

SMART Mobility

Modeling Workflow Development, Implementation, and
Results Capstone Report

July 2020

(This Page Intentionally Left Blank)

Foreword

The U.S. Department of Energy’s Systems and Modeling for Accelerated Research in Transportation (SMART) Mobility Consortium is a multiyear, multi-laboratory collaborative, managed by the Energy Efficient Mobility Systems Program of the Office of Energy Efficiency and Renewable Energy, Vehicle Technologies Office, dedicated to further understanding the energy implications and opportunities of advanced mobility technologies and services. The first three-year research phase of SMART Mobility occurred from 2017 through 2019, and included five research pillars: Connected and Automated Vehicles, Mobility Decision Science, Multi-Modal Freight, Urban Science, and Advanced Fueling Infrastructure. A sixth research thrust integrated aspects of all five pillars to develop a SMART Mobility Modeling Workflow to evaluate new transportation technologies and services at scale.

This report summarizes the work of the SMART Mobility Modeling Workflow effort. The SMART Mobility Modeling Workflow was developed to evaluate new transportation technologies such as connectivity, automation, sharing, and electrification through multi-level systems analysis that captures the dynamic interactions between technologies. By integrating multiple models across different levels of fidelity and scale, the Workflow yields insights about the influence of new mobility and vehicle technologies at the system level. For information about the other Pillars, please refer to the relevant pillar’s Capstone Report.

Acknowledgments

This material is based upon work supported by the U.S. Department of Energy, Office of Energy Efficiency and Renewable Energy (EERE), specifically the Vehicle Technologies Office (VTO) under the Systems and Modeling for Accelerated Research in Transportation (SMART) Mobility Laboratory Consortium, an initiative of the Energy Efficient Mobility Systems (EEMS) Program.

This report was prepared as an account of work sponsored by an agency of the United States Government. Neither the United States Government nor any agency thereof, nor any of its employees, makes any warranty, express or implied, or assumes any legal liability or responsibility for the accuracy, completeness, or usefulness of any information, apparatus, product, or process disclosed, or represents that its use would not infringe privately owned rights. Reference herein to any specific commercial product, process, or service by trade name, trademark, manufacturer, or otherwise does not necessarily constitute or imply its endorsement, recommendation, or favoring by the United States Government or any agency thereof. The views and opinions of authors expressed herein do not necessarily state or reflect those of the United States Government or any agency thereof.

The following DOE Office of Energy Efficiency and Renewable Energy (EERE) managers played important roles in establishing the project concept, advancing implementation, and providing ongoing guidance: David Anderson, Michael Berube, Erin Boyd, Heather Croteau, and Prasad Gupte.

The SMART Mobility Modeling Workflow acknowledges the contributions of: Aymeric Rousseau¹, Colin Sheppard², Joshua Auld¹, Felipe de Souza¹, Annesha Enam¹, Vincent Freyermuth¹, Max Gardner³, Venu Garikapati⁴, Zachary Needell², Monique Stinson¹, Omer Verbas¹, and Eric Wood⁴.

Affiliation during research effort:

¹ Argonne National Laboratory

² Lawrence Berkeley National Laboratory

³ University of California – Berkeley

⁴ National Renewable Energy Laboratory

This work was authored for the U.S. Department of Energy (DOE) by Argonne National Laboratory under Contract No. DE-AC02-06CH11357, Lawrence Berkeley National Laboratory under Contract No. DE-AC02-05CH11231, Idaho National Laboratory under Contract No. DE-AC07-05ID14517, National Renewable Energy Laboratory under Contract No. DE-AC36-08GO28308, and Oak Ridge National Laboratory under Contract No. DE-AC05-00OR22725. Funding provided by U.S. Department of Energy, Office of Energy Efficiency and Renewable Energy, Vehicle Technologies Office.

List of Acronyms

ABM	agent-based model
ACC	adapted cruise control
AMRF	Argonne Advanced Mobility Research Facility
Argonne	Argonne National Laboratory
AV	automated vehicle
BAU	business-as-usual
BEV	battery-electric vehicle
CACC	cooperative adapted cruise control
CAGR	compound annual growth rate
CAV	connected and automated vehicle
Conv	conventional vehicle
CTA	Chicago Transit Authority
DCFC	direct-current fast charging
DOE	U.S. Department of Energy
DTA	dynamic traffic assignment
EVI-Pro	Electric Vehicle Infrastructure Projection
EVSE	electric vehicle supply equipment (i.e., charging station)
EEMS	Energy Efficient Mobility Systems
FCSPan	Fast Charging Station Plan
GHG	greenhouse gas

HD	heavy-duty
HEV	hybrid electric vehicle
HH	household
HOV	high-occupancy vehicle
I2V	infrastructure-to-vehicle communication
IEA	International Energy Agency
LBNL	Lawrence Berkeley National Laboratory
LDV	light-duty vehicle (i.e., passenger cars including sports-utility vehicles and light trucks)
LLNL	Lawrence Livermore National Laboratory
MATSim	Multi-Agent Transportation System Framework
MD	medium-duty
MEP	mobility energy productivity metric
NREL	National Renewable Energy Laboratory
ORNL	Oak Ridge National Laboratory
P&D	parcel and delivery
PEV	plug-in electric vehicle (i.e., PHEV or BEV)
PHEV	plug-in hybrid electric vehicle
PHT	productive hours travelled
PMT	productive miles travelled
PUMS	U.S. Census Public Use Microdata Sample
PUMA	public use microdata area

R&D	research and development
SAV	shared automated vehicle
SMART	Systems and Modeling for Accelerated Research in Transportation
SOC	battery state of charge
SOV	single-occupancy vehicle
SUV	sports utility vehicle
TNC	transportation network company (i.e., ride-hailing)
TSDC	Transportation Secure Data Center
V2I	vehicle-to-infrastructure communication
V2V	vehicle-to-vehicle communication
VHT	vehicle hours travelled
VMT	vehicle mile travelled
VOTT	value of travel time
VTO	Vehicle Technologies Office
xEV	electrified powertrain (i.e., HEV, PHEV, BEV)
ZOV	zero-occupancy vehicle
ZOV miles	deadheading for an automated vehicle

Executive Summary

Research to increase the energy efficiency of the transportation system has traditionally emphasized the importance of vehicles and vehicle components. Today, however, dramatic changes in transportation and communication technologies—from vehicle electrification and automation to shared mobility, e-commerce, and telecommuting—are disrupting the transportation system and increasing the need to understand the systemic energy impacts of human behaviors in the context of so many new choices.

The U.S. Department of Energy (DOE) Systems and Modeling for Accelerated Research in Transportation (SMART) Mobility Consortium is a multi-year, multi-laboratory collaborative dedicated to further understanding the energy implications and opportunities of advanced mobility technologies and services. The SMART Mobility Consortium consists of five pillars of research: Connected and Automated Vehicles, Mobility Decision Science, Multi-Modal Freight, Urban Science, and Advanced Fueling Infrastructure.

The SMART Mobility Consortium creates tools and generates knowledge about how future mobility systems may evolve while identifying ways to improve their overall system efficiency and affordability. The consortium also identifies research and development (R&D) gaps that DOE's Office of Energy Efficiency and Renewable Energy, Vehicle Technologies Office's Energy Efficient Mobility Systems (EEMS) Program may address through its advanced research portfolio and generates insights that will be shared with mobility stakeholders.

Recent studies have shown a wide range of potential impacts that individual vehicle technologies could have on energy and travel demand. While the opportunity exists for inexpensive, reliable, and accessible mobility to lead to significant benefits, there is also a substantial risk for increased congestion, energy use, and urban sprawl. Cities are already home to more than half of the world population, and would be the first to experience these impacts.

The SMART Mobility modeling workflow has been developed to evaluate new transportation technologies such as connectivity, automation, sharing, and electrification through multi-level systems analysis that captures the dynamic interactions between technologies. Through integration of multiple models across different levels of fidelity and scale (i.e., individual vehicles to entire metropolitan areas), the workflow yields insights about the influence of new mobility and vehicle technologies at the system level:

- At the individual vehicle level, detailed models are created to represent powertrain component technologies and control algorithms across powertrain and vehicle classes.
- Multi-vehicle models are used to implement connected and automated vehicle (CAV) enabled vehicle and powertrain control algorithms, evaluate the impact of connectivity (e.g., vehicle to infrastructure [V2I] and vehicle-to-vehicle [V2V] communication), and quantify the potential energy benefits.
- Micro-simulation models that represent tens of thousands of vehicles are then used to quantify the impact of those new controls on intersection and corridor traffic flow, based on specific travel patterns and traffic levels.
- Mesoscopic transportation system models are used to model travel behavior at the city or regional scale, and to assess the impact of new transportation technologies and services on hundreds of thousands or even millions of travelers in the mobility system.

This report describes the SMART Mobility modeling workflow, and discusses results and insights generated through two implementations of the workflow for two different cities (Chicago and San Francisco) based on a common set of scenarios.

ES.1 New SMART Mobility Modeling Workflow

By creating a multi-fidelity, end-to-end modeling workflow (Figure ES-1), SMART Mobility researchers advanced the state of the art in transportation system modeling and simulation. The consortium developed a software toolchain that captures the complex interactions among mobility decision-making, technology implementation, different mobility service models and modes, land use, and electric vehicle (EV) charging infrastructure. This unique capability integrates freight and passenger movement and allows researchers to evaluate the energy, mobility, and affordability outcomes of potential future transportation scenarios.

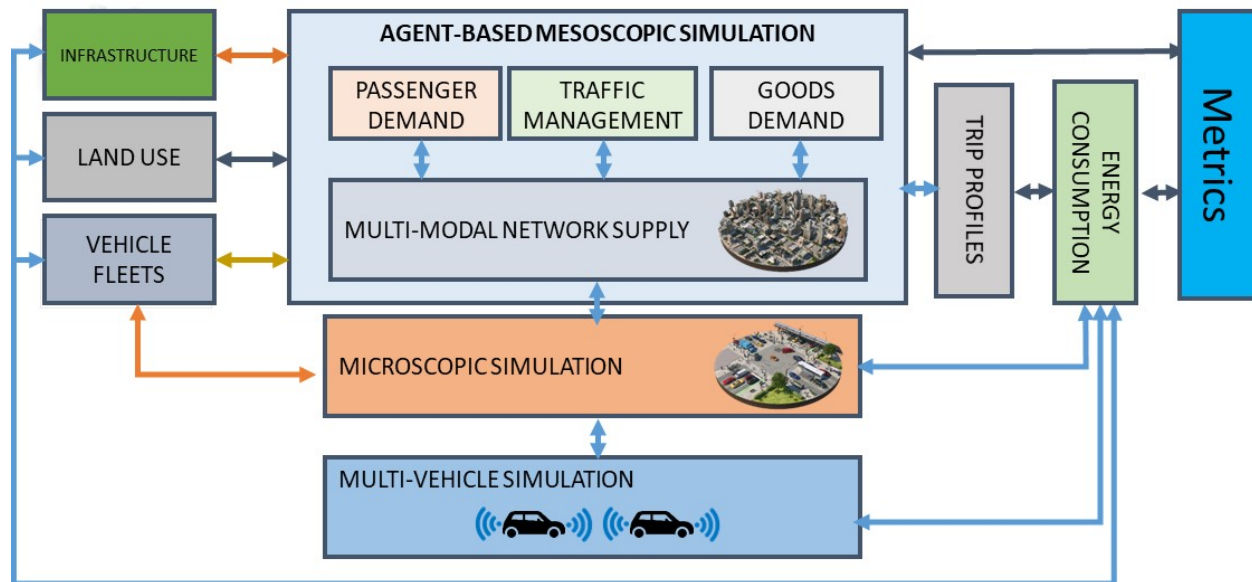


Figure ES-1. SMART Mobility Workflow

The workflow is built around two core agent-based models (ABMs) that simulate the transportation system. These two implementations of the SMART Mobility workflow were developed in parallel, and demonstrate that different tools with different levels of fidelity can be used interchangeably, employing a similar set of assumptions:

- One implementation is built around Planning and Operations Language for Agent-based Regional Integrated Simulation (POLARIS), a high-performance, open-source ABM framework developed by Argonne National Laboratory, designed for simulating large-scale transportation systems.
- Another implementation is built around the Behavior, Energy, Autonomy, and Mobility (BEAM), a modeling framework for behavior, energy, autonomy, and mobility developed by Lawrence Berkeley National Laboratory (LBNL), which extends the Multi-Agent Transportation System Framework (MATSim) to enable scalable analysis of urban transportation systems.

While both workflow implementations rely on different models to address each specific steps (e.g., vehicle energy consumption), they share some common elements:

- UrbanSim: a microsimulation platform for forecasting the growth and development of metropolitan regions over decade-scale time horizons, including changes to land use, demographics, and employment.

- Electric Vehicle Infrastructure Projection (EVI-Pro): a tool used to determine public charging station location and type based on plug-in vehicle (PEV) trip demand.
- Aimsun: a commercial traffic microsimulation tool used to generate traffic flow fundamental diagrams, such as the relationship between the speed, flow rate, and density of vehicles on a given transportation link, for different market penetrations of automated vehicles.
- Mobility energy productivity (MEP): a methodology that quantifies the energy, cost, and time-weighted opportunity space within a reachable area—how many goods, services, and destinations can be reached by a given mode of transport, in a specified amount of time.

ES.2 Common Scenarios and Assumptions

Several major trends, such as vehicle connectivity, automation, sharing, and electrification are poised to have a significant impact on the transportation system. How these trends evolve (e.g., whether partial or full automation is incorporated into vehicles, what the market penetration is for new technologies or mobility services) remains uncertain. In addition, dynamic system interactions among these trends are complex, and may impact the transportation system in ways that are not fully understood. For example, full powertrain electrification of shared mobility service fleets would lead to different vehicle use patterns, charging requirements, and potentially radical changes in land use. Although the overall objective of the SMART Mobility Consortium is to quantify the impact of each individual technology and their combination at the system level, a limited number of scenarios were initially selected to highlight some of the key parameters that influence traffic flow, travel behavior, and transportation system control.

To quantify the impact of new mobility technologies independently from other parameters including land use, vehicle technology and freight, consortium members developed a series of current and future baseline scenarios that assume no/low/high vehicle technology development, but with no changes in vehicle connectivity, automation, and sharing. Three main future scenarios (Figure ES-2) were then created to quantify the impact of connectivity, automation, and sharing relative to the baselines:

1. Scenario A: High Sharing, Low Automation. This scenario represents a near-term future with a moderate increase in vehicle ride-hailing fleets along with the penetration of partially automated vehicle technologies (e.g., advanced driver assistance systems).
2. Scenario B: High Sharing, High Automation. This scenario represents a longer term future where fully automated driverless vehicles are owned by fleet operators and widely shared by large segments of the population. E-commerce is common among households.
3. Scenario C: Low Sharing, High Automation. Like Scenario B, Scenario C represents the longer term future with fully automated driverless vehicles. In Scenario C, however, those vehicles are owned by individuals and shared within the household (i.e., privately owned AVs). It is thus a low ride-hailing case alternative to Scenario B. E-commerce is common among households.



Figure ES-2. High-Level Scenario Description.

Selected results and conclusions reached by implementing the SMART Mobility Modeling Workflow on these common assumptions are described below.

ES.3 Pooled Ride-hailing without Repositioning Decreases Vehicle Miles Travelled

In the Chicago metropolitan area, high-sharing scenarios without vehicle repositioning to search for riders (i.e., Scenarios A and B) achieve lower vehicle miles travelled (VMT) due to the efficient use of ride-hailing, the small share of VMT without a passenger (below 15%), and a significant amount of ride pooling (22%–27%). As shown in Figure ES-3, shared automation (Scenario B5/B6) produces a substantial increase in ride-hail travel compared to the other scenarios (up to 112 million daily miles traveled). The shared automation scenarios (B5/B6) also have the highest percentage of pooling, with up to 27% of total ride-hail VMT being pooled; this more than offsets the 12%–14% share of deadheading trips for passenger pickup. These results are consistent with existing literature that estimates that the share of empty miles would be between 14% and 22%. Overall, this result, where pooling largely offsets the empty travel miles, can be attributed to several factors: (i) high household vehicle retirement rates (more ride-hailing requests due to vehicle disposal leads to more opportunity for pooling, especially because the high vehicle disposal rates tend to occur in dense urban areas); (ii) reduced wait times due to larger fleet sizes; and (iii) reduced labor costs in the automated ride-hailing vehicles. The share of deadheading VMT, however, is still highest in the high sharing scenarios (B5/B6), because there are more ride requests per vehicle than the other scenarios due to overall higher ridership. This leads to a lower share of vehicles available at a given time and therefore an increase in the distance between the traveler and an available vehicle, thereby increasing overall empty VMT.

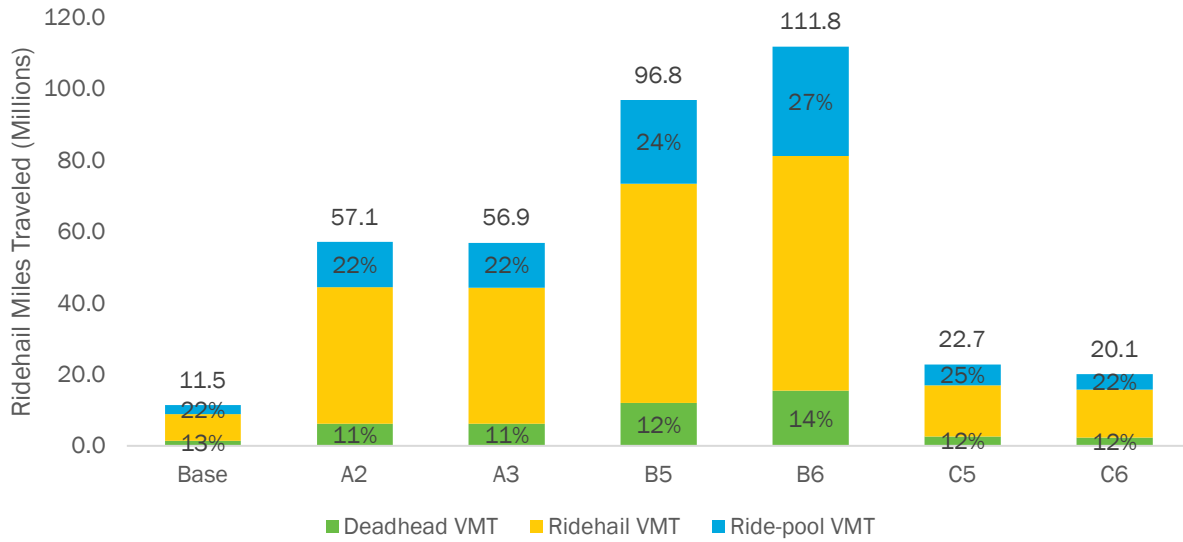


Figure ES-3. POLARIS Ride-hailing Operational Characteristics by Scenario.

ES.4 Ride-hailing Repositioning Leads to Increased Empty Miles

In the San Francisco metropolitan area, ride-hailing vehicles in a heavily utilized fleet are often empty and unmatched to passengers. If ride-hailing vehicles reposition to increase their chances of picking up a passenger – including pooled passengers – with low wait time, the increase in empty VMT from this repositioning overwhelms any VMT reductions from increased pooling, even with low prices and no consumer aversion to shared rides. These results are sensitive to ride-hailing repositioning and matching algorithms. As shown in Figure ES-4, Scenario B, where household vehicle ownership is low and preference for sharing is high, leads to more vehicle miles traveled than Scenario C, even though the latter scenario assumes more single-occupancy car dependence. This effect is largely due to reduced performance of the ride-hailing fleet in Scenario B. Simulation results show that VMT is higher in Scenario B than in either the long-term baseline (Base 5/6) or Scenario C. Despite a preference for shared rides among travelers, the matching and rebalancing algorithms simulated are unable to substantially increase the average occupancy of ride-hail vehicles from baseline levels; indeed, the occupancy of ride-hail vehicles is on average even less than in the baseline scenario, largely due to frequent repositioning of the ride-hail fleet as it attempts to maximize the number of trips it can serve. Because automated ride-hail vehicles operate all day, there is an oversupply of them during off-peak times. When local supply is higher than demand, some idle ride-hail vehicles will move to locations where expected demand is higher to increase their likelihood of matching a request; this portion is calibrated to match deadhead portions observed in current ride-hailing fleets. When supply outstrips demand during a large portion of the day, as in Scenario B, this repositioning to meet anticipated demand further inflates nonproductive VMT.

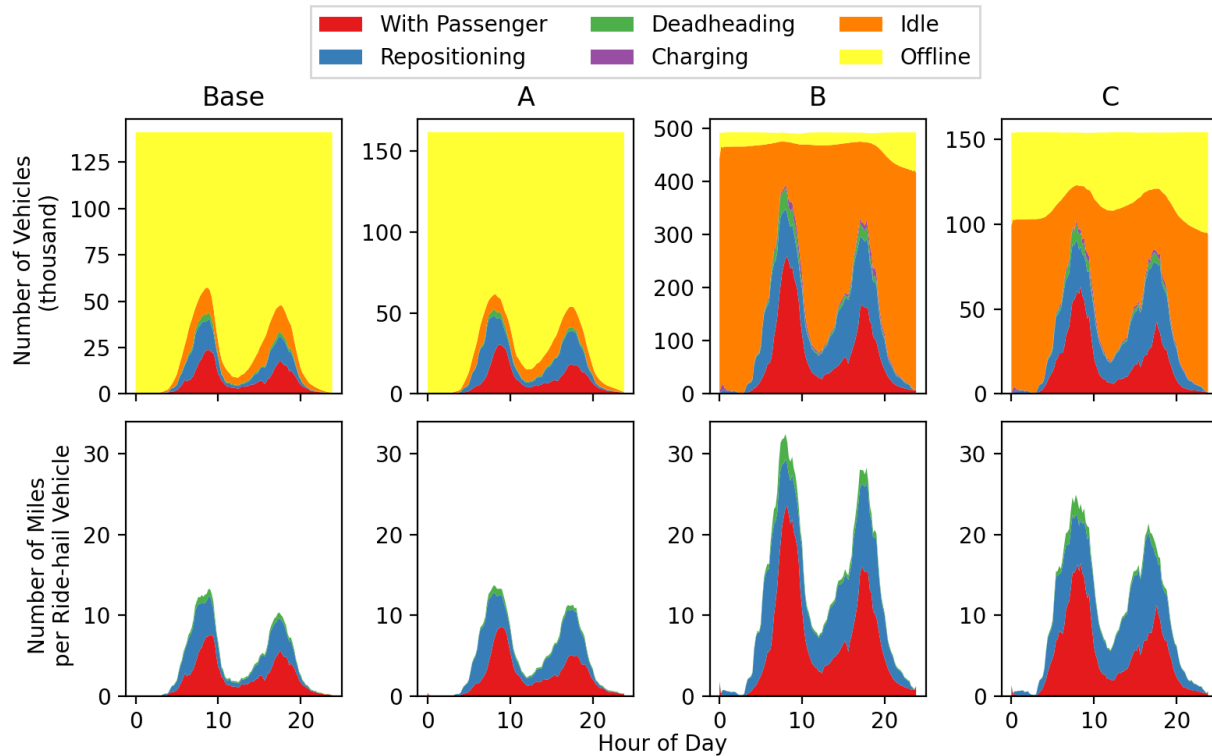


Figure ES-4. Use of the Ride-hail Fleet in Base 0 and the Three Vehicle Technologies Office (VTO) scenarios (columns) in BEAM. Top: number of ride-hail vehicles in a state at a given time of day. Bottom: total number of miles (per hour (normalized by the number of unique ride-hail vehicles)) by the ride-hail fleet with different purposes.

ES.5 Personally Owned Driverless Vehicles Increase VMT

The use of privately owned automated vehicles (AVs) leads to drastically increased VMT and greatly increased unloaded vehicle travel, with 1 out of 7 all vehicles in the system being empty, compared to 1 out of 25 in the high-sharing, high-automation case (Scenario B6). In the Chicago metropolitan area, a 52% penetration of privately owned, fully automated vehicles (Scenario C6) leads to an increase of 25% in VMT compared to Base 6. This occurs due to two primary phenomena: the increase in VMT with no passenger due to increased vehicle repositioning in the privately owned AV case, and the increase in overall travel resulting from the assumed reduction in value of travel time (VOTT) in an AV. As shown in Figure ES-5, the temporal distribution of vehicle hours traveled (VHT) by type (ownership, automation level, passenger load) and by time of day clearly demonstrates a significant travel increase in Scenario C6 largely driven by lower VOTT, with much of that taking place in privately owned AVs (represented by the solid orange color in Figure ES-5). However, there is also additional unloaded travel for both for ride-hail and shared automated vehicles (SAVs). In Scenario C6, almost 22% of the privately owned AV travel is done by unloaded or empty vehicles. Overall, 15% of all travel hours in the system are driven unloaded in Scenario C6; in Scenario B6, unloaded travel occurs only in the SAV (automated ride-hail) vehicles, and only 14% of total SAV travel hours are unloaded.

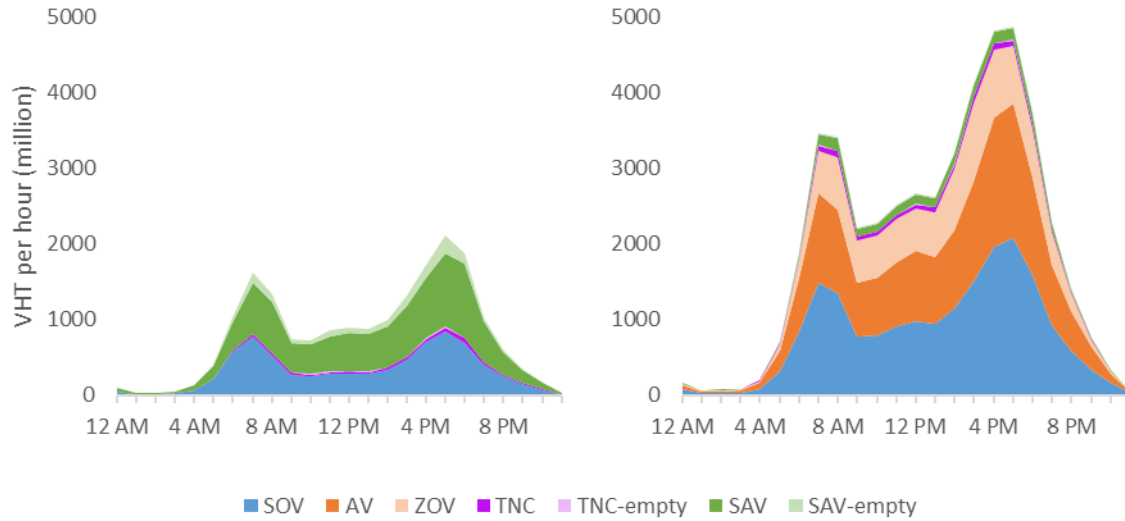


Figure ES-5. Temporal Distribution of VHT by Auto Modes for (a) Shared AV (Scenario B6) and (b) Private AV (Scenario C6) in POLARIS.

ES.6 Personally Owned Driverless Vehicles Impact Travel Behavior

Households with AVs exhibit substantially different travel behavior compared to households without AVs. This behavior includes a propensity to travel longer during peak evening hours and to take more single-occupancy vehicle (SOV) trips. As shown in Figure 6, households with AVs exhibit higher travel time compared to households without AVs; average trip travel time for AV households is approximately 7 minutes higher than for non-AV households during peak periods. In general, households with AVs tend to travel farther and for longer durations, especially for discretionary activities: for these activities, the average travel time is more than 6 minutes longer and the average travel distance is 4 miles farther than for households without AVs. The share of SOV trips for AV households is also 7% higher than that of non-AV households. These households travel farther and for longer durations by SOV, high-occupancy vehicle (HOV), and ride-hail modes compared to households without AVs. The reduced VOTT for AV travel is the major factor contributing to the differences in the travel behavior between households with and without AVs, along with unloaded vehicle repositioning as household members share the use of the AV.

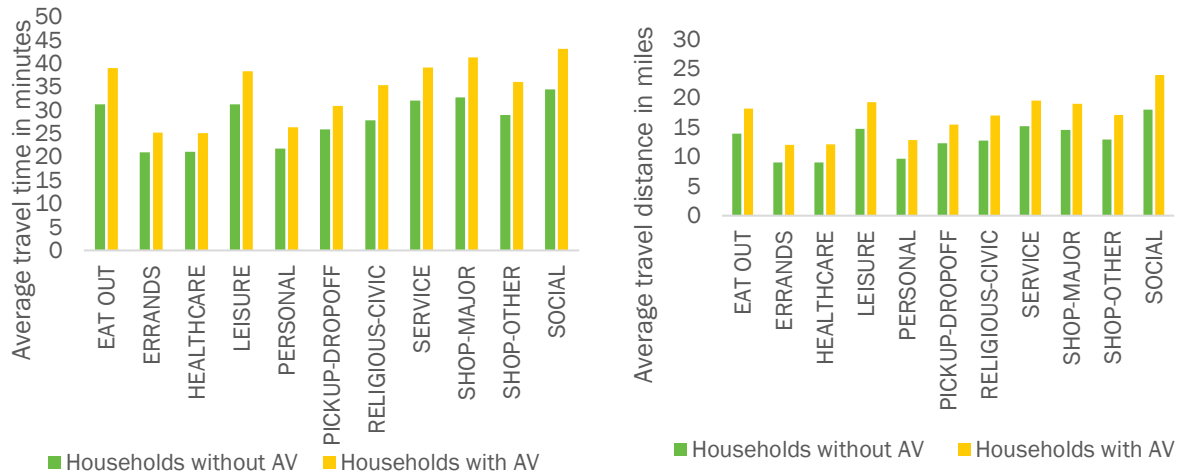


Figure ES-6. Average Travel Time by Mode, and Travel Distance by Mode in POLARIS.

ES.7 Transit is Critical to Mobility

Transit is vital to the overall transportation system. In a Chicago metropolitan area-based scenario with no transit, all mobility and energy metrics become substantially worse in the urban core: there is a 52% increase in VHT and a 23% decrease in travel efficiency (passenger miles per kilowatt-hours). To analyze the effect of transit on regional mobility, an additional scenario was implemented to analyze a no-transit case. This no-transit scenario was the same as the Base 0 scenario, but with all transit links and vehicles removed in the Chicago metropolitan area. The findings shown in Figure ES7 indicate there would be substantial adverse effects on mobility and energy use throughout the entire region, but the negative effects are more pronounced in the urban area.

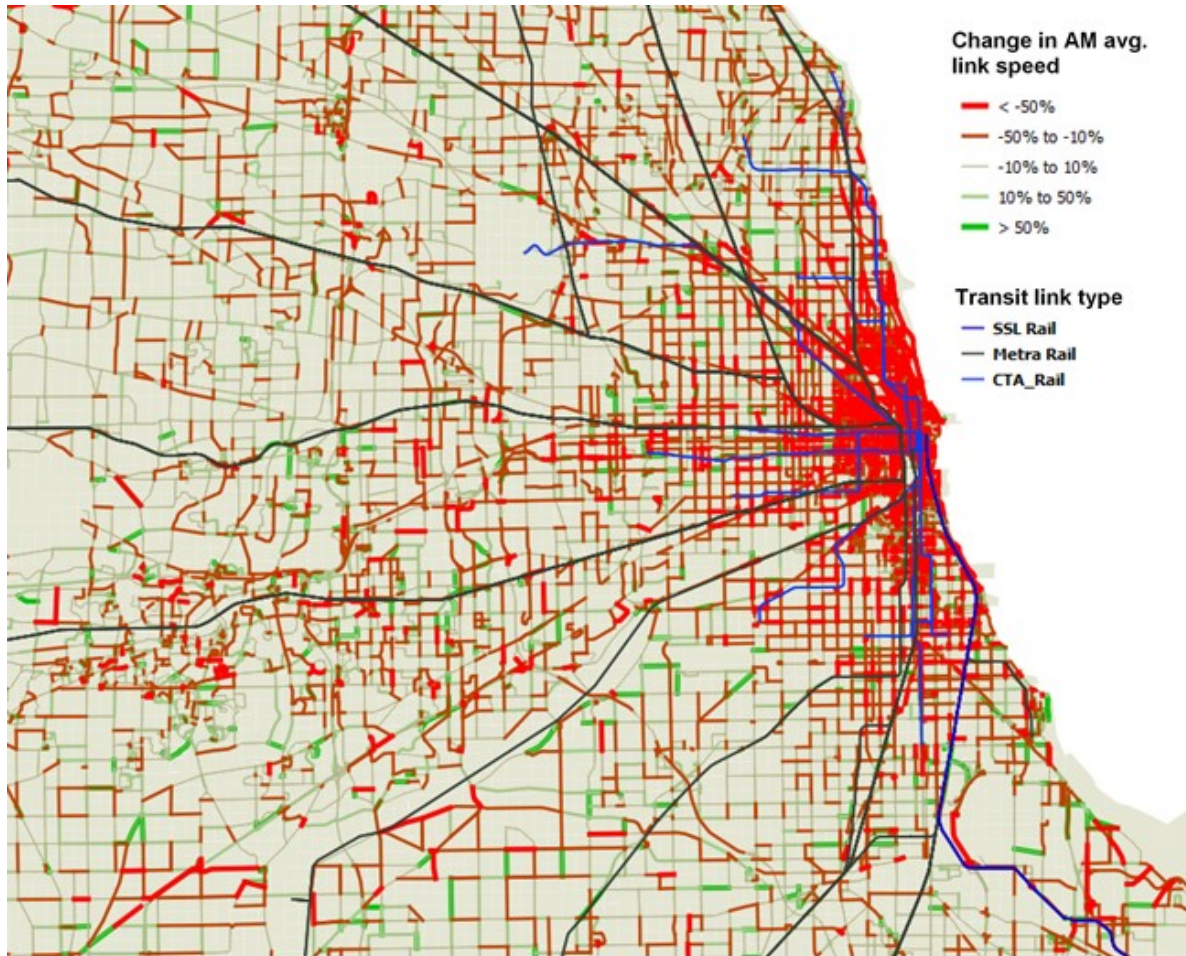


Figure ES-7. Impact of No-Transit Scenario in POLARIS.

ES.8 Freight Movement Will Be Increasingly Important to Transportation Energy Use

Based on scenario analysis in the Chicago metropolitan area, medium- and heavy-duty (MD and HD) vehicles currently account for 33% the overall transportation energy. This share is expected to grow to 50% in the future due to light-duty vehicle efficiency improvements enabled by electrification combined with increased freight demand. As shown in Figure ES7, MD/HD truck energy represents 33% of the total energy for the Base 0 scenario and Scenario A, up to 50% for Scenario B, and up to 40% for Scenario C. The increased portion of MD/HD truck energy in future scenarios can primarily be explained by the lower level of electrification in MD/HD trucks, and the fact that their VMT is expected to increase over time. Note that in Scenario B, MD/HD trucks consume 50% of the total energy, although they are responsible for only 10% of VMT.

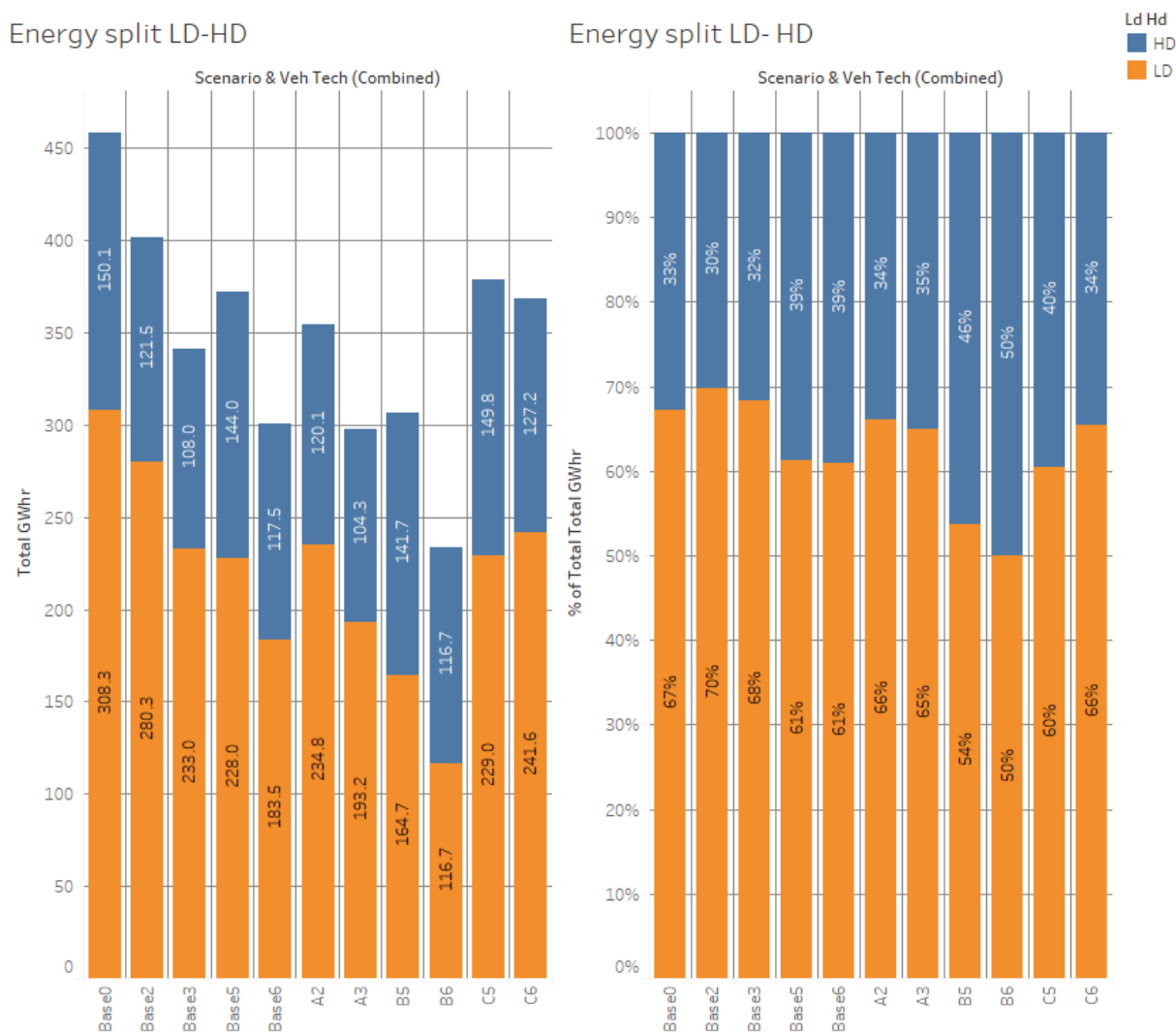


Figure ES-8. Autonomie Energy Split between LDV and MD/HD Trucks.

ES.9 An Increase in E-Commerce Lowers Overall System VMT and Energy

E-commerce is expected to generate a large increase in last-mile delivery of goods. However, after accounting for shopping trip reductions and vehicle technology changes, simulations show that there will be an overall net reduction in VMT (34–56%) and energy use (29–54%) across the Chicago metropolitan area. The e-commerce delivery rate is assumed to increase from one delivery per household per week in the current baseline (Base 0–Base 6) to three per week in the near term (Scenarios A2, A3), and five per week in the long term (Scenarios B5, B6, C5, C6). Because the average shopping trip is 7–8 miles long and shopping trips currently constitute approximately 7% of total VMT, there is substantial potential for VMT and energy to decrease if shopping trips are replaced by deliveries. As shown in Figure ES-9, if household e-commerce deliveries triple in the short term compared to the base year (Base 0), retail-based VMT could decrease by 31%, and retail-based energy consumption could decrease by 39%–49%. Over the long term, if household e-commerce deliveries were to grow to five days per week, retail-based VMT and energy consumption could decline by 36%–50% and 54%–72%, respectively. The VMT savings are even greater when comparing the future (Scenarios A, B, C) to their respective baselines (Base 1, Base 2, Base 3 and Base 4, Base 5, Base 6).

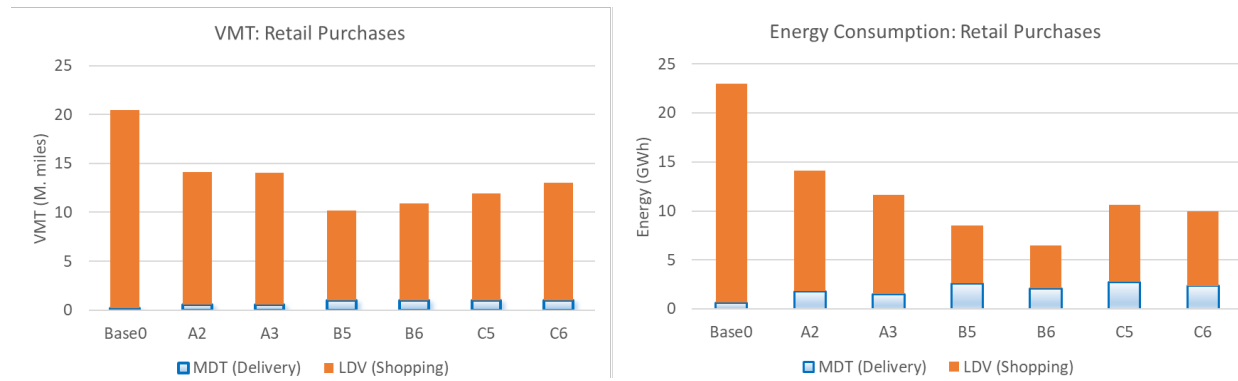


Figure ES-9. VMT (Left) and Energy Consumption (Right) Associated with Retail Purchasing from POLARIS Workflow.

ES.10 Shared Mobility Improves Mobility Energy Productivity (MEP)

MEP improvements are greater in the high sharing, high automation scenarios (B5/B6) than in the low sharing, high automation scenarios (C5/C6), demonstrating that shared mobility has additional travel cost, time, and energy benefits beyond those due to vehicle technology improvements alone. As shown in Figure ES-10, for both workflow implementations, MEP score improvements are higher in Scenario B5/B6 than in Scenario C5/C6. This shows reduced network congestion and increased vehicle occupancy brought out by shared mobility augment the benefits associated with vehicle technology improvements. In the privately-owned CAV scenario (Scenario C), networks are more congested compared to shared-mobility scenarios, which causes MEP scores to drop. As a result, the calculated MEP in Scenario C is lower than MEP in Scenario B with similar vehicle technology improvements.

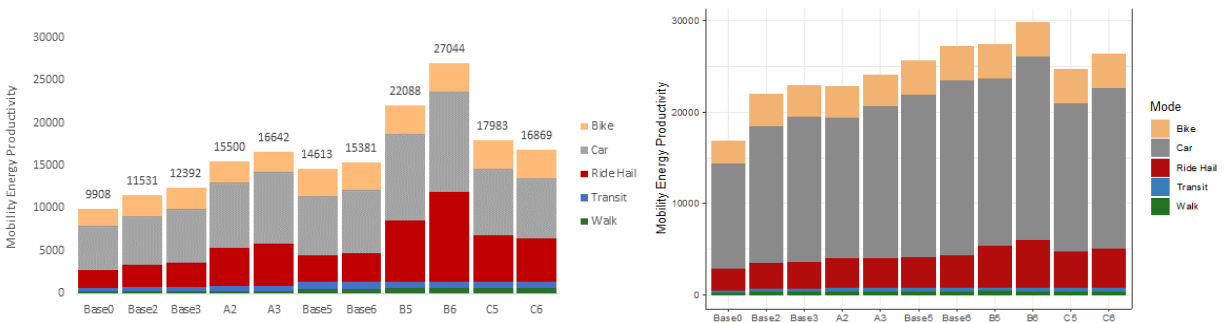


Figure ES-10. Aggregate MEP Values for the Workflow Scenarios (left: POLARIS/Chicago; right: BEAM/San Francisco).

Table of Contents

Executive Summary	vi
ES.1 New SMART Mobility Modeling Workflow	vii
ES.2 Common Scenarios and Assumptions	viii
ES.3 Pooled Ride-hailing without Repositioning Decreases Vehicle Miles Travelled	ix
ES.4 Ride-hailing Repositioning Leads to Increased Empty Miles	x
ES.5 Personally Owned Driverless Vehicles Increase VMT	xi
ES.6 Personally Owned Driverless Vehicles Impact Travel Behavior.....	xii
ES.7 Transit is Critical to Mobility.....	xiii
ES.8 Freight Movement Will Be Increasingly Important to Transportation Energy Use.....	xiv
ES.9 An Increase in E-Commerce Lowers Overall System VMT and Energy	xv
ES.10 Shared Mobility Improves Mobility Energy Productivity (MEP)	xvi
1 Overview	1
2 Approach	3
2.1 SMART Mobility Modeling Workflow	3
2.1.1 Workflow Implementation using POLARIS	4
2.1.2 Workflow Implementation Using BEAM	17
2.2 High-Level Workflow Implementation Comparisons	24
2.3 Mobility Energy Productivity (MEP) Metric	25
3 Common Scenarios and Assumptions	29
3.1 Scenarios	29
3.2 Main Assumptions.....	31
3.2.1 Individual Parameters.....	31
3.2.2 Vehicle Assumptions and Fleet Distribution.....	35
4 Results from POLARIS Workflow Implementation.....	45
4.1 Individual Traveler Behavior Changes	52
4.2 Ride-Hailing	56
4.3 Privately Owned AVs.....	61
4.4 Multi-Modal Travel	65
4.5 MEP	67
4.6 Light-Duty Vehicle Charging Infrastructure.....	71
4.7 Goods Delivery.....	72
4.8 Vehicle Technology Impact and Vehicle Class Contribution to Energy Consumption.....	77
5 Results from BEAM Workflow Implementation.....	85
5.1 Impact of VTO Research Targets	93
5.2 Ride-hailing.....	96
5.3 Household CAVs.....	99
5.4 Land Use	101
5.5 Light-Duty Vehicle Charging Infrastructure.....	103
6 Conclusions	106

References	109
APPENDIX A – Models Validation	113
APPENDIX B – POLARIS Household E-Commerce Demand Model	130
APPENDIX C – Main Vehicle Technologies Assumptions	131
APPENDIX E – Main Vehicle Fleet Assumptions	135
APPENDIX F – GREET Greenhouse Gas Emission Factors	138

List of Figures

Figure 1. SMART Mobility Coordinated Research Plan.....	3
Figure 2. Generic SMART Mobility Workflow.....	4
Figure 3. Workflow Implementation Centered around POLARIS.	5
Figure 4. POLARIS Transportation Systems Simulator Overview.	8
Figure 5. SVTrip–RoadRunner–Aimsun Workflow for CAVs Control in Traffic.	9
Figure 6. UrbanSim-POLARIS Workflow for Land Use Consideration.	10
Figure 7. EVI-Pro–POLARIS Workflow for Charging Station Locations.	11
Figure 8. POLARIS Charging Decision Algorithm.	12
Figure 9. Chicago Estimated Residential Charging Availability by PUMA as a Function of Assumed PEV Penetration.....	13
Figure 10. POLARIS-simulated PEV Public Charging Demand from Unconstrained Network (Background) and EVI-Pro Synthesized Charging Station Locations	13
Figure 11. POLARIS Last-mile E-commerce Supply and Demand Development.	14
Figure 12. Aimsun-POLARIS Workflow to Represent CAVs Penetration Impact on Traffic Flow	16
Figure 13. Common Autonomous Vehicle Models Reused across Multiple Tools.....	16
Figure 14. Data Flow between ADOPT, FASTSim, Route-E, and BEAM.	19
Figure 15. Data Flow between UrbanSim, ActivitySynth, and BEAM.	21
Figure 16. Modeling Workflow between BEAM, EVI-Pro, and FCSPlan (Fast-Charging Station Plan) to Site Charging Infrastructure for BEAM Simulations.....	22
Figure 17. BEAM-simulated PEV Public Charging Demand from Unconstrained Network (Background) and EVI-Pro Synthesized Charging Station Locations.	23
Figure 18. CACC Impact on Highway and Arterial Road Capacity in BEAM (based on Work by Hao et al. 2018).	24
Figure 19. Thirty-minute isochrone for biking.....	26
Figure 20. MEP Calculation Workflow.	27
Figure 21. MEP Baseline Maps Incorporating POLARIS and BEAM Data	28
Figure 22. High-Level Scenario Descriptions.	30
Figure 23. SMART Mobility Scenarios.	31
Figure 24. Baseline Vehicle Fleet Assumption (Source: POLK).	38
Figure 25. Light-Duty Vehicle Class of Car Stock Assumptions.	39
Figure 26. Light-Duty Vehicle Powertrain of Car Stock Assumptions across Scenarios.	39

Figure 27. Light-Duty Powertrain Electrification across Classes (Continued on Next Page)..... 41

Figure 28. Light-Duty Vehicle Automation Assumptions across Scenarios..... 42

Figure 29. MD and HD Vehicle Powertrain Assumptions across Scenarios. 42

Figure 30. MD and HD Powertrain Electrification across Classes..... 43

Figure 31. MD and HD Vehicle Automation Assumptions across Scenarios..... 44

Figure 32. POLARIS Scenario Results for (a) VMT and PMT, (b) VHT and PHT, (c) VMT and PMT per Capita, (d) VHT and PHT per Capita, and (e) Average Speed. 50

Figure 33. POLARIS Total Energy Use, and Energy Use by Powertrain Type. 51

Figure 34. POLARIS Mode Shares by Scenario. 53

Figure 35. POLARIS Household Vehicle Disposal Rates by Traffic Analysis Zone for Scenarios (a) A2, (b) B2, and (c) C2..... 54

Figure 36. POLARIS Mode Share across Central Business District (CBD), City Center, Suburban, and Exurban Areas for Households Relinquishing at Least One Vehicle..... 56

Figure 37. Disparity between Households That Do and Do Not Own Vehicles in POLARIS. 56

Figure 38. POLARIS Ride-hailing Operational Characteristics by Scenario. 57

Figure 39. Cumulative Distribution of Daily Trips per Ride-hailing Vehicle in Scenarios Base 0, A3, B6, and C6. 58

Figure 40. Cumulative Distribution of Total Daily Miles Driven by Ride-hailing Vehicles in Scenarios Base 0, A3, B6, and C6. 58

Figure 41. Fleet Operation Profile in POLARIS for Scenarios Base 0, A3, B6, and C6. 59

Figure 42. Trips Served by Time of Day with and without Ride-pooling in POLARIS..... 60

Figure 43. Travel Time (Pickup and Drop-off Combined) and Average Speed of Ride-hailing Vehicles in Scenarios B6 and C6. 60

Figure 44. POLARIS (a) PMT and VMT, and (b) PHT and VHT per Capita by AV Ownership (Scenario C6)..... 61

Figure 45. Comparison of (a) Average Travel Time by Activity Type, (b) Average Travel Distance by Activity Type, (c) Average Travel Time across the Day, (d) Average Travel Time by Mode, (e) Mode Share, and (f) Travel Distance by Mode in POLARIS (Scenario C6)..... 63

Figure 46. Temporal Distribution of VHT by Auto Modes for (a) Shared AV (Scenario B6) and (b) Private AV (Scenario C6) in POLARIS. 64

Figure 47. POLARIS Transit Mode Share in the Baseline Scenario and Percent Change under Scenarios A3, B6, and C6..... 65

Figure 48. POLARIS TNC Mode Share in the Baseline Scenario and Percent Change under Scenarios A3, B6, and C6..... 66

Figure 49. Comparison between Ride-hailing and Transit Mode Share Changes in POLARIS (Scenario B6)..... 66

Figure 50. Ride-hailing MEP Scores, Energy Intensity, and Cost Values. 68

Figure 51. MEP and PMT Results from POLARIS. 68

Figure 52. MEP Evolution across Each Main POLARIS Scenario. 70

Figure 53. Simulated Charging Demand across Chicago. 71

Figure 54. Base 0 MD/HD Shares of VMT (Million Miles) and Fuel (Million..... 74

Figure 55. Impacts of Commodity Flow Growth and Vehicle Technology Changes on Freight VMT and Energy Consumption from POLARIS Workflow..... 75

Figure 56. VMT (Left) and Energy Consumption (Right) Associated with Retail Purchasing from POLARIS Workflow. 76

Figure 57. Passenger Shopping Generates 7% of Regional VMT (Base0). 76

Figure 58. MD/HD Truck Impacts on VMT and Energy Use across Scenarios from POLARIS Workflow. 77

Figure 59. Energy and VMT Split between by Powertrain (PWT) and Class (Light-duty Vehicles [LDV] and MD/HD Trucks) from POLARIS Workflow. 78

Figure 60. GHGs and GHGs/Mile for Light-duty and MD/HD Vehicles from POLARIS Workflow..... 79

Figure 61. Autonomie Energy Split between Light-duty Vehicles and MD/HD Trucks. 80

Figure 62. Energy Benefits of Meeting VTO Technology Targets (High Vehicle Technologies) Compared to Business-as-Usual (BAU - Low Vehicle Technologies) from POLARIS Workflow..... 81

Figure 63. Fuel and Electrical Energy Consumption from POLARIS Workflow. 82

Figure 64. Average Light-Duty Vehicle Fuel Economy (MPGGE). 83

Figure 65. Impact of Automation on Vehicle Fuel Economy (Scenario B6). 84

Figure 66. Modal Market Shares for Commute in San Francisco Bay Area across Scenarios. 89

Figure 67. Total Commuting Travel Distance per Capita in the San Francisco Bay Area, Disaggregated by Mode Taken. 90

Figure 68. Baseline Mode Splits (Top) and Absolute Change in Portion of Commute Trips Taken by Different Modes (Bottom) from Baseline to Workflow Scenarios, Disaggregated by Trips of Different Distances. 90

Figure 69. Left: Overall Average Travel Speed (for All Modes), Right: Average Travel Speed for Car, CAV, and Ride-hailing Trips Only..... 91

Figure 70. Aggregate BEAM MEP Values for the Workflow Scenarios 92

Figure 71. Relationship between MEP and Average Light-duty Vehicle Fuel Economy across Scenarios, Showing a Strong Positive Relationship..... 93

Figure 72. Total Light-duty Vehicle Energy Consumption by Fuel Type for the San Francisco Bay Area..... 94

Figure 73. Total VMT for Commuting by Mode for the San Francisco Bay Area. 95

Figure 74. VMT by Ride-hails for the San Francisco Bay Area across Scenarios, Differentiating between Miles without a Passenger (Hatched) and Miles with Multiple Passengers (Purple). 97

Figure 75. Utilization of Ride-hail Fleet in Base 0 and the Three VTO Scenarios. Top: Number of Ride-hail Vehicles in a State at a Given Time of Day. Bottom: Total Number of Miles Driven (Averaged per hour) by Ride-hail Fleet with Different Purposes. 98

Figure 76. Light-duty VMT Disaggregated by Automation Level across Workflow Scenarios..... 100

Figure 77. Average Travel Times from Home to Work for Manually Operated Car Trips, Used by Home and Workplace Location Choice Models in Urbansim. 101

Figure 78. Relationship between Rent and Accessibility, Measured as Number of Jobs That Can Be Reached by Car within a Given Generalized Travel Time..... 102

Figure 79. Relationship between Job Density and Accessibility, Measured as Number of Jobs That Can Be Reached by Car within a Given Generalized Travel Time. 103

List of Tables

Table 1. Assumed Probability of Access to Residential Charging based on Residence Type and Tenure. 22

Table 2. MEP Inputs Used from Various Models 27

Table 3. Baseline Scenarios Main Parameters. 33

Table 4. Advanced Mobility Scenario Main Parameters..... 33

Table 5. Baseline Vehicle Fleet Assumptions. 36

Table 6. Advanced Mobility Scenarios Main Vehicle Fleet Assumptions. 37

Table 7. POLARIS Key System Performance Metrics (Light Duty+MD/HD) across Scenarios. 47

Table 8. POLARIS Key System Performance Metrics (Light Duty Only) across Scenarios..... 48

Table 9. Percentage Change in Mobility and Energy Metrics with No transit in POLARIS (vs Base0) ... 67

Table 10. Summary of EVI-Pro Public Charging Networks Simulated for POLARIS Workflow. 72

Table 11. POLARIS Freight Impact Results Summary..... 73

Table 12. Differences in Various Aggregate Metrics from Baseline across the Workflow Scenarios..... 88

Table 13. Distribution of Light-duty Vehicle VMT across Usage (Personal vs. Ride-hail) and Powertrain Type. 99

Table 14. Summary of EVI-Pro Public Charging Networks Simulated for BEAM Workflow. 105

(This Page Intentionally Left Blank)

1 Overview

Research to increase the energy efficiency of the transportation system has traditionally focused on vehicle and powertrain technology development. Today, however, dramatic changes in transportation and communication technologies—from vehicle electrification and automation to shared mobility, e-commerce, and telecommuting—are disrupting the transportation system and increasing the need to understand the systemic energy impacts of human behaviors in the context of so many new choices.

The U.S. Department of Energy (DOE) Systems and Modeling for Accelerated Research in Transportation (SMART) Mobility Consortium is a multi-year, multi-laboratory collaborative dedicated to further understanding the energy implications and opportunities of advanced mobility technologies and services. The SMART Mobility Consortium focuses on five pillars of research:

- **Connected and Automated Vehicles (CAVs):** Identifying the energy, technology, and usage implications of connectivity and automation and identifying efficient CAV solutions.
- **Mobility Decision Science (MDS):** Understanding the human role in the mobility system, including travel decision-making and technology adoption in the context of future mobility.
- **Multi-Modal Freight (MMF):** Evaluating the evolution of freight movement and understanding the impacts of new modes for long-distance goods transport and last-mile package delivery.
- **Urban Science (US):** Understanding the linkages between transportation networks and the built environment and identifying the potential to enhance access to economic opportunity.
- **Advanced Fueling Infrastructure (AFI):** Understanding the costs, benefits, and requirements for fueling/charging infrastructure to support energy efficient future mobility systems.

The SMART Mobility Consortium creates tools and generates knowledge about how future mobility systems may evolve while identifying ways to improve their overall system efficiency and affordability. The consortium also identifies research and development (R&D) gaps that the DOE's Energy Efficient Mobility Systems (EEMS) Program may address through its advanced research portfolio and generates insights that will be shared with mobility stakeholders.

Recent studies have shown that individual vehicle technologies have a wide range of potential impacts on energy and travel demand:

- There is opportunity for inexpensive, reliable, and accessible mobility to lead to significant benefits. Proper vehicle size selection (i.e., right-sizing the vehicle for its use), advanced vehicle and powertrain technologies (e.g., electrification, light-weighting, and engine improvements), reducing the number of stops at traffic lights, shorter distances between vehicles, and platooning could all improve overall system efficiency.
- There is also substantial risk for increased congestion, energy use, and urban sprawl. Cities are already home to more than half of the world population. By 2030, that figure is projected to be more than 60% [1], with urban residents accounting for more than 90% of growth in energy consumption globally [2]. Increased population means increased travel demand and congestion. As new transportation technologies and services make travel more affordable and convenient, travel demand may increase. Empty miles resulting from ride-hailing/taxis or fully automated vehicles, substitution from transit to car-based modes, and new travel demand from previously underserved populations may increase vehicle miles travelled (VMT). In addition, rapidly increasing e-commerce may continue to add to the demand for goods delivery.

The SMART Mobility Modeling Workflow has been developed to evaluate new transportation technologies such as connectivity, automation, sharing, and electrification through multi-level systems analysis that captures the dynamic interactions between technologies. By integrating multiple models across different levels of fidelity and scale (i.e., individual vehicles to entire metropolitan areas), the Workflow yields insights about the influence of new mobility and vehicle technologies at the system level.

- At the individual vehicle level, detailed models represent powertrain component technologies and control algorithms across powertrain and vehicle classes.
- Multi-vehicle models implement CAVs-enabled vehicle and powertrain control algorithms, evaluate the impact of connectivity (e.g., vehicle to infrastructure [V2I], vehicle to vehicle [V2V]), and quantify the potential energy benefits.
- Micro-simulation models that represent tens of thousands of vehicles then quantify the impact of those new controls on intersection and corridor traffic flow based on specific travel patterns and traffic levels.
- Mesoscopic transportation system models model travel behavior at the city or regional scale, and assess the impact of new transportation technologies and services on hundreds of thousands or even millions of travelers in the mobility system.

This report describes the SMART Mobility Modeling Workflow, and discusses results and insights generated through two implementations of the workflow for two different cities (Chicago and San Francisco) based on a common set of scenarios.

2 Approach

SMART Mobility researchers implemented a coordinated research plan to analyze the impact of a wide range of mobility and vehicle technologies at the system level (Figure 1). Common scenarios feed parameters into the workflow to calculate the impacts of new technologies on a wide range of metrics, including VMT, vehicle hours travelled (VHT), energy, cost, and mobility energy productivity (MEP) [3] to generate insights.

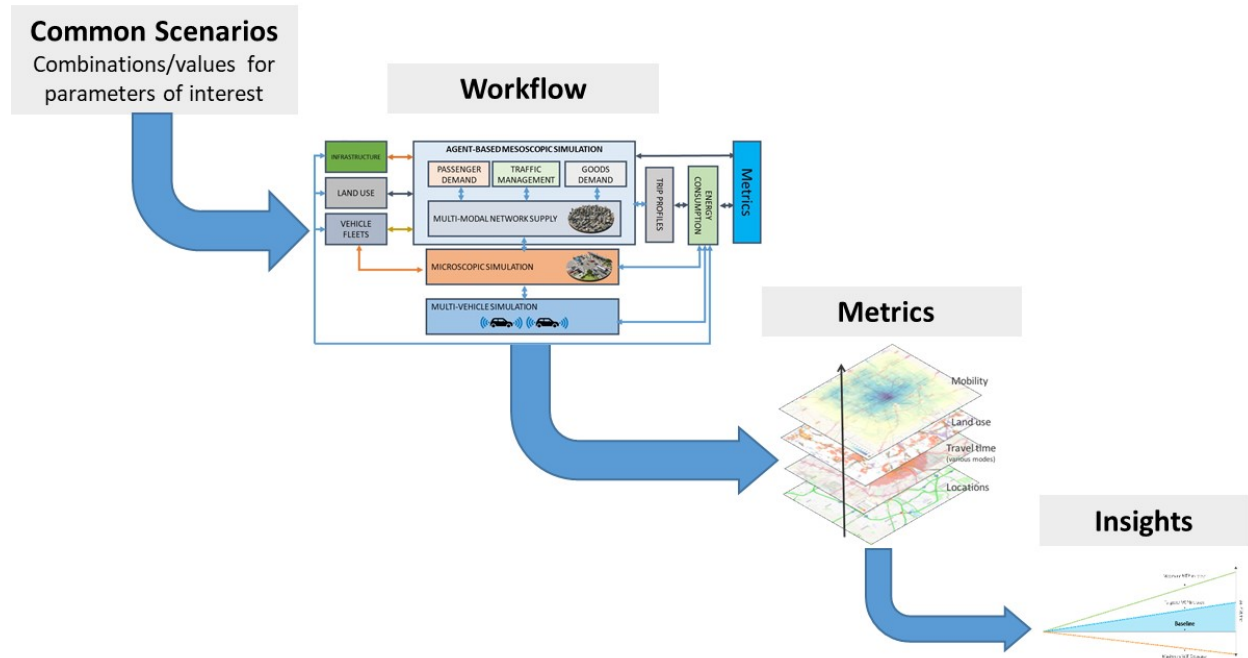


Figure 1. SMART Mobility Coordinated Research Plan.

2.1 SMART Mobility Modeling Workflow

A taskforce composed of the main technical leads for each model within the Workflow led its development and application, with the initial task of (1) confirming the model linkages identified during a review of all the available models and (2) ensuring that models of different fidelities could be used for different implementations of the workflow. The successful development of individual model linkages led to the SMART Mobility workflow as shown in Figure 2.

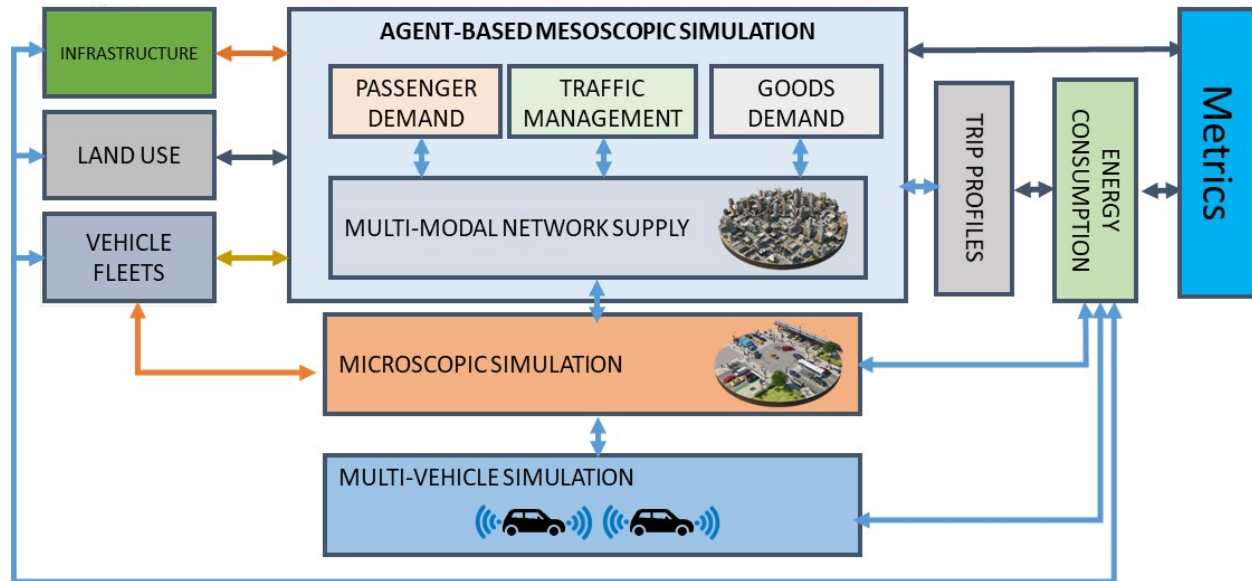


Figure 2. Generic SMART Mobility Workflow.

The Workflow is built around two core agent-based models (ABMs) that simulate the transportation system. These two implementations of the SMART Mobility Workflow were developed in parallel, and demonstrate that different tools with different levels of fidelity can function interchangeably, using a similar set of assumptions:

- One implementation is built around POLARIS, a high-performance, open-source ABM framework developed by Argonne, designed for simulating large-scale transportation systems.
- One implementation is built around BEAM, a modeling framework for behavior, energy, autonomy, and mobility developed by Lawrence Berkeley National Laboratory (LBNL), which extends the Multi-Agent Transportation System Framework (MATSim) to enable scalable analysis of urban transportation systems.

The following sections describe both workflow implementations.

2.1.1 Workflow Implementation using POLARIS

The workflow implementation built around POLARIS leverages unique expertise from six national laboratories and seven universities, as shown in Figure 3. POLARIS, Argonne's agent-based transportation systems simulator [4], forms the core of this workflow implementation. It links with multiple models to simulate land use, charging station location, vehicle market penetration, and microscopic traffic flow impacts. Outputs from POLARIS are then fed into the other simulation tools; for example, POLARIS provides travel demand patterns to the microscopic traffic flow model, network level of service characteristics to the land use model, and electric vehicle charging demand patterns to the fueling infrastructure model. POLARIS also generates simulated travel episodes and trip profiles that can estimate energy consumption using the Autonomie model [5]. The outputs of the workflow include many characteristics of the mobility system (e.g., energy consumption, miles traveled, hours traveled, network speed and congestion), and ultimately are used to calculate the MEP metric.

Nearly 10% of VMT and more than 30% of fuel consumption in the transportation sector are associated with the movement of goods and freight. The transport of finished goods is also responsible for a significant portion of traffic, especially in urban areas. POLARIS is unique among transportation system ABMs because it includes both passenger and freight movement, and represents the interactions between passenger and goods

demand. POLARIS generates both passenger trips and trips for trucks that carry goods, and simulates an integrated traffic system with both passenger and commercial freight vehicles. The interactions between passenger and goods demand is a primary driver of mobility and energy.

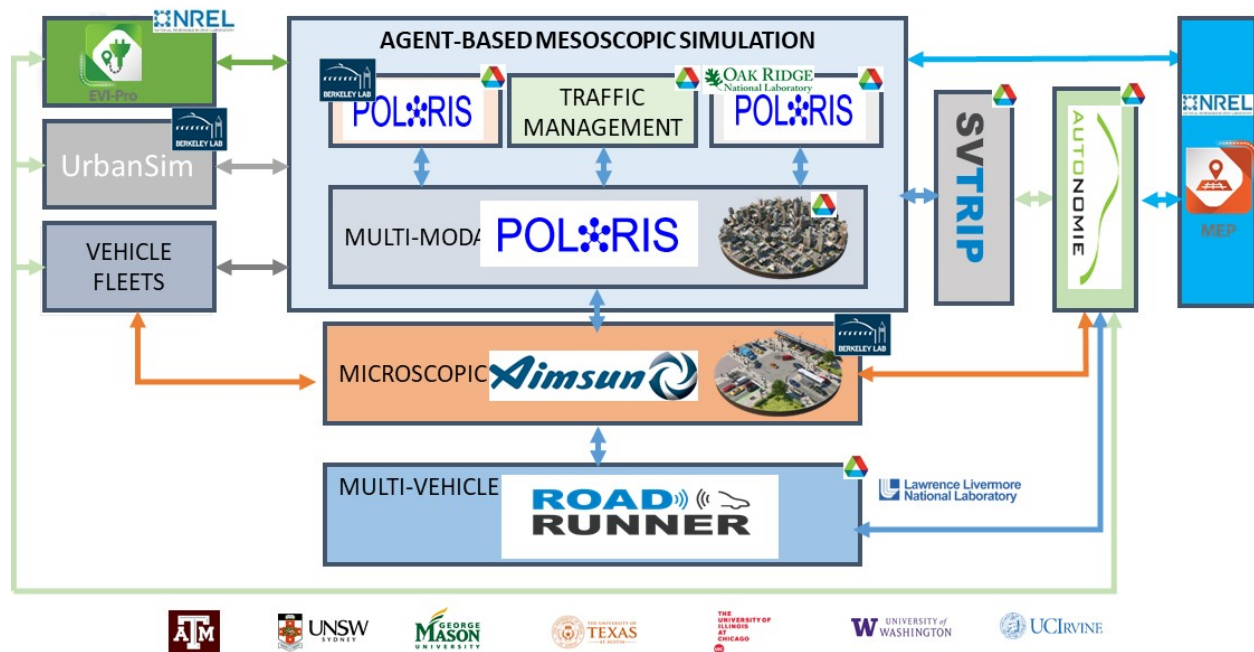


Figure 3. Workflow Implementation Centered around POLARIS.

The workflow taskforce selected the following models for inclusion in the POLARIS implementation of the workflow after reviewing the inputs, outputs, and level of fidelity of each model:

- POLARIS: An agent-based, mesoscopic transportation system simulation tool used to generate travel demand and traffic flow at the metropolitan area level.
- Aimsun: A traffic microsimulation tool used to generate traffic flow fundamental diagrams (i.e., the relationships between the speed, flow rate, and density of vehicles on a given transportation link) for different market penetrations of AVs, used as an input to POLARIS.
- RoadRunner: A multi-vehicle simulation tool used to estimate the impact of new control algorithms at the vehicle and component levels using Autonomie powertrain models and vehicle aerodynamic data.
- UrbanSim: A microsimulation platform for forecasting the growth and development of metropolitan regions over decade-scale time horizons, including changes to land use, demographics, and employment. Outputs are provided to POLARIS for scenario runs.
- Electric Vehicle Infrastructure Projection (EVI-Pro): A tool used to determine public charging station location and type based on plug-in electric vehicle (PEV) trip demand generated by POLARIS.
- Stochastic Vehicle Trip Profile (SVTrip): A tool to synthesize vehicle speed dynamics (i.e., acceleration, deceleration) from detailed POLARIS information (i.e., average vehicle speed per link, road type, potential stop duration) for use by Autonomie to properly estimate vehicle energy consumption.
- Autonomie: A high-fidelity vehicle simulation tool used to estimate vehicle energy consumption from SVTrip speed traces across vehicle classes, powertrains, and component technologies.

- MEP: A computation using outputs from UrbanSim, POLARIS, and Autonomie in an aggregate calculation that includes the energy, time, and cost of mobility.

The contributions of the university partners to the workflow implemented around POLARIS are as follows:

- George Mason University: Automated behavior model calibration.
- University of California Irvine: Ride-hailing repositioning optimization in CPLEX.
- University of Illinois at Chicago: Activity scheduling and resource allocation POLARIS models.
- University of New South Wales: Value of time and time use POLARIS models.
- University of Texas at Austin: Dynamic rideshare modeling in POLARIS.
- University of Texas A&M: Improvement of CAV traffic flow model using CAV-specific fundamental diagrams in POLARIS.
- University of Washington: Ride-hailing driver behavior and travel survey.

2.1.1.1 POLARIS Transportation System Simulation

The POLARIS agent-based transportation systems simulator [4] developed by Argonne forms the core of the workflow implementation. Multiple elements such as land use modeling, vehicle market penetration modeling, and microscopic traffic flow impacts provide inputs into and inform the POLARIS model. POLARIS, in turn, generates simulated travel episodes (i.e., measure of time spent on one activity or traveling), network performance characteristics, and activity demands that are used by the other components of the workflow (e.g., by the Autonomie model to estimate energy consumption [5]). The results of the workflow are input into the MEP calculation, which is used as a basis for evaluating the combined effect of mobility and energy impacts associated with a given scenario.

POLARIS is a high-performance ABM framework designed to simulate large-scale transportation systems. It features integrated travel demand, network flow, and a traffic assignment model to capture key aspects of travel decisions (activity planning, route choice, and tactical-level driving decisions) simultaneously and in a continuous, fully integrated manner. The model covers individual decision-making on long-term, mid-term, and within-day timeframes for various travel-related decisions. The mid-term and within-day travel behavior decisions (e.g., the process of individual activity episode planning and engagement) are captured in a computational process model representation of decision-making [4]. These decisions are constrained by long-term choices regarding home/workplace choice and household vehicle choices, which in turn influence activity and travel episode planning and realization. The network model includes a mesoscopic representation of vehicle movements based on Newell's kinematic wave model [6]; updates represent interactions with traffic control infrastructure. The traveler agents in the model can react in real time to changing or unexpected network conditions based on either direct observation or information provision, using an en-route rerouting and re-planning model.

For long-term choices, fleet definitions within POLARIS can either come from external market penetration forecasts [7] coupled with baseline vehicle registration data, or from household-level choice modeling [8]. An additional CAV technology choice process uses models based on stated-preference survey data [9] to determine the willingness-to-pay for various levels of CAV technology for each household vehicle. This transportation simulation framework connects to the Autonomie vehicle-level energy simulation model through the SVTrip stochastic trip reconstruction process. For more detail on the POLARIS framework, see Auld et al. [4], and for an example of the use of POLARIS in energy estimation see Auld et al. [10].

Several key features have been added to the POLARIS framework to represent future mobility technologies, including:

- A household-level AV-sharing optimization model was implemented to allow households to access privately owned AVs. This model optimizes the household members' schedules in order to minimize costs (fuel, parking, tolls, time costs, etc.) subject to a variety of constraints including spatiotemporal limitations, vehicle availability, activity flexibility, and others. Formulation of the optimization function and details of its solution using the CPLEX solver can be found in Javanmardi et al. [11].
- The transit model (bus, rail, commuter rail) and active modes (walking and biking) on a multilayered network was improved to allow for fully intermodal movements such as walk-to-transit and park-and-ride. Travelers walk or drive to a transit stop, then wait for a transit trip; they may then board, sit, stand, alight, transfer, get rejected to board, reroute, and so forth. These movements are guided by a time-dependent point-to-point intermodal routing algorithm [12].
- New SAV agents for operators and vehicles have been developed to model the operations of both transportation network company (TNC) vehicles and SAV fleets. The SAV operator receives trip requests from traveler agents, assigns the nearest idle vehicle to pick up travelers, and suggests repositioning moves for vehicles that have been idled for long periods—a dispatching strategy similar in concept to that proposed by Bischoff and Maciejewski [13]. Ride-hailing fleets are modeled using the same agents, with different cost structures, fleet sizes, and vehicle types, and with the drivers' ability to refuse trips and stop working at any time. More details on this model can be found in the CAVs Capstone report. Note that currently SAV/TNC vehicles that are electric vehicles currently go out of service when batteries are depleted, rather than charging and re-entering the fleet.
- Whether an AV is part of a shared fleet or privately owned, its impact on traffic flow is similar. In both cases, it is modeled as an adjustment to the link capacity parameter in the mesoscopic flow model based on the instantaneous penetration rate on each link [14]. The capacity adjustment is derived from simulation studies of link performance under different cooperative adapted cruise control (CACC) penetration rates, as described in Lu et al. [15].
- POLARIS was improved to allow all instances of travel time costs entering choice utility functions (e.g., mode choice, destination choice, and route choice) to be modified by a value of time adjustment factor meant to capture the increased comfort and convenience of AV modes. The parameters are typically varied over ranges from 0.35 to 1.0 rather than set by a model, because this is still a new area of research (see [16, 17, 18, 19]) with few empirical estimates of VOTT changes. More details about the model can be found in the MDS Capstone report.
- Agent-based freight transportation was implemented into POLARIS and is fully integrated with key passenger features including dynamic traffic assignment (DTA). The model synthesizes a population of business establishments, simulates their trade partnerships with each other, and subsequently generates the scheduling and routing of individual MD and HD trucks. More details about the model and about the initial agent-based and commodity-flow based implementations can be found in the MMF Capstone report.

Figure 4 depicts the POLARIS simulator, with these specific model enhancements. POLARIS has been extensively validated using test data (Appendix A). The SMART Mobility workflow has been exercised for the Chicago Metropolitan area. The relationships between different tools are described below.

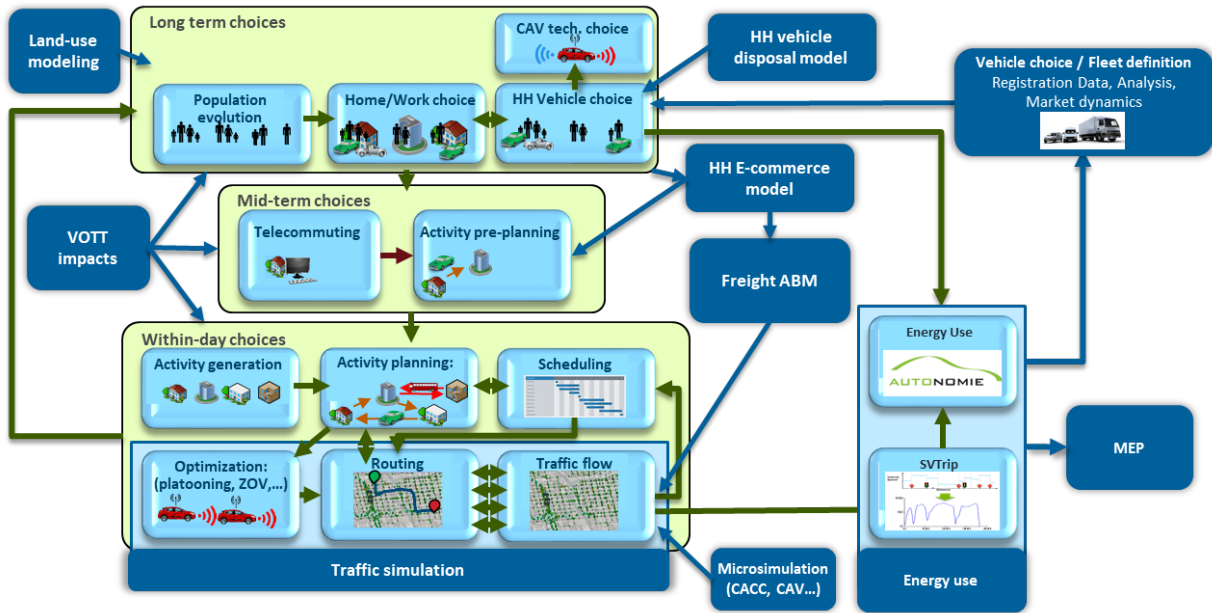


Figure 4. POLARIS Transportation Systems Simulator Overview.

2.1.1.2 Traffic Flow Impact on Multi-vehicle Control

CAVs have the potential to save significant energy by improving vehicle operation (e.g., vehicle speed and/or powertrain optimization) within safety and travel time constraints. This research is performed using a new dedicated tool developed by Argonne called RoadRunner. RoadRunner is a software framework that simulates multiple vehicles with full powertrain models, as well as the interactions between vehicles and their environment. RoadRunner uses powertrain models from Autonomie and adds new capabilities such as multivehicle simulation, models of road characteristics, causal models of human driving, V2X (“vehicle to everything”) communications, and sensors.

RoadRunner can simulate, in the same environment, both powertrain dynamics (e.g., engine torque, fuel flow, battery state of charge [SOC]) and vehicle longitudinal dynamics (e.g., speed, acceleration). As a result, it presents a unique capability for researchers and automotive engineers to develop energy-saving techniques that rely on a combination of powertrain controls, driving automation, connectivity, and sensing. SMART Mobility researchers use RoadRunner to develop and evaluate the benefits of energy-focused CAV controls. As an essential part of the SMART workflow, RoadRunner also enables vehicle-in-the-loop research, where one simulated vehicle is replaced by an actual vehicle on a dynamometer.

To ensure that the eco-driving controllers designed in RoadRunner are robust, the algorithms were evaluated under different traffic flow conditions. To do so, two complimentary approaches were implemented (Figure 5):

- Using the linkage with SVTrip to generate the second-by-second vehicle speed profile from macroscopic attributes of the trip segments, researchers can run fast CAV simulations with exogenous traffic for any road scenario. In this approach, a lead vehicle serves as a proxy for traffic and represents all vehicles the following vehicles would encounter throughout the trip. This process allows SMART researchers to quickly run a very large number of traffic flow scenarios.
- Using the linkage with Aimsun, a commercial microscopic traffic flow simulation tool, SMART researchers can consider more complex traffic dynamics with a larger number of vehicles, although the more detailed process required for each scenario limits the number of scenarios that can be run.

In summary, this new capability enables interactions between vehicle-level (RoadRunner) and road-level simulation (e.g., Aimsun) tools, allowing traffic dynamics to be considered as part of vehicle-level control development and evaluation.

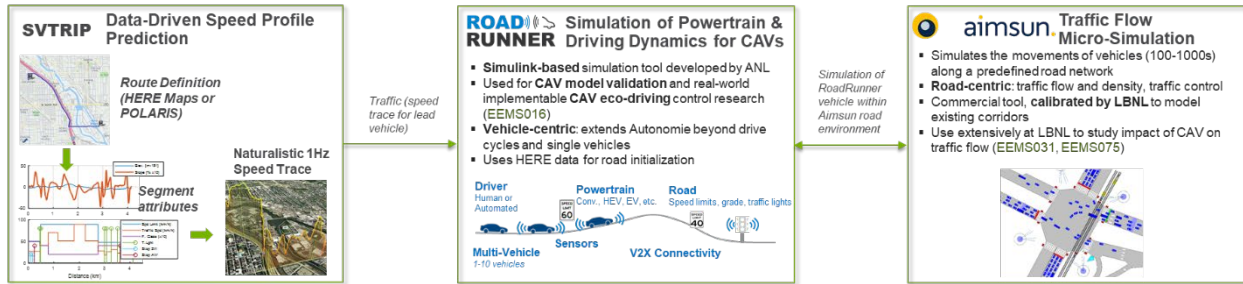


Figure 5. SVTrip–RoadRunner–Aimsun Workflow for CAVs Control in Traffic.

RoadRunner vehicle controls have been extensively validated using vehicle dynamometer test data (Appendix A)

2.1.1.3 Land Use Impact on the Transportation System

The population in large metropolitan areas is expected to significantly increase in the future. To model land use changes, University of California (UC) Berkeley’s UrbanSim was paired with POLARIS in a closed-loop simulation. The iterative process shown in Figure 6 includes the following steps:

- POLARIS generates sets of travel times, costs, distances, and other factors by mode and time of day between each pair of zones in the modeled region. It then provides this information to UrbanSim.
- Urbansim uses these network performance measures to predict where population will shift and where new development will occur for a future year.
- This future-year set of population, employment, and land use data is then used as input to POLARIS to estimate future network performance. This process continues until the population and network performance estimates converge.

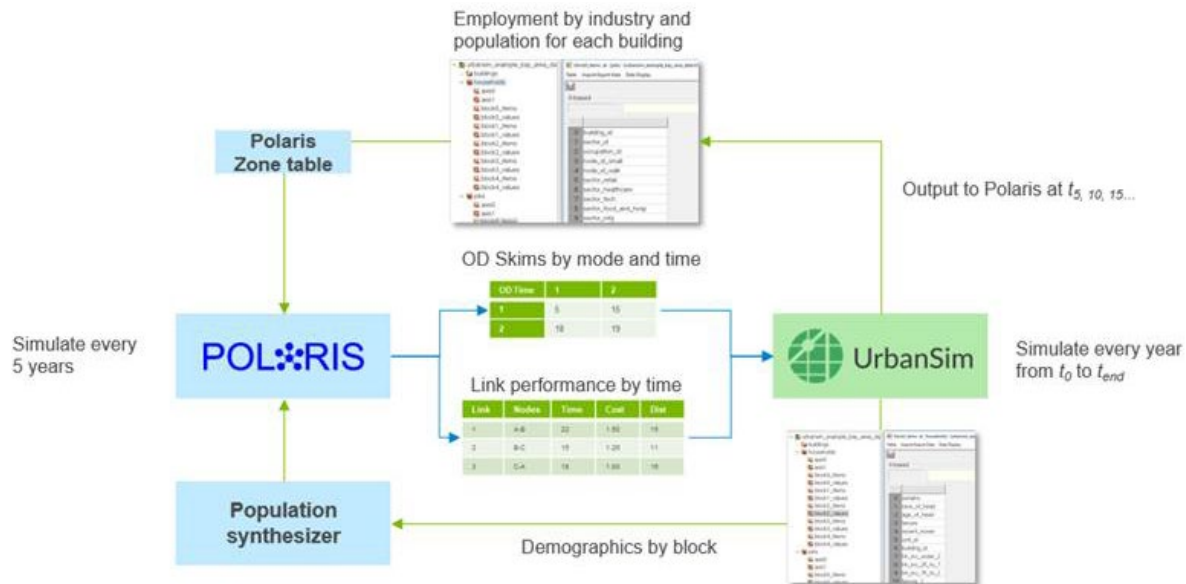


Figure 6. UrbanSim-POLARIS Workflow for Land Use Consideration.

2.1.1.4 Fueling/Charging Infrastructure Impact on the Transportation System

Charging decisions related to PEVs affect traveler behavior and have transportation system-wide impacts. Factors that influence charging decisions include the location, type, and availability of charging stations, vehicle design, battery SOC, and whether the vehicle is privately owned or fleet-owned. To effectively evaluate the impacts that electric-drive vehicles may have on future mobility, it is critical to properly represent PEV charging station locations and types for different vehicle usage and market penetrations.

A workflow between POLARIS and Electric Vehicle Infrastructure Projection model (EVI-Pro) has been developed to support residential and public charging network designs. EVI-Pro uses detailed data on personal vehicle travel patterns, electric vehicle attributes, and charging station characteristics in bottom-up simulations to estimate the quantity and type of charging infrastructure necessary to support regional adoption of electric vehicles and their resulting charging load profiles. EVI-Pro has been used for detailed studies in Massachusetts [20], Columbus [21], California [22], and Maryland [23], and for a National Analysis of U.S. communities and corridors [24].

As shown in Figure 7, an iterative multi-step process has been adopted:

1. POLARIS synthesizes a population of approximately 10 million individuals living in around 3 million households within the metropolitan region of Chicago. The information associated with members of the population includes sociodemographic characteristics and vehicle ownership.
2. POLARIS provides the population data to EVI-Pro, which then uses it to estimate the availability of residential charging for each household based on residence type, tenure, household density, income, and availability of residential parking.
3. EVI-Pro provides household-level residential charging availability information back to POLARIS. Assuming an unconstrained network of public chargers and modeled at-home charging availability, POLARIS uses a SOC vehicle model to simulate all of the PEVs in the network, along with other passenger vehicles, taxis, ride-hailing vehicles, buses, and trucks. Based on the traffic conditions, speeds, and distance traveled, the electricity consumption of these PEVs are calculated second by second using a

machine-learning algorithm. As the SOC of each PEV decreases, a charging decision is made using a rule-based algorithm based on the traveler’s current state (Figure 8).

4. EVI-Pro uses the public charging demand placed on the unconstrained network to design a public network of Level 2 and direct-current fast-charging stations to meet driver demand realistically.
5. POLARIS re-simulates the region (Figure 8) using the constrained public charging network and the charging decision algorithm.

The charging decision is handled using a rule-based algorithm as follows:

- If the vehicle is already going home and a charging station exists there, the decision becomes “charge at home.”
- If the vehicle is not going home, the SOC is below 50%, and the scenario is “unconstrained charging,” the traveler decides to charge on the spot.
- Otherwise, the traveler searches for the nearest public charging station and obtains the expected travel time to that location.
 - If the travel time and the expected charging time do not interfere with their next activity, the traveler decides to charge the PEV.
 - If the new charging activity overlaps with the next activity, the decision is based on the flexibility of the next activity.
 - If the next activity has a high priority, and low start time and duration flexibility, the agent decides to postpone the charging event.
 - If the next activity is not very urgent and the start time can be postponed, the agent decides to charge the PEV.

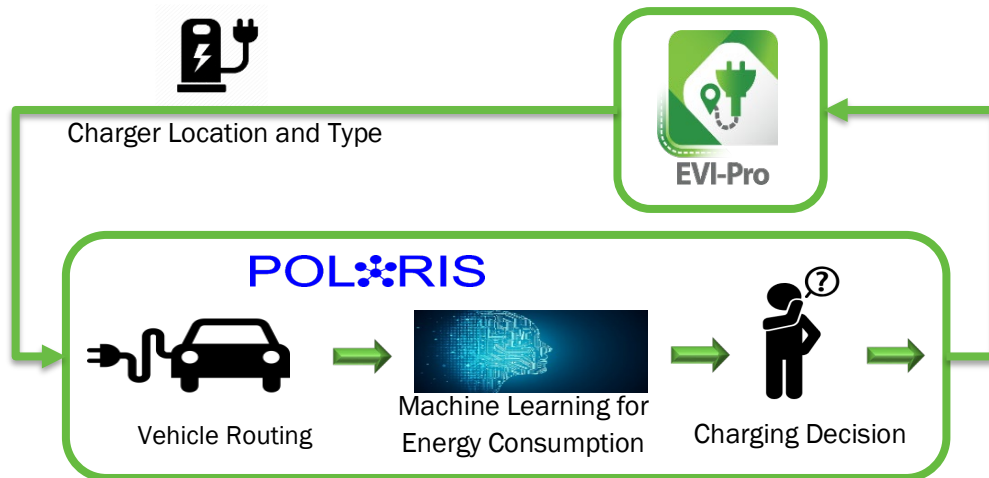


Figure 7. EVI-Pro-POLARIS Workflow for Charging Station Locations.

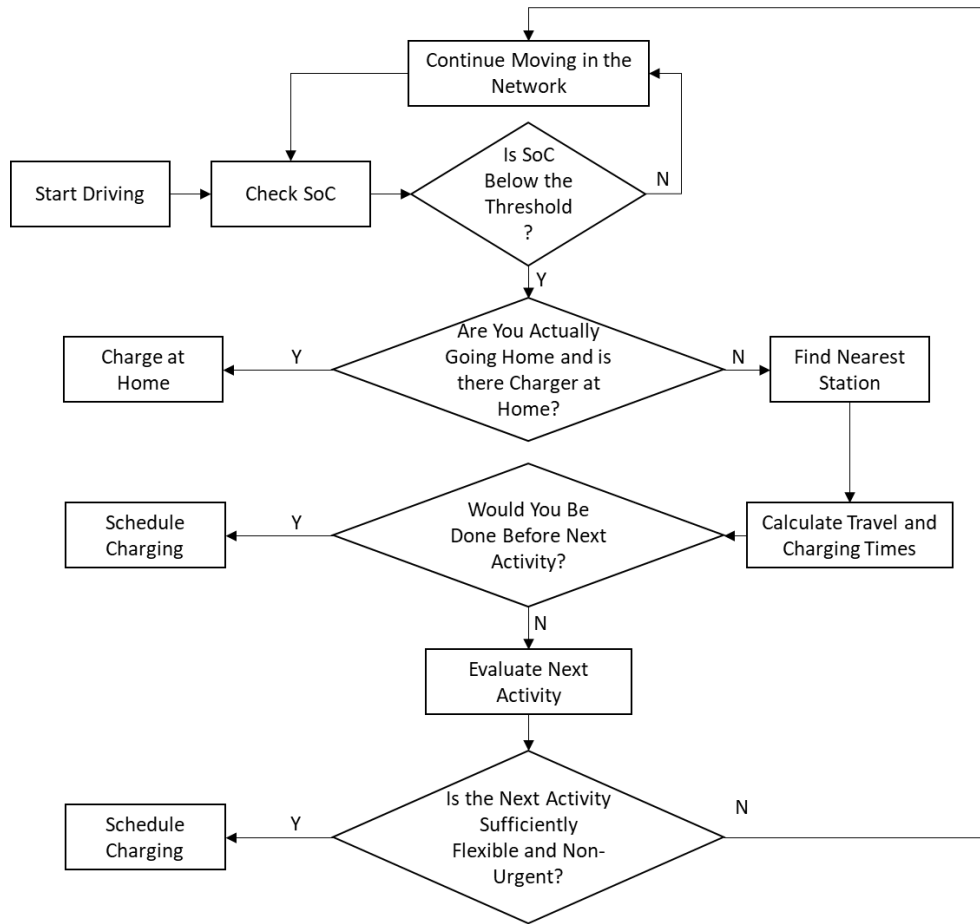


Figure 8. POLARIS Charging Decision Algorithm.

To estimate residential charging availability across Chicago, the present-day data from the US Census Public Use Microdata Sample (PUMS) database is utilized. The PUMS data breaks the Chicago area into geographies defined by the U.S. Census as Public Use Microdata Areas (PUMAs). These PUMAs are roughly equivalent in size to zip codes and tend to contain populations of at least 100,000 individuals. For each PUMA, distributions of residence type, tenure, light-duty vehicle ownership, income, and availability of residential parking are calculated.

These housing-type distributions are coupled with present-day survey data from UC Davis [25] that describes the availability of residential charging with respect to residence type. Given that residence type (and by extension residential charging availability) vary by income, households within each PUMA in the Chicago region are sequenced in descending order by household income to quantify changes in residential charging availability as a function of the size of the PEV market, as shown in Figure 9. Using household-level PEV owner locations from POLARIS, residential charging availability for each SMART workflow scenario is calculated at the PUMA level.

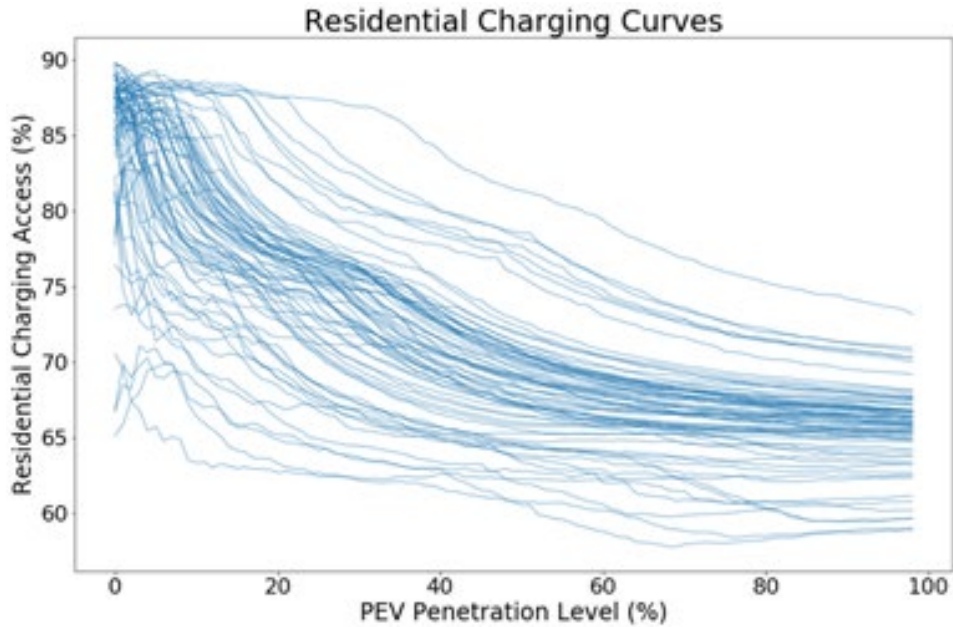


Figure 9. Chicago Estimated Residential Charging Availability by PUMA as a Function of Assumed PEV Penetration.

Using EVI-Pro’s residential charging network, POLARIS is then used to simulate public charging demand in Chicago, assuming an unconstrained network of chargers with vehicles utilizing charging stations as necessary. Simulated demand from the unconstrained network is then spatially aggregated using a hierarchical clustering algorithm in EVI-Pro to generate a set of discrete charging locations, each with a limited number of plugs and charging capacity. Figure 10 illustrates POLARIS-simulated PEV public charging demand and EVI-Pro synthesized charging station locations in and around Chicago.

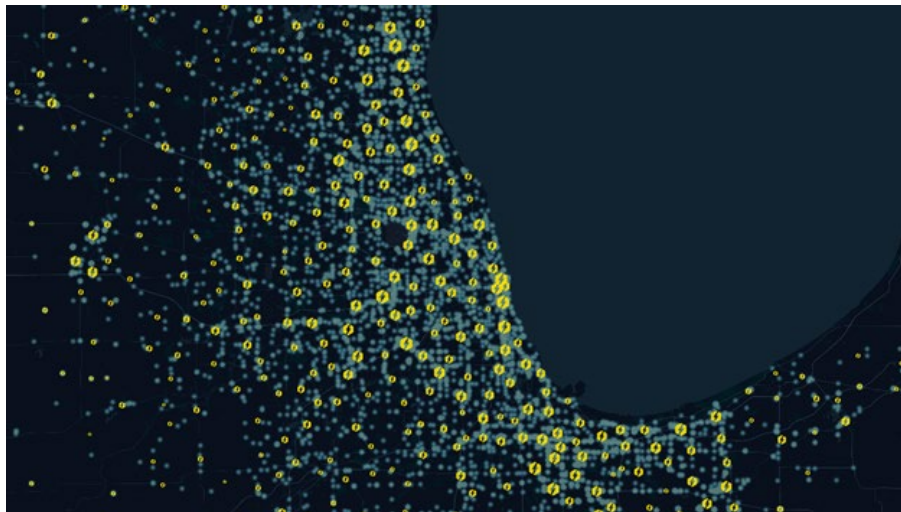


Figure 10. POLARIS-simulated PEV Public Charging Demand from Unconstrained Network (Background) and EVI-Pro Synthesized Charging Station Locations .

2.1.1.5 Freight Impact on Transportation System

The movement of goods has a significant impact on the overall transportation system. Freight transportation includes both long-haul commodities transport and “last-mile” delivery, which denotes the transport of goods from regional distribution centers to consumers. The development of the POLARIS freight model is described in detail in the Multimodal Freight Capstone report.

The development of the POLARIS e-commerce framework is shown in Figure 11 and can be described as follows:

- SMART researchers developed a behavioral model of household e-commerce delivery demand using data collected under the WholeTraveler transportation behavioral study. (Refer to the MDS Capstone report for more details on WholeTraveler.) The behavioral model simulates the number of e-commerce deliveries that each household in the region generates for a given day.
- The simulated household e-commerce demand data are input to the parcel-delivery tour generation procedure. (Refer to the Multimodal Freight Capstone report for more details on this procedure.) Using the demand information, this process creates parcel delivery truck tour itineraries for carrying e-commerce goods to households throughout the Chicago metropolitan area. Each delivery stop maps to one household that has an e-commerce delivery, as simulated in the first step.
- The delivery trips (which are assumed to use medium-duty [MD] trucks) are then input to POLARIS. The trips are modeled using DTA in a fully integrated fashion with all other trips in the region. VMT is estimated as part of the DTA.
- Finally, similar to passenger travel, the POLARIS parcel-delivery simulation results are provided to SVTrip and Autonomie for energy analysis.

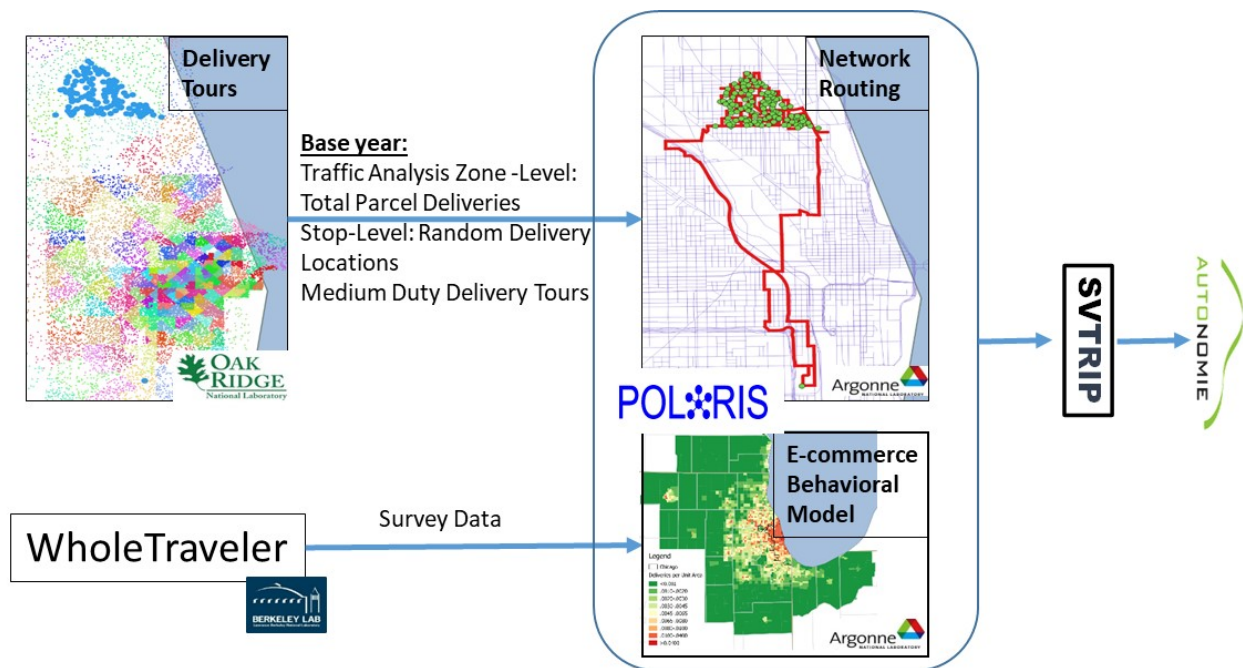


Figure 11. POLARIS Last-mile E-commerce Supply and Demand Development.

2.1.1.6 E-commerce Behavioral Model Using WholeTraveler Data

Data from the WholeTraveler survey were used to develop a two-stage, household-level model of e-commerce demand. The first stage identifies whether a household participates in e-commerce. Subject to the participation decision, the second model quantifies the ratio of delivery to retail shopping for that household. Currently, each e-commerce shopping event is assumed to replace one in-person shopping trip. Appendix B provides the estimation results of the joint binary probit model (first stage) and ordered probit model (second stage).

In general, the model produces intuitive results:

- A household is more likely to participate in e-commerce if the household has:
 - Relatively few adults,
 - Higher income, and/or
 - Lower access to transit.
- Among the households participating in e-commerce, a household tends to make more online orders if the household has:
 - Higher income,
 - Relatively few adults,
 - Relatively few vehicles, and/or
 - Less walkability.

The model was implemented in POLARIS to (i) identify the households that participate in e-commerce; and (ii) modify the shopping-trip generation rate for the households that participate in e-commerce. The model constants and thresholds are adjusted for each e-commerce scenario to calibrate the model output so that the average delivery rate matches the rate defined for the scenario. Therefore, when the calibrated model is applied, total e-commerce demand is summed over all households. Dividing this total by the number of households yields the average household e-commerce delivery rate, which matches the rate associated with the given scenario.

To quantify the impact of e-commerce on regional travel and energy consumption, the household delivery demand model is integrated with a last-mile parcel delivery supply model. More information on the supply model can be found in the Multimodal Freight Capstone Report.

2.1.1.7 Microsimulation to Mesoscopic Transportation System Model

To simulate millions of agents, mesoscopic models rely on fundamental diagrams of traffic flow that relate speed, flow, and density of travel on a road link. Because CAVs enable a reduction of the spacing between vehicles on the roadway, determining how the technology will impact the fundamental diagrams for different market penetration levels is essential to properly simulate traffic.

SMART researchers used the Aimsun traffic microsimulation tool to generate fundamental diagrams and then incorporate them into the POLARIS traffic simulator (Figure 12). This work was based on previous activities by UC's PATH Program, based on the Next Generation Simulation (NGSIM) Oversaturated Flow Model implemented on the Aimsun microsimulation platform. These models include many enhancements to the default Aimsun driver model to produce more realistic representations of normal drivers' car following and lane changing behavior, plus car-following models for cooperative and uncooperative (autonomous) adaptive cruise control systems for cars and heavy trucks that were calibrated directly from PATH experiments on full-scale cars and trucks.

Most of these efforts focused on characterizing the impact of adapted cruise control (ACC) and CACC systems on highways; areas for potential model enhancements include representations of signalized arterial driving conditions for vehicles using ACC and CACC systems, coordinated merging and lane-changing behaviors under both manual and automatic vehicle control, and V2I/I2V coordinated eco-driving strategies for signalized intersections and corridors.

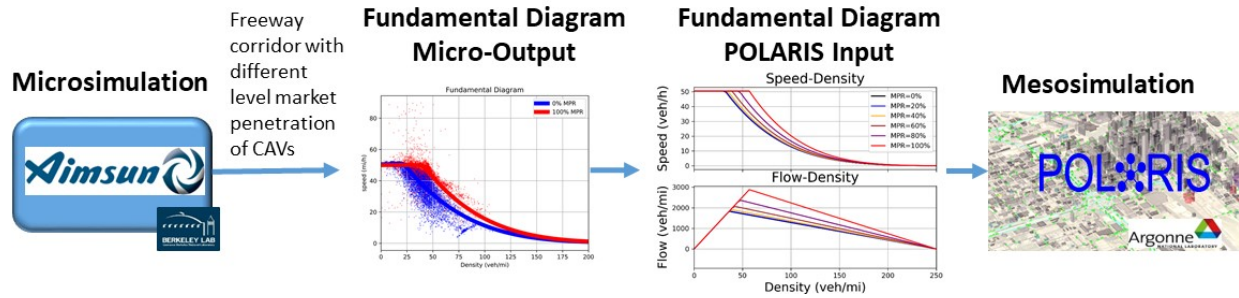


Figure 12. Aimsun-POLARIS Workflow to Represent CAVs Penetration Impact on Traffic Flow

2.1.1.8 Vehicle Energy Consumption

Autonomie is a vehicle system simulation tool developed by Argonne that is designed to estimate the impacts of new vehicle technologies on energy, performance, and cost. Autonomie has been extensively used to support DOE’s Vehicle Technologies Office (VTO) on a wide range of projects, including developing VTO research targets, and assessing the benefits of individual technologies and the entire VTO portfolio under standard and real-world operating conditions across timeframes, vehicle classes, powertrains, and components. Autonomie has been validated across a large number of vehicle classes, powertrain and component technologies (Appendix A)

As shown in Figure 13, a workflow has been developed to allow the reuse of the same vehicle models and fleets across different tools, including Aimsun, VISSIM, and POLARIS. This facilitates the comparison of results between different tools and studies.

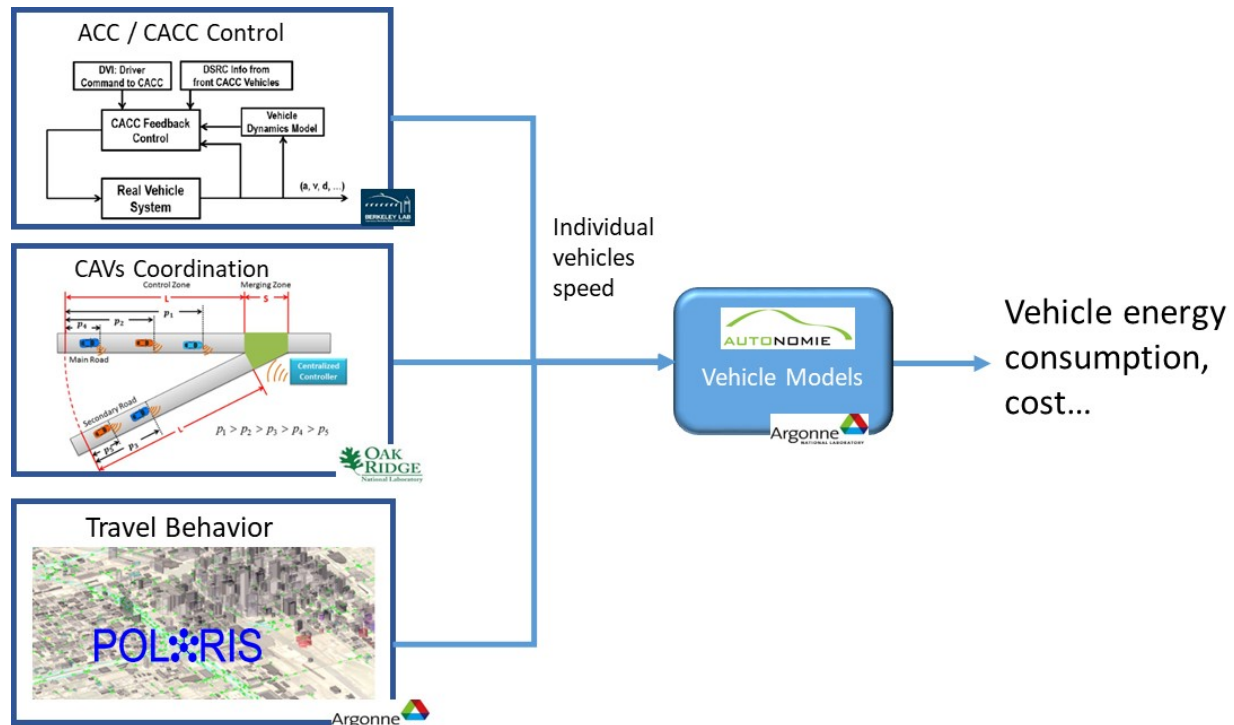


Figure 13. Common Autonomie Vehicle Models Reused across Multiple Tools.

2.1.2 Workflow Implementation Using BEAM

2.1.2.1 BEAM Transportation System Simulation

BEAM is an integrated, agent-based travel demand simulation framework. It models a set of spatially resolved resource markets, including the road network, parking and charging infrastructure, and the transit system. BEAM also models a synthetic population, with different household characteristics, home and work locations, vehicle ownership, and valuations of travel time. Travelers choose to consume these resources by taking trips on different modes based on characteristics such as travel times and crowding, and mobility providers such as ride-hailing companies dynamically operate their fleets to maximize service and productivity. By simulating travelers' choices and the performance of the transportation system in common workflow scenarios, BEAM approximates an equilibrium outcome that captures many of the complex interactions that determine regional travel patterns. BEAM incorporates numerous constraints on mobility associated with personal schedules, vehicle technology, the transport network, and operational realities of different modes. This allows SMART researchers to evaluate the feasibility of different potential mobility futures and better understand the directionality and relative magnitude of the relationship between different technology and policy developments and system-wide outcomes. In these SMART workflow simulations, some of the levers modeled are associated with clear impacts on system wide performance, while others are associated with more complex interactions that cannot be characterized as easily.

BEAM is an extension to the MATSim (Multi-Agent Transportation Simulation) model [26], where agents employ reinforcement learning across successive simulated days to maximize their personal utility through plan mutation (exploration) and selecting between previously executed plans (exploitation). The utility of these plans considers both the performance of the transportation network and individual preferences. To model the road network, BEAM uses the Java Discrete Event Queue Simulation (JDEQSim) event-based traffic simulation model [27] that captures the impact of personal car and ride-hail vehicle use on congestion and travel times. The workflow uses UrbanSim for land-use evolution, ActivitySynth for daily activity plans, EVI-Pro for public charging infrastructure siting, and Aimsun to characterize the relationship between vehicle automation and traffic flow. The future vehicle fleet powertrain mix scenarios are informed by the Automotive Deployment Options Projection (ADOPT) consumer choice model (based on relatively low versus high progress on vehicle component technology improvements over different timeframes). The outputs of BEAM in combination with the other models incorporated in the workflow are ultimately used to calculate the MEP metric, which incorporates the energy, time, and cost associated with mobility.

For the workflow implementation using BEAM:

- UrbanSim performs population synthesis, simulates how real-estate markets evolve over time, and performs workplace and residential choice for the synthetic agents.
- ActivitySynth (a submodel of UrbanSim) synthesizes home and work activities for each member of the population from UrbanSim.
- BEAM uses land use, population, and activity data to simulate travel mode choice, vehicle assignment and scheduling, traffic flow and DTA, ride-hailing market behavior, parking behavior, and electric vehicle charging.
- FASTSim simulates vehicle energy consumption based on 1-Hz drive-cycle profiles.
- RouteE establishes a correlation between vehicle energy consumption and aggregated driving conditions such as average speed of traffic, grade, and road class.
- Fast-Charging Station Plan (FCSPan) is responsible for siting fast-charging power networks for fleets of electric automated ride-hail vehicles.

The outcome of BEAM is the user equilibrium state for the transportation system along with complete fidelity over the individual choices and movements of all agents in the simulation. BEAM currently focuses on passenger travel, and does not yet simulate goods movement or truck traffic.

ActivitySynth [28], developed by UC Berkeley, generates activity plans for use in travel modeling. Currently, ActivitySynth ingests a synthetic population (e.g., SynthPop) and then performs operations for workplace location choice, automobile ownership, primary commute mode choice, time of departure (home to work and work to home), and activity plan file generation. ActivitySynth solely focuses on workplace commuting trips, and does not consider any discretionary trips (trips for shopping, leisure, etc.), intra-household coordinated activity planning, or school location choice.

For the BEAM implementation of the workflow applied to San Francisco, vehicle energy consumption modeling leverages the connected tool chain shown in Figure 14 between the ADOPT consumer preference model, the integrated FASTSim vehicle powertrain model, and custom-trained RouteE models to estimate road-link-level energy consumption for each vehicle in the BEAM simulation. This approach does not require an exact second-by-second driving profile for each vehicle/link journey, because it relies on average energy consumption for specific average vehicle speed bins. For the first step of the process, it aligns the income bins from ADOPT for estimating future vehicle powertrain adoption under each scenario with income bins in BEAM for making household vehicle assignments. These characteristic vehicles created by ADOPT vary in terms of physical characteristics such as mass, drag coefficient, and powertrain efficiency. In particular, battery capacities range from 28 to 70 kWh for battery electric vehicles (BEVs), associated with ranges of between approximately 100 and 250 miles, and they vary with income bin and vehicle technology scenario. Ride-hail BEV ranges are not assumed to differ from BEV ranges in the personal vehicle fleet. Across the income bins, representative FASTSim models are created that correspond to each powertrain type from the ADOPT fleet estimates. Based on this set of (non-automated) powertrain models for each scenario simulation, parallel sets of partially automated and fully automated powertrain models are created (resulting in higher vehicle accessory load requirements in the partially automated relative to the non-automated vehicle, and higher still for the fully automated vehicle).

The powertrain and automation makeup of the personal and ride-hail fleets were determined by a three-dimensional iterative proportional fitting procedure, which allows scenarios to assume different distributions of automation level by vehicle use (personal or ride-hail) while also ensuring that overall fleet-wide distribution of powertrain type and automation level match scenario definitions. In practice, this meant that in scenarios where ride-hailing and personal vehicle fleets had different levels of automation they also had different powertrain makeups; that fully automated vehicles being more likely to be fully electric means that scenarios with a highly automated ride-hailing fleet also, by consequence of the scenario assumptions, had a particularly un-electrified personal vehicle fleet. In addition, privately owned fully automated vehicles are assumed to only belong to households in the top half of the income distribution. This household vehicle shedding/retirement is simulated by matching each household vehicle to a commute by a household member. Excess vehicles (in households with more vehicles than workers) are retired first, and then vehicles associated with shorter commutes are preferentially retired until overall fleet size is met. Finally, the ride-hailing fleet is sized according to joint objectives of maximizing the amount of service provided and maximizing the utilization of existing ride-hailing vehicles. This sizing is done by tuning the effective number of personal vehicles that each ride-hailing vehicle replaces, changing the number of unique vehicles that enter the simulation. The combination of these factors means that different scenarios, where vehicles with different powertrain types and automation levels are allocated differently across different users, may have the same aggregate fleet of vehicles but that different types of vehicles may be used in substantially different amounts.

The next step of the process creates custom road-link-level RouteE models that correspond to each FASTSim vehicle model. BEAM accesses the trained RouteE models for this application in the form of multidimensional lookup tables [29]. These tables associate an energy consumption rate (energy/distance) to each vehicle based on road and traffic conditions encountered through the simulation (e.g., roadway type, number of lanes, typical

free-flow speed, current average traffic speed, and road grade). To train each RouteE vehicle model, the corresponding FASTSim model is simulated over approximately a million miles of actual on-road driving data from the Transportation Secure Data Center (TSDC)—spanning the range of road segment driving conditions used for the RouteE energy consumption correlations. Adjustments to the partially and fully automated RouteE vehicle models are informed by microsimulation results for traffic streams with varying levels of (cooperative) AV penetrations. This is accomplished by running FASTSim models over the second-by-second driving profiles from the microsimulations and comparing the modeled fuel consumption rate in consistent traffic speed conditions under varying levels of AV penetration. After creating RouteE models across the powertrain penetration scenarios for non-automated as well as a partially and fully automated vehicle cases, these vehicle models are assigned to agents in the BEAM simulation according to the mix of powertrains as well as non-automated, partially automated, and fully automated vehicles assumed for each given scenario.

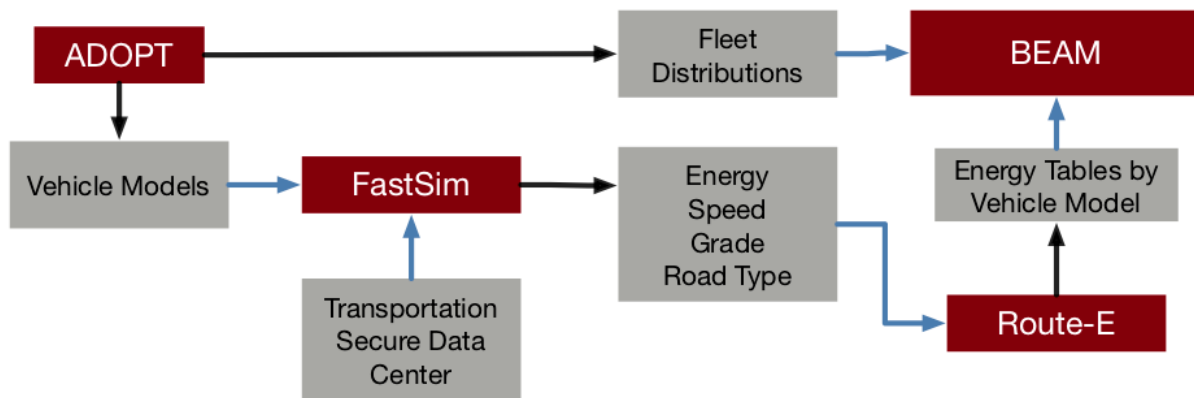


Figure 14. Data Flow between ADOPT, FASTSim, Route-E, and BEAM.

BEAM simulates the operation of ride-hailing fleets, finding an equilibrium between ride-hailing supply and demand that is sensitive to variations in traveler value of time, ride-hail fleet automation and charging requirements, road network speeds, and the spatial distribution of travel demand. Human ride-hailing vehicle drivers are assumed to follow shifts that average approximately 4 hours in duration and coincide with the temporal distribution of travel demand, while automated ride-hailing vehicles are assumed to be available all day except when they are charging. Ride-hailing ride pricing is modeled as having a fixed component, a distance component, and a time component, with parameters estimated from ride-hailing operations data published by the City of Chicago. Automated (driverless) ride-hailing vehicles are assumed to be priced without a time component, lowering prices for travelers because the labor costs for operators are lower. Idle ride-hailing vehicles are matched with trip requests using an adaptation of the Alonso-Mora pooling algorithm [28], which prioritizes maximizing vehicle occupancy while constraining the added waiting and travel time associated with forming pooled itineraries. Idle ride-hail vehicles are modeled as probabilistically deciding to relocate to areas with higher demand; the likelihood of rebalancing is calibrated to bring the proportion of empty ride-hailing VMT in the baseline scenario in line with currently observed values. The result of this algorithm is that empty ride-hail vehicles tend to move from lower-demand areas to higher-demand areas at a rate proportional to overall demand—so repositioning and its associated empty VMT are concentrated in the morning and evening peak hours.

BEAM also simulates the impacts of different levels of vehicle automation between the different vehicle technologies cases. In the ride-hailing fleet, fully automated vehicles are assumed to operate all day rather than in shifts. This increases the effective size of the ride-hailing fleet but sometimes leads to oversupply in off-peak periods. Privately owned fully automated vehicles are assumed to be shared among family members for commuting activities, with each CAV's schedule optimized to maximize its utilization throughout the day.

Vehicle automation also impacts traffic flow; partially and fully automated vehicles are simulated as participating in CACC, increasing road capacity as the portion of CACC-equipped vehicles increases.

As part of BEAM development, various input parameters were calibrated in order to reproduce current travel conditions. These calibration parameters include components of the mode choice model, the relative size of the ride-hailing fleet and its propensity for rebalancing empty vehicles, traffic-flow parameters of the road network, and the aggregate supply of parking spaces. These parameters were adjusted to align simulation outputs with observed distributions of commute mode choice, ride-hailing demand and deadhead ratios, and average commute travel times. In particular, calibrating to match the distribution of commute travel times yielded average network speeds that were higher than observed values. The calibration is explored in more detail in Appendix A.

2.1.2.2 Land Use Impact on the Transportation System

As shown in Figure 15, BEAM couples with the land use model UrbanSim to generate activity patterns for travelers and simulate how changes in transportation network performance interact with changes in land development patterns. Starting with current demographic data, ActivitySynth produces a set of work activity locations and start and end times for the synthetic population of the San Francisco Bay area. This population and its commuting plans are used as inputs into BEAM, which simulates travel behavior and transport network performance until the system converges. As part of its mesoscopic simulation, BEAM produces a matrix of measurements of the generalized time and cost associated with trips between different origins and destinations on the network. UrbanSim uses this matrix to estimate the accessibility and desirability of different locations for housing and firm development and location, allowing individual agents to bid prices up or down until market equilibrium is approached. As part of this process, some households move or find new work locations, generating a new set of plans for the next BEAM run. In this set of workflow runs, this full handoff is completed twice, BEAM runs three times at 15-year intervals, and UrbanSim runs twice.

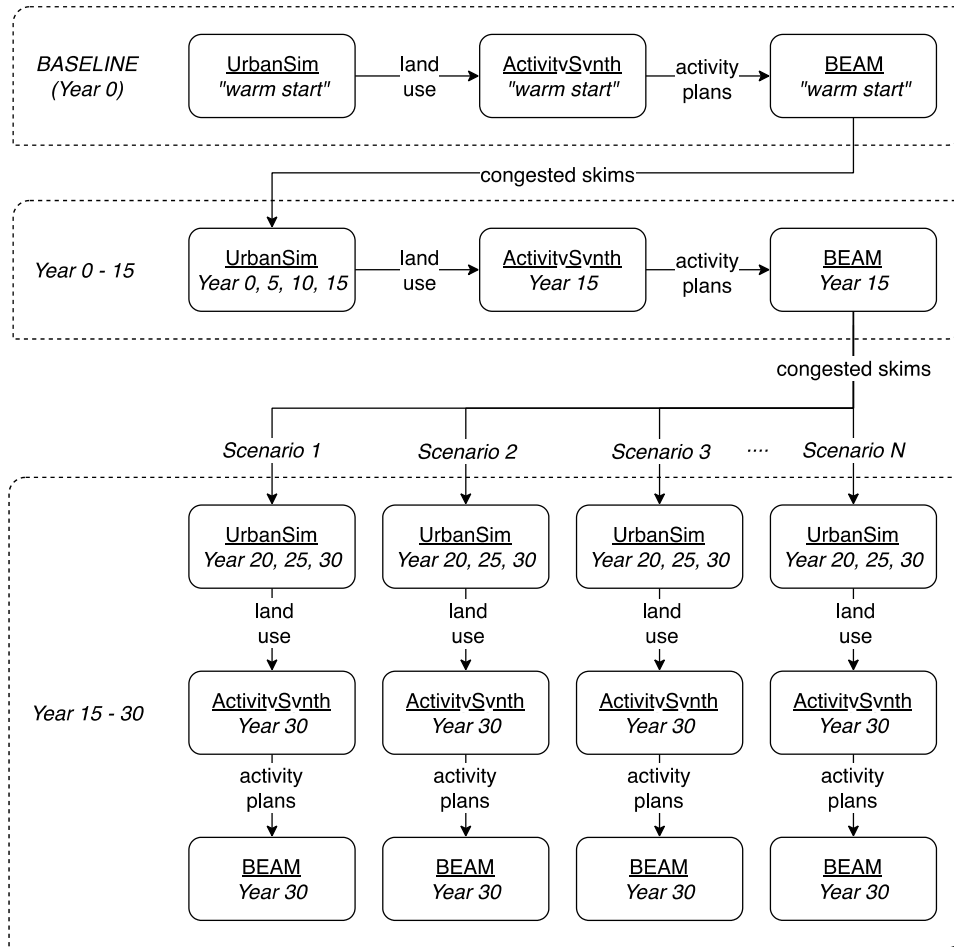


Figure 15. Data Flow between UrbanSim, ActivitySynth, and BEAM.

2.1.2.3 Infrastructure Impact on the Transportation System

Residential and public charging network designs for BEAM workflow simulations are provided using the National Renewable Energy Laboratory’s (NREL’s) EVI-Pro. EVI-Pro was developed in collaboration with the California Energy Commission and with additional support from the VTO. EVI-Pro uses detailed data on personal vehicle travel patterns, electric vehicle attributes, and charging station characteristics in bottom-up simulations to estimate the quantity and type of charging infrastructure necessary to support regional adoption of electric vehicles, and their resulting charging load profiles.

As shown in Figure 16, the SMART Mobility workflow has adopted an iterative multistep process. For each simulation scenario, BEAM determines which households across San Francisco will be simulated as owning a BEV based on vehicle adoption distributions. These distributions are conditioned on the household income of each home. For each household that owns a BEV, BEAM uses housing stock characteristics from UrbanSim (i.e., tenure, residency type) in order to make on-the-fly estimates of residential charging availability based on EVI-Pro residential charging assumptions. Household-level residential charging availability estimates are used within BEAM to simulate utilization of an unconstrained public charging network. EVI-Pro uses public charging demand placed on the unconstrained network to design a public network of Level 2 and direct current fast-charging stations to meet driver demand realistically. A final round of BEAM simulations is conducted using the constrained public charging network supplied by EVI-Pro. A similar approach is taken by FCSPlan—a tool developed under the SMART Mobility Alternative Fueling Infrastructure pillar—to design a dedicated network of fast-charging stations for the automated ride-hail fleet in BEAM [31].

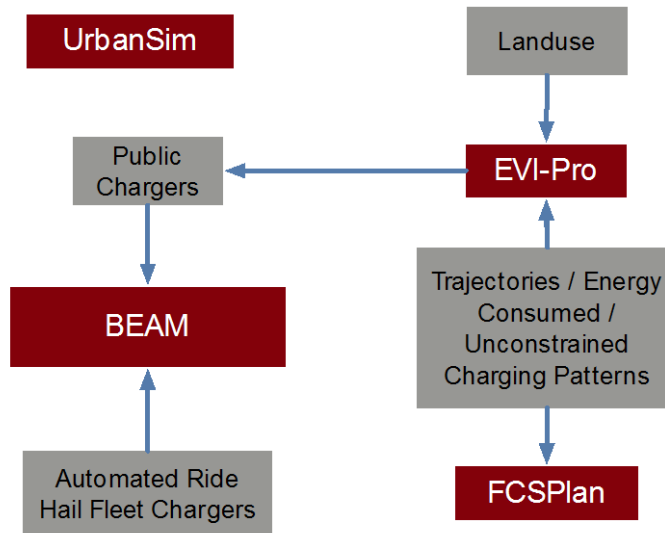


Figure 16. Modeling Workflow between BEAM, EVI-Pro, and FCSPan (Fast-Charging Station Plan) to Site Charging Infrastructure for BEAM Simulations.

In order to estimate residential charging availability across San Francisco, projected housing stock characteristics from UrbanSim are utilized, specifically residence type and tenure. UrbanSim housing type information is used to assign residential chargers from a weighted distribution informed by present-day survey data from UC Davis describing availability of residential charging with respect to residence type. Assumed residential charging availability probabilities are shown in Table 1.

Table 1. Assumed Probability of Access to Residential Charging based on Residence Type and Tenure.

Home Type	Property Owner	Property Renter
Single family home	90%	80%
Multi-family unit	50%	40%

Using estimated residential charging availability from EVI-Pro, BEAM simulations are conducted for all SMART workflow scenarios assuming access to an unconstrained network of public charging stations. Simulated public charging demands placed on the unconstrained network are provided back to EVI-Pro in order to design a public charging network that closely matches the needs of the PEVs in each scenario. EVI-Pro locates public charging stations by implementing hierarchical clustering of spatial charging demand as simulated by BEAM. Figure 17 provides a map of BEAM-simulated PEV public charging demand and EVI-Pro synthesized charging station locations from the San Francisco Bay area.



Figure 17. BEAM-simulated PEV Public Charging Demand from Unconstrained Network (Background) and EVI-Pro Synthesized Charging Station Locations.

2.1.2.4 Microsimulation to Mesoscopic Transportation System Model

In Hao et al. (2018), the microsimulation framework Aimsun was used to explore the impact of CACC on the maximum flow capacity of highways and major arterial roads. The results of this study were integrated into BEAM by adapting the flow capacity field in each highway and large arterial network link based on the instantaneous fraction of vehicles on the link that have CACC (i.e., level 3 automation or above). Figure 18 shows the data available in Hao et al. (2018) [30] alongside the road link capacities in BEAM, as recorded during events logging.

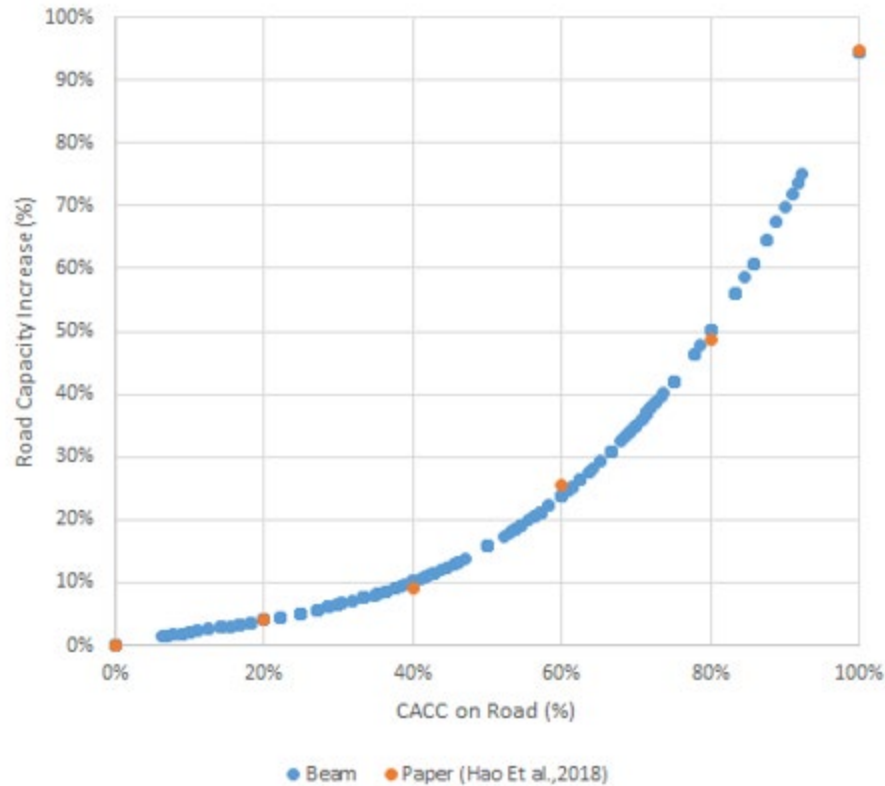


Figure 18. CACC Impact on Highway and Arterial Road Capacity in BEAM (based on Work by Hao et al. 2018).

2.2 High-Level Workflow Implementation Comparisons

Although most trends from the San Francisco results are similar to the Chicago implementation, different modeling assumptions and model components were used:

- For passenger movement, only travel commuting activities (i.e., home to work and work to home) were considered in the San Francisco implementation, whereas in the Chicago implementation agents also took discretionary (e.g., shopping and recreational) trips.
- Higher network speeds in BEAM across the entire metropolitan area are potentially due to modeling commute-only trips, lack of residential roads in the network, and the fact that network parameters were calibrated based on travel times. This could result in a mismatch between the trip lengths in the commute data used to calibrate UrbanSim's workplace location choice model compared to real-world trip lengths. As a result, the simulated average road network speed in the San Francisco Baseline scenario was found to be 43 miles per hour, substantially faster than real-world conditions.
- Unlike the Chicago implementation, the San Francisco implementation did not consider goods movement. The additional load on the transportation system due to freight/goods movement yields additional VMT and associated congestion and energy use in the Chicago implementation.
- The San Francisco implementation simulated repositioning movements and charging activities of ride-hailing vehicles, while the Chicago implementation did not. These repositioning and charging movements decrease the average occupancy (productive miles travelled [PMT]/VMT) and increase the added congestion associated with heavy reliance on ride-hailing in the San Francisco implementation.

- The two workflow implementations used different methods of allocating vehicle types to the personal and ride-hailing fleets. This led to differences in the relative utilization of different powertrain types.
- The BEVs simulated in the San Francisco implementation had lower all-electric range (100–250 miles) than in the Chicago implementation. This shorter range means that all electric personal and ride-hailing vehicles needed to spend more time driving to and using charging stations.

2.3 Mobility Energy Productivity (MEP) Metric

New technologies and services can influence many transportation-related metrics across a metropolitan area, including energy, productivity, mobility, and affordability. SMART Mobility researchers at NREL developed the MEP metric to quantify the mobility potential of a geographic area with respect to time, cost, and energy. The metric measures accessibility and appropriately weights it with travel time, cost, and energy intensity of modes that provide access to opportunities in any given location. The metric can be computed from readily available data sources, or it can be derived from outputs of travel demand models such as those used in the SMART Mobility modeling workflow. Ultimately, the MEP metric can be used to reflect the overall impacts of new mobility technologies (e.g., AVs and electrified powertrain vehicles [xEVs]), business models (e.g., car sharing and bike sharing), and land-use practices (e.g., transit-oriented development) on sustainable urban mobility. This section describes the integration of the MEP metric with the SMART workflow process. The MEP value for any given location represents the mobility potential of that location, so a high MEP score indicates higher access to opportunities, in a more energy-, cost-, and time-efficient manner.

The MEP metric is based upon accessibility measures that extend existing accessibility theory and methodologies, assessing the number of jobs, goods, and service opportunities available within prescribed travel times from a location. This approach is fundamentally a geospatial analysis, providing both a visual map for comparative analysis and a numeric score to baseline performance metrics. Data to support travel-time calculations and land use (i.e., available goods, services, and employment opportunities) are readily available using third-party travel data or outputs from regional travel-demand models along with land-use data from cities, MPOs, or commercial entities. Isochrones (i.e., lines on a map of a region showing what can be accessed within a given timeframe using a selected mode of travel) are constructed for each mode. Figure 19. is an example of a 30-minute isochrone showing reachable opportunities (color coded by land use) by bicycle from a location in Columbus, Ohio.

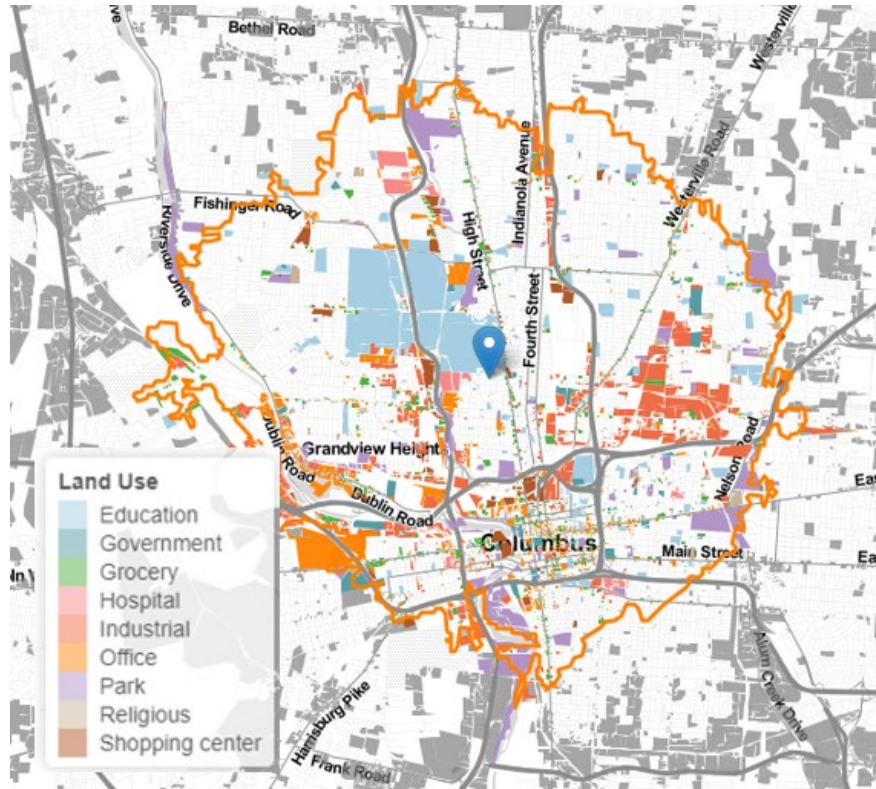


Figure 19. Thirty-minute isochrone for biking

The MEP formulation creates isochrones for each location (grid cell) and each mode to reflect how far an individual can travel within 10, 20, 30, and 40 minutes from a location by walking, biking, driving, or using public transit. The calculation then counts the job opportunities, grocery stores, restaurants, recreation facilities, medical service providers, and other destinations located within an isochrone. These opportunity counts are appropriately weighted based on travel time, affordability, and energy use of each mode. Each opportunity count (job, grocery stores, medical services, etc.) is also appropriately weighted based on the frequency with which people make those sorts of trips, as revealed by travel surveys. Land use is indexed to purpose (e.g., education, shopping-retail, health) as well as to job-opportunity potential (number of employees or jobs). Each of these steps is further elaborated in the MEP project description within the Urban Science capstone report, and in a journal article that describes the MEP [3].

The MEP code (written in statistical programming language R) was customized to use data provided by various model components within each workflow implementation. Table 2 shows the data inputs to MEP from various components of the workflow.

Table 2. MEP Inputs Used from Various Models

Model	Data Generated
BEAM/POLARIS	Study area boundary
	Travel times by mode
	Ride-hailing wait times
	Activity engagement frequencies
	Operational cost (per passenger mile) by mode
UrbanSim	Land use (establishments of different activity types)
	Population (number of people per block)
	Employment (no. of jobs by activity type)
Autonomie/Route E	Energy consumption (per passenger mile) by mode
Default	Coefficients for time/cost/energy parameters

Using the model outputs, the MEP calculation procedure is executed as follows:

1. Import input data.
2. Generate isochrones.
3. Count opportunities that can be accessed.
4. Calculate MEP.

Figure 20 illustrates the workflow of the MEP calculation process.

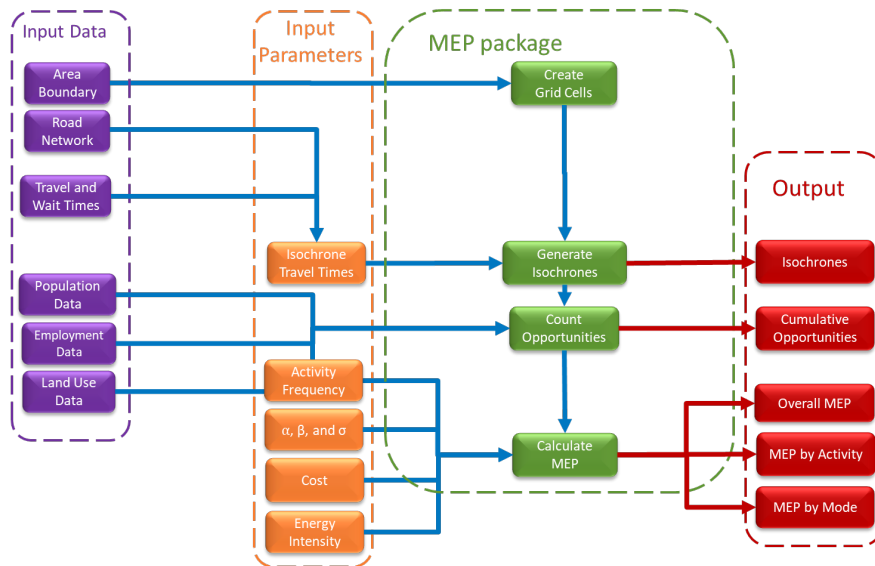
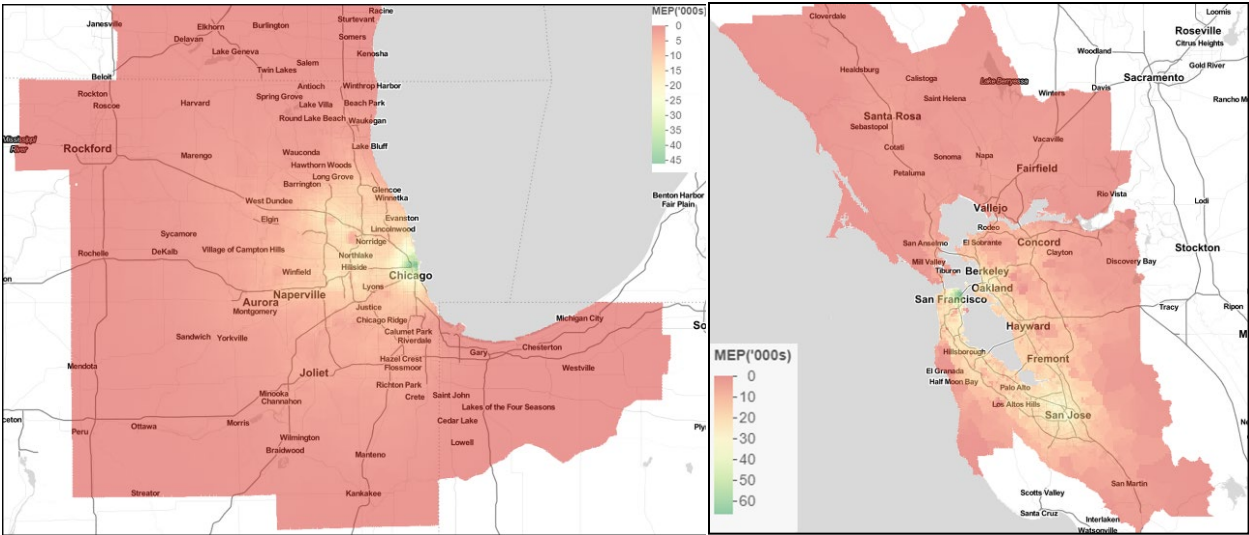


Figure 20. MEP Calculation Workflow.

Figure 21 illustrates the spatially resolved MEP calculations for Chicago and San Francisco. The maps are color-coded using a gradient scale where dark red depicts a score of zero (indicating low MEP), and dark green indicates maximum MEP in the region. Note that the MEP scores for Chicago and San Francisco are different in magnitude. The intent of the MEP metric is to provide a means to compare the changes in MEP results for a region with respect to any scenario changes within that region. The MEP results should not be compared between the two regions; differences in modeling approaches, geography, demographics, and other regional characteristics may result in MEP calculations of different magnitudes.



(a) Chicago (POLARIS)

(b) San Francisco (BEAM)

Figure 21. MEP Baseline Maps Incorporating POLARIS and BEAM Data

For any given scenario, the MEP uses information associated with land use changes, network travel times, energy consumption, and cost of travel segmented by various modes as critical inputs. The calculation incorporates this information to compute a MEP metric for each square kilometer “pixel” in a given city or region. Note that: (1) MEP scores are computed for a representative hour in the day (morning peak hour) for both workflows; and (2) MEP scores reported in this report were computed based on observed, but not perceived, travel times. When individuals perceive travel to be less onerous in certain modes compared to others (e.g., in fully automated vehicles), their travel productivity is expected to increase. Because this perceived increase in productivity cannot be applied uniformly to all individuals within the mobility system, the MEP calculation currently does not take this effect into account. The pixel level MEP scores can be aggregated to the city level by weighting each pixel by population to calculate an overall MEP result. More detail on the MEP calculation procedure appears in the Urban Science capstone report.

3 Common Scenarios and Assumptions

3.1 Scenarios

Several major trends, such as vehicle connectivity, automation, sharing, and electrification are poised to have significant impacts on the transportation system in the future. How these trends evolve (e.g., which automated features are incorporated into vehicles, what the market penetration is for new technologies or mobility services) remains uncertain. In addition, dynamic system interactions among these trends are complex and may impact the transportation system in ways not fully understood. For example, full powertrain electrification of shared mobility service fleets would lead to different vehicle use patterns and charging requirements, and potentially radical changes in land use. Although the overall objective of the SMART Mobility Consortium is to quantify the impact of each individual technology and their combination at the system level, a limited number of scenarios were initially selected to highlight some key parameters that influence traffic flow, travel behavior, and transportation system control.

To quantify the impact of population growth and improvement in vehicle technologies without any changes in vehicle connectivity, automation and sharing, a set of seven baseline scenarios were developed as shown in Figure 23. They consider the following:

- Three options for land use and freight (current, short-term, and long-term).
- Five options for powertrain and vehicle technologies:
 - Current technology;
 - Business-as-usual, short-term improvements based on historical trends;
 - More aggressive short-term improvements based on VTO technical targets;
 - Business-as-usual, long-term improvements based on historical trends; and
 - More aggressive long-term improvements based on VTO technical targets.

As shown in Figure 22, three main future scenarios were selected to quantify the impact of connectivity, automation and sharing:

- Scenario A: A near-term future with moderate increase in vehicle ride-hailing fleets along with increased penetration of partially automated vehicle technologies (e.g., advanced driver assistance systems).
- Scenario B: A longer term future where fully automated driverless vehicles are owned by shared fleet operators. These vehicles are widely shared by large segments of the population. E-commerce is common among households.
- Scenario C: Like Scenario B, Scenario C represents a longer term future with fully automated driverless vehicles. However, in Scenario C those vehicles are owned by individuals and shared within the household (i.e., privately owned AVs). It is thus a low ride-hailing case alternative to Scenario B. E-commerce is common among households.

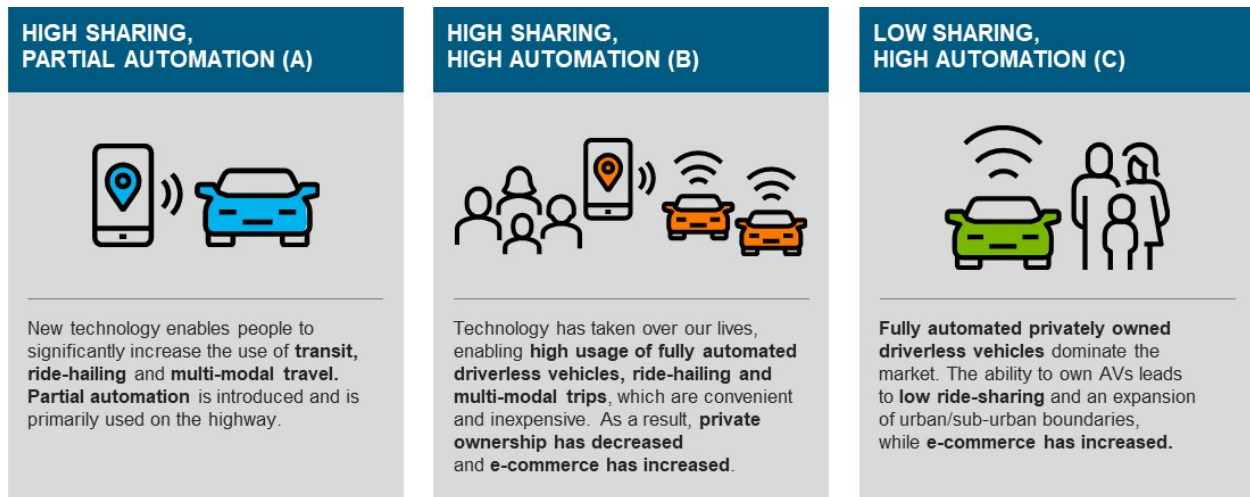


Figure 22. High-Level Scenario Descriptions.

The current workflow implementation was designed to explore a set of scenarios representing possible future vehicle and mobility technologies to highlight their impacts on the movement of passengers and goods. In addition to mobility technologies including partial and full automation as well as ride-hailing, each scenario includes two vehicle technology developments:

- A low-technology case (business as usual) representing historical year-over-year technology evolution driven by the automotive industry.
- A high-technology case (aggressive evolution that would require breakthroughs) representing achievement of research targets from the VTO along with additional vehicle improvements (see Appendix C).

Advances in powertrains (e.g., HEV, PHEV, and BEV), components (e.g., engine, transmission, electric machine, and energy storage system), light-weighting, aerodynamics, and tire rolling resistance are all considered in the study. Figure 22 summarizes the 13 scenarios considered.

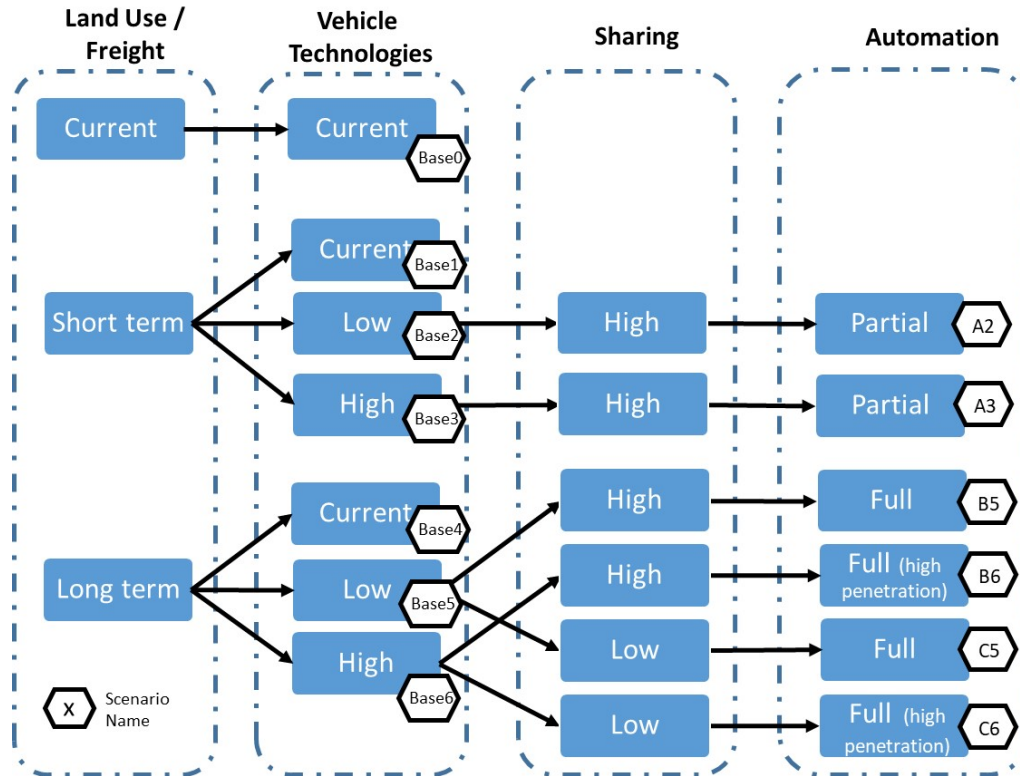


Figure 23. SMART Mobility Scenarios.

Section 3.2 describes the scenarios considered along with the main assumptions. All the parameters have been applied to both workflow implementations except the freight parameters, which have only been implemented in the POLARIS workflow.

3.2 Main Assumptions

3.2.1 Individual Parameters

The SMART Mobility Workflow Taskforce selected the following common parameters for each scenario:

- Land use: Population and establishment distribution across the region at a given time.
- Vehicle retirement rate: Percentage (with respect to the corresponding baseline scenario) of household vehicles that are relinquished in a given scenario compared to the baseline.
- Vehicle market penetration: Percentages for each combination of vehicle class, powertrain, and automation level.
- Level of automation (partial and full): Percentage of vehicles that are partially (i.e., requires a driver) and fully (i.e., capable of driverless operation) automated.
- Shared use penalty: Indicates higher preference for ride-pooling service (compared to riding alone for ride-hailing modes).
- Value of travel time (VOTT) multiplier: Set as a fraction between 0 and 1. A fraction below 1 indicates a lower sensitivity to the travel time compared to the baseline scenario (where the VOTT multiplier is set to 1) and therefore an increased preference for a given trip or mode. This factor is applied to automobile modes (i.e., single-occupancy vehicles [SOVs] and high-occupancy vehicles [HOVs]). For example, if a

traveler's commuting VOTT is \$30/hour under the baseline scenario for the automobile mode, a future scenario with a VOTT multiplier of 0.5 would change the VOTT to \$15/hour.

- Long-haul commodity flows: Compound annual growth rate (CAGR) for MD and heavy-duty (HD) truck trips relative to the base year.
- Propensity of non-car modes: VOTT adjustment factor for non-car modes (e.g., walking, bicycle, and transit). Similar to the VOTT multiplier for auto modes, this parameter is set as a fraction less than 1. For example, if a traveler's commuting VOTT is \$20/hour under the baseline scenario for the bus mode, a future scenario with a VOTT multiplier of 0.75 would change the VOTT to \$15/hour.
- E-commerce delivery rates: Average number of package deliveries per person, or per household, per day.

The key parameters describing the different baselines and advanced mobility scenarios are shown in Tables 3 and 4, respectively.

It is important to note that the values of different parameters must be internally consistent within each scenario. For example, a scenario with high levels of automated ride-hailing would include a large number of advanced vehicle technologies with low VOTT and high vehicle retirement rates.

For freight, the commodity flow CAGRs are applied to all trucks that carry commodities. Commodity-carrying trucks include all intercity HD trucks, two-thirds of intraregional HD trucks, and one-third of MD trucks. CAGRs were obtained from IHS Global, Inc. [37]. A rate of 1.0% CAGR is used to represent moderate economic growth.

The baseline e-commerce delivery rate is 0.08 deliveries per person per day, based on data from the 2017 National Household Travel Survey [36]. The moderate rate is 0.20, which is the current rate in Seoul, South Korea [34]. Finally, as a "corner case" a high rate of 0.35 is assumed. This rate equates to five deliveries per week for a two-person household. To model the joint traffic and energy impacts of delivery truck and passenger shopping trips, the modeling workflow assumed that each delivery replaces exactly one passenger shopping trip. This assumption is based on results from the WholeTraveler survey, in which respondents reported that one delivery substitutes for about one shopping trip. Additional opportunities exist to refine this estimate to account also for merchandise returns or other factors.

In addition to the parameters described in Table 4, changes in VOTT were also considered. The specifications on VOTT change (Appendix D) impact the baseline VOTT, which vary depending on mode, travel component (e.g., walking, waiting, and sitting in a vehicle all have different time valuations), personal characteristics (e.g., income), and other factors. Travelers with a lower VOTT for a particular travel mode tend to spend more time travelling because the VOTT is a ratio of time disutility (u/hr) to cost disutility (u/\$). As a result, reduced VOTT is equivalent to lowering the time disutility; therefore travelers are willing to travel longer at the same cost.

The VOTT high-impact and low-impact ranges (Appendix D) apply to partially and fully automated vehicles. The difference in VOTT between the two related to the uncertainty of VOTT changes under AV and improvement of the technology over time. The increased utility of a fully automated vehicle is evident in the table. For example, a partially automated vehicle has limited increase in utility in most driving situations because the driver must remain alert and ready to take over the driving task, limiting the benefits of partial automation; therefore, the reduction in VOTT is lower for a partially automated vehicle than for a full AV. Additional factors considered include the time sensitivity of travel (i.e., if the traveler is under scheduling pressure with no time flexibility), the congestion level of the roads the vehicle is traveling on, and the functional class of the road (i.e., highway versus arterial).

Table 3. Baseline Scenarios Main Parameters.

	Parameter	Baseline	Baseline Short-Term			Baseline-LongTerm			
			Base	Low	High	Base	Low	High	
Scenario Names		Base0	Base1	Base2	Base3	Base4	Base5	Base6	
General	Land Use	Current	Short term baseline			Long term baseline			
	Component Technology	Current	Current	Short term BAU	Short term VTO Targets	Current	Long term BAU	Long term VTO Targets	
	Additional accessory load		400	400	400	400	400	400	
	Partial Automation (W)	1900	1900	1900	1900	1900	1900	1900	
	Full Automation (W)	0	0	0	0	0	0	0	
Passenger	Vehicle retirement rate (%)	0	0	0	0	0	0	0	
	VOTT Factor	1	1	1	1	1	1	1	
	Shared Use	Partial Automation	1.3	1.3	1.3	1.3	1.3	1.3	1.3
		Full Automation							
	Market Penetration	Partial Automation (%)	0	0	0	0	0	0	0
		Full Automation (%)	0	0	0	0	0	0	0
Freight	Long Haul Commodity Flow - CAGR (%)	1	1	1	1	1	1	1	
	E-Commerce Delivery Rates	Per Person/day	0.08	0.08	0.08	0.08	0.08	0.08	0.08
		Per Household/day	0.16	0.16	0.16	0.16	0.16	0.16	0.16
	Propensity of non car mode	1	1	1	1	1	1	1	
	Market Penetration	Partial Automation (%)	0	0	0	0	0	0	0
Full Automation (%)		0	0	0	0	0	0	0	

Table 4. Advanced Mobility Scenario Main Parameters.

SMART Mobility Modeling Workflow Development, Implementation, and Results

	Parameter	Baseline	A		B		C		
			Low	High	Low	High	Low	High	
Scenario Names		Base0	A2	A3	B5	B6	C5	C6	
General	Land Use	Current	Short term		Long Term		Long Term		
	Component Technology	Current	Short term BAU	Short term VTO Targets	Long term BAU	Long term VTO Targets	Long term BAU	Long term VTO Targets	
	Additional accessory load	Partial Automation (W)	400	400		400		400	
		Full Automation (W)	1900	1900		1900		1900	
Passenger	Vehicle retirement rate (%)	0	45	45	68	75	15	20	
	VOTT Factor	1	Low impact		High impact		High impact		
	Shared Use	Partial Automation	1.3	1		1		1.3	
		Full Automation						1.6	
	Market Penetration	Partial Automation (%)	0	10	11	5	8	5	8
		Full Automation (%)	0	0	0	17.5	51.5	17.5	51.5
Freight	Long Haul Commodity Flow - CAGR (%)	1	1		1		1		
	E-Commerce Delivery Rates	Per Person/day	0.08		0.35		0.35		
		Per Household/day	0.16		0.4		0.7		
	Propensity of non car mode	1	0.5		1		1		
	Market Penetration	Partial Automation (%)	0	5	10	20	40	20	40
Full Automation (%)		0	0	0	2	15	2	15	

3.2.2 Vehicle Assumptions and Fleet Distribution

To properly quantify the impact of new mobility technologies on energy consumption, it is critical to consider different fleet scenarios. Each fleet was defined based on the following criteria:

- Timeframe:
 - Near term (~10 years).
 - Long term (20+years).
- Vehicle classes:
 - Light-duty vehicles: compact car, midsize car, full-size car, compact sports utility vehicle (SUV), midsize SUV, full-size SUV, pickup truck.
 - MD and HD vehicles: Class 3 pickup and delivery, Class 4, Class 6, transit bus, line haul.
- Powertrains:
 - Conventional internal combustion engine.
 - Engine start-stop (micro-hybrid).
 - HEV: power split for light-duty, pre-transmission for MD and HD.
 - PHEV: 50 miles all-electric range.
 - BEV: 200 miles range on U.S. standard cycles for light-duty, class-specific for MD and HD.
- Component technologies [36]:
 - Current improvement rate consistent with historical trends,
 - VTO technical targets (Appendix C).
- Automation level:
 - Additional electrical accessory loads (400 W for partially automated and 1.9 kW for fully automated driverless-capable vehicles) are considered.
 - Increased accessory loads due to automation have cascading effects (e.g., larger battery packs to meet the desired range, increased electric machine power to maintain performance with a larger battery pack) that are also considered.

Tables 5 and 6 describe the composition of vehicle classes and powertrains within each scenario considered.

Table 5. Baseline Vehicle Fleet Assumptions.

	Parameter		Baseline	Baseline Short-Term			Baseline-LongTerm		
				Base	Low	High	Base	Low	High
Scenario Names			Base0	Base1	Base2	Base3	Base4	Base5	Base6
Passenger	Market Penetration	Classes	Compact car (21.6%) Midsize car (20.5%) Large Car (7.1%) Compact SUV (15%) Midsize SUV (20%) Fullsize SUV (4%) Pickup (11.8%)	Compact car (21.6%) Midsize car (20.5%) Large Car (7.1%) Compact SUV (15%) Midsize SUV (20%) Fullsize SUV (4%) Pickup (11.8%)	Compact car (18.5%) Midsize car (21%) Large Car (7.7%) Compact SUV (17.5%) Midsize SUV (20%) Fullsize SUV (4%) Pickup (12%)	Compact car (18.5%) Midsize car (21.5%) Large Car (7%) Compact SUV (18%) Midsize SUV (20%) Fullsize SUV (4%) Pickup (11%)	Compact car (21.6%) Midsize car (20.5%) Large Car (7.1%) Compact SUV (15%) Midsize SUV (20%) Fullsize SUV (4%) Pickup (11.8%)	Compact car (13) Midsize car (22%) Large Car (6%) Compact SUV (27.5%) Midsize SUV (18%) Fullsize SUV (3%) Pickup (10.5%)	Compact car (13%) Midsize car (23%) Large Car (6%) Compact SUV (26.5%) Midsize SUV (18%) Fullsize SUV (3%) Pickup (10.5%)
		Powertrains	Conv gas (95.8%) Conv gas 48V (0%) Conv diesel (2%) HEV (2%) PHEV (0.1%) BEV (0.1%)	Conv gas (95.8%) Conv gas 48V (0%) Conv diesel (2%) HEV (2%) PHEV (0.1%) BEV (0.1%)	Conv gas (67%) Conv gas 48V (16%) Conv diesel (1%) HEV (9%) PHEV (3%) BEV (4%)	Conv gas (59%) Conv gas 48V (21%) Conv diesel (1%) HEV (7%) PHEV (5%) BEV (7%)	Conv gas (95.8%) Conv gas 48V (0%) Conv diesel (2%) HEV (2%) PHEV (0.1%) BEV (0.1%)	Conv gas (11%) Conv gas 48V (35%) Conv diesel (0.5%) HEV (28%) PHEV (7.5%) BEV (18%)	Conv gas (16%) Conv gas 48V (21%) Conv diesel (0.5%) HEV (12%) PHEV (11.5%) BEV (39%)
Freight	Market Penetration	Classes	Class 3 Box (13%) Class 3 Shuttle (2%) Class 4 Delivery (20%) Class 6 P&D (20%) Transit Bus (5%) Line Haul (40%)	Class 3 Box (13%) Class 3 Shuttle (2%) Class 4 Delivery (20%) Class 6 P&D (20%) Transit Bus (5%) Line Haul (40%)			Class 3 Box (13%) Class 3 Shuttle (2%) Class 4 Delivery (20%) Class 6 P&D (20%) Transit Bus (5%) Line Haul (40%)		
		Powertrains	Conv gas (15%) Conv gas 48V (0%) Conv diesel (82.5%) Conv diesel 48V (0%) HEV (2.5%) PHEV (0%) BEV (0%)	Conv gas (15%) Conv gas 48V (0%) Conv diesel (82.5%) Conv diesel 48V (0%) HEV (2.5%) PHEV (0%) BEV (0%)	Conv gas (12%) Conv gas 48V (3%) Conv diesel (60%) Conv diesel 48V (10%) HEV (5%) PHEV (0%) BEV (0%)	Conv gas (7%) Conv gas 48V (6%) Conv diesel (56%) Conv diesel 48V (20%) HEV (13%) PHEV (0%) BEV (2%)	Conv gas (15%) Conv gas 48V (0%) Conv diesel (82.5%) Conv diesel 48V (0%) HEV (2.5%) PHEV (0%) BEV (0%)	Conv gas (0%) Conv gas 48V (5%) Conv diesel (52%) Conv diesel 48V (16%) HEV (20%) PHEV (0%) BEV (11%)	Conv gas (0%) Conv gas 48V (5%) Conv diesel (44%) Conv diesel 48V (12%) HEV (22%) PHEV (4%) BEV (15%)

Table 6. Advanced Mobility Scenarios Main Vehicle Fleet Assumptions.

		Parameter	Baseline	A		B		C	
				Low	High	Low	High	Low	High
Scenario Names		Base0	A2	A3	B5	B6	C5	C6	
Passenger	Market Penetration	Classes	Compact car (21.6%) Midsize car (20.5%) Large Car (7.1%) Compact SUV (15%) Midsize SUV (20%) Fullsize SUV (4%) Pickup (11.8%)	Compact car (18.5%) Midsize car (21%) Large Car (7%) Compact SUV (17.5%) Midsize SUV (20%) Fullsize SUV (4%) Pickup (12%)	Compact car (18.5%) Midsize car (21.5%) Large Car (7%) Compact SUV (18%) Midsize SUV (20%) Fullsize SUV (4%) Pickup (11%)	Compact car (13) Midsize car (22%) Large Car (6%) Compact SUV (27.5%) Midsize SUV (18%) Fullsize SUV (3%) Pickup (10.5%)	Compact car (13%) Midsize car (23%) Large Car (6%) Compact SUV (26.5%) Midsize SUV (18%) Fullsize SUV (3%) Pickup (10.5%)	Compact car (13) Midsize car (22%) Large Car (6%) Compact SUV (27.5%) Midsize SUV (18%) Fullsize SUV (3%) Pickup (10.5%)	Compact car (13%) Midsize car (23%) Large Car (6%) Compact SUV (26.5%) Midsize SUV (18%) Fullsize SUV (3%) Pickup (10.5%)
		Powertrains	Conv gas (95.8%) Conv gas 48V (0%) Conv diesel (2%) HEV (2%) PHEV (0.1%) BEV (0.1%)	Conv gas (67%) Conv gas 48V (16%) Conv diesel (1%) HEV (9%) PHEV (3%) BEV (4%)	Conv gas (59%) Conv gas 48V (21%) Conv diesel (1%) HEV (7%) PHEV (5%) BEV (7%)	Conv gas (11%) Conv gas 48V (35%) Conv diesel (0.5%) HEV (28%) PHEV (7.5%) BEV (18%)	Conv gas (16%) Conv gas 48V (21%) Conv diesel (0.5%) HEV (12%) PHEV (11.5%) BEV (39%)	Conv gas (11%) Conv gas 48V (35%) Conv diesel (0.5%) HEV (28%) PHEV (7.5%) BEV (18%)	Conv gas (16%) Conv gas 48V (21%) Conv diesel (0.5%) HEV (12%) PHEV (11.5%) BEV (39%)
Freight	Market Penetration	Classes	Class 3 Box (13%) Class 3 Shuttle (2%) Class 4 Delivery (20%) Class 6 P&D (20%) Transit Bus (5%) Line Haul (40%)	Class 3 Box (13%) Class 3 Shuttle (2%) Class 4 Delivery (20%) Class 6 P&D (20%) Transit Bus (5%) Line Haul (40%)	Class 3 Box (13%) Class 3 Shuttle (2%) Class 4 Delivery (20%) Class 6 P&D (20%) Transit Bus (5%) Line Haul (40%)	Class 3 Box (13%) Class 3 Shuttle (2%) Class 4 Delivery (20%) Class 6 P&D (20%) Transit Bus (5%) Line Haul (40%)	Class 3 Box (13%) Class 3 Shuttle (2%) Class 4 Delivery (20%) Class 6 P&D (20%) Transit Bus (5%) Line Haul (40%)	Class 3 Box (13%) Class 3 Shuttle (2%) Class 4 Delivery (20%) Class 6 P&D (20%) Transit Bus (5%) Line Haul (40%)	
		Powertrains	Conv gas (15%) Conv gas 48V (0%) Conv diesel (82.5%) Conv diesel 48V (0%) HEV (2.5%) PHEV (0%) BEV (0%)	Conv gas (12%) Conv gas 48V (3%) Conv diesel (60%) Conv diesel 48V (10%) HEV (5%) PHEV (0%) BEV (0%)	Conv gas (7%) Conv gas 48V (6%) Conv diesel (56%) Conv diesel 48V (20%) HEV (13%) PHEV (0%) BEV (2%)	Conv gas (0%) Conv gas 48V (5%) Conv diesel (52%) Conv diesel 48V (16%) HEV (20%) PHEV (0%) BEV (11%)	Conv gas (0%) Conv gas 48V (5%) Conv diesel (44%) Conv diesel 48V (12%) HEV (22%) PHEV (4%) BEV (15%)	Conv gas (0%) Conv gas 48V (5%) Conv diesel (52%) Conv diesel 48V (16%) HEV (20%) PHEV (0%) BEV (11%)	Conv gas (0%) Conv gas 48V (5%) Conv diesel (44%) Conv diesel 48V (12%) HEV (22%) PHEV (4%) BEV (15%)

The current fleet distribution, shown in Figure 24, was developed based on POLK data for light-duty vehicles and latest available sales for MD and HD vehicles (e.g., Statista).

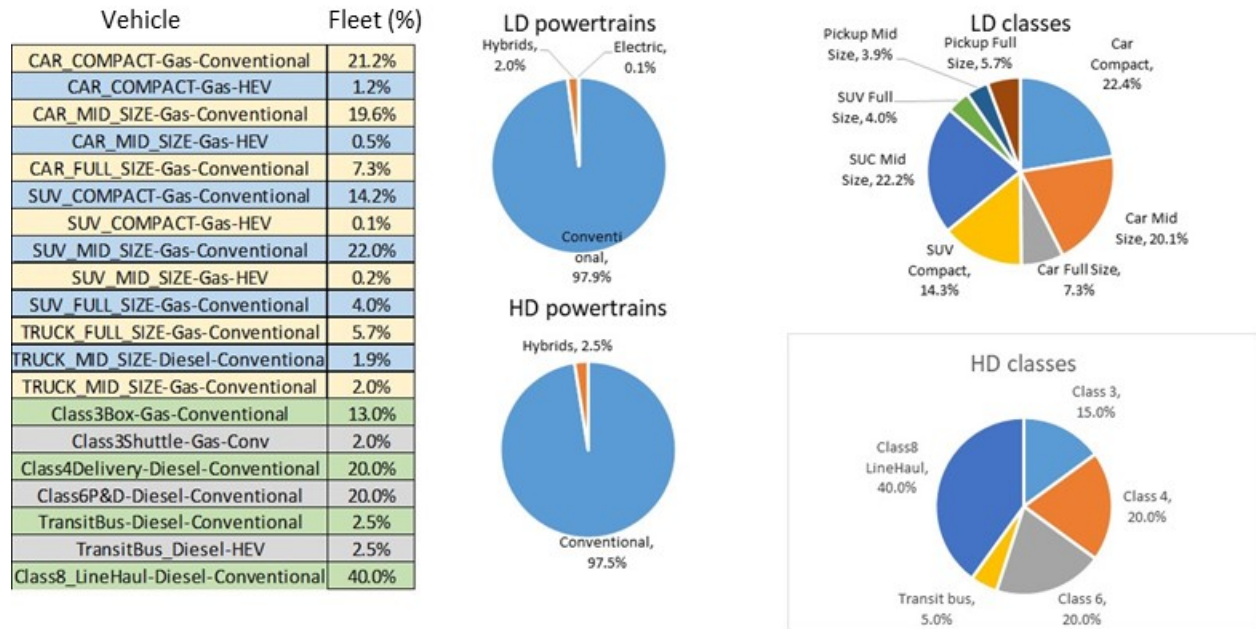


Figure 24. Baseline Vehicle Fleet Assumption (Source: POLK).

Section 3.2.2.1 provides additional details on assumptions related to vehicle class, powertrain and level of automation for LDV, MD trucks, and HD trucks. See Appendix E for detailed tables.

3.2.2.1 Light-Duty Vehicle Assumptions Detail

Based on historical trends and predictions from International Energy Agency [37], an increase in SUV market share was assumed (39% to 47.5%) at the expense of passenger cars, as shown in Figure 25.

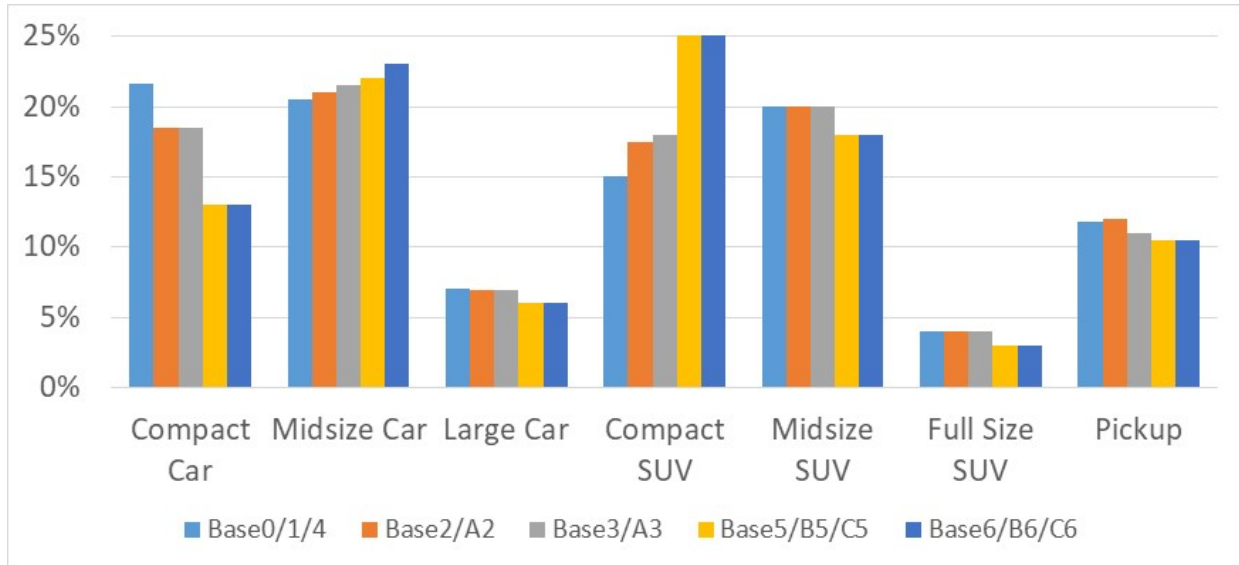


Figure 25. Light-Duty Vehicle Class of Car Stock Assumptions.

Figure 26 illustrates the fleet distribution of different powertrains across all vehicle classes for each scenario. The proportion of electrified vehicles (HEV, PHEV, and BEV) rapidly increases from 2% under Base 0 to 16% in Scenarios Base 2 and A2, and further increases to 62.5% under Scenarios Base 6, B6, and C6.

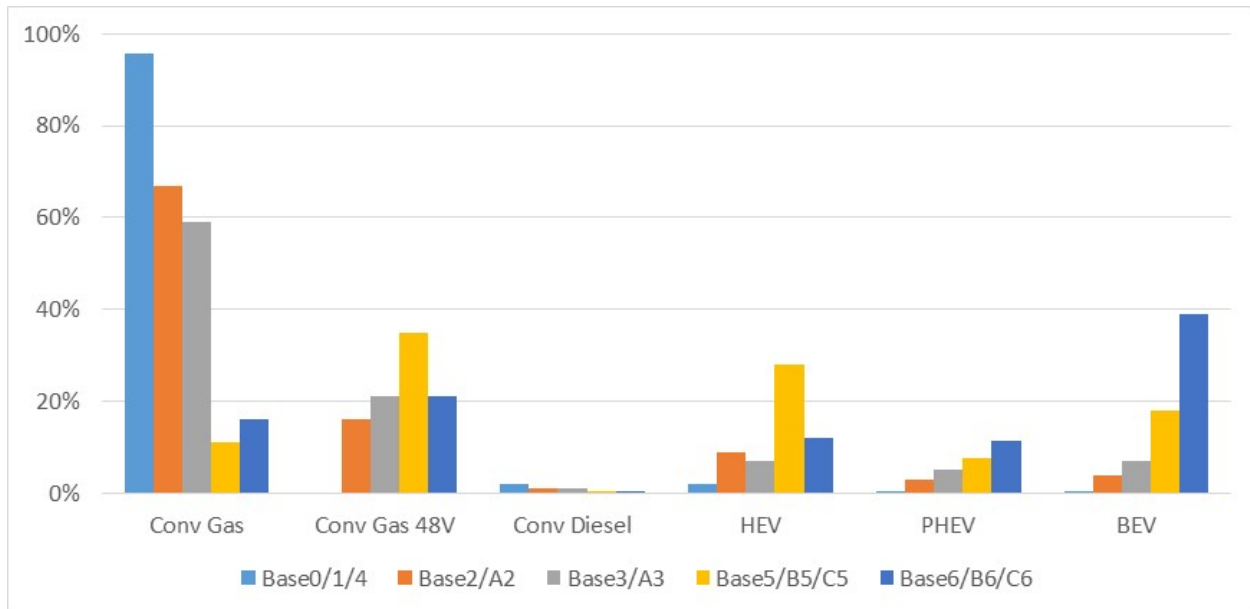


Figure 26. Light-Duty Vehicle Powertrain of Car Stock Assumptions across Scenarios.

Figure 27 illustrates the distribution of electrified powertrains (HEV, PHEV, and BEV) assumptions across each light-duty vehicle class. The greatest market penetration is assumed to occur across classes with the highest sales volume (i.e., midsize car and compact SUV), except for BEV, which has the greatest penetration for compact cars.

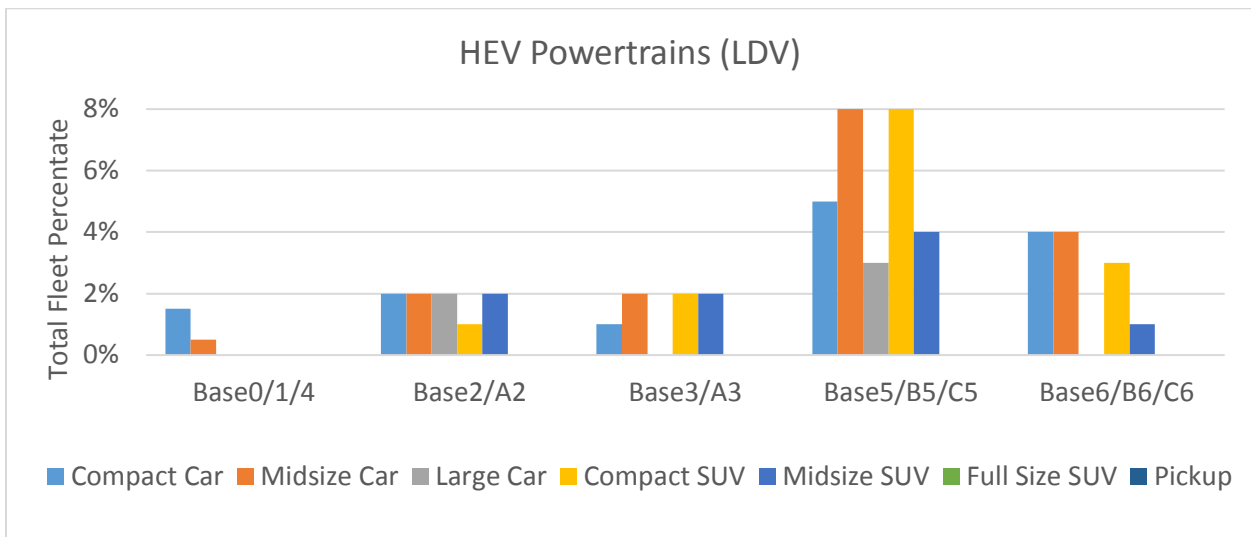
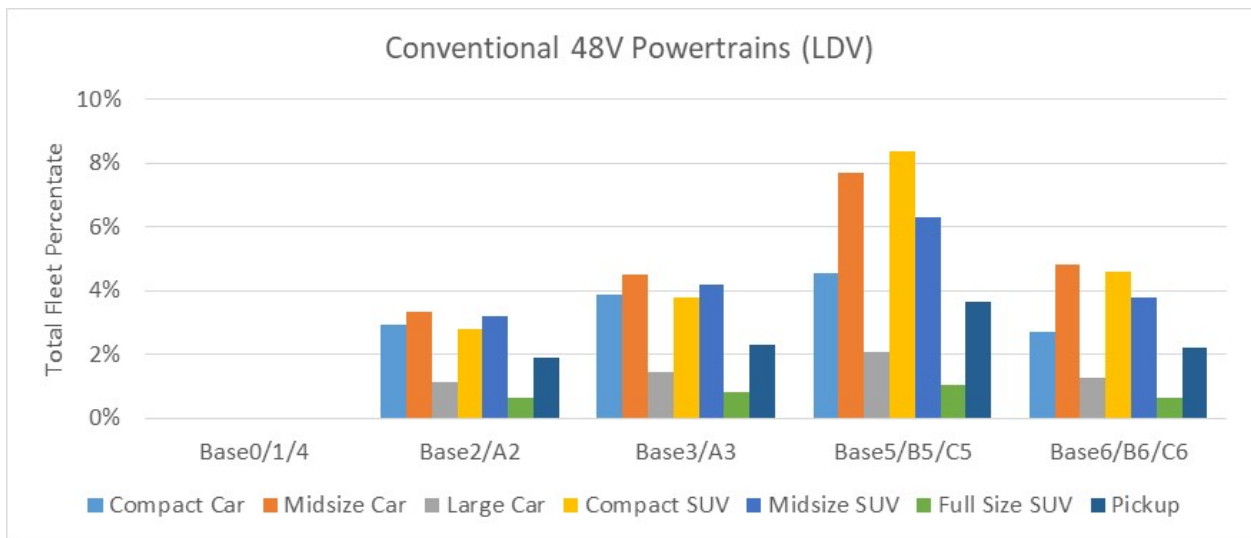
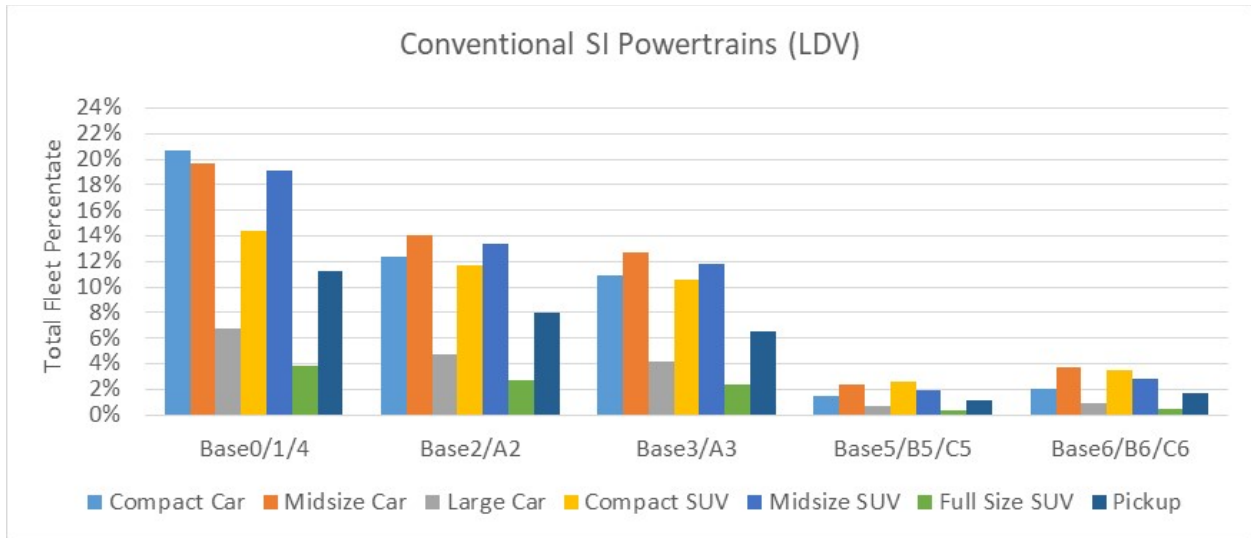


Figure 27. Light-Duty Powertrain Electrification across Classes (Continued on Next Page)

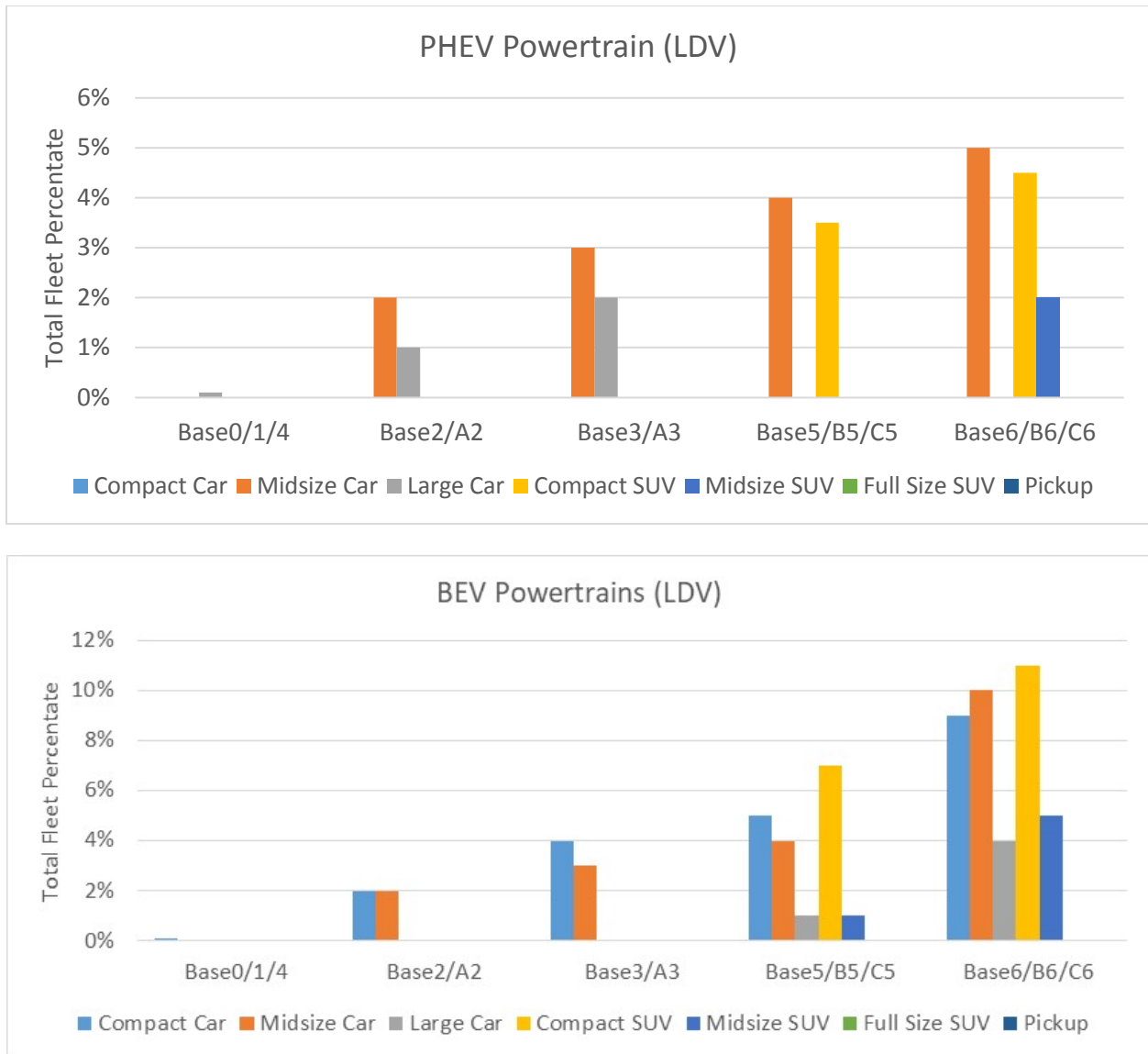


Figure 27. (Continued from Previous Page)

As shown in Figure 28, under Scenario A, only partial automation is considered (10–11%). Scenarios B and C include a mix of partial and fully automated vehicles. Fully automated vehicles enable zero-occupancy driving.

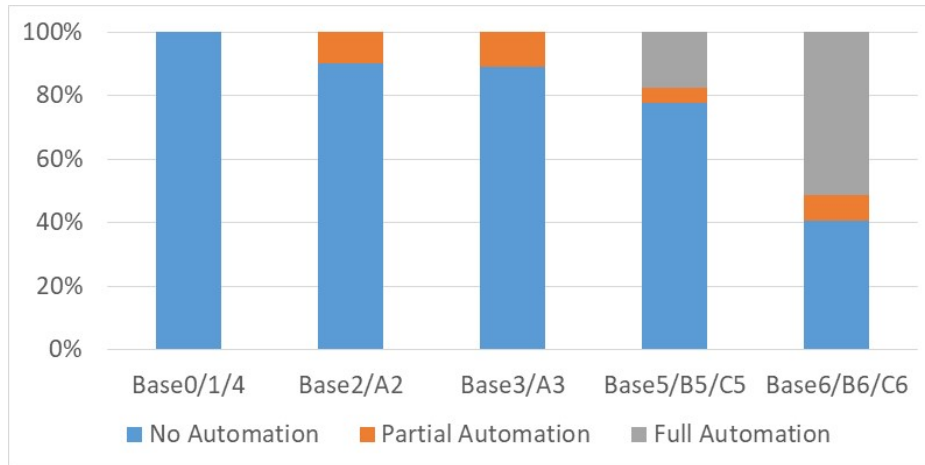


Figure 28. Light-Duty Vehicle Automation Assumptions across Scenarios.

3.2.2.2 Medium- and Heavy-Duty Vehicle Assumptions Details

For MD and HD vehicles, the distribution of classes was maintained constant across all scenarios:

- Class 3 box (13%),
- Class 3 shuttle (2%),
- Class 4 delivery (20%),
- Classes 5 and 6 (20%),
- Transit bus (5%), and
- Classes 7 and 8 tractor/trailer (40%).

Due to different vehicle requirements, especially in terms of range, a smaller penetration of electrified powertrain was considered, as shown in Figure 29.

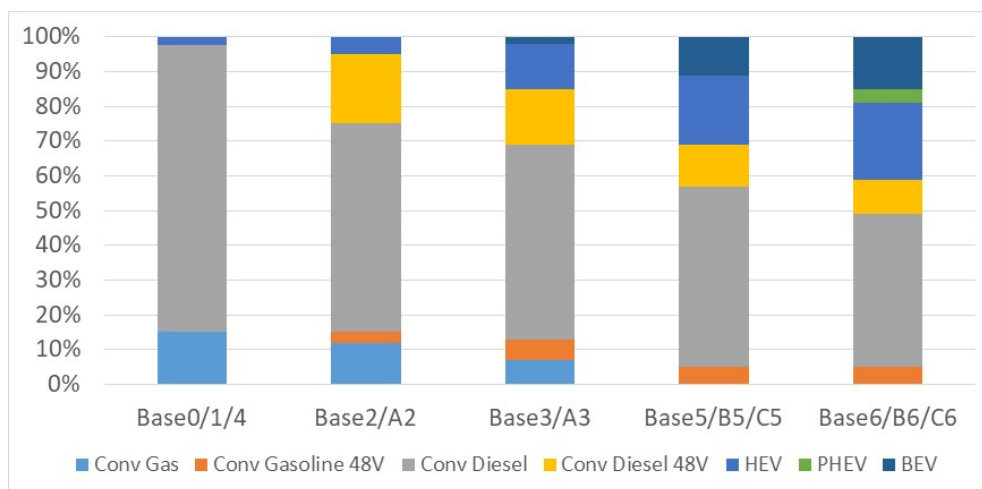


Figure 29. MD and HD Vehicle Powertrain Assumptions across Scenarios.

As shown in Figure 30, some vehicle classes (e.g., transit bus, class 4 delivery) were more aggressively electrified than others (e.g., line haul).

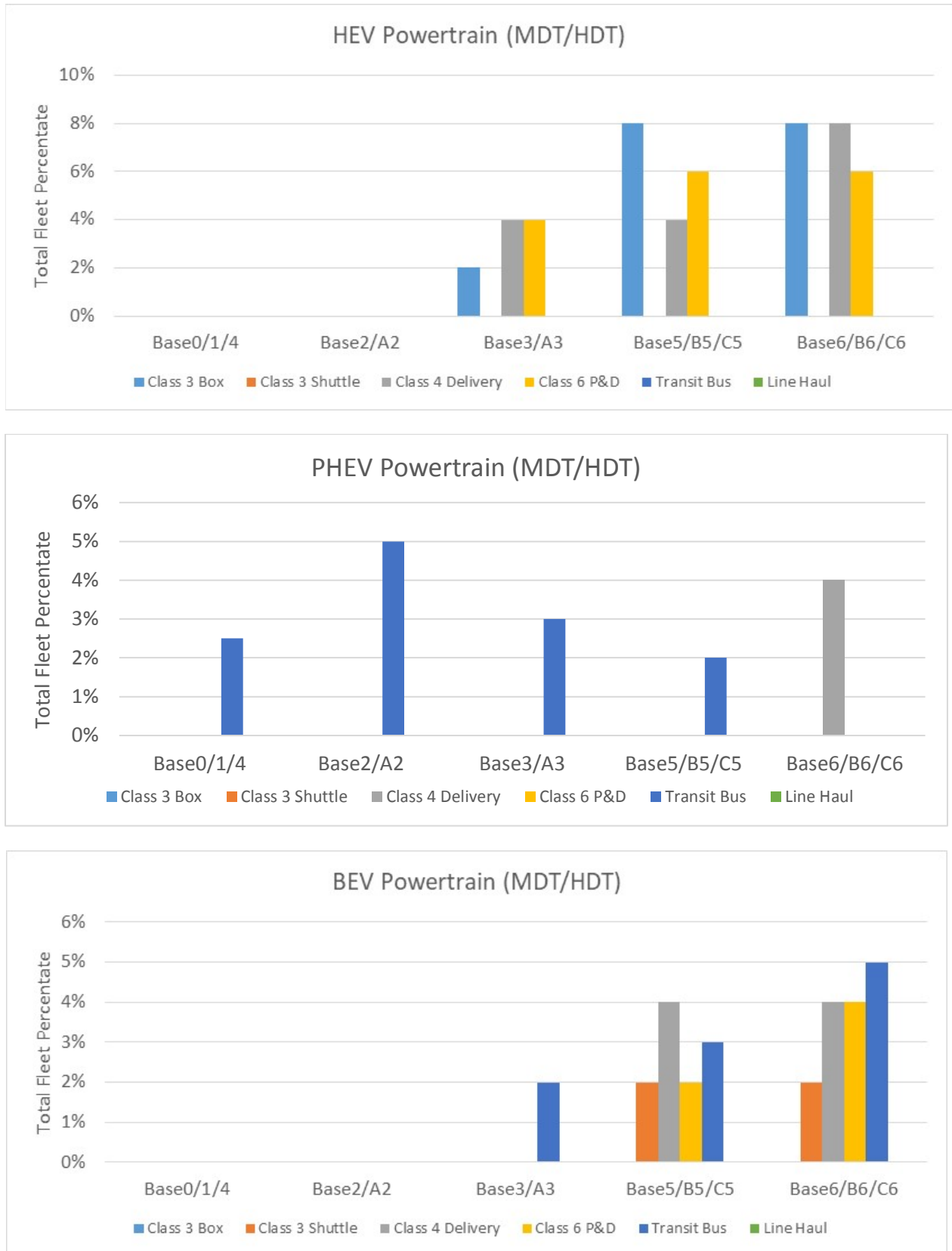


Figure 30. MD and HD Powertrain Electrification across Classes.

Partial automation was considered across all future scenarios with primary implementation on highway (e.g., cooperative adaptive cruise control). As shown in Figure 31, full automation was considered in Scenarios B and C for classes with high BEV penetration (e.g., transit, Class 4 parcel and delivery [P&D], Class 6).

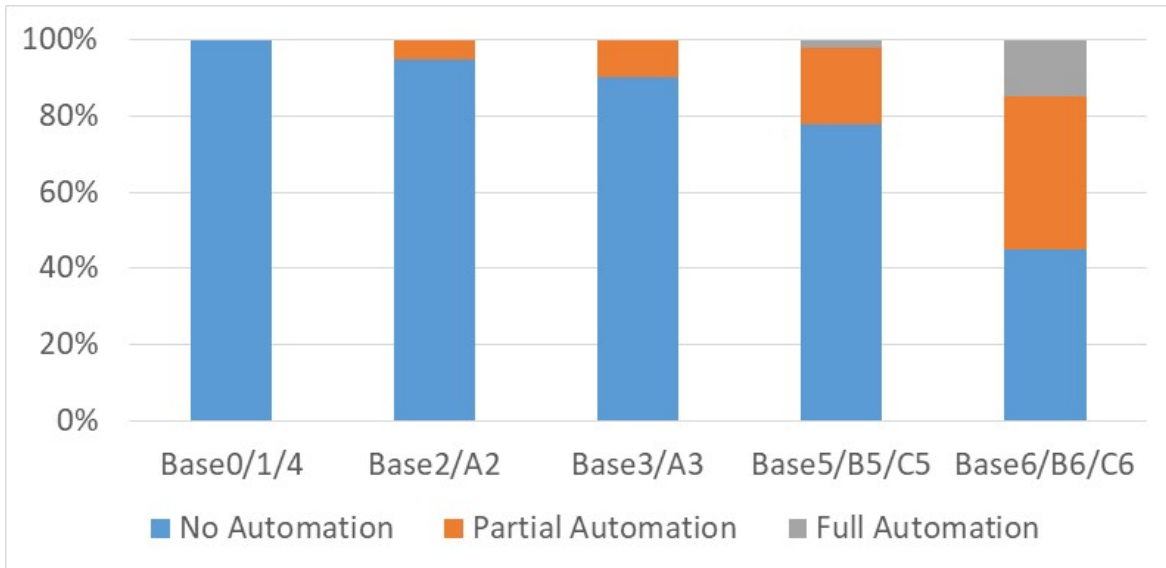


Figure 31. MD and HD Vehicle Automation Assumptions across Scenarios

4 Results from POLARIS Workflow Implementation

The POLARIS implementation of the SMART Mobility modeling workflow was applied to the Chicago metropolitan area using the set of common future scenarios and assumptions described in Section 3. The key results and insights generated by this application of modeling workflow include:

- Applying the SMART Mobility workflow to Chicago demonstrates that shared ride-hailing fleets can improve the energy efficiency of travel by nearly 30%, providing the same mobility as the corresponding baseline in terms of PMT while also reducing congestion. On the other hand, privately owned fully automated vehicles may increase PMT up to 7% but also increase congestion.
- Despite significant market penetration of electric-drive vehicles and improvements in powertrain technologies in the future, the potential increase in VMT resulting from privately owned, fully automated vehicles could offset or even increase overall transportation energy consumption.
- Travel behavior:
 - Transit and active modes of transportation (such as walking and biking) increase in the high-sharing scenarios. This is compounded by the trip-chaining effect where transit or ride-hailing is selected as the commute mode and discretionary activities on the same travel tour are then done at nearby locations by walk or bike, or at more distant locations using additional transit or ride-hail trips.
 - Households that dispose of at least one vehicle tend to shift to public transit and ride-hailing. This decision is highly dependent on geographical location; urban households tend to choose public transit (15% point increase), and suburban households tend to choose ride-hailing (44% point increase) because these become the remaining options with the highest travel utility.
- Ride-sharing:
 - High-sharing scenarios without vehicle repositioning to search for riders (i.e., Scenarios A and B) achieve lower vehicle miles travelled (VMT) due to the efficient use of ride-hailing, the small share of VMT without a passenger (below 15%), and a significant amount of ride pooling (22–27%).
 - Assuming an average of three daily trips for a private auto, a single ride-hailing vehicle can replace about five personally owned vehicles. This number can be increased by different pricing, more efficient repositioning, and increased ride-pooling.
 - Overall congestion is a key factor in ride-hailing performance because vehicles can perform more trips with smaller travel times in less congested networks. Therefore, the increased network speed in Scenarios B5 and B6 provides an additional performance benefit and allows smaller fleet sizes to meet the same demand.
- Personally owned fully automated (driverless-capable) passenger vehicles:
 - Households with privately owned, fully automated vehicles (Scenario C6) show substantially higher productive miles travelled (PMT, 57%) and productive hours travelled (PHT, 38%) relative to households without AVs.
 - Households with AVs exhibit substantially different travel behavior compared to households without AVs. This behavior includes a propensity to travel longer during peak evening hours and to take more single-occupancy vehicle (SOV) trips.

- The use of privately owned automated vehicles (AVs) leads to drastically increased VMT and greatly increased unloaded vehicle travel, with 1 out of 7 vehicles in the system being empty, compared to 1 out of 25 in the high-sharing, high-automation case (Scenario B6).
- Multi-modal travel:
 - Even without changes to the existing transit infrastructure and schedules in Chicago, the mode share of transit will increase by 67% and 100% under Scenarios A3 and B6, respectively, due to reduction in vehicle ownership of 45% and 75%, and increased acceptance of shared and non-auto-based travel modes.
 - In a hub-and-spoke system like the Chicago region, ride-hailing and transit can be complimentary, with transit being a key mobility provider in the urban core and ride-hailing providing personal mobility in the suburbs.
 - Transit is vital to the overall transportation system. In a Chicago metropolitan area-based scenario with no transit, all mobility and energy metrics become substantially worse in the urban core: there is a 52% increase in VHT and a 23% decrease in travel efficiency (passenger miles per kilowatt-hours).
- MEP:
 - The increase in MEP and travel efficiency for the shared mobility scenarios (Scenarios A and B) show that shared mobility has an additional travel efficiency impact beyond that provided by vehicle technology improvements alone.
 - Increased congestion and lower transportation system efficiency in the case of privately owned, fully automated vehicles (Scenario C6) offset the improvements associated with VTO technology targets, leading to a moderate MEP increase and a travel efficiency decrease (changes of +10% and -12%, respectively, compared to Base 6).
- Freight:
 - At a moderate rate of commodity flow growth (1% CAGR), total freight VMT in the Chicago region will grow by 27% in the long term (Bases 4, 5, 6 versus Base 0). There will be detrimental impacts on energy consumption (as shown in Base 4) unless energy-efficient vehicle technologies are adopted more widely (represented by moderate and aggressive technology improvements in Base 5 and Base 6, respectively).
 - E-commerce is expected to generate a large increase in last-mile delivery of goods. However, after accounting for shopping trip reductions and vehicle technology changes, simulations show that there will be an overall net reduction in VMT (34–56%) and energy use (29–54%) across the Chicago metropolitan area.
 - Even though the VMT generated by e-commerce delivery are projected to grow at a much faster rate than VMT generated by other commodity types (assumption based on FAF forecasts), e-commerce delivery trucks constitute a maximum of only 3% of MD/HD VMT. This underscores the importance of analyzing the other types of freight traffic that make up the rest of truck VMT.
- Light-duty, MD, and HD vehicle energy consumption and greenhouse gas (GHG):
 - Although overall energy consumption from light-duty vehicles decreases over time due to vehicle technology improvements, the energy consumption by MD and HD vehicles remains relatively

constant because efficiency gains from vehicle technology improvements are countered by the expected increase in MD and HD VMT.

- Based on scenario analysis in the Chicago metropolitan area, medium- and heavy-duty (MD and HD) vehicles currently account for 33% of the overall transportation energy (compared to 28% in the United States estimated by EIA [38]). This share is expected to grow to 50% in the future due to light-duty vehicle efficiency improvements enabled by electrification combined with increased freight demand.
- Achieving VTO light-duty vehicle technology research targets will lead to system-level energy savings compared to business as usual in all scenarios considered (15%, 24%, and 2% savings for Scenarios A, B, and C, respectively). Meeting VTO technology targets for MD/HD trucks is required in the personally owned AV scenario (Scenario C) to compensate for the light-duty vehicle energy increase caused by higher VMT.
- Technology improvements over time provide significant reduction in energy per mile for powertrains with internal combustion engines. This effect is reduced for electrified powertrains due to the increase in accessory load from automation (e.g., electrical loads from LiDAR, radars, and other sensors and computing devices).

The key metrics related to mobility and energy use for both passenger and freight for each scenario are shown in Table 7 (all vehicle classes) and Table 8 (MD and HD vehicles only).

Table 7. POLARIS Key System Performance Metrics (Light Duty+MD/HD) across Scenarios.

Metric	Unit	Reference baselines			%Δ from Base0						%Δ from short-term ¹		%Δ long-term ¹			
		Base0	Base 1/2/3	Base 4/5/6	A2	A3	B5	B6	C5	C6	A2	A3	B5	B6	C5	C6
Vehicle hours traveled (VHT)	M hours	10	11	11	-18%	-19%	-23%	-24%	15%	62%	-21%	-22%	-29%	-30%	5%	49%
Vehicle miles traveled (VMT)	M miles	307	323	348	-7%	-8%	-7%	-7%	18%	42%	-12%	-12%	-18%	-18%	4%	25%
Prod.-hours of travel	M hours	16	17	18	8%	8%	14%	16%	16%	37%	2%	2%	1%	2%	2%	20%
Prod.-miles of travel (PMT) ²	M miles	450	477	515	5%	5%	12%	14%	14%	23%	-1%	-1%	-2%	0%	-1%	7%
Per capita PMT	M miles	45	45	45	-2%	-2%	-4%	-2%	-2%	6%	-1%	-1%	-2%	0%	-1%	7%
Per capita VMT	M miles	31	30	30	-13%	-14%	-20%	-20%	2%	22%	-12%	-12%	-18%	-18%	4%	25%
Avg. vehicle travel speed	MPH	30	30	31	14%	15%	21%	22%	3%	-12%	11%	12%	16%	17%	-1%	-16%
Avg. trip speed	MPH	28	28	28	-2%	-2%	-2%	-2%	-2%	-10%	-2%	-3%	-3%	-2%	-2%	-11%
Total energy	GWh	458	481	531	-23%	-35%	-33%	-49%	-17%	-19%	-12%	-13%	-18%	-23%	2%	22%
MEP metric	000s	9908.0	10844	12832	56%	68%	123%	173%	81%	70%	34%	34%	51%	76%	23%	10%
			11531	14613												
			12392	15381												
Travel efficiency	mi/KWh	1.0	1.0	1.0	36%	62%	67%	124%	37%	53%	13%	14%	19%	29%	-2%	-12%
			1.2	1.4												
			1.4	1.8												
			0.16	0.14												
Cost - Drive	(\$/mile)	0.18	0.16	0.14	-7%	-15%	-18%	-26%	-18%	-23%	-1%	-1%	-1%	-1%	-1%	3%
Cost - Ridehail	(\$/mile)	1.75	1.75	1.75	-23%	-23%	-37%	-65%	-44%	-51%	-23%	-23%	-37%	-65%	-44%	-51%

Table 8. POLARIS Key System Performance Metrics (Light Duty Only) across Scenarios.

Metric	Unit	Reference baselines			%Δ from Base0						%Δ from short-term ¹		%Δ long-term ¹			
		Base0	Base 1/2/3	Base 4/5/6	A2	A3	B5	B6	C5	C6	A2	A3	B5	B6	C5	C6
Population	M	9.9	10.6	11.5	7%	7%	16%	16%	16%	16%	0%	0%	0%	0%	0%	0%
Vehicle hours traveled (VHT)	M hours	9.7	10.0	10.4	-20%	-20%	-26%	-28%	12%	61%	-22%	-23%	-31%	-33%	4%	50%
Vehicle miles traveled (VMT)	M miles	284.1	299.6	319.0	-8%	-8%	-10%	-10%	17%	43%	-13%	-13%	-20%	-20%	4%	27%
Prod.-hours of travel ²	M hours	15.3	16.2	17.3	8%	8%	14%	16%	14%	36%	2%	2%	1%	2%	1%	20%
Prod.-miles of travel (PMT) ²	M miles	426.8	453.3	485.2	5%	5%	11%	13%	13%	22%	-1%	-1%	-2%	0%	-1%	8%
Per capita PMT	M miles	43.1	42.8	42.2	-2%	-2%	-4%	-2%	-3%	5%	-1%	-1%	-2%	0%	-1%	8%
Per capita VMT	M miles	28.7	28.3	27.7	-14%	-14%	-23%	-23%	1%	23%	-13%	-13%	-20%	-20%	4%	27%
Avg. vehicle travel speed	MPH	29.3	30.1	30.7	14%	15%	22%	24%	5%	-11%	11%	12%	16%	18%	0%	-15%
Avg. trip speed	MPH	27.9	28.0	28.1	-2%	-3%	-3%	-2%	-1%	-10%	-3%	-3%	-3%	-3%	-2%	-10%
Total energy	GWh	308	325	343	-23%	-35%	-33%	-49%	-17%	-19%	-12%	-13%	-18%	-23%	2%	22%
			233	184												
MEP metric	000s	9908.0	10844	12832	56%	68%	123%	173%	81%	70%	34%	34%	51%	76%	23%	10%
			11531	14613												
travel efficiency	mi/KWh	0.9	1.4	1.4	36%	63%	66%	123%	36%	52%	13%	14%	19%	29%	-2%	-12%
			1.6	2.1												
			1.9	2.6												

1. Scenario A2 vs. Base 2, A3 vs. Base 3, B5 & C5 vs. Base 5, B6 & C6 vs. Base 6

2. Productive Miles Traveled - All traveler miles (by any mode) plus freight miles traveled. Excludes transit driver miles, TNC/taxi driver miles and unloaded SAV/CAV miles.

Additional key mobility metrics shown in Table 7 are used for more detailed analysis, including:

- Vehicle miles traveled (VMT): Total number of miles traveled by all vehicles in the system for each scenario, representing a measure of the load on the system from the transportation network perspective.
- Productive miles traveled (PMT): Total person-miles traveled by all travelers in any mode (i.e., cars, ride-hailing/taxi vehicles, transit vehicles, walking, and biking), plus all freight delivery miles, minus unloaded miles (e.g., taxi, ride-hailing vehicles, or fully automated vehicles without a passenger, freight delivery vehicles without a load). This represents a measure of the load on the system from a user perspective (i.e., how much mobility is the system providing), with higher ratio of PMT to VMT indicating better system performance:

$$PMT = PMT_{pass} + PMT_{freight}$$

$$\text{with } PMT_{pass} = \sum D_{SOV} + \sum D_{HOV} + \sum D_{bike} + \sum D_{walk} + \sum D_{ride-hailing} \times \text{passengers} + \sum D_{transit} \times \text{passengers}$$

$$PMT_{pass} = \sum D_{MD/HD}$$

- Vehicle hours traveled (VHT): Total travel time for all vehicles in the system, representing another measure of the transportation system load. When VHT increases faster than VMT, this indicates growing congestion and delay in the system.
- Productive hours traveled (PHT): Total travel time for all users in the system, with users defined the same as for PMT.
- Average vehicle travel/network speed: Ratio of VMT/VHT.
- Average trip/travel speed: Ratio of PMT/PHT.
- Travel efficiency: Average energy required to move a person or a good 1 mile (PMT/total energy).

Note: In the rest of this section, unless otherwise noted, comparisons between scenarios and baselines will always refer to the corresponding baseline in terms of population growth and vehicle technology. For example, Scenario C6 will be compared to Base 6, Scenario B5 to Base 5 and so on, unless otherwise stated.

Applying the SMART Mobility workflow to Chicago demonstrates that shared ride-hailing fleets can improve the energy efficiency of travel by nearly 30%, providing the same mobility as the corresponding baseline in terms of PMT while also reducing congestion.

On the other hand, privately owned fully automated vehicles may increase PMT up to 7% but also increase congestion. As shown in Figure 32(a), overall, mobility (PMT) increases only under Scenario C6 (7%); it remains either flat or slightly reduced for the other scenarios compared to their respective baselines. For Scenarios A and B, this nearly constant mobility is associated with a drastic decrease on the system load (12% and 18% lower VMT respectively). Those results demonstrate the benefits of increasing ride-hail fleets and ride-pooling utilization because similar mobility is provided under much lower loads. The system efficiency improvements are also highlighted by the VHT in Figure 32(b); VHT decreases faster than VMT, indicating substantial congestion reduction. Vehicle travel speeds also increase by 11% to 17%, although average trip speeds, accounting for all transit and non-motorized travel, is reduced slightly because travelers deflect to slower modes. In other words, more travelers are using slower options (e.g., transit, walking), which increases overall vehicle speeds for those still using auto-based modes. However, for the C scenarios, VHT grows faster than VMT, indicating growing congestion. In fact, under Scenario C6, overall average travel speeds are reduced by 16%; VHT increases by 49% while VMT only increases by 25%, suggesting a substantial increase in traffic congestion.

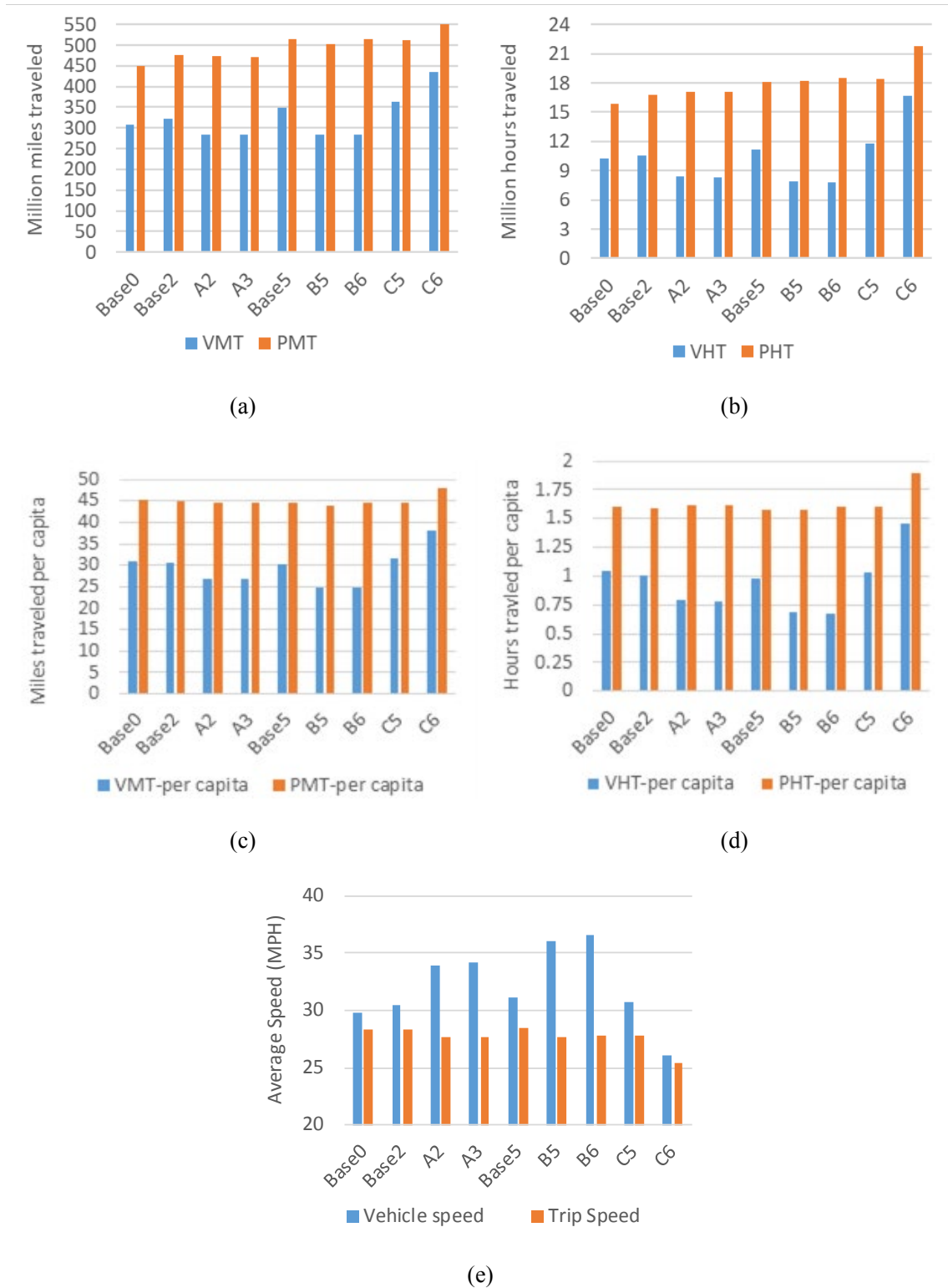


Figure 32. POLARIS Scenario Results for (a) VMT and PMT, (b) VHT and PHT, (c) VMT and PMT per Capita, (d) VHT and PHT per Capita, and (e) Average Speed.

Despite significant market penetration of electric-drive vehicles and improvements in powertrain technologies in the future, the potential increase in VMT resulting from privately owned, fully automated vehicles could offset or even increase overall transportation energy consumption.

Compared to the baseline scenario (Base 0), the assumed increase in vehicle electrification and improved vehicle technologies under Scenarios B and C leads to reduced overall energy consumption despite an increase in SUV and pickup sales. Indeed, although Base 0 has a total energy consumption of 458 GWh, energy consumption is reduced by nearly 50% (to 233 GWh) under the high-sharing Scenario B6 (Figure 33). Under those conditions, reduced congestion (represented by higher average vehicle speed) at the same mobility level (no change in PMT) contributes to the overall benefits along with advanced vehicle technologies and increased powertrain electrification. The most aggressive vehicle technology improvements assumed (under Scenario C) achieve similar energy reduction benefits as Scenario A2. The mobility increases in the C scenarios resulting from fully automated privately owned vehicles combined with increased freight movement offset or even increase overall system energy consumption, compared to their respective baselines (Scenarios Base 5 and Base 6).

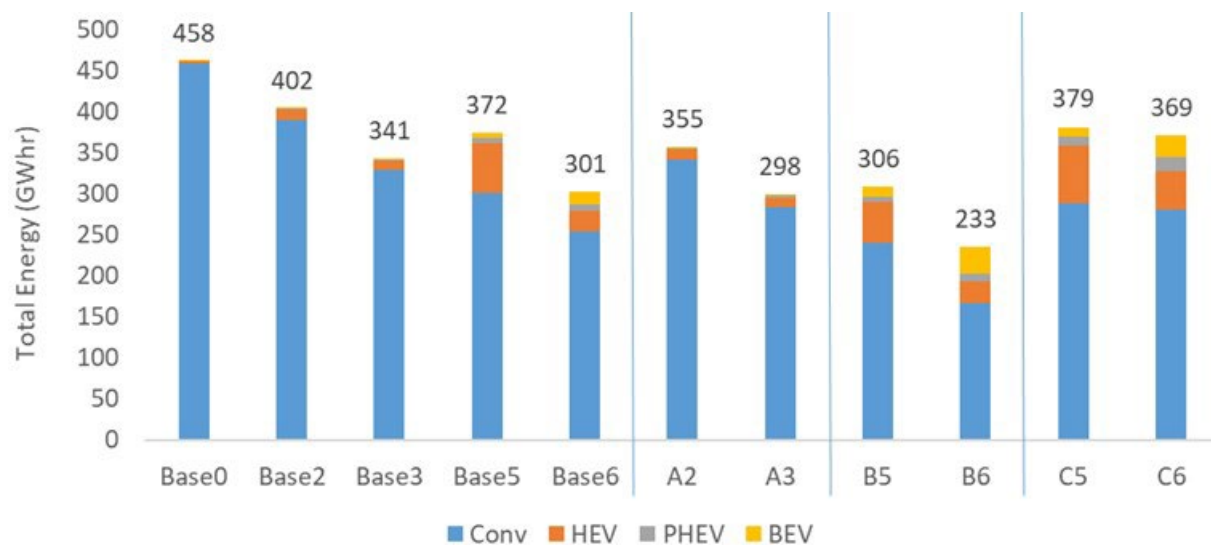


Figure 33. POLARIS Total Energy Use, and Energy Use by Powertrain Type.

A detailed analysis of each scenario, based on Table 7, highlights the impact of technologies on the different metrics:

- In the high-technology partially-automated high-sharing Scenario A3, PMT and PHT remain relatively constant compared to Base 3, but there is a 22% reduction in VHT. Furthermore, in addition to the 35% energy reduction due to increased powertrain efficiency, there is an additional 13% reduction in energy consumption primarily due to a 12% reduction in VMT. The result is a 14% increase in travel efficiency over Base 3 (67% over Base 0). The non-automobile-drive mode share increases by 90% due to the increased availability of ride-hailing vehicles, which drives down wait times, and the disposal of 45% of household vehicles assumed to be caused by that ride-hailing availability.
- In the high-technology shared AV case (Scenario B6), the total PMT remains nearly constant compared to Base 6, while VMT decreases by 18%, primarily due to increased ride-pooling and travelers switching to transit and non-motorized modes. As a result of this shift, average vehicle speeds on the road network increase because there less congestion, while average trip speeds (for all modes) remain constant. By providing the same mobility with a reduced load on the road network, this scenario leads to increased system efficiency. The mode share for non-privately owned automobiles also increases to 68% (Figure 33) due to the widespread availability of SAVs. Travel energy efficiency improves by 44% compared to

Base 6 (172% compared to Base 0), while energy use decreases by 29% relative to Base 6 (49% relative to Base 0), primarily due to improvements in powertrain technology, even though travel is now less efficient due to unloaded VMT. Interestingly, since PHT and miles of travel are essentially constant compared to the long-term baseline (Base 6), the use of shared AVs provides a similar level of mobility with greatly increased travel efficiency.

- The fully automated privately owned scenario (Scenario C6) shows many of the opposite effects from Scenario B. PMT and PHT increase by 7% and 20%, respectively, compared to Base 6 because there is a reduced VOTT. This indicates travelers are taking advantage of increased travel opportunities to reach more attractive discretionary travel destinations. Total VHT increases even more (49%) due to reduced VOTT as well as empty fully automated vehicles repositioning themselves to accommodate sharing among household members. In fact, empty vehicle travel in this scenario represents 15% of total system VMT. As a result, the system energy use increases by 22% over the long-term baseline (in contrast to the 23% reduction seen in Scenario B6), which results in a 12% decrease in travel efficiency compared to Base 6.
- A favorable future scenario can be defined by the following characteristics: higher network speeds, lower energy consumption from travel, and lower cost of travel. The MEP metric, which combines the time (represented by travel speed in mph), energy (in terms of kilowatt-hours per passenger mile), and affordability (in dollars per passenger mile) of travel increases the most (76%) in the high-sharing, high-automation, high-technology case (Scenario B6), where network speeds increase (by 17%) because there are fewer vehicles in the road network as a result of high degree of shared trips, total energy consumption decreases (by -23%), and the cost of traveling in car and ride-hailing modes is reduced the most (with respect to their respective baselines). On the other hand, MEP improvements are the lowest in the low-sharing, high-automation, high-technology case (Scenario C6) because there are lower road network speeds (16% reduction) and higher energy consumption (22% increase) due to the higher VMT induced by the AV technology.

The following subsections describe in greater detail the key factors and their resulting outcomes observed across scenarios, including individual traveler behavior, ride-hailing/SAV performance, CAV impacts, and multimodal travel.

4.1 Individual Traveler Behavior Changes

Mode share, a key traveler behavior response, varies substantially over the scenarios. The use of SOVs is most prevalent in the baseline scenario and Scenario C6, but is as low as 15% under Scenario B6 and 36% under Scenario A3. This is consistent with differences in personal vehicle disposal and VOTT, as expected.

Transit and active modes increase in the high-sharing scenarios, and this is compounded by the trip-chaining effect where transit or ride-hailing is selected as the commute mode and discretionary activities on the same travel tour are then done at nearby locations by walk or bike, or more distant locations using additional transit or ride-hail trips.

Figure 34 shows that there is significant variation across scenarios in terms of travel by SOVs and ride-hailing. Scenario B represents the highest transit share, which is 5 percentage points greater than Base0. This scenario also results in the highest ride-hailing and walk share, 31% and 12%, which are respectively 27% and 10% greater than Base 0. The major mode shifts in Scenario B are mostly driven by the considerable reduction in private vehicle ownership and a high penetration of shared AV technology. Bicycle and HOV shares do not vary considerably across the scenarios and demonstrates 2 and 4 percentage point increases, respectively, in Scenario B compared to Base 0. The highest transit, ride-hailing, walk and bike shares are observed in Scenario B6 resulting from a 75% reduction in private vehicle ownership and high penetration of shared AV technology. In Scenario C, with a high proportion of privately owned, fully automated vehicles, the SOV and

AV share nearly matches the base SOV share, whereas the ride-hailing share increases by only 2 to 3 percentage points.

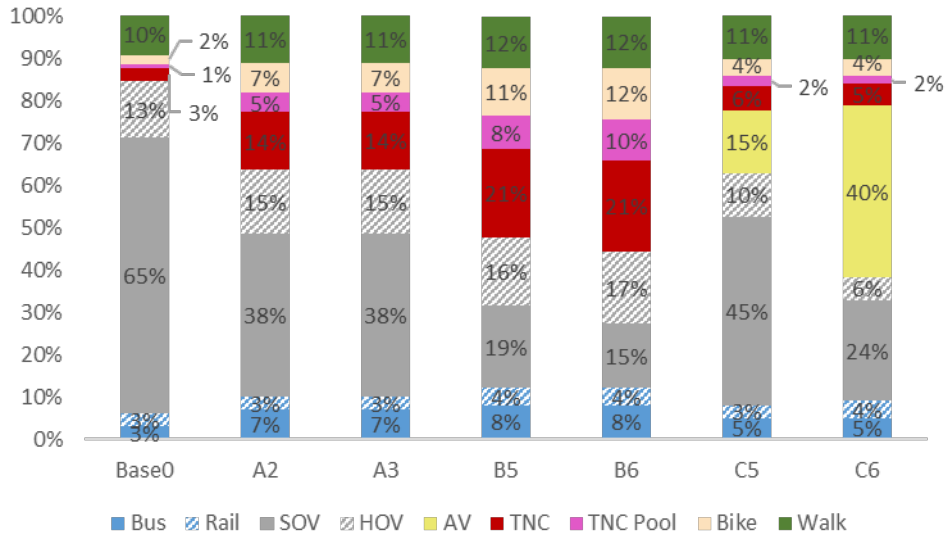


Figure 34. POLARIS Mode Shares by Scenario.

A key driver of the results is household vehicle retirement, assumed to be driven by the increased availability of ride-hailing and shared modes of transportation. The household vehicle retirement rate was set as an input parameter, as discussed in Section 3.2, with values of 45% for the high-sharing, partial-automation case (Scenarios A2 and A3), 68% and 75% for the high-sharing, high-automation cases (Scenarios B5 and B6), and 15% and 20% for the low-sharing, high-automation cases (Scenarios C5 and C6). Note that these rates are assumptions based on the scenario definition (i.e., Scenarios A and B are high-sharing scenarios, so they have higher retirement rates), that would in reality have complex interactions between ride-hail operating characteristics and pricing, vehicle pricing, household travel needs, and other factors which are currently not fully explored. Current trends indicate that households do retire vehicles and use more ride-hailing as these fleets expand [40, 41], but further modeling of this phenomenon is necessary to move beyond assumed retirement rates [42]. These retirement rates represent an average, although household vehicles are unlikely to be disposed of uniformly. For example, residents in urban areas and those near high-quality transit are much more likely to dispose of vehicles than households with lower accessibility to other modes of transportation (e.g., rural areas and locations without adequate transit systems). To account for this in the workflow common scenarios, the household vehicle disposal model developed by Menon et al. [39], was adapted for POLARIS and implemented in the simulation code. Figure 35 shows the proportion of households disposing of personally owned vehicles by zone for Scenarios A3, B6, and C6.

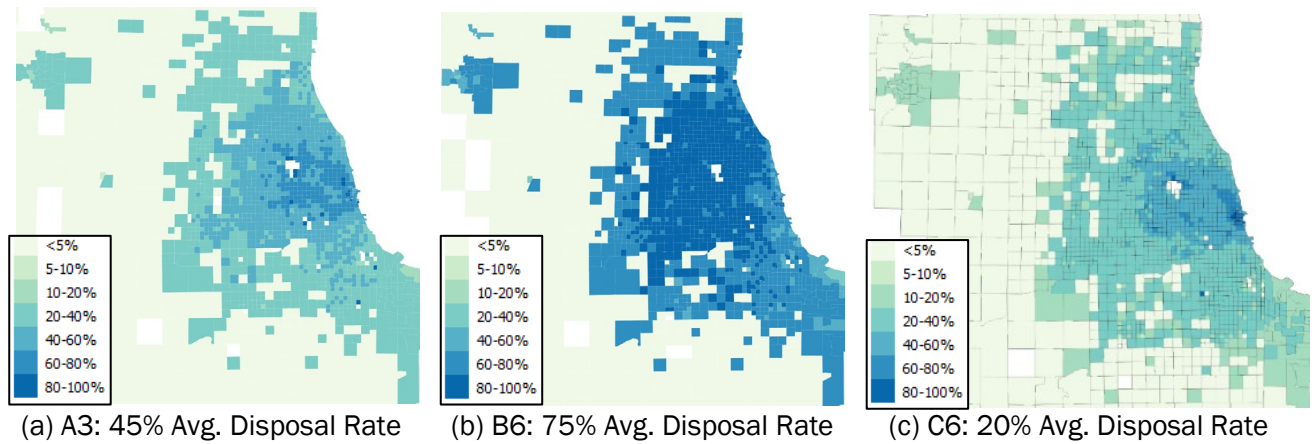
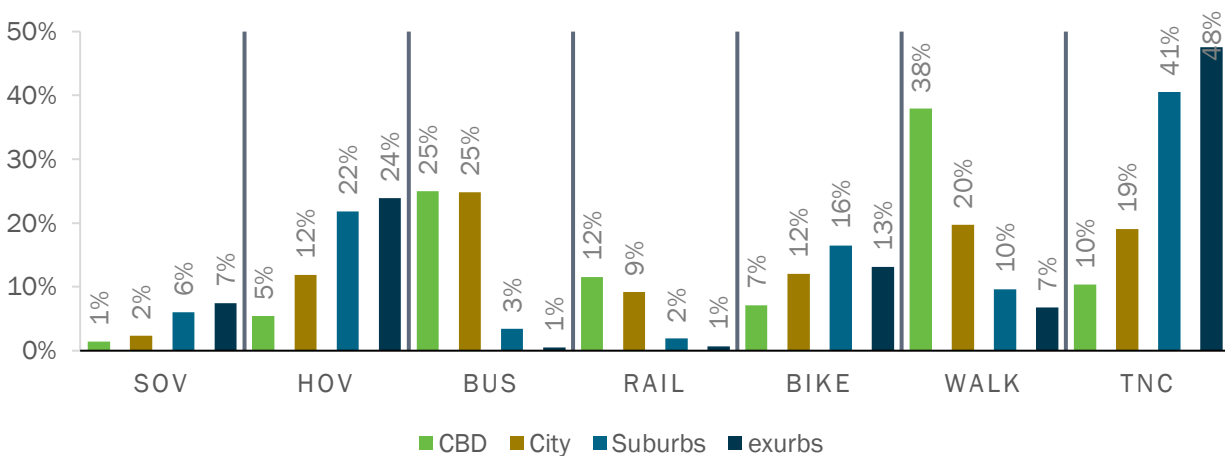


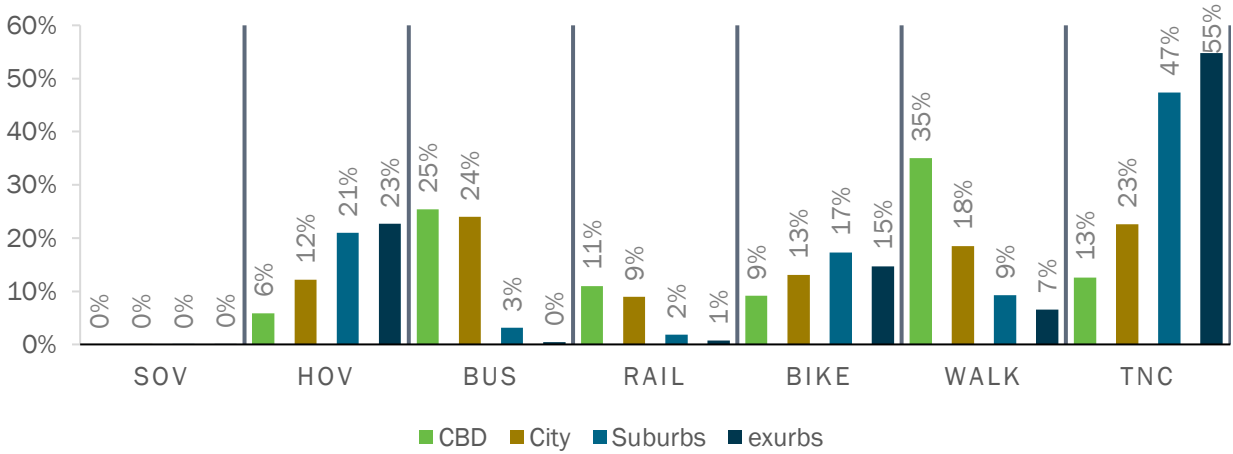
Figure 35. POLARIS Household Vehicle Disposal Rates by Traffic Analysis Zone for Scenarios (a) A2, (b) B2, and (c) C2.

Households that dispose of at least one vehicle tend to shift to public transit and ride-hailing. This decision is highly dependent on geographical location; urban households tend to choose public transit (15% point increase), and suburban households tend to choose ride-hailing (44% point increase) as these become the remaining options with the highest travel utility.

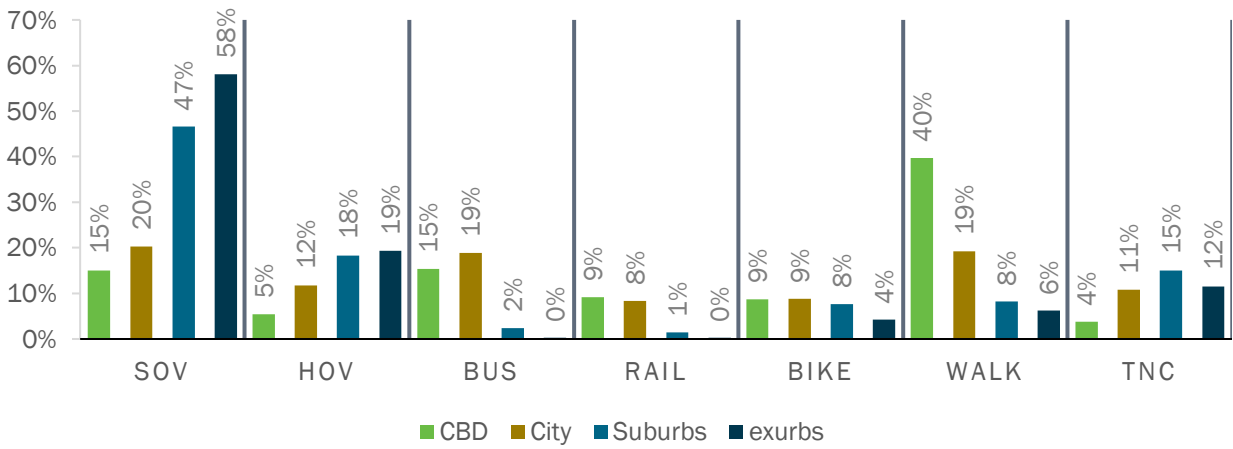
As shown in Figure 36, households located in the Chicago Central Business District and in the city center mostly depend on public transit and walking to meet their mobility needs while households located in the suburbs and exurbs mainly rely on biking and ride-hailing companies after disposing of their vehicle. For example, in Scenarios A3 and B6, ride-hailing represents 48% and 55% of the mode share, respectively, in the exurban areas; this is substantially higher than the 5% share in Base 0. In addition, there are observable differences across the scenarios due to different vehicle retirement rates and ride-hailing penetration. In Scenario B6 (representing 75% household vehicle retirement and very high ride-hailing penetration), SOVs are almost nonexistent. In addition, households in the suburb and exurb areas meet their demand through ride-hailing with additional biking trips. Scenario A3, which also represents high sharing, has similar trends. In Scenario C6 (representing only 20% vehicle retirement and high dependency on privately owned AVs), although the SOV share decreases considerably in the suburban and exurban areas compared to Base 0 (Figure 34), the decrease is minimal in the city center (from 17% in Base 0 to 15% in Scenario C6).



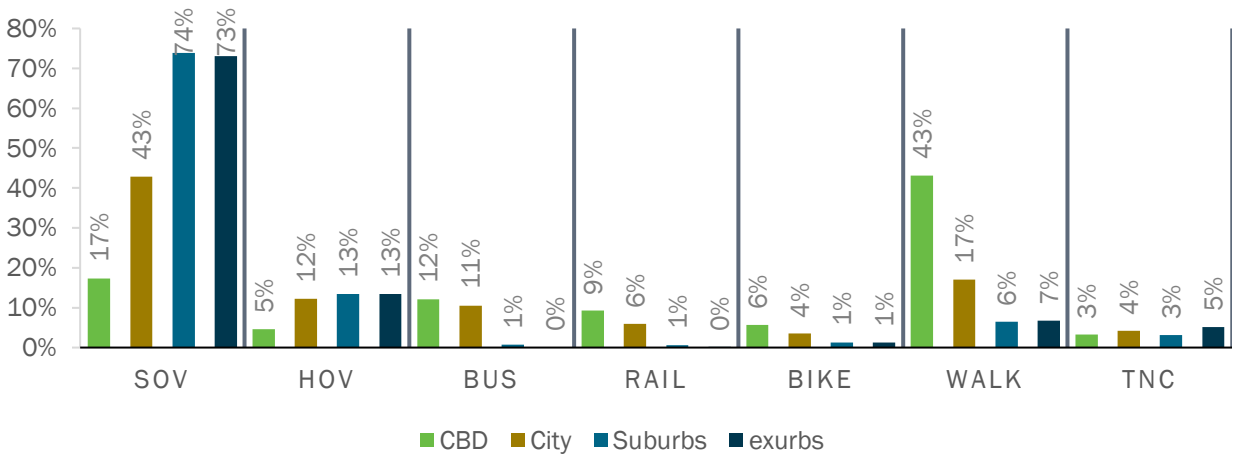
(a) Scenario A3 (High Sharing, Partial Automation)



(b) Scenario B6 (High Sharing, High Automation)



(c) Scenario C6 (Low Sharing, High Automation)



(d) Base 0

Figure 36. POLARIS Mode Share across Central Business District (CBD), City Center, Suburban, and Exurban Areas for Households Relinquishing at Least One Vehicle.

Households that retain their personally owned vehicles are increasingly responsible for the increase in both VMT and PMT as sharing decreases and automation increases. As shown in Figure 37, households with vehicles contribute substantially more to per-capita PMT, VMT, and VHT because persons without vehicles are more likely to use modes that contribute to PMT but not VMT (i.e., transit, walking, and biking). However, from Scenario A2 to Scenario C6, this difference becomes more and more pronounced as automation increases (Scenarios A to B) and sharing decreases (Scenarios B to C). When comparing households with and without vehicles (Scenarios A3 and C6), results show that although households in Scenario A3 can rely on shared modes like ride-hail/ride pool to meet their mobility needs, the households in Scenario C6 without a car do not have such options; this leads to a much higher PMT disparity compared to households with vehicles. Similarly, in Scenario C6, the contribution to the per-capita PMT and VMT by households that own vehicles are respectively 20 and 22 miles higher compared to the households that do not own vehicles, for the same reasons mentioned above, with the addition of extra travel for the households that own AVs due to reduced VOTT and extra ZOV miles. In other words, households that own vehicles travel significantly more than households that do not—an effect that is magnified as automation increases.

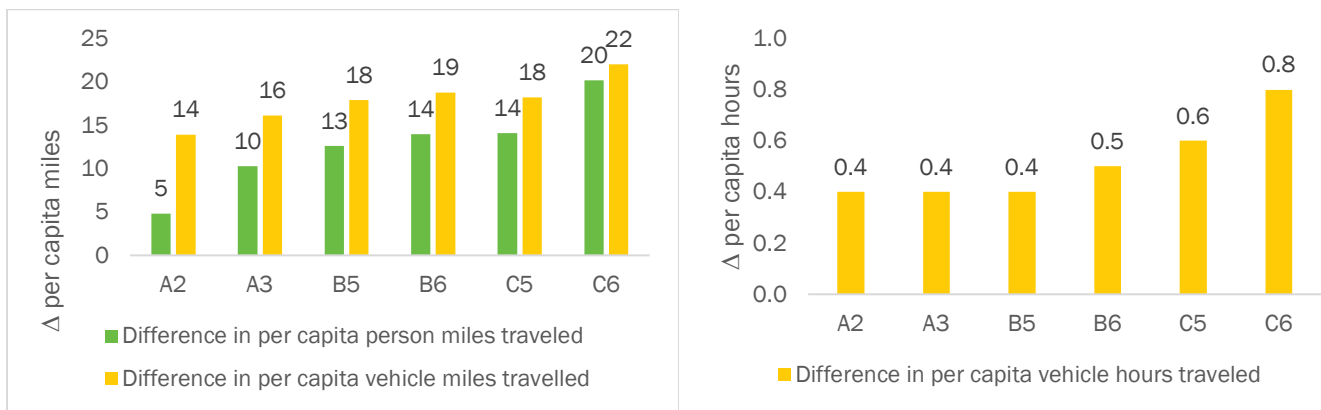


Figure 37. Disparity between Households That Do and Do Not Own Vehicles in POLARIS.

4.2 Ride-Hailing

Ride-hailing fleets are modeled jointly from both the demand and supply perspectives in POLARIS. For demand, POLARIS generates ride-hailing requests using a household vehicle ownership model and a mode-choice model that includes fares and travel times to identify the preferred mode. For supply, POLARIS allows the operation of multiple ride-hailing operators. When a traveler agent requests a ride, the operator assigns a vehicle to serve the respective request. POLARIS also simulates dynamic ride-pooling. Pooling occurs depending on the delay experienced by each passenger, as well as the delay incurred by the path diversion being less than a given threshold (6 minutes). In other words, if a passenger in a ride-pool-eligible vehicle has already been delayed up to the threshold due to other pickups and drop-offs, that vehicle will no longer pool until all such passengers have left the vehicle.

High-sharing scenarios without vehicle repositioning to search for riders (i.e., Scenarios A and B) achieve lower VMT due to the efficient use of ride-hailing with a small share of miles without a passenger (below 15%) combined with significant amount of ride pooling (22%–27%).

Figure 38 shows that shared automation (Scenario B) produces a substantial increase in ride-hail travel compared to the other scenarios (up to 112 million daily miles traveled). Scenario B6 also has the highest

percentage of pooling; 27% of total ride-hail VMT is pooled, more than offsetting the 14% share of deadheading trips for repositioning and passenger pickup. These results are consistent with existing literature that estimates the share of empty miles between 14% and 22% [43, 44, 45]. Overall, this result, with pooling largely offsetting the empty miles of travel, may be attributed to several factors: (i) high household vehicle retirement rates (more ride-hailing requests due to vehicle disposal leads to more opportunity for pooling, especially because the high vehicle disposal rates tend to occur in dense urban areas); (ii) reduced wait times due to larger fleet sizes; and (iii) reduced labor costs in the automated ride-hailing vehicles. Increased ride-hailing fleet size and utilization also help to increase the pooling rate, and can help to reduce the amount of deadheading travel, depending on overall utilization. The share of deadheading VMT is still highest for Scenario B6 due to the overall large scale of ride-hailing utilization, with more ride requests per vehicle than in other scenarios. The overall low empty miles share observed over all scenarios is driven largely by the high fleet sizes for each scenario, so further analysis can be performed to explore more efficient tradeoffs between fleet size, empty miles, wait times, and other factors of ride-hailing operations.

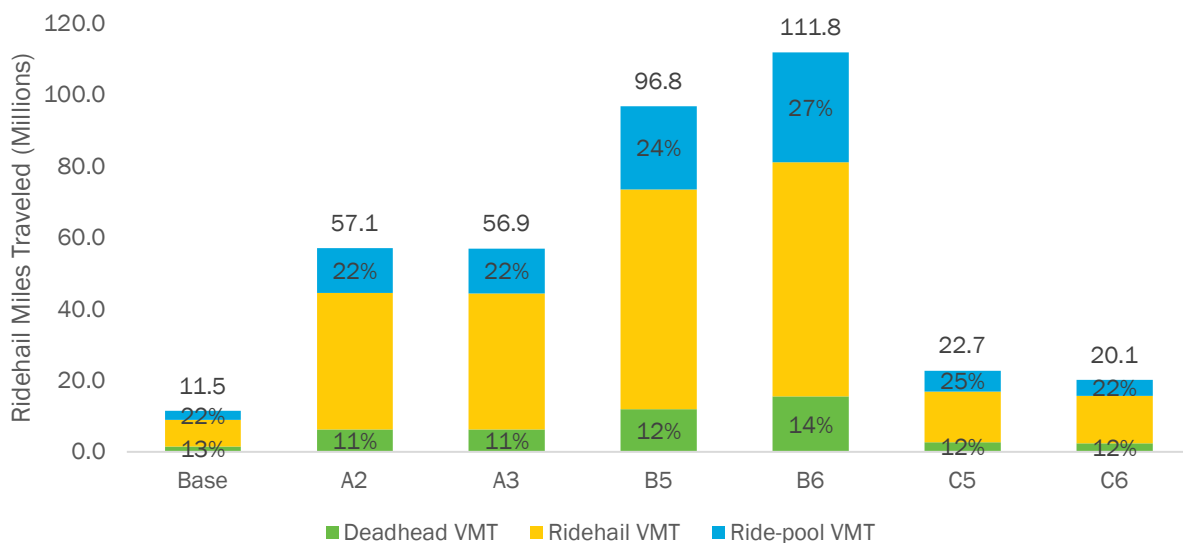


Figure 38. POLARIS Ride-hailing Operational Characteristics by Scenario.

Assuming an average of three daily trips for a private auto, a single ride-hailing vehicle can replace about six personally owned vehicles. This number can be increased by different pricing, more efficient repositioning, and increased ride-pooling, up to about 7–8 vehicles.

Figure 39 shows the cumulative distribution of the number of trips per vehicle for Base 0, Scenario A3, Scenario B6, and Scenario C6. Most ride-hailing vehicles in the high-sharing scenarios (Scenarios A3 and B6) complete 18–27 customer trips each day, although a few vehicles complete up to 50 trips. The median number of trips served increases substantially from Base 0 (18 trips per day) to Scenarios A3 and B6 (23 trips per day), due to higher ride-hailing mode share and lower background congestion. Meanwhile, the low-sharing, high-automation scenario (Scenario C6) is similar to the baseline because there is increased congestion from private AV travel. The daily travel distance distribution for ride-hailing vehicles follows a similar pattern, as shown in Figure 40.

Typical ride-hailing vehicles in Base 0 drive about 3,100 miles per day, which increases to 360 miles in Scenario B6. Scenario C6, meanwhile, has a median of only 280 daily miles driven for ride-hailing vehicles. This reduction is due to lower utilization of each ride-hailing vehicle and higher traffic congestion. Note that the results for individual vehicles are highly dependent on the fleet size assumptions, with larger fleets causing vehicles to travel less on average. The fleets in each scenario were sized so that the percentage of idle vehicles

in the peak usage period was approximately 10%, while average wait times were not raised beyond 7 minutes, as evaluated through successive runs of the simulation. The fleet size difference changes the pick-up trip VMT and wait time marginally, although high-level scenario results do not change significantly.

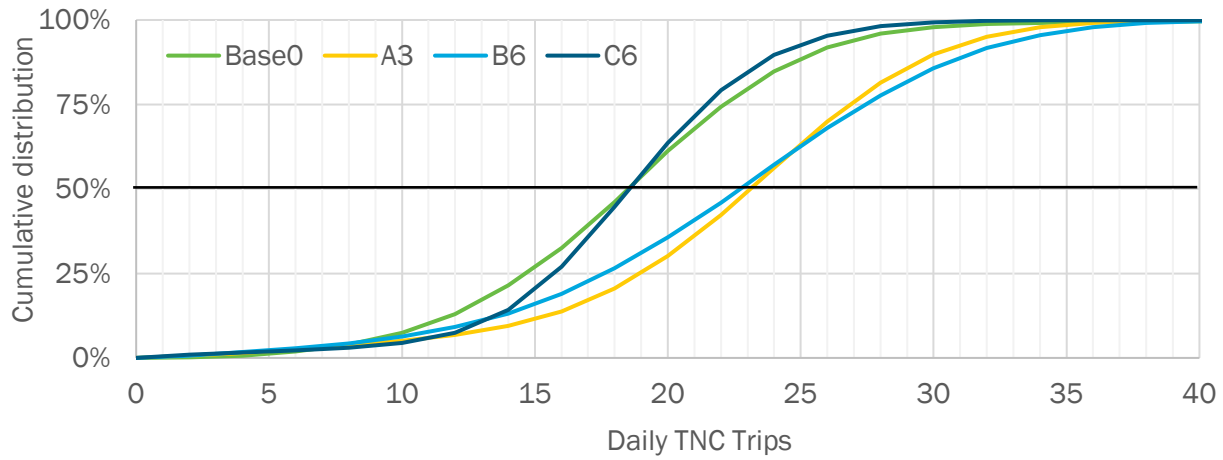


Figure 39. Cumulative Distribution of Daily Trips per Ride-hailing Vehicle in Scenarios Base 0, A3, B6, and C6.

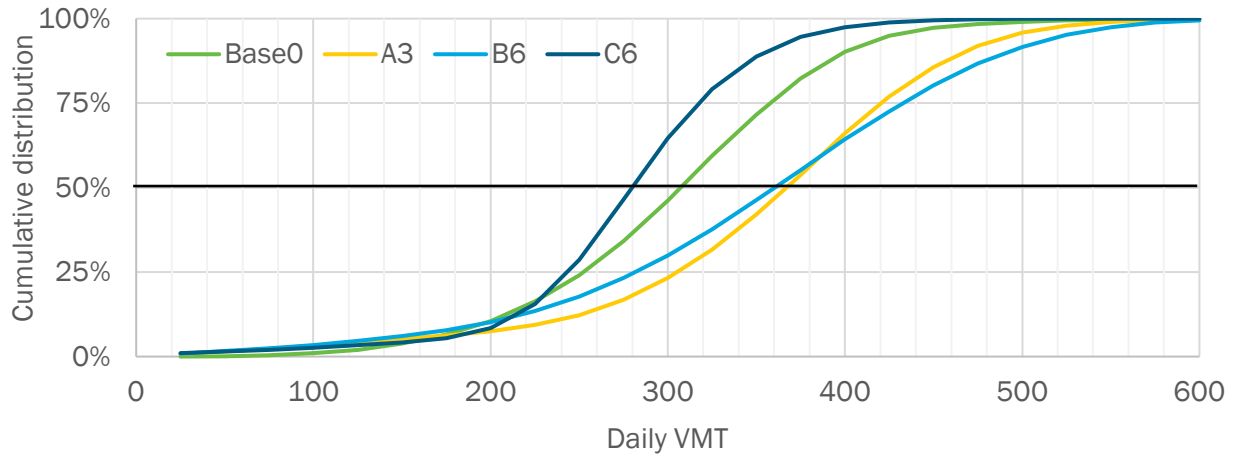


Figure 40. Cumulative Distribution of Total Daily Miles Driven by Ride-hailing Vehicles in Scenarios Base 0, A3, B6, and C6.

Figure 41 illustrates the share of vehicles performing pickup (traveling to a passenger) and drop-off (taking a passenger to a destination) operations or remaining idle for the baseline and Scenarios A3, B6, and C6. For much of the day in the baseline, less than 80% of ride-hailing vehicles are being utilized at any moment, and even fewer are utilized at off-peak times in the high-sharing scenarios. Therefore, SAV fleet sizes can be reduced by incentivizing the shifting of some trips to the off-peak periods.

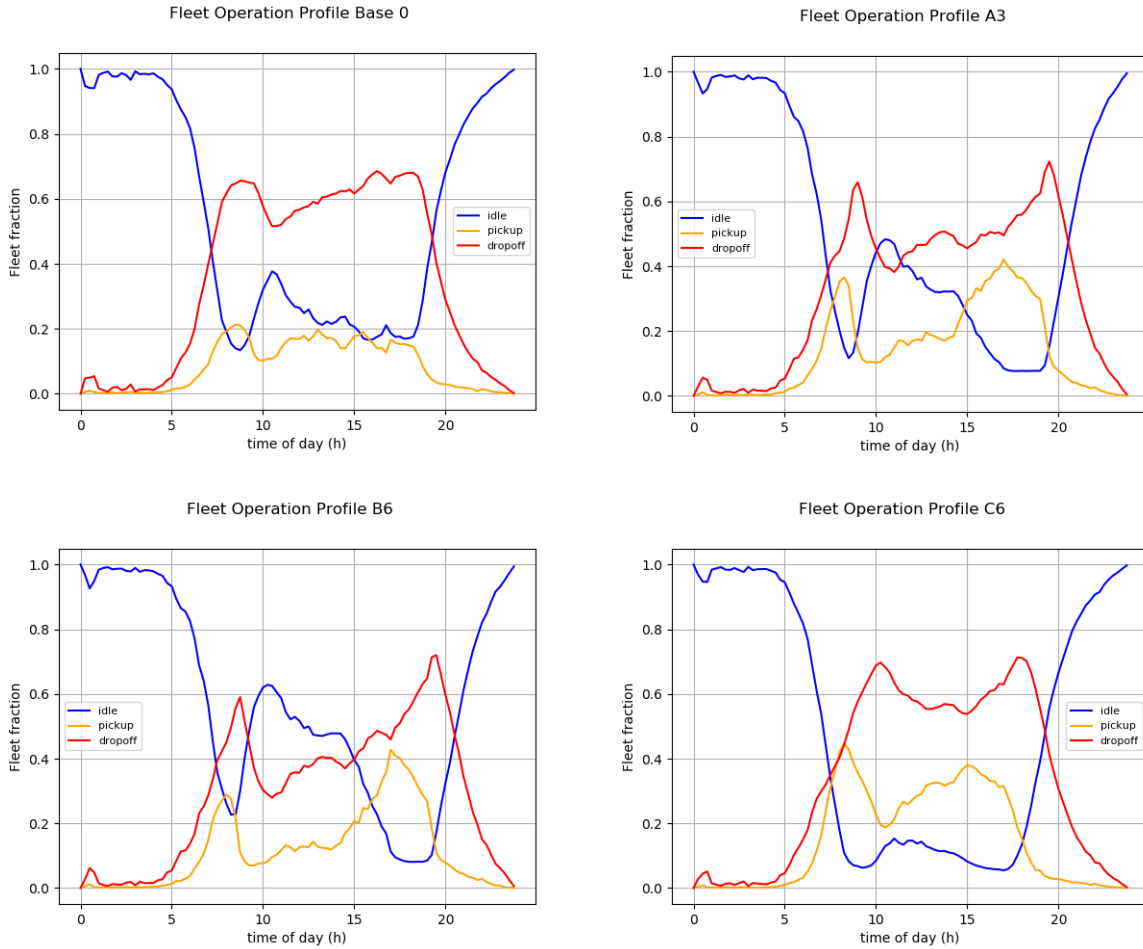


Figure 41. Fleet Operation Profile in POLARIS for Scenarios Base 0, A3, B6, and C6.

Ride-sharing allows more efficient fleet utilization by successfully serving more trips with smaller required fleet sizes and fewer VMT for the same level of mobility. Figure 42 shows the number of trips throughout the day in Scenario B6 with pooled ride-hailing (multiple customers can share the ride at the same time) and without (the vehicle can only carry one customer at a time). At the evening peak, pooled ride-hailing allows an increase of approximately 20% in the number of served trips compared to no pooling. The highest share of pooled ride-hailing occurs exactly at the peaks.

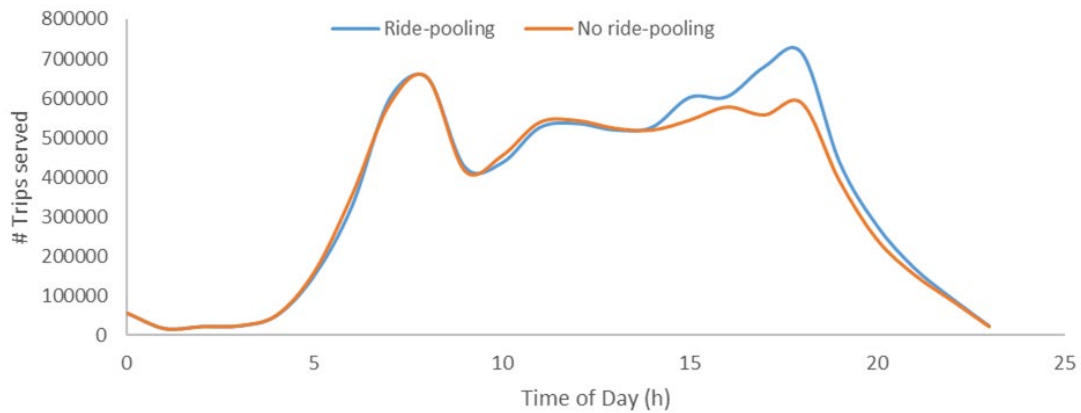


Figure 42. Trips Served by Time of Day with and without Ride-pooling in POLARIS.

Overall congestion is a key factor in ride-hailing performance because vehicles can perform more trips with shorter travel times in less congested networks. Therefore, the reduced VMT in Scenarios B5 and B6 give additional performance benefits and allow for smaller fleets to meet the same demand.

Figure 43 (left) depicts the average ride-hailing trip time (pickup + drop-off) for Scenarios B6 and C6. Most of the time, the trip times are significantly higher in Scenario C6. This travel time difference is an outcome of the lower average speed of ride-hailing vehicles in Scenario C6, as shown in Figure 42 (right). The higher travel time and lower speed in Scenario C6 are caused by the congestion created by the empty miles from private vehicles, which slows ride-hailing vehicles and prevents them from serving more trips. Because there is lower congestion in Scenario B6, a significant share of vehicles were able to perform more than 30 trips for Scenario B6 compared to a negligible share for Scenario C6, as shown in Figure 43. In other words, an additional benefit of lower congestion in Scenario B is the ability of a smaller ride-hailing fleet size to serve the same travel demand.

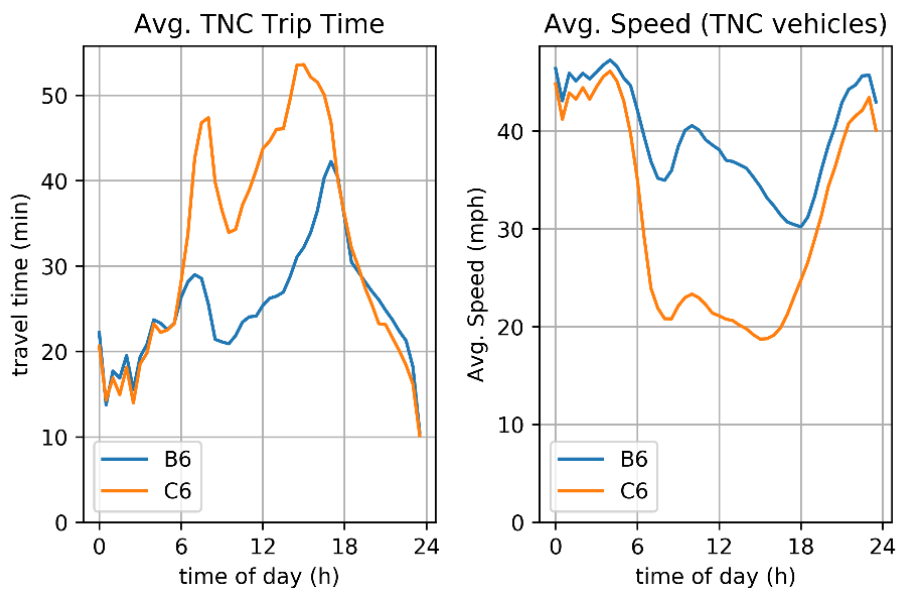


Figure 43. Travel Time (Pickup and Drop-off Combined) and Average Speed of Ride-hailing Vehicles in Scenarios B6 and C6.

4.3 Privately Owned AVs

Travel behavior is a key driver of the results observed across the various scenarios; much of the behavioral change is driven by assumed changes in VOTT and household vehicle disposal. From the choice of modes, destination, and start times to trip rerouting and re-planning in response to changing congestion patterns, travel behavior forms the core of the POLARIS simulation model and the workflow. Many of the behaviors observed are the result of key scenario assumptions, primarily the change in VOTT in AVs and the household vehicle disposal response to growing ride-hailing availability. Both of these factors have a major influence on the simulation results, with the VOTT changes based on vehicle automation level impacting the mode, destination, start time, and route choices. Research conducted as a part of the Mobility Decision Science pillar on the sensitivity of POLARIS to VOTT changes has shown strong elasticity at -0.25 (i.e., a 2.5% reduction in travel for a 10% increase in VOTT parameter for an individual), although this response is highly dependent on context and geography. For more details, please refer to the Mobility Decision Science Capstone report section entitled “Mobility and Energy Impacts of the Value of Travel Time.” Given the range of VOTT changes specified as scenario inputs in Section 3.2 of this report, with AV VOTT reduction ranging from 30% to 65% for a fully automated vehicle, a substantial increase in travel for households that own AVs is expected.

Households with privately owned, fully automated vehicles (Scenario C6) show substantially higher PMT (57%) and PHT (38%) relative to households without AVs. As shown in Figure 44, the per-capita PHT for households that own fully automated vehicles increases to almost 2 hours per day, a substantial increase over the average of 1.3 hours per day for non-automated vehicles owners in Scenario C6. In addition, VMT increases by 82% for households with an AV. As previously stated, this is a result of the assumed VOTT reduction in the fully automated vehicle case, which represents the ability of travelers to multitask and engage in other activities during AV travel [46, 47], along with vehicle repositioning trips.



Figure 44. POLARIS (a) PMT and VMT, and (b) PHT and VHT per Capita by AV Ownership (Scenario C6).

Households with AVs exhibit substantially different travel behavior compared to households without AVs. This behavior includes a propensity to travel longer during peak evening hours and to take more SOV trips. Figure 45 shows many of the key traveler behavior indicators for those in households with and without AVs for Scenario C6. Households with AVs exhibit higher travel times compared to households without AVs, with an average trip travel time for AV households being approximately 7 minutes higher than the non-AV households during peak periods. In general, households with AVs tend to travel longer distances and for longer durations especially for discretionary activities. For discretionary activities, the average travel time may be more than 6 minutes higher and the average travel distance may be 4 miles higher than the households without AVs. The share of SOV trips for AV households is also 7% higher than that of non-AV households. Additionally, these households travel longer distances for longer durations by SOV, HOV, and ride-hail modes compared to the households without AVs. The reduced VOTT for AV travel is the major factor contributing to

the differences in the travel behavior between households with and without AVs, along with unloaded vehicle repositioning as household members share the use of the AV.

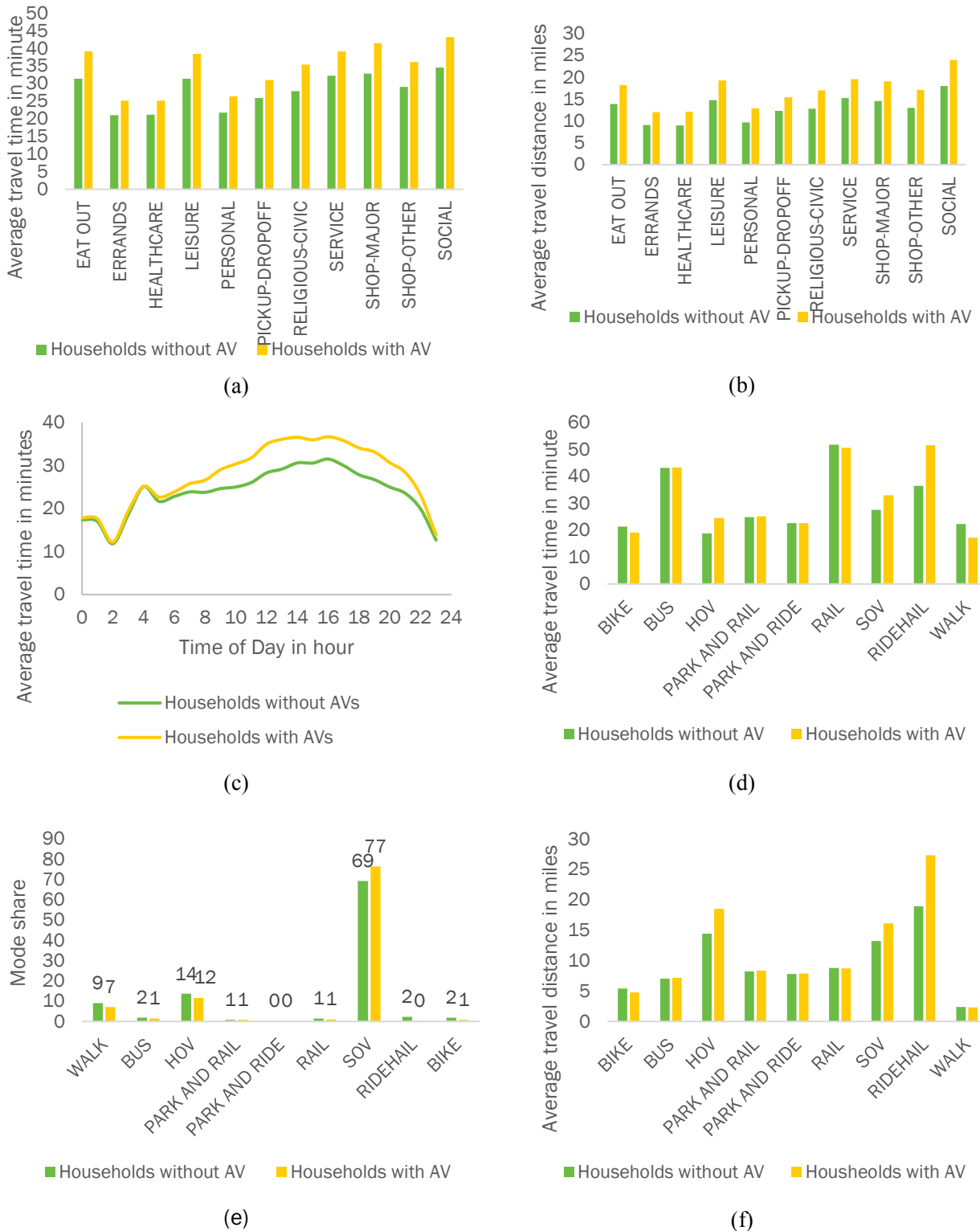


Figure 45. Comparison of (a) Average Travel Time by Activity Type, (b) Average Travel Distance by Activity Type, (c) Average Travel Time across the Day, (d) Average Travel Time by Mode, (e) Mode Share, and (f) Travel Distance by Mode in POLARIS (Scenario C6).

The use of privately owned AVs leads to drastically increased VMT and greatly increased unloaded vehicle travel, where 1 out of 7 vehicles in the system is empty, compared to 1 out of 25 in the high-sharing, high-automation case (Scenario B6). A 52% penetration of private fully automated vehicles (Scenario C6) leads to an increase of 25% in VMT compared to Base 6. This occurs due to two primary phenomena: the increase in unloaded VMT due to increased vehicle repositioning in the privately owned AV case, and the increase in overall travel resulting from the assumed reduction in VOTT in an AV. Figure 46b shows the temporal distribution of VHT by type (ownership, automation level, passenger load) and by time of day. The distribution clearly demonstrates a significant travel increase in Scenario C6. This is largely driven by lower VOTT, with much of the increase taking place in privately owned AVs (represented by orange). However, there is also additional unloaded travel for both ride-hail vehicles and SAVs. In Scenario C6, almost 22% of privately owned AV travel is done by unloaded/empty vehicles. Overall, 15% of all travel hours in the system are driven unloaded in Scenario C6; in Scenario B6, unloaded travel occurs only in the SAV (automated ride-hail) vehicles, with only 14% of total SAV travel hours unloaded.

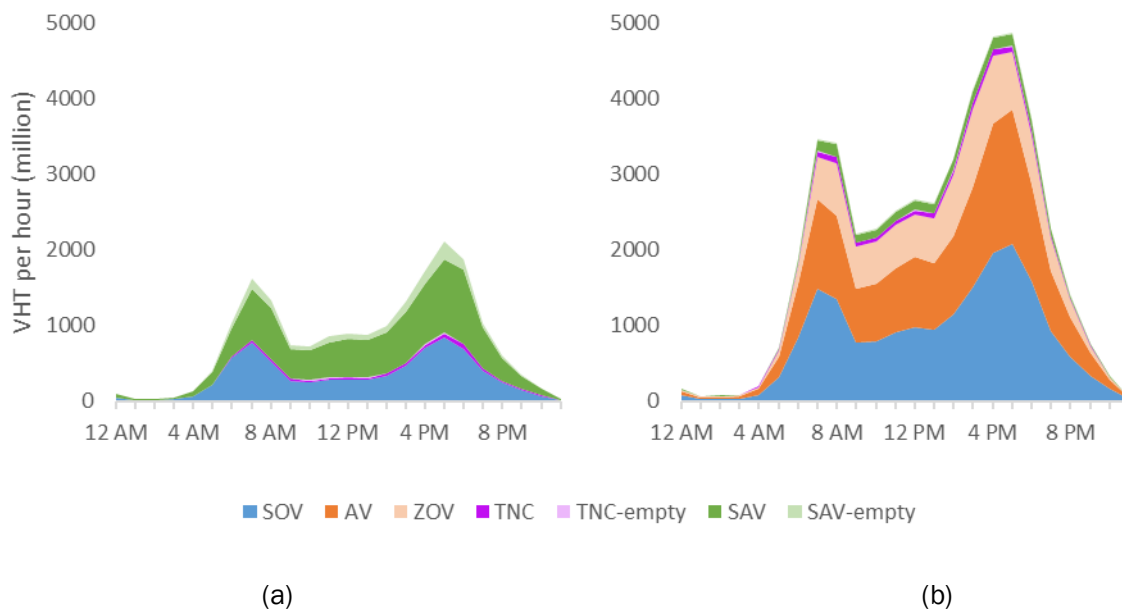


Figure 46. Temporal Distribution of VHT by Auto Modes for (a) Shared AV (Scenario B6) and (b) Private AV (Scenario C6) in POLARIS.

The finding that privately owned AVs result in higher VMT is corroborated by previous studies, including a field study conducted by Herb et al. [17], who found an 85% increase in total household VMT. However, their naturalistic experiment produced a higher percentage of unloaded or zero-occupancy vehicle (ZOV) trips, which resulted in somewhat higher VMT compared to the current study. This could be due to the fact that in Harb et al. [17] unloaded trips (driven by chauffeurs) were taken to perform household errands, whereas in the current study such ZOV trips were conducted exclusively to reposition the vehicle without any opportunity to address household needs independent of household travelers. In addition, in the current study only 52% of households owned an AV, so if ownership was extended to 100% the VMT increase of 25% would have been higher. Overall, the household level increase in the simulations of 82% is very close to the experimental finding of 85% increase, in spite of the lack of induced household errand trips conducted by the vehicle in ZOV mode in the simulation. Additionally, the lack of congestion increases shown in [17] is due to the small sample size of the field experiment.

The findings of the shared and private AV scenarios studied here are generally consistent with previous simulation observations regarding VMT and VHT increases as well. The 25% increase in VMT (Scenario C6 versus Base 6) observed in this study is substantially higher than the 16% observed in the AV scenario by [48].

However, that study did not simulate AV repositioning, which may account for the smaller increase [48] compared to this study, and may explain why that study found a greater VMT increase in the SAV scenario than the AV scenario, contrary to the finding here. Rodier [49] also found a lower increase in VMT, up to 11% in AV and 18% in SAV scenarios, in contrast to the findings in this study. In this case, the lower VMT can be explained by the modest reduction in drive VOTT assumed (25%), along with the lack of vehicle repositioning trips. Zhao and Kockelman [8] also found a VMT increase up to 41%, although significant limitations are mentioned in the study due to the use of a four-step travel demand model, such as the lack of repositioning travel.

4.4 Multi-Modal Travel

Even without changes to the existing transit infrastructure and schedules in Chicago, simulation results show that the mode share of transit will increase by 67% and 100% under Scenarios A3 and B6, respectively, due to reduction in vehicle ownership of 45% and 75% and increased acceptance of shared and non-auto-based travel modes. The Chicago metropolitan region resembles a hub-and-spoke system when it comes to transit service. Major urban rail lines operated by the Chicago Transit Authority (CTA), as well as the commuter rail lines operated by Metropolitan Rail (Metra) provide services that start or terminate in the Central Business District. Moreover, there are major bus lines operated by the CTA in the urban core and suburban bus lines operated by PACE. As shown in Figure 47, mode share of transit is very high in the urban core for the baseline scenario. Figure 46 also illustrates a substantial increase in the mode share of transit in the downtown region under Scenario A3 and even more so under Scenario B6. On the other hand, there is no change, or even a small decrease, in transit use in the outer regions under all scenarios, with the highest decrease under Scenario C6. This is expected, because many in these areas shift to greater utilization of private mobility and are more likely to purchase AVs. Decreases in the outer regions under other scenarios are due to vehicle disposal making the drive-to-transit mode less available.

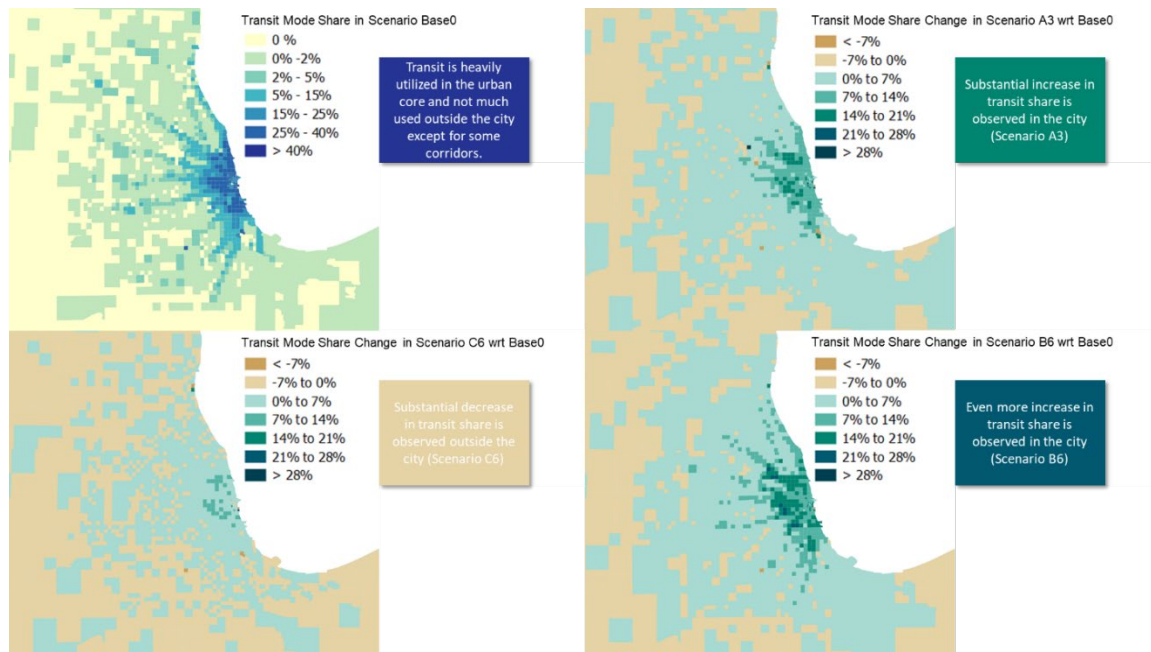


Figure 47. POLARIS Transit Mode Share in the Baseline Scenario and Percent Change under Scenarios A3, B6, and C6.

In a hub-and-spoke system like the Chicago region, ride-hailing and transit can be complimentary, with transit being a key mobility provider in the urban core and ride-hailing providing personal mobility in the suburbs. As shown in Figure 48, the mode share of ride-hailing increases heavily under Scenarios A3 and B6, especially in the areas surrounding the urban core. In this way, ride-hailing and transit complement each other: people rely on ride-hailing where the transit service is not very frequent and reliable, and travelers choose transit in the

urban core where it has high frequency and lower travel times as the urban core gets congested. Please refer to Figure 49 for a direct comparison of the changes in transit and ride-hailing mode share.

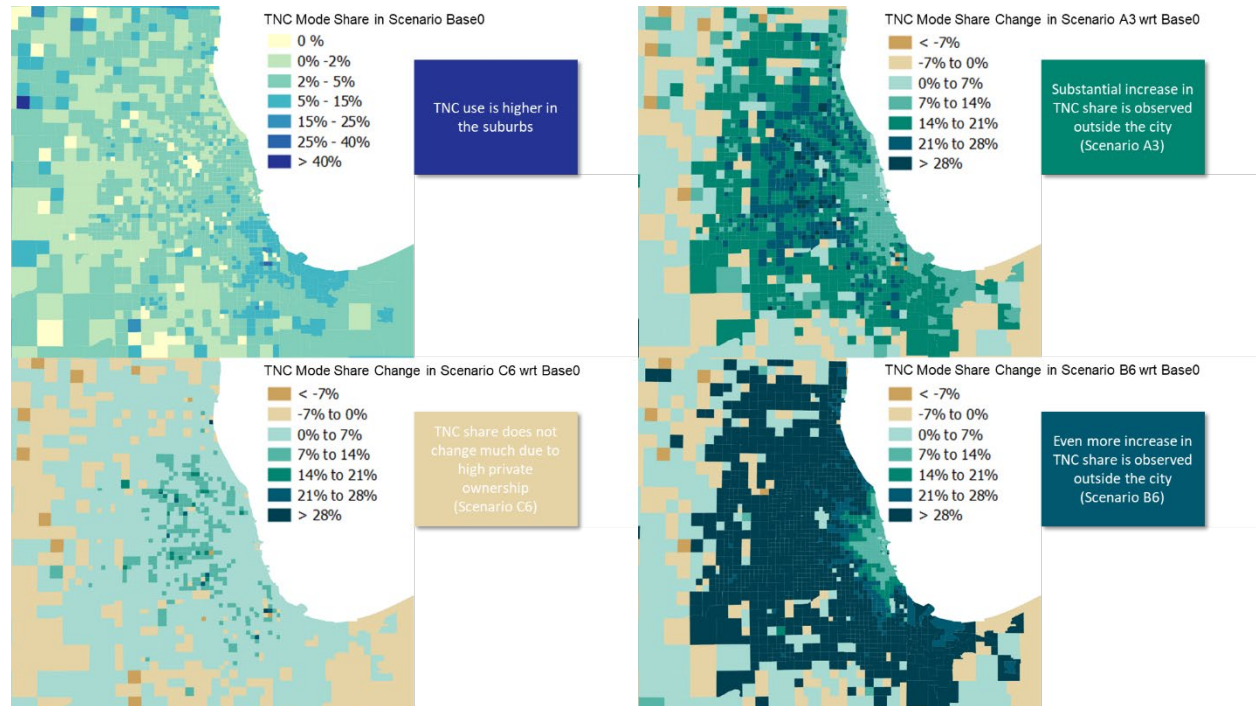


Figure 48. POLARIS TNC Mode Share in the Baseline Scenario and Percent Change under Scenarios A3, B6, and C6.

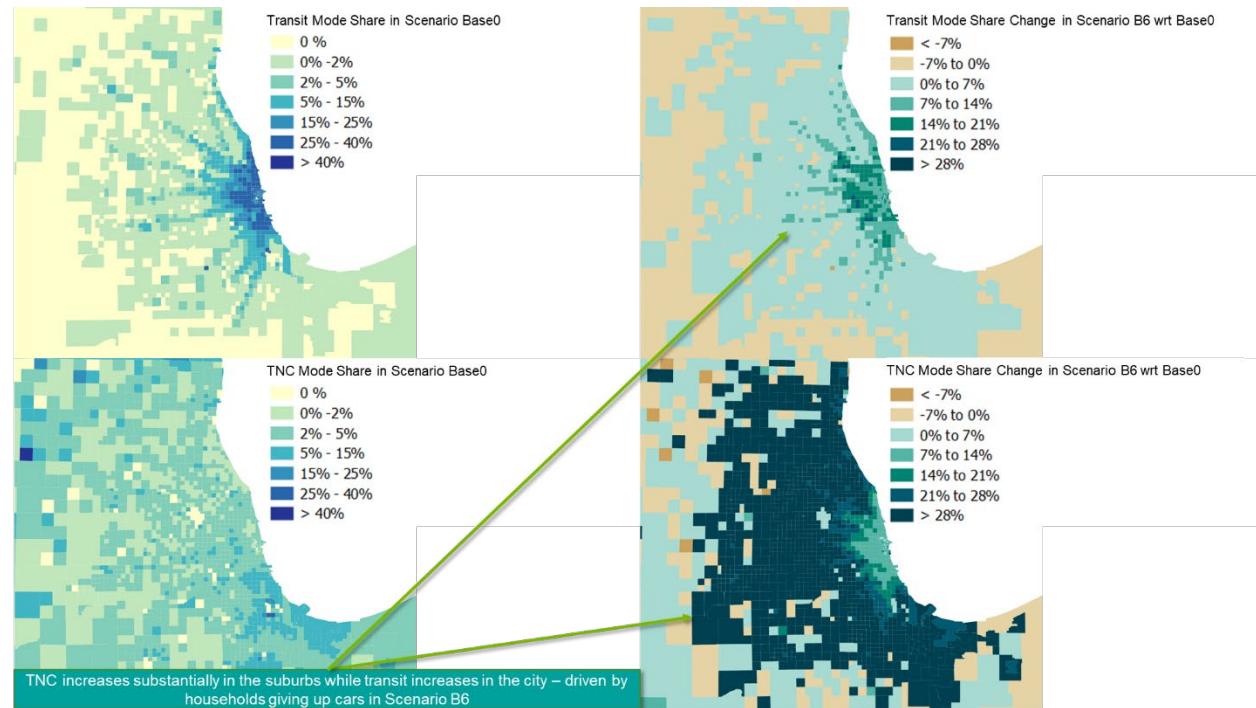


Figure 49. Comparison between Ride-hailing and Transit Mode Share Changes in POLARIS (Scenario B6).

Transit is vital to the overall transportation system. In a scenario with no transit, all mobility and energy metrics become substantially worse in the urban core; there is a 52% increase in VHT and a 23% decrease in travel efficiency (passenger miles per kilowatt-hours). In order to analyze the effect of transit on regional mobility, an additional scenario was implemented to analyze a no-transit case. This no-transit scenario was the same as Base 0, but with all transit links and vehicles removed in the Chicago metropolitan region. The findings are shown in Table 9 and indicate there would be substantial adverse effects on mobility and energy use in the entire region, while the negative effects are more emphasized in the urban area.

Table 9. Percentage Change in Mobility and Energy Metrics with No transit in POLARIS (vs Base0)

Factor	Base 0		% Change with No Transit	
	Metropolitan Region	City of Chicago	Metropolitan Region	City of Chicago
VMT (million miles)	296.6	32.4	+6%	+37%
VHT (million hours)	10.3	1.5	+13%	+52%
Average speed (mph)	28.8	21.3	-7%	-10%
Energy (GWh)	435.3	42.6	+4%	+29%
Travel efficiency (passenger-miles/kWh)	0.94	1.40	-4%	-23%

4.5 MEP

In addition to the travel and energy parameters presented in Table 8, the MEP computation takes into account the affordability (or cost) of travel in different modes, including operational cost associated with driving and ride-hail modes in various scenarios. Table 9 shows that cost of ride-hailing drops significantly in Scenarios B and C, while the cost of driving stays relatively stable (except for a slight increase in Scenario C6 due to reduced fuel economy resulting from increased congestion).

The increase in MEP and travel efficiency for the shared mobility scenarios (Scenarios A and B) shows that shared mobility has an additional travel efficiency impact beyond that provided by the vehicle technology improvements alone. Changes in MEP across scenarios can be attributed to increases or reductions in energy intensity, cost of travel, and the speed of the network in each of the scenarios. The improvement in MEP scores for each scenario (relative to their respective baselines) demonstrates that the greatest improvements are possible with a combination of increased network speeds, coupled with reduced energy and cost of travel (with MEP improvements of 51% and 76% for Scenarios B5 and B6, relative to their respective baselines Base 5 and Base 6). When long-term technology improvements are taken out of the equation and partial automation is considered rather than full automation, there is a slight reduction in travel speeds on the network in Scenario A compared to Scenario B, and MEP scores still improve by 34% in both Scenarios A2 and A3 compared to their respective baselines. Finally, even as the technology improves and levels of vehicle automation increase, if private vehicle ownership remains dominant, the resulting MEP improvements turn out to be the smallest of all scenarios (23% and 10%, respectively, for Scenarios C5 and C6, relative to their respective baselines Base 5 and Base 6).

The MEP improvements in the high-sharing, high-automation scenario are driven by major improvements in ride-hailing-specific MEPs (i.e., ride-hailing-MEP improved by 380% in Scenario B6 with respect to Base 0). Assumptions associated with vehicle retirement (~70% in Scenario B6), coupled with ride-hailing having large improvements in energy intensity (63% reduction in energy intensity per passenger mile with respect to Scenario B0) and affordability (65% reduction in cost/passenger mile with respect to Scenario B0) lead to these high ride-hailing-MEP scores in Scenario B6. Similar trends can be discerned from the right panel of Figure 50, which depicts improvements in ride-hailing scores in comparison with respective baselines. While Scenario C5 shows a drop in both energy intensity and cost values with respect to Base 5, leading to a 74% improvement in ride-hailing MEP score, Scenario C6 shows a decrease in cost but an increase in the energy intensity of ride-hailing (with respect to Base 6). This results in an increase in ride-hailing MEP that is less

than that in Scenario C5, illustrating that a higher MEP results from a case in which both energy intensity and the cost of travel are reduced.

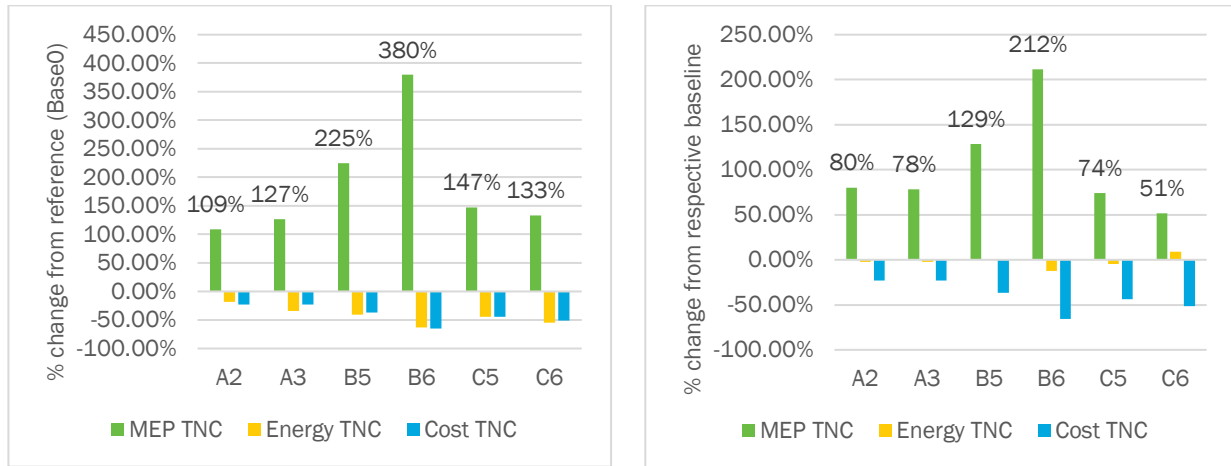


Figure 50. Ride-hailing MEP Scores, Energy Intensity, and Cost Values.

The MEP increase (Figure 51) is greatest for Scenario B6, with a 173% increase relative to Base 0 and a 76% increase over the long-term baseline (Base 6). Scenario C6 only increases by 10% with respect to Base 6 with the same technology level; this demonstrates the benefits of high-technology shared-mobility scenarios.

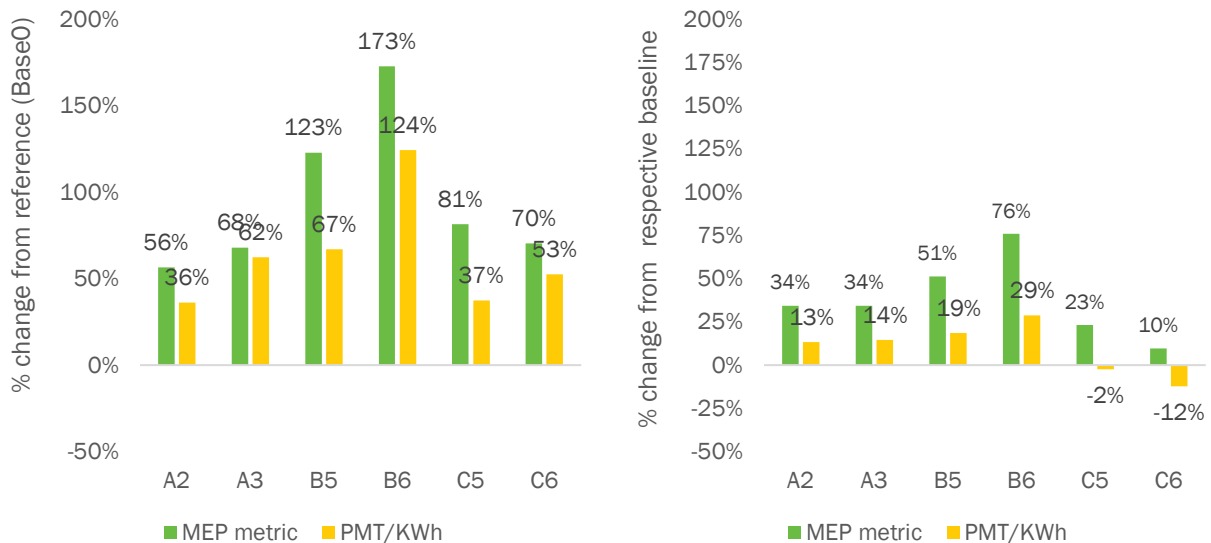


Figure 51. MEP and PMT Results from POLARIS.

Figure 51 also shows the PMT per kilowatt hour consumed, defined as travel efficiency. This measure is calculated by dividing all PMT provided by the transportation system in each scenario by the total energy consumption, and is a direct measure of realized energy productivity. The MEP metric, on the other hand, is a measure of the potential MEP that could be provided by the system in each scenario.

Increased congestion and lower transportation system efficiency in the case of privately owned, fully automated vehicles (Scenario C6) leads to a moderate MEP increase and a travel efficiency decrease (changes of +10% and -19%, respectively, compared to Base 6). Scenario C uses similar vehicle class and powertrain assumptions as Scenario B, in addition to having a higher penetration of privately owned AVs. However, the

improvement in MEP in the low-sharing, high-automation case (Scenario C) is lower than that for the high-sharing, high automation case (Scenario B). This is consistent with expectations; Scenario C assumes a lower vehicle retirement rate, which means that most individuals travel in a privately owned AV. Improvements in energy intensity and cost factors in Scenario C are dwarfed in comparison to the congestion effects associated with increased travel from a high penetration of personally owned AVs, resulting in lower MEP scores for that scenario compared to Scenario B.

Figure 52 provides the spatially resolved MEP calculations across each scenario compared with their respective baseline. As previously discussed, Scenario B, which primarily focuses on pooled ride-hailing, demonstrates the highest MEP growth. In addition, MEP improvement is not evenly spatially distributed; the greatest increase occurs in dense urban areas. Figure 51 illustrates the change in the MEP calculation between each scenario and its corresponding baseline run (e.g., Scenario B5 versus Base 5), and between the low- and high-technology runs for each scenario (e.g., Scenario C6 versus Scenario C5), along with a comparison between each of the high technology scenarios (Scenarios A3 to B6, and B6 to C6). The results for the A scenarios show MEP increasing moderately in the downtown area and along several major highway corridors near downtown, as congestion decreases due to increased ride-hail and transit usage. The slight MEP increase throughout the region is also influenced by reduced energy consumption due to improved vehicle technology.

In Scenario B6 there is a much larger and more widespread increase in MEP in the high-tech scenario because many more households in the dense urban areas retire vehicles and use pooled rideshare. This causes network conditions to improve and fuel consumption to decrease, especially in areas well served by transit and along most major highway corridors. Comparing Scenario B6 to Scenario B5 shows that the general vehicle technology and ride-share service improvements cause a widespread increase in MEP throughout most of the City of Chicago and inner-ring suburbs.

The low-sharing, high-automation scenarios are possibly the most interesting from a MEP perspective. In Scenario C5, as private use of AVs starts to increase, congestion and fuel use in outlying wealthier suburbs that are poorly served by transit increase, reducing the MEP. In Scenario C5, however, the vehicle retirement and increased ride-hail use, counteract much of this effect in many areas, still leading to some MEP increases.

Finally, in Scenario C6, the use of private AVs has increased to such an extent that MEP begins to decrease in many areas. Those living in the Chicago downtown core tend not to travel as far because they already have high access to quality activity spaces, so congestion increases less here, and increased transit and ride-hail use still lead to modest overall MEP increases. However, the rest of the suburban areas, especially in wealthier locations (where adoption is highest) or outlying areas (where there is more opportunity for much further travel as VOTT is reduced), see widespread use of private AV leading to drastically increased congestion and travel times. This coupled with the additional unloaded VMT that decreases energy efficiency by the automobile mode, decreases MEP throughout much of the region. It is important to note, however, that the increased travel times that lower MEP do not account for the perceived reduction in travel burden from reduced VOTT. Therefore, an MEP calculation based on perceived accessibility rather than observed travel times would not show such drastic reductions, and would likely increase in many areas due to productive in-vehicle time use from AVs.

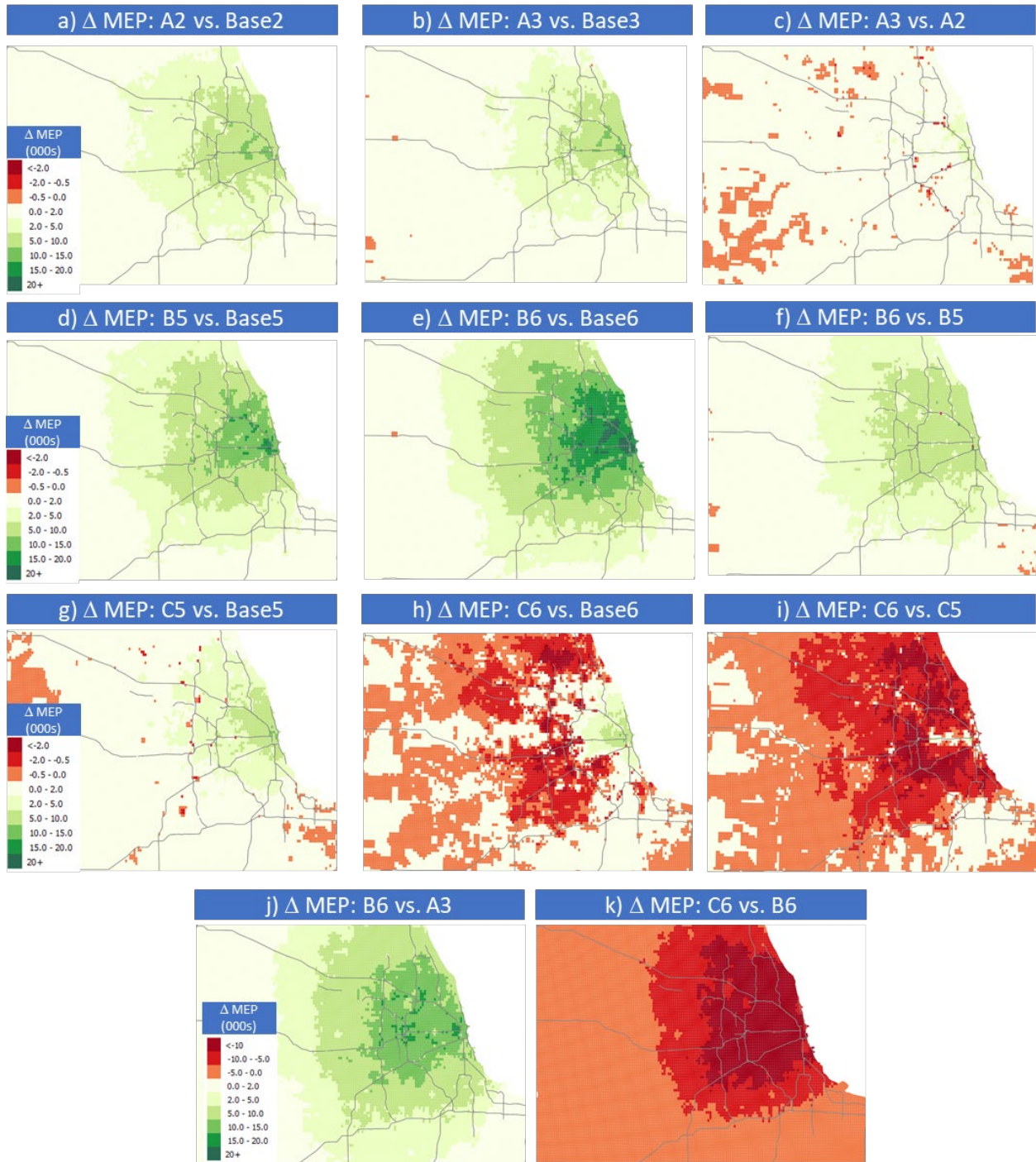


Figure 52. MEP Evolution across Each Main POLARIS Scenario.

4.6 Light-Duty Vehicle Charging Infrastructure

Scenario C6 considered 450,000 personal BEVs in Chicago, suggesting that 6,880 fast-charging plugs could be necessary to meet the demand of privately owned vehicles (a 35× increase over existing infrastructure) based on the assumed PEV market penetrations. The current study did not consider the electric charging demand of ride-hailing or freight. Figure 53 shows maps of POLARIS-simulated charging demand overlaid with public charging networks from EVI-Pro (Table 10 provides quantitative results for each workflow scenario). As the total BEV population increases across each scenario, as expected, the count of public charging events also increases. However, the increase is not proportional, because increased levels of BEV adoption result in better charging network utilization (events per plug increases with fleet size). As real-world travel data at this scale is either nonexistent or costly to acquire, POLARIS provides an efficient approach to exploring infrastructure requirements for high-penetration electrification scenarios.



Figure 53. Simulated Charging Demand across Chicago.

Table 10. Summary of EVI-Pro Public Charging Networks Simulated for POLARIS Workflow.

Parameter	Scenario					
	A2	A3	B5	B6	C5	C6
<i>Number of personal BEVs</i>	15,732	30,148	73,240	173,612	158,868	454,436
<i>Public charge events</i>	2,412	4,976	11,324	27,068	23,132	73,012
<i>Public stations</i>	564	804	1,232	1,828	1,664	2,724
<i>Public L2 EVSE</i>						
<i>Plug count</i>	672	1,376	3,096	7,064	6,292	19,236
<i>Average events/plug</i>	1.4	1.3	1.3	1.4	1.3	1.3
<i>Average plugs/station</i>	1.2	1.7	2.5	3.9	3.8	7.1
<i>Average plugs/1,000 BEVs</i>	42.7	45.6	42.3	40.7	39.6	42.3
<i>Public DCFC</i>						
<i>Plug count</i>	588	896	1,764	3,452	2,908	6,880
<i>Average events/plug</i>	2.5	3.5	4.1	5.1	5.1	6.9
<i>Average plugs/station</i>	1.0	1.1	1.4	1.9	1.7	2.5
<i>Average plugs/1,000 BEVs</i>	37.4	29.7	24.1	19.9	18.3	15.1

4.7 Goods Delivery

Goods are an essential part of the overall transportation system, accounting for a significant amount of VMT, congestion, and energy. Table 11 shows the main POLARIS results by scenario for the various goods-related market segments included in the analysis. The first section includes results for all MD and HD trucks, while the second section (e-commerce and retail shopping only) only includes parcel delivery MD trucks and passenger shopping trip results. Percent changes in Table 11 are all computed with respect to their associated baselines (e.g., Scenario A2 versus Base 2, Scenario A3 versus Base 3, Scenario B5 versus Base 5, etc.).

Table 11. POLARIS Freight Impact Results Summary

Market	Metric	Unit	Reference baselines			%Δ from Base0 ²						%Δ from short-term ³		%Δ from long-term ³			
			Base0	Base 1/2/3 ¹	Base 4/5/6 ¹	A2	A3	B5	B6	C5	C6	A2	A3	B5	B6	C5	C6
			All MDT, HDT Trips	Vehicle miles traveled (VMT)	M miles	23	23	29	3%	1%	31%	32%	32%	34%	1%	-1%	2%
VMT, HDT	M miles	20		20	26	-0.2%	-2%	28%	30%	30%	31%	-1%	-3%	-1%	0%	0%	1%
VMT, MDT	M miles	2.6		2.9	3.2	24%	23%	50%	51%	51%	55%	12%	13%	25%	25%	26%	29%
Vehicle hours traveled (VHT)	M hours	0.6		0.7	0.8	-1%	-4%	25%	31%	58%	77%	-5%	-9%	-6%	-1%	18%	33%
VHT, HDT	M hours	0.53		0.56	0.70	-3%	-6%	24%	31%	56%	71%	-7%	-10%	-9%	-3%	15%	27%
VHT, MDT	M hours	0.09		0.10	0.11	13%	11%	35%	36%	68%	113%	5%	0%	11%	12%	38%	76%
Fuel	M gallons	4.5		4.6	5.6	-20%	-31%	-6%	-23%	-0.5%	-16%	-1%	-3%	-2%	-1%	4%	8%
				3.2	3.5												
Fuel, HDT	M gallons	4.2		4.3	5.3	-21%	-31%	-6%	-22%	-0.7%	-16%	-2%	-4%	-3%	-2%	3%	7%
				3	3.3												
Fuel, MDT	M gallons	0.28		0.32	0.34	-1%	-17%	-4%	-28%	1.8%	-18%	12%	11%	24%	25%	31%	41%
				0.21	0.16												
Fuel	GWh	151		122	145	-20%	-31%	-6%	-22%	-0.2%	-15%	-1%	-3%	-2%	-1%	4%	8%
				108	118												
Electricity	GWh	0		0	0.4			0.5	0.9	0.5	0.9				15%	25%	19%
			0	0.7													
Total Energy	GWh	151	122	145	-20%	-31%	-6%	-22%	0%	-15%	-1%	-3%	-2%	-1%	4%	8%	
			109	118													
E-commerce & Retail Shopping Only	VMT: Total	M miles	20	22	23	-31%	-32%	-50%	-47%	-42%	-36%	-34%	-35%	-56%	-53%	-49%	-44%
	VMT, MDT Delivery	M miles	0.2	0.2	0.2	244%	243%	474%	484%	473%	491%	198%	200%	433%	444%	432%	450%
	VMT, LDV Shopping	M miles	20	21	23	-34%	-34%	-55%	-51%	-46%	-41%	-36%	-37%	-60%	-57%	-53%	-48%
	Total Energy	GWh	23	24	26	-39%	-49%	-63%	-72%	-54%	-57%	-33%	-33%	-50%	-54%	-38%	-29%
				18	14												
	Energy, MDT Delivery	GWh	0.7	0.8	0.7	175%	129%	294%	221%	320%	260%	195%	196%	408%	420%	441%	483%
			0.5	0.4													
Energy, LDV Shopping	GWh	22	24	25	-45%	-55%	-74%	-81%	-65%	-66%	-40%	-40%	-65%	-68%	-53%	-45%	
			17	14													

1. Each of the 'Short' and 'Long' baselines has two sub-cases shown as business as usual / VTO program success
 2. Change in electricity is shown as magnitude (MD/HD has zero electrification in Base0, so % change cannot be obtained)
 3. Scenario A2 vs. Base2, A3 vs. Base3, B5 & C5 vs. Base5, B6 & C6 vs. Base6

In the baseline scenario (Base 0), freight transportation generates approximately 10% of regional VMT but consumes about 30% of fuel (Figure 54), due to the lower fuel economy of commercial freight vehicles compared to passenger cars. This comparison is consistent with other studies, which indicate that freight traffic has a disproportionately high impact on energy consumption [41]. As a result, potential improvements in MD/HD vehicle energy efficiency could have dramatic impacts on transportation energy consumption. Part of the energy consumption impacts of trucking are due to traffic congestion, which is caused by both passenger and freight vehicles. (Refer to Table 7 for metrics of system wide mobility and congestion including both freight and passenger modes). For example, comparing the percentage changes in truck VMT versus VHT for Scenarios C5 and C6 to Base 0 shows that for each additional mile traveled, truck VHT increases at a greater rate (Table 11). In other words, increased truck travel comes at the cost of slower travel speeds.

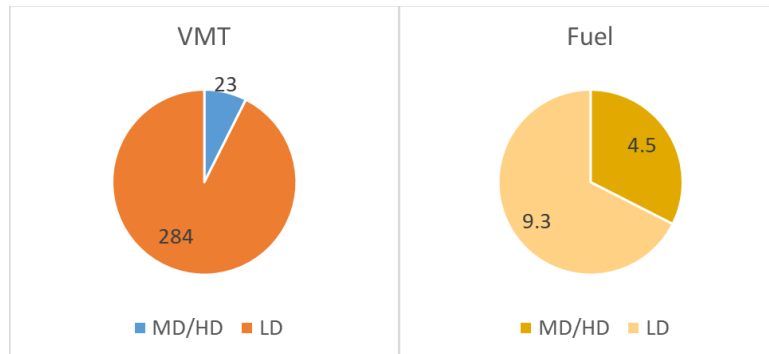


Figure 54. Base 0 MD/HD Shares of VMT (Million Miles) and Fuel (Million Gallons) from POLARIS Workflow.

At a moderate rate of commodity flow growth (1% CAGR), total freight VMT in the Chicago region will grow by 27% in the long term (Bases 4, 5, 6 versus Base 0) with detrimental impacts on energy consumption (as shown in Base 4), unless energy-efficient vehicle technologies are adopted more widely (represented by moderate and aggressive technology improvements in Bases 5 and 6, respectively). As Figure 55 shows, with the same technology as today, there would be a 25% increase in truck fuel use in the long term (Base 4 over Base 0); more efficient technologies, however, could enable a 4% to 22% energy reduction (in the low-technology Base 5 and high-technology base long-term baseline scenarios, respectively, relative to Base 0). Full electrification plays a small role in improving energy efficiency in Bases 5 and 6. Similar conclusions apply for the short term; however the impact is smaller because there would be less time for technology advancement. VMT increases slightly from the baseline (Base 0) to the short term (Base 1–Base 3), with energy consumption increasing commensurately by 5 GWh with no technology improvements (Base 0 to Base 1) and decreasing significantly by 29 and 42 GWh, respectively, with technology improvements (Base 2 and Base 3 compared to Base 0).

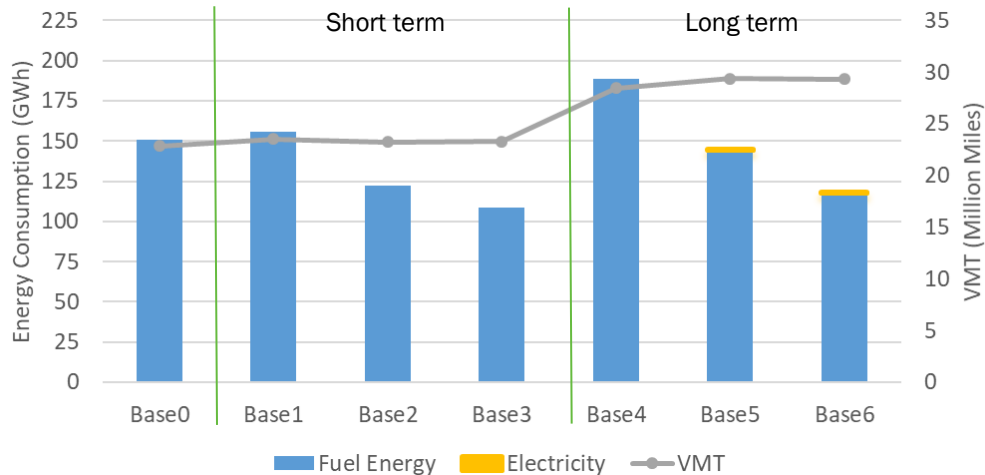


Figure 55. Impacts of Commodity Flow Growth and Vehicle Technology Changes on Freight VMT and Energy Consumption from POLARIS Workflow.

Although e-commerce is expected to generate a large increase in last-mile delivery, an overall net reduction in VMT (34–56%) and energy use (30–55%) is estimated to occur after also accounting for reduction in passenger vehicle shopping trips and improvements in vehicle technology. Table 11 shows how these estimates are derived by comparing Scenarios A, B, and C to Scenarios Base 2/3 and Base 5/6, while Figure 56 shows the VMT and energy results attributed to retail purchasing with shopping and delivery impacts for the scenarios in comparison with Base 0.

Results for the e-commerce analysis are also reported separately for MD delivery trucks and light-duty passenger vehicles for shopping trips. The e-commerce delivery rate is assumed to increase from one delivery per household per week in the current baseline (Scenarios Base 0–Base 6) to three per week in the near-term (Scenarios A2, A3), to five per week in the long-term (Scenarios B5, B6, C5, C6). Because the average shopping trip is 7–8 miles long [46] and shopping trips constitute approximately 7% of total VMT (Figure 56), the potential VMT and energy reduction associated with replacing a shopping trip with deliveries is substantial. In comparison with the base year (Base 0), if household e-commerce deliveries triple in the short term, retail-based VMT could decrease by 31%, accompanied by a 39–49% decrease in retail-based energy consumption.

In the long term, if household e-commerce deliveries were to grow to five days per week, retail-based VMT and energy consumption could decline by 36–50% and 54–72%, respectively. The VMT savings is even greater when comparing the future scenarios (Scenarios A, B, C) to their respective baselines (Base 1/2/3 and Base 4/5/6 in Table 11), which estimate that retail VMT will grow by about 5% in the short term and 14% in the long term (in comparison to Base 0), assuming household delivery rates remain at today’s levels.

Finally, total retail-related energy consumption is approximately 33% less in Scenarios A2 and A3 than in Scenarios Base 2 and Base 3 (Table 11), demonstrating that increased e-commerce leads to energy savings beyond the efficiency benefits of new vehicle technologies. Results for the long term are similar, with energy savings of 29–54% in Scenarios B and C compared to Scenarios Base 5 and Base 6.

Scenario B has lower VMT and energy use than Scenario C due to differences in household behavior, particularly the differences in trip length when passengers use ride-hailing (predominantly in Scenarios B5 and B6) versus privately owned AVs (predominantly in Scenarios C5 and C6). Passenger trips (including shopping trips) that use privately owned AVs are estimated to be longer on average than those that use ride-hailing. Therefore, although the number of passenger shopping trips is relatively constant in all B and C scenarios, these trips generate more VMT and energy use in Scenarios C5 and C6 than in Scenarios B5 and B6. Energy

use by MD delivery trucks is also higher in Scenarios C5 and C6—and VMT is the same or slightly higher—even though the number of deliveries is the same in the B and C scenarios. The differences for MD trucks are due to the additional congestion in Scenario C relative to Scenario B, because the increases in passenger travel result in more congestion, slower roadway speeds, and more circuitous routing.

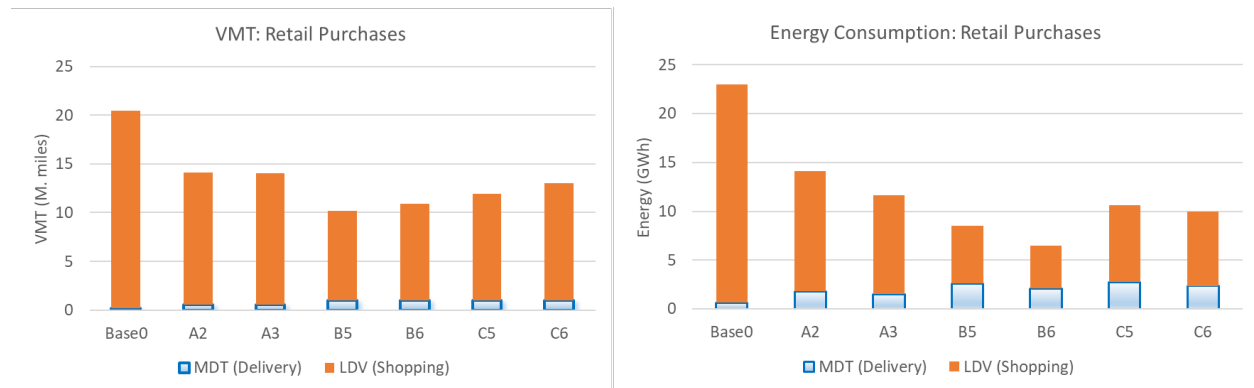


Figure 56. VMT (Left) and Energy Consumption (Right) Associated with Retail Purchasing from POLARIS Workflow.



Figure 57. Passenger Shopping Generates 7% of Regional VMT (Base0).

Even though the VMT generated by e-commerce delivery is projected to grow much more quickly than VMT generated by commodity types other than e-commerce based retail goods (based on Freight Analysis Framework forecasts), e-commerce delivery trucks constitute a maximum of only 3% of MD/HD VMT, which underscores the importance of analyzing the other types of freight traffic that make up the rest of truck VMT. The small percentage attributable to e-commerce is due mainly to the nature of last-mile delivery, where each delivery trip (in an efficient delivery system) adds only a small amount of mileage (based on parcel carrier data that shows approximately 120 stops per delivery tour). Other MD and HD truck trips tend to be much longer. For example, the in-region portion of HD truck trips averages 35 miles in the POLARIS Chicago model. As shown in Figure 58, total truck VMT are highest in the B and C scenarios, which are associated with growth in commodity flows over the long term as well as the highest e-commerce rates. Improved vehicle technology helps to mitigate energy consumption in Scenarios A, B, and C, with greater energy savings consistently achieved in the high-tech scenarios (Scenarios A3, B6, C6) compared to the low-tech scenarios (Scenarios A2, B5, C5).

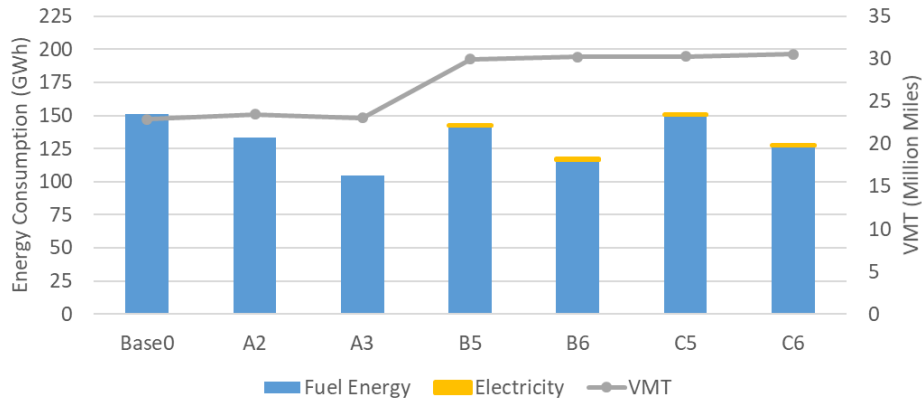


Figure 58. MD/HD Truck Impacts on VMT and Energy Use across Scenarios from POLARIS Workflow.

4.8 Vehicle Technology Impact and Vehicle Class Contribution to Energy Consumption

While overall energy consumption from light-duty vehicles decreases over time due to vehicle technology improvements, the energy consumption by MD and HD vehicles remains relatively constant because efficiency gains from vehicle technology improvements are countered by the expected increase in MD and HD vehicle VMT. Figure 59 illustrates energy and VMT for both light-duty vehicles and MD/HD trucks. For light-duty vehicles, even in Scenario C6 which has the largest VMT, energy consumption is less than that of Base 0. Powertrain electrification and other vehicle technology improvements are the primary drivers of lower light-duty vehicle energy consumption. For MD/HD trucks, fewer opportunities for powertrain electrification result in a much smaller impact on energy consumption. Other technology improvements (e.g., engine, transmission, light-weighting and aerodynamics) have a significant impact on vehicle efficiency but the VMT increase offsets the benefits from the vehicle technology improvement.

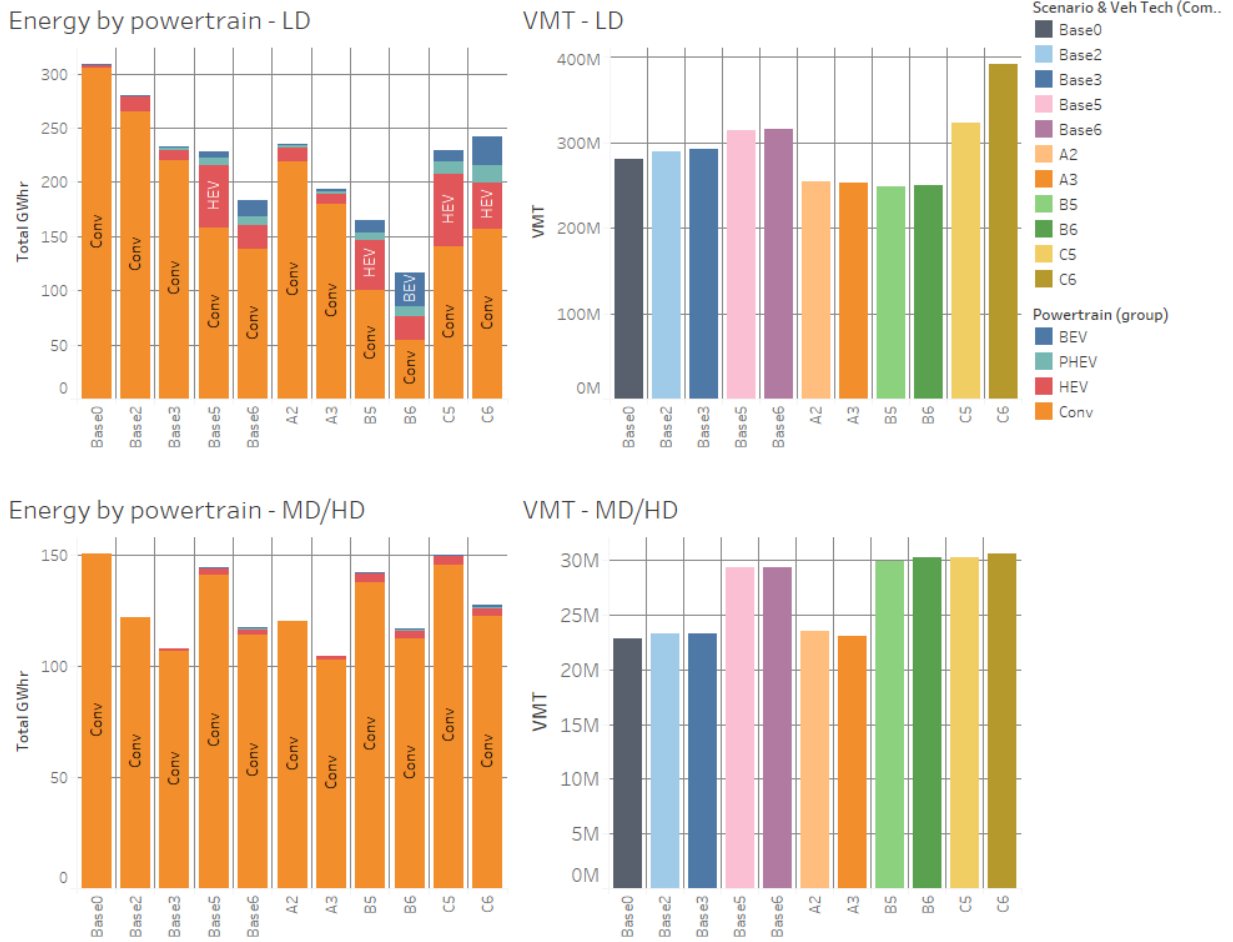


Figure 59. Energy and VMT Split between by Powertrain (PWT) and Class (Light-duty Vehicles [LDV] and MD/HD Trucks) from POLARIS Workflow.

GHGs were calculated using GREET well-to-wheel emission factors and Autonomie vehicle modeling for the three timeframes under consideration. Appendix F lists the emission factors used for the GHG calculation in Figure 60. GHGs per mile are expected to decrease in future scenarios across all vehicle classes, driven by light-duty vehicles. Trends in GHG numbers closely track energy trends. Figure 60 shows total GHGs and GHGs per mile for light-duty vehicles and MD/HD vehicles. While GHGs are dependent on geographical location for electricity generation and method of extraction for fossil fuels, this study uses U.S. aggregate numbers. GHGs per mile decrease for all scenarios compared to the current baseline. Scenario B6 results in the lowest light-duty vehicle GHGs per mile, reflecting long-term technology improvements and low road congestion. Scenarios C5 and C6 have higher GHGs per mile compared to Scenarios B5 and B6 because of higher congestion leading to slower, inefficient traffic.

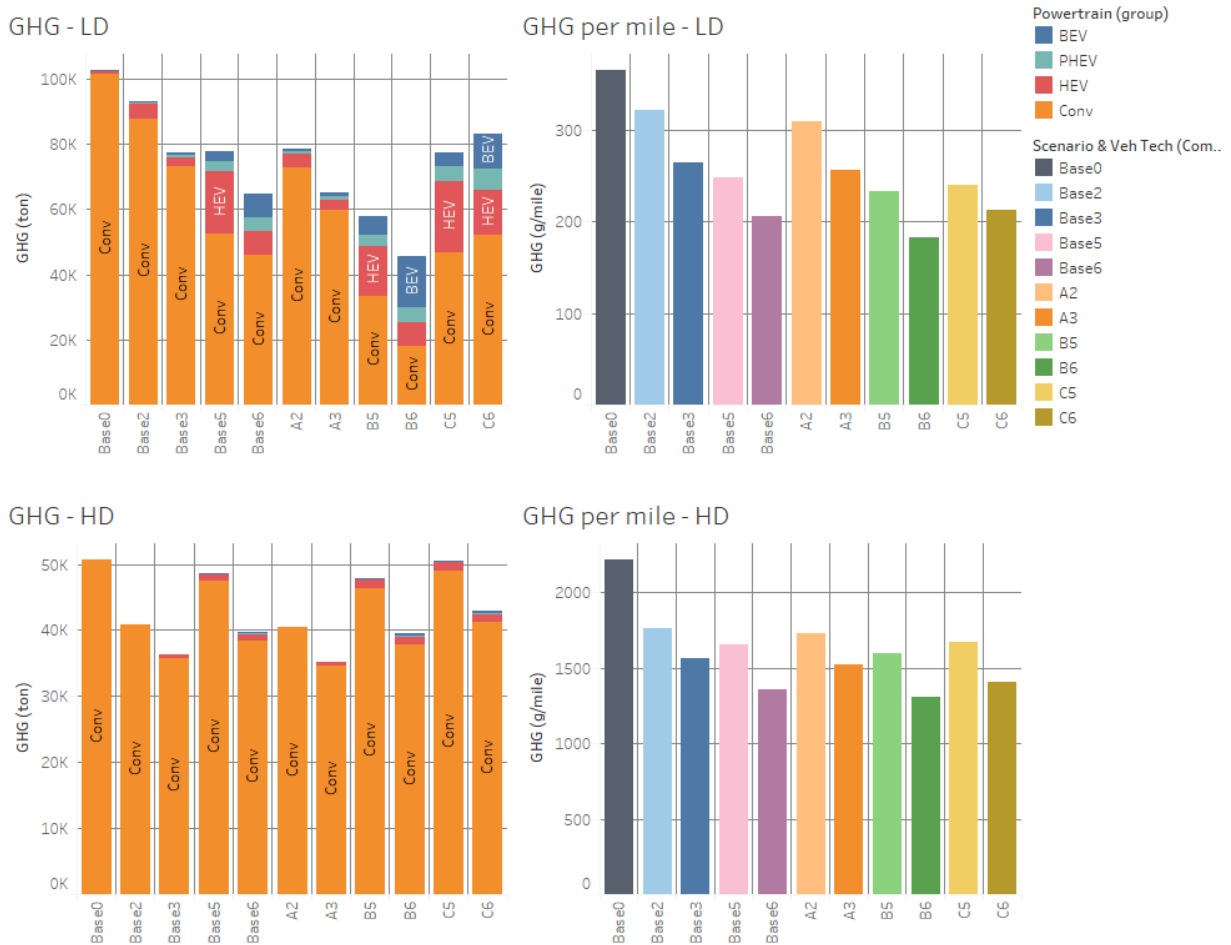


Figure 60. GHGs and GHGs/Mile for Light-duty and MD/HD Vehicles from POLARIS Workflow.

Based on scenario analysis in the Chicago metropolitan area, MD and HD vehicles currently account for 33% of the overall transportation energy in the United States. This share is expected to grow to 50% in the future, driven by increased light-duty vehicle electrification combined with increased freight demand. Figure 61 highlights the energy split between light-duty vehicles and MD/HD trucks. MD/HD truck energy represents 33% of the total energy for Base 0 and Scenario A, up to 50% for Scenario B and up to 40% for Scenario C. The increased portion of MD/HD truck energy in future scenarios is primarily explained by the smaller opportunity for electrification in MD/HD trucks combined with increased MD/HD VMT. Note that in Scenario B, MD/HD trucks consume 50% of the total energy, but they only constitute 10% of VMT.

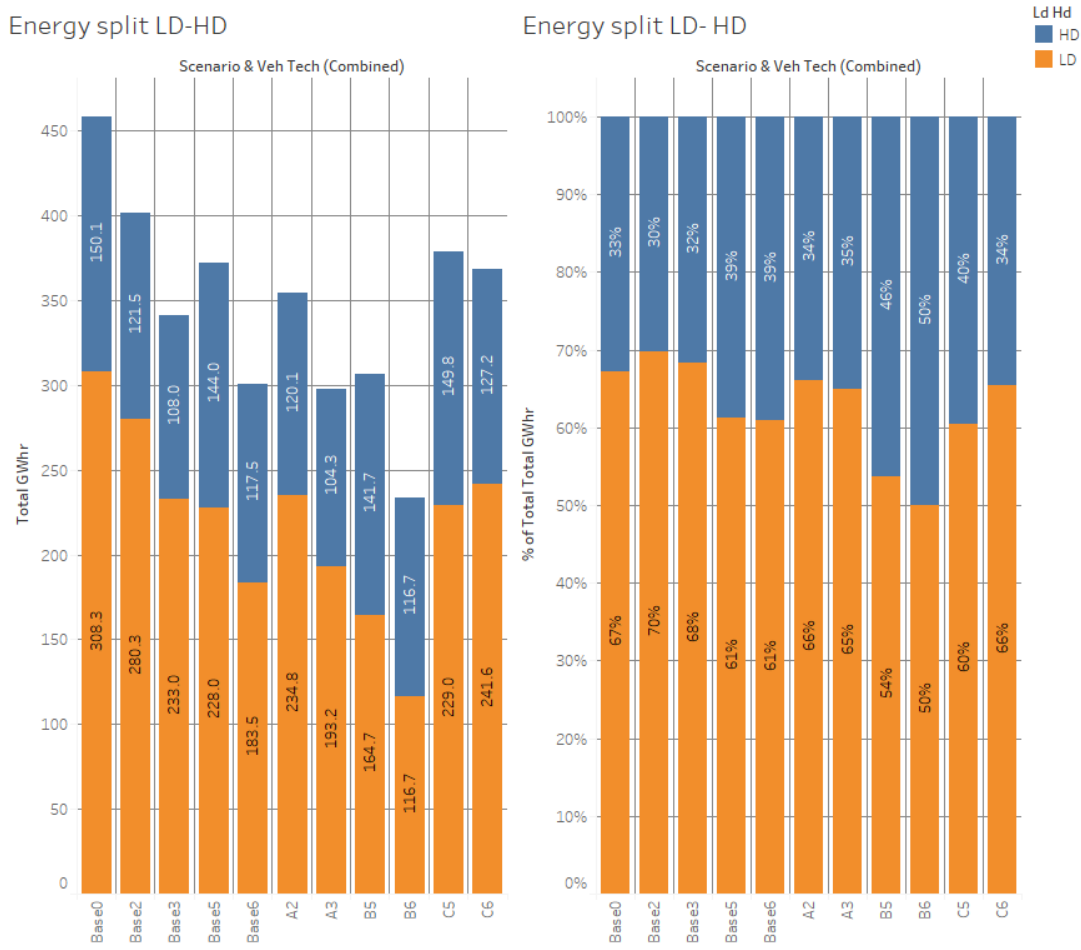


Figure 61. Autonomie Energy Split between Light-duty Vehicles and MD/HD Trucks.

Achieving VTO light-duty vehicle technology research targets will lead to 18% system-level energy savings compared to business as usual for Scenario A and 29% for Scenario B (Figure 62). In the personally owned AV scenario (Scenario C), the energy savings from achieving the technology targets are insufficient to offset the impact of increased VMT, resulting in a 6% energy increase. While vehicle technology improvements consistently provide significant energy reduction on a per-mile basis, the VMT increase resulting from new mobility technologies could be sufficient to lead to an overall increase in light-duty vehicle energy consumed. As a result, meeting VTO technology targets for MD/HD trucks is required in Scenario C to compensate for the light-duty vehicle energy increase.



Figure 62. Energy Benefits of Meeting VTO Technology Targets (High Vehicle Technologies) Compared to Business-as-Usual (BAU - Low Vehicle Technologies) from POLARIS Workflow

Assumed technology improvements at the vehicle and powertrain levels are sufficient to overcome the energy consumption increase due to automation (e.g., increased electrical loads due to cameras, LiDAR, radar, and computing power) for internal combustion engine vehicles, but not for electrified vehicles. Since electrified vehicles are more efficient than conventional powertrains, they are more sensitive to added electrical loads. As shown in Figure 63, fuel-based powertrains consume on average 1.1 kWh per mile in Base 0, improving to 0.65–0.8 kWh per mile for the long-term scenarios (Scenarios B5, B6, C5, C6). Electrified powertrains however, which consume on average 0.26 kWh per mile in Base0, will see their energy consumption increase to 0.32 to 0.33 kWh per mile in the long-term scenarios due the higher electrical accessory loads (assumed to be 400 W for partially automated vehicles and 1.9 kW for fully automated driverless vehicles) resulting from automation.

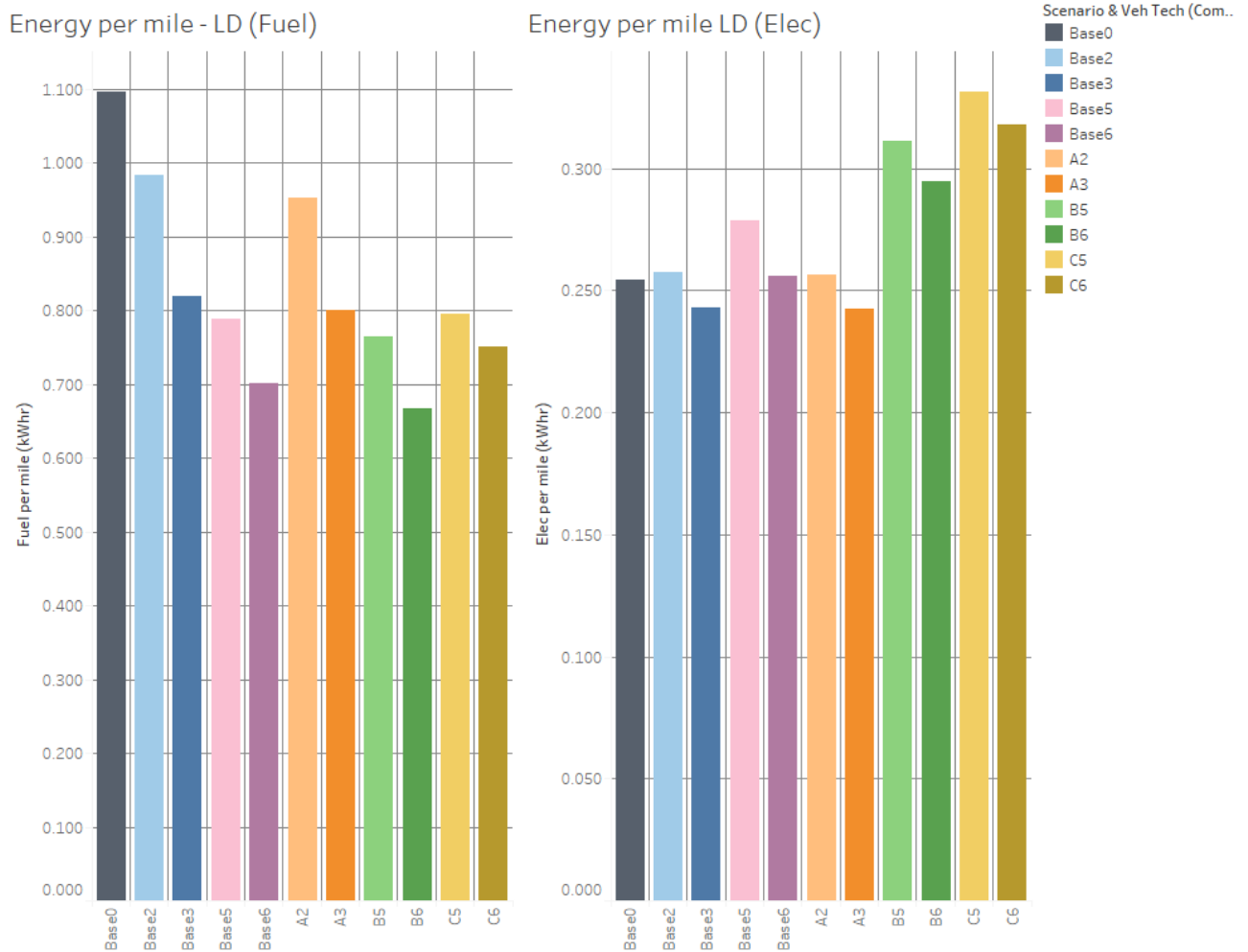


Figure 63. Fuel and Electrical Energy Consumption from POLARIS Workflow.

Figure 64 illustrates the average light-duty vehicle efficiency increase in terms of MPG-gasoline-equivalent (MPGGe, which combines fuel and electricity) across all scenarios. While Scenarios Base 6, B6, and C6 have the same light-duty vehicle fleet composition, Scenario B6 has the highest MPGGe value due to lower congestion and higher system efficiency. In Scenario C6, the extra congestion lowers average speed and overall vehicle efficiency.

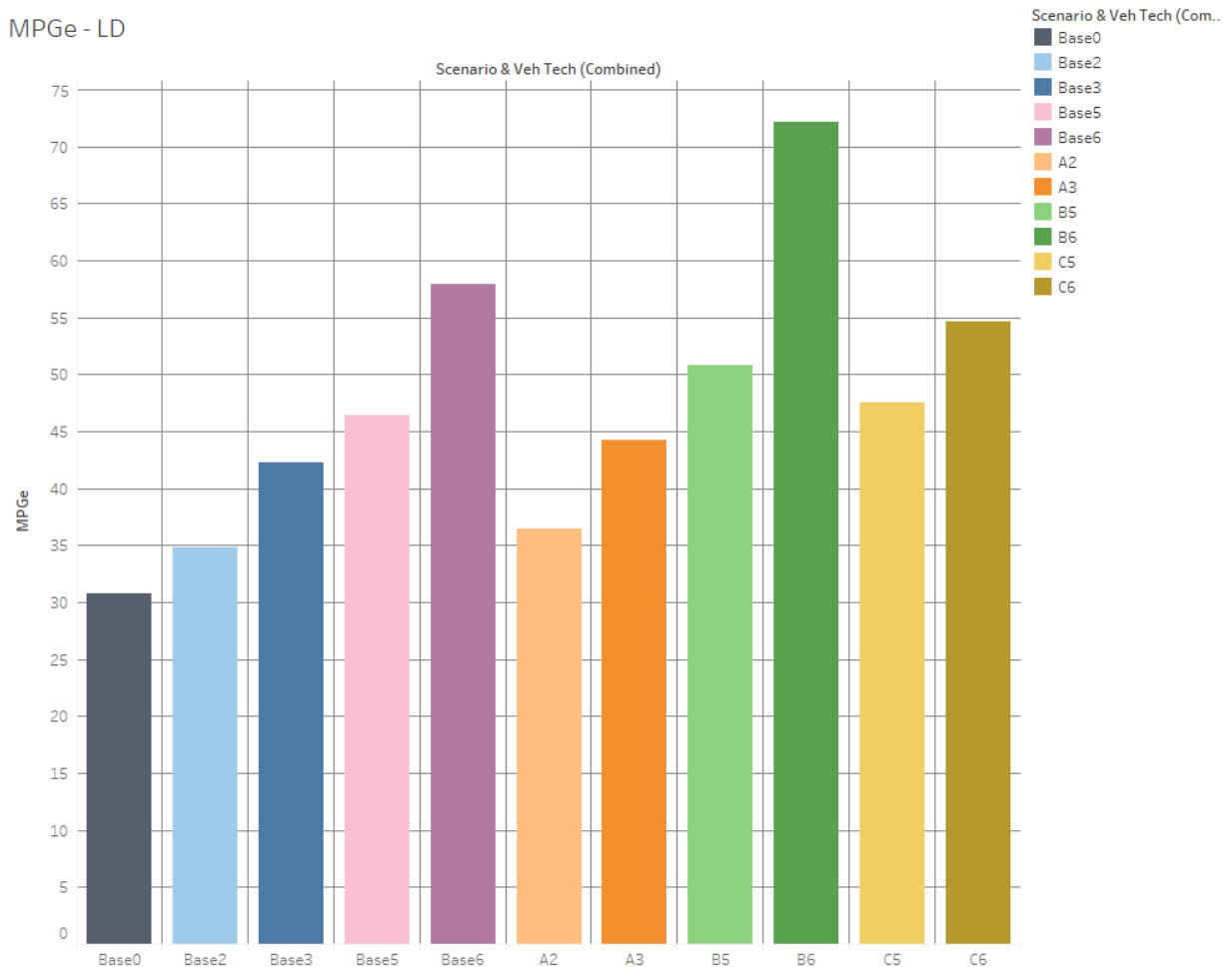


Figure 64. Average Light-Duty Vehicle Fuel Economy (MPGGE).

Significant vehicle powertrain efficiency improvements are required to offset the additional accessory electric load required by fully automated vehicles. For a given powertrain, fully automated vehicle (e.g., SAE Level 4-5) energy consumption is greater than that of non-automated vehicles (SAE Level 0). Figure 65 highlights this for conventional vehicles and BEVs for Scenario B6. In other words, automation by itself has a negative impact on fuel consumption due to the added load on the system. However, fully automated vehicles are assumed more likely to be electric vehicles. Because electric vehicles have a higher fuel economy compared to non-electrified vehicles, the effect of added load for fully automated vehicles is mitigated. Therefore, when considering all fully automated vehicles together for all powertrains, their fuel efficiency is better than that of non-automated vehicles. In other words, the higher level of electrification for fully automated vehicles overcomes the efficiency penalty that otherwise comes from the increased accessory load compared to non-automated vehicles.

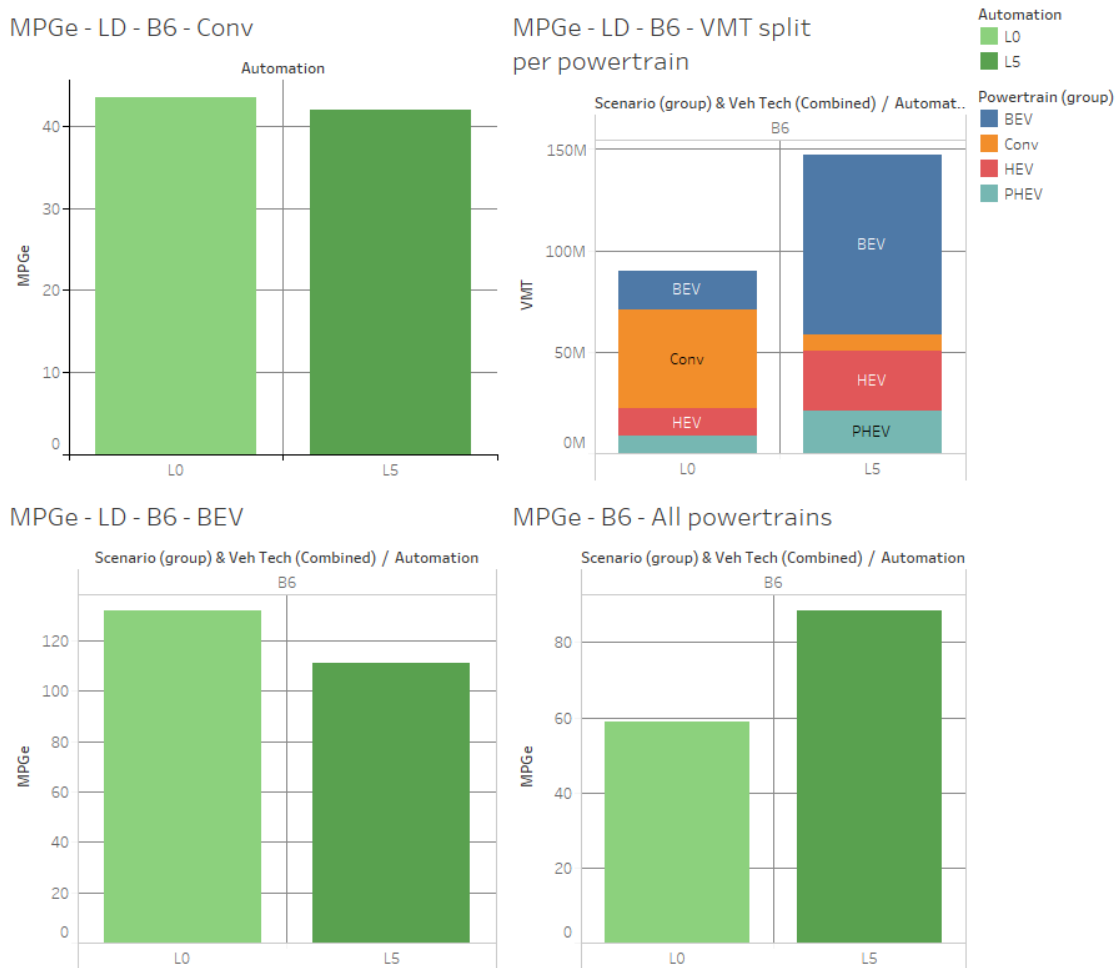


Figure 65. Impact of Automation on Vehicle Fuel Economy (Scenario B6).

5 Results from BEAM Workflow Implementation

Agent-based modeling in BEAM allows the simulation of a range of scenarios to determine the relationships between technological and behavioral change and the efficiency of a regional transportation system. The common scenarios modeled in both workflow implementations start from shared sets of high-level assumptions related to travel preferences and levels of technology advancement. Within each workflow implementation, different modeling approaches, low-level assumptions, and geographic differences lead to different outcomes in terms of overall mobility patterns, aggregate energy consumption, and MEP. The results highlighted below are from the San Francisco Bay Area implementation of the workflow using BEAM. After simulation, the network state resulting from each scenario is then used to compute MEP, quantifying access to all opportunities weighted by time, energy, and cost efficiency.

The main findings can be summarized as follows:

- Household vehicle ownership assumptions and different valuations of travel time are the main drivers of variation in commuting mode share across scenarios, and private car trips remain the dominant mode without changes in both. Neither preference for non-motorized and shared modes (Scenario A) nor moderate personal vehicle retirement rates (Scenario C) keep personal car travel from staying the primary mode (reduction of approximately 15 percentage points in Scenario A and roughly unchanged in Scenario C), but dramatic vehicle retirement and preference for shared mobility reduce reliance on private cars by 40–45 percentage points.
- As commuting travelers shed their personally owned vehicles and change travel preferences, they shift to non-car travel, but the mode share for transit does not greatly increase. Indeed, the increased preference for non-car travel in Scenario A actually leads to a decrease in transit mode share. In both shared-mobility scenarios, longer car trips shift from car (6% decrease in private car mode share in Scenario A, 50% in Scenario B) to transit (5% increase in Scenario A, 29% increase in Scenario B). However, in the case where non-car modes are preferred, short trips also shift from transit (38% decrease in mode share for short trips in Scenario A) to walking and biking (2.5× increase in mode share in Scenario A), cancelling out increases in transit mode share.
- The transportation system exists at an equilibrium between faster car modes and less expensive non-car modes, where changes that would tend to decrease congestion lead to additional capacity on the road network that will be partially filled by other cars. Reducing the valuation of travel time for non-car modes (Scenario A, increasing road speeds by 2% while increasing average travel times by 15%) or increasing the cost of car modes (Scenario B, increasing road speeds by 4% while increasing average travel times by 15%) shifts this equilibrium away from cars, and the addition of population growth reduces speeds across the board (up to 7% by 2040).
- MEP results are strongly tied to vehicle energy efficiency and roadway speeds. Vehicles in Scenarios A3, B6, and C6 (i.e., high-technology scenarios) are by definition more energy efficient than their corresponding scenarios with business-as-usual technology progress (Scenarios A2, B5, and C5, respectively), leading to higher absolute MEP calculations when VTO technical research targets are met. However, the network congestion created from CAVs in Scenarios C5 and C6 (which experience the largest reduction in travel speed, coupled with increased energy consumption, with respect to Scenarios Base 5 and Base 6, respectively), results in lowest MEP scores across all scenarios (a reduction of ~3–4% from their respective baselines, i.e., Scenarios Base 5 and Base 6). MEP results for shared mobility scenarios (Scenarios A and B) are higher than their respective baselines, but they are lower for the privately owned automobile scenario (Scenario C), indicating shared mobility can augment vehicle technology improvements. While the magnitudes of impacts are different between workflows, the MEP scores (reflecting the comprehensive impact of travel time, energy, and affordability changes across scenarios), show consistent trends.

- VTO research target impact
 - Even business-as-usual technology advancement is expected to lead to substantial decreases in per-capita light-duty vehicle energy consumption (up to a 32% reduction in Base 5). Advanced vehicle technologies, including powertrain electrification, remain the primary factor influencing future transportation energy consumption, having a greater impact than either vehicle sharing or automation.
 - Meeting VTO targets, holding behavioral preferences constant, has the most substantial benefits in scenarios with the most reliance on light-duty vehicles (27% decrease in per-capita energy consumption in Scenario C, versus 19% in Scenario A and 15% in Scenario B). Given conservative assumptions of the sensitivity of trip distances and frequency to perceived travel time, automation does not increase energy use more in a low-sharing versus high-sharing future. Thus, the differences in light-duty vehicle fleet powertrain makeup between scenarios have a larger impact on energy use than differences in adoption of fully automated vehicles.
 - While pooling (increasing occupancy of light-duty vehicles) is normally expected to enable a more efficient future transportation system, scenarios focused on pooling (i.e., Scenarios B5 and B6) perform no better than those with baseline behavior and the same powertrains. This happens in part due to diseconomies of scale in the ride-hail business model. At low mode shares, ride-hail services naturally provide the trips they can serve most efficiently. Achieving higher mode share (over a third of all trips in Scenario B6) requires serving longer trips (ride-hail trips are about 10% longer in Scenario B6 than in Base 6) that are difficult to cover with low amounts of deadheading and a high degree of pooling. This inefficiency is exacerbated in Scenario B6 where the personal vehicle fleet is 22% smaller than in Scenario B5 and 21% less efficient than in Scenario C6.
- Ride-hailing
 - Increasing ride-hail occupancy while maintaining high enough quality service to attract travelers is a fundamentally difficult problem. Increased preference for pooled ride-hail leads to longer wait times and detours as ride-hail vehicles string together more trips, degrading customer experience and pushing riders toward solo rides. This effect limits the ability of pooled ride-hail to make up for overall fleet deadheading, even when traveler preference for pooling is very high.
 - Ride-hailing vehicles in a heavily utilized fleet are often empty and unmatched to passengers. If ride-hailing vehicles reposition to increase their chances of picking up a passenger with low wait time, even if such movements happen with low probability, the result is a large number of unproductive VMT. This increase in empty VMT overwhelms reductions due to pooling, even with low prices and no consumer aversion to shared rides. These results are sensitive to ride-hailing repositioning and matching algorithms.
 - Differences in the relative utilization of vehicles can lead to dramatic differences in energy consumption between scenarios with the same light-duty vehicle powertrain makeup (over 20% in some cases). This means that the distribution of powertrain types across different classes of uses is an important driver of system wide energy outcomes. In these high-sharing scenarios, disproportionate savings can be achieved by improving energy efficiency of the vehicles making up the smaller (69% smaller in Scenario B6 than Scenario C6) but more heavily used vehicles (63% more VMT per vehicle) personal vehicle fleet.
 - Vehicle automation will likely make in-car travel more comfortable and productive, and as a result has the potential to greatly increase travel distances and times. While this may be the case, this analysis uncovers several factors that will serve to limit increases to VMT in scenarios with high

personal ownership of AVs, suggesting in particular that any substantial increases to travel distances are likely to come from discretionary (non-mandatory) trips.

The key metrics related to mobility and energy use for passenger travel for each scenario are shown in Table 12.

Household vehicle ownership assumptions and different valuations of travel time are the main drivers of variation in commuting mode share across scenarios, and private car trips remain the dominant mode without changes in both. Neither preference for non-motorized and shared modes (Scenario A) nor moderate personal vehicle retirement rates (Scenario C) keep personal car travel from staying the primary mode (reduction of approximately 15 percentage points in Scenario A and remaining roughly unchanged in Scenario C), but dramatic vehicle retirement and preference for shared mobility reduce reliance on private cars by 40–45 percentage points.

The Base 0 scenario represents current commute travel patterns in the San Francisco region, with over 70% of trips taken by car (Figure 66). In Scenarios A2 and A3, the portion of travelers relying on non-motorized modes increases by a factor of 3 and the portion of ride-hail requests that are for pooled travel increases by a factor of 2.5. Despite these differences, the majority of trips are still taken in personally owned cars due to low personal vehicle retirement rates (Table 4) and car travel's continued advantage in terms of cost and travel time. This demonstrates how the region's built environment and transit infrastructure constrains potential changes in travel behavior.

In Scenarios B5 and B6, changes to modal split are more dramatic. In these scenarios, lower personal vehicle ownership and a larger ride-hail fleet influence many travelers to choose ride-hailing over personally owned vehicle trips. The greater availability of fully automated driverless vehicles and the cheaper fares associated with removing the ride-hail driver cost in Scenario B6 further increase ride-hail mode share, including an increase in first- and last-mile connections to transit trips. In Scenarios C5 and C6, human-driven car trips from Base 0 are replaced by a combination of household-owned CAV trips and ride-hail trips though fewer of the ride-hail trips are pooled compared to Scenarios B5 and B6.

Table 12. Differences in Various Aggregate Metrics from Baseline across the Workflow Scenarios.

Metric	Reference Baselines					% Change from Base0						% Change from Base2 and Base 3		% Change from Long-term Base5 and Base6			
	Base0	Base2	Base3	Base5	Base6	A2 / Base0	A3 / Base0	B5 / Base0	B6 / Base0	C5 / Base0	C6 / Base0	A2 / Base2	A3 / Base3	B5 / Base5	B6 / Base6	C5 / Base5	C6 / Base6
Population (millions)	7.80	8.90	8.90	9.30	9.30	14%	14%	19%	19%	19%	19%	0.0%	0.0%	0.0%	0.0%	0.0%	0.0%
VMT (million miles)	332	383	383	399	398	10%	10%	17%	22%	25%	25%	-4%	-4%	-2%	2%	4%	4%
VMT/capita (miles)	43	43	43	43	43	-4%	-3%	-2%	2%	5%	4%	-4%	-4%	-2%	2%	4%	4%
VHT (million hours)	8	10	10	10	10	14%	16%	27%	28%	40%	38%	-9%	-7%	2%	3%	12%	11%
PMT (million miles)	358	412	412	427	426	11%	11%	16%	15%	19%	14%	-4%	-4%	-2%	-4%	0%	-4%
PMT/capita (miles)	46	47	47	46	46	-3%	-3%	-3%	-4%	-1%	-5%	-4%	-4%	-2%	-4%	0%	-4%
PHT (million hours)	10	13	13	13	13	37%	39%	40%	32%	28%	18%	11%	12%	14%	7%	3%	-5%
Avg. Vehicle Speed (mi/h)	43	40	40	40	40	-4%	-5%	-8%	-5%	-11%	-10%	4%	4%	1%	3%	-3%	-2%
Avg. Trip Speed (mi/h)	35	32	32	32	33	-19%	-20%	-17%	-13%	-7%	-3%	-14%	-14%	-11%	-8%	0%	3%
Energy/capita (kWh)	34	30	24	23	16	-20%	-35%	-32%	-44%	-28%	-49%	-9%	-8%	0%	20%	7%	10%
Energy (GWh)	264	265	214	213	147	-8%	-26%	-19%	-33%	-13%	-39%	-9%	-8%	0%	20%	7%	10%
Fuel Economy (MPGe)	44	51	63	66	96	20%	48%	45%	83%	45%	104%	5%	4%	-2%	-15%	-3%	-6%
MEP	17000	22000	23000	26000	27000	35%	43%	62%	76%	46%	56%	4%	5%	7%	10%	-4%	-3%
Cost Drive (\$/pax-mile)	\$ 0.19	\$ 0.17	\$ 0.17	\$ 0.13	\$ 0.11	-16%	-19%	-28%	-18%	-24%	-33%	-7%	-8%	6%	44%	12%	18%
Cost Ride-Hail (\$/pax-mile)	\$ 1.71	\$ 1.78	\$ 1.76	\$ 1.78	\$ 1.79	-6%	-9%	-18%	-36%	-16%	-23%	-10%	-12%	-21%	-29%	-20%	-26%

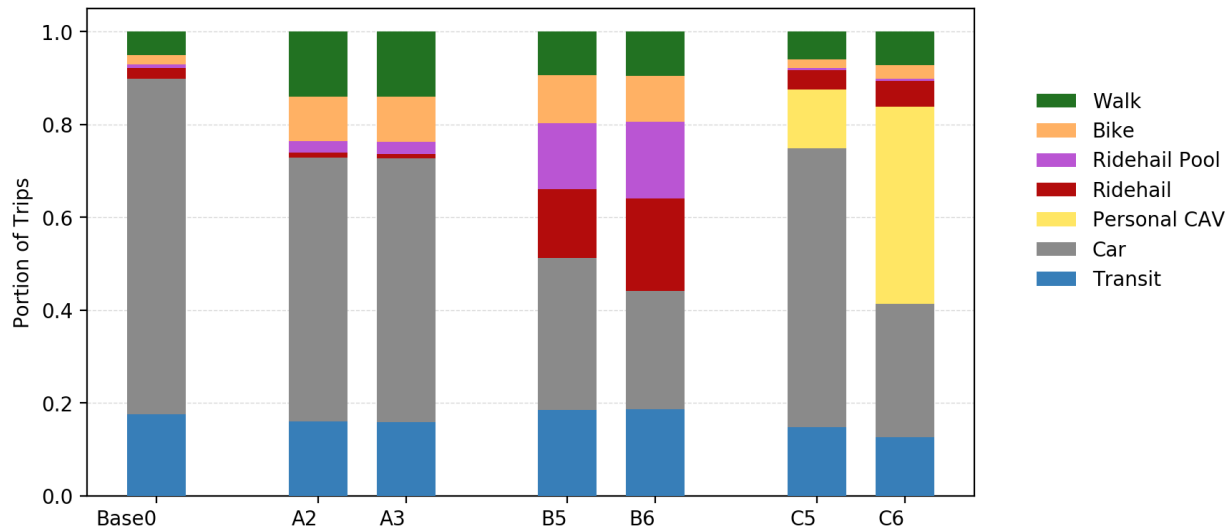


Figure 66. Modal Market Shares for Commute in San Francisco Bay Area across Scenarios.

As commuting travelers shed their personally owned vehicles and shift to non-car travel, the mode share for transit stays relatively constant. This is because the transition from car travel to transit for longer commutes is offset by a shift from transit to walking and biking for shorter trips.

Longer car trips shift from car (6% decrease in private car mode share in Scenario A, compared to a 50% decrease in Scenario B) to transit (5% increase in Scenario A, and 29% increase in Scenario B), but short trips shift from transit (38% decrease in mode share for short trips in Scenario A) to walking and biking (2.5× increase in mode share in Scenario A), cancelling out increases in transit mode share.

More subtle differences in mode choice between scenarios can also be explained by varying behavioral and technology assumptions. In Scenarios A2 and A3, travelers have a weaker aversion to time spent on transit and non-motorized modes compared to Baseline and Scenarios B and C. As a result of this change in value of time and assumptions about vehicle retirement (45% decrease in the number of household cars), there are substantial increases in the number of non-motorized trips in Scenario A (almost tripling) but not an increase in the number of transit trips (Figure 67). When a traveler is choosing between a short walk or bike trip and a slightly faster but more expensive transit trip, decreasing the perceived disutility associated with travel time makes the cheaper but slower non-motorized trip look more favorable in comparison. However, when a traveler is choosing between a longer transit trip and a car or ride-hail trip, the transit trip is often slower but lower cost, especially when parking, tolls, and gasoline costs are factored in for car trips. Thus, decreasing the valuation of non-light-duty vehicle travel time tends to lead to fewer short transit trips and more long ones, causing per-capita transit person miles traveled (PMT) to increase slightly in Scenario A when compared to Base 0 (Figure 68). In Scenario B, the portion of transit trips increases by approximately 5% and the portion of PMT increases by almost 10%, despite transit not having the same reduced valuation of travel time as in Scenario A. These distance-specific mode shift effects are shown in Figure 66; for example, the non-motorized share of all short trips increases by 43 percentage points from Base 3 to Scenario A3, coming in part at the expense of an 8 percentage point decrease in transit mode share, despite travelers having an equivalent preference for both modes. In going from Base 6 to Scenario B6, the share of long trips taken via transit increases by 5 percentage points (at the expense of car trips) despite travelers in Scenario B6 not having a preference for transit. This effect is likely due to the greater degrees of personal vehicle retirement in Scenario B than in Scenario A (68% and 75% for Scenarios B5 and B6 versus 45% for Scenarios A2 and A3), meaning that more travelers with relatively long commutes do not have access to a personal car in Scenario B and therefore are choosing between transit and a more expensive ride-hail option.

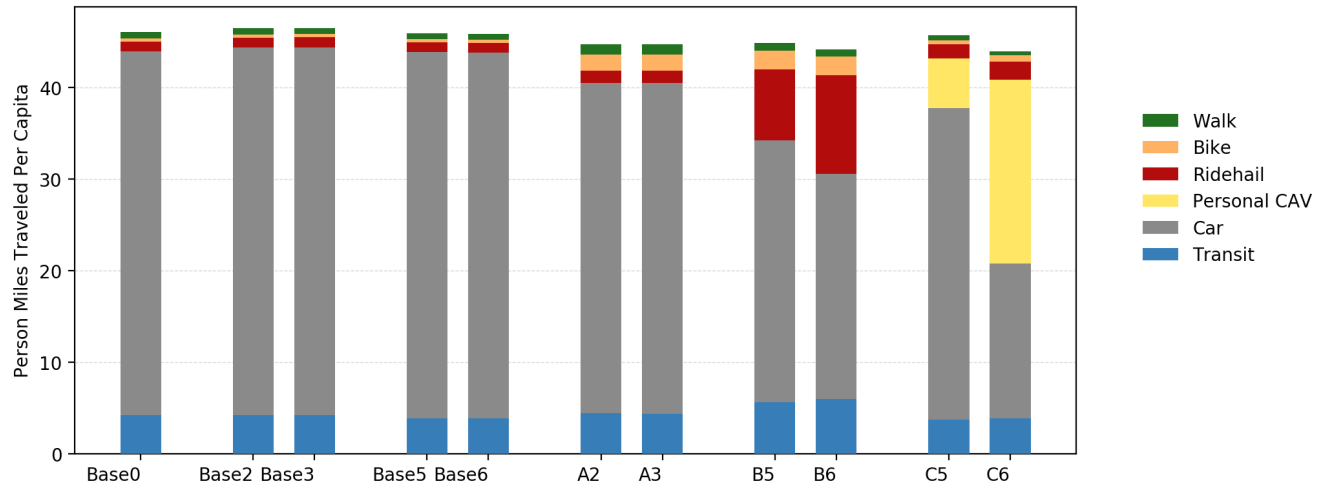


Figure 67. Total Commuting Travel Distance per Capita in the San Francisco Bay Area, Disaggregated by Mode Taken.

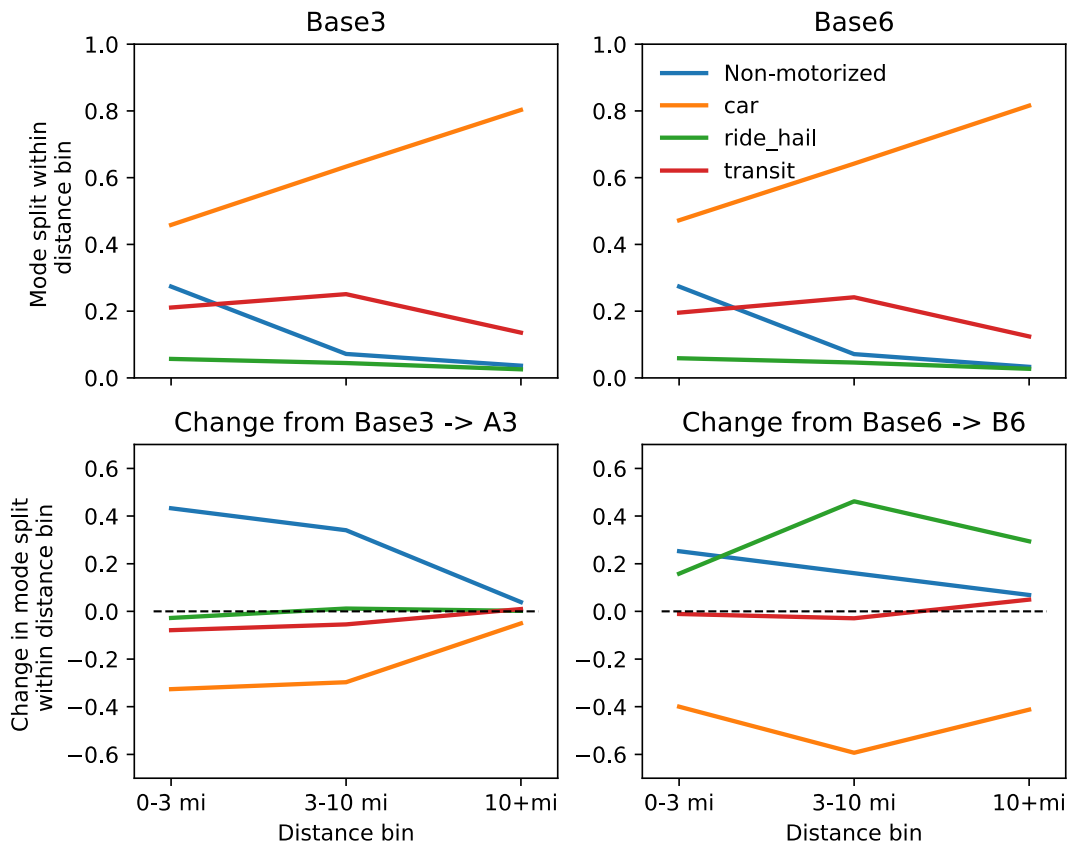


Figure 68. Baseline Mode Splits (Top) and Absolute Change in Portion of Commute Trips Taken by Different Modes (Bottom) from Baseline to Workflow Scenarios, Disaggregated by Trips of Different Distances.

The transportation system exists at an equilibrium between faster car modes and less expensive non-car modes, where changes that would tend to decrease congestion lead to additional capacity on the road network that will

be partially filled by other cars. Reducing the valuation of travel time for non-car modes (Scenario A, increasing road speeds by 2% while increasing average travel times by 15%) or increasing the cost of car modes (Scenario B, increasing road speeds by 4% while increasing average travel times by 15%) shifts this equilibrium away from cars, and the addition of population growth reduces speeds across the board (up to 7% by 2040).

Changes in travel time valuation also influence overall travel speeds in a complex fashion, clarifying important feedback loops in the transportation system (Figure 69). Comparing Scenarios A and B to Base 0, overall person speeds (defined as the total number of passenger miles traveled divided by the total number of passenger hours of travel) decrease (in contrast to road network speeds, which are defined as car VMT traveled divided by car VHT). When travelers’ VOTT decreases, they are willing to tolerate longer travel times. In this case, lower VOTT means switching from expensive car (due to tolls, fuel, and parking) and ride-hail (due to fares) modes to cheaper modes like walking and biking (especially for short trips) and transit for longer trips. Due to the set of modes available in the Bay Area, lower VOTT on non-car modes produces secondary effect of freeing up road capacity and allowing road network speeds to increase slightly, making those modes more favorable than they would be if this feedback were not captured. This equilibrium is seen in comparing the current baseline to the longer term baselines—scenarios with similar behavior and vehicle fleets but increasing population and congestion.

Changes to travel speeds in the Workflow scenarios are driven both by baseline population growth (which tends to increase congestion) and differing behavioral and technology assumptions. Comparing Base 1 to Base 0, population increases by 14%, road speeds (car VMT divided by car VHT) decrease by 7%, and non-motorized and transit mode shares increase by 4% and 1%, respectively, showing that population growth alone will decrease road speeds and push travelers away from car travel. Shared mobility assumptions lead to an even greater shift away from car modes while reversing the increases in congestion due to population growth; for example, in Scenario A3 the equilibrium road network speed is 2% higher than in Base 1 because travelers prefer slower non-car modes. In Scenario C, overall travel speeds are higher than in Scenario B because in Scenario C travelers do not prefer time spent in non-car modes. This effect is dampened because a switch to more car and CAV travel increases congestion on the road network, bringing speeds between car and non-car modes closer to equilibrium. Also note that the average speed in the current baseline is 43 miles per hour, which is higher than many estimates for the San Francisco Bay Area. This is due in part to the lack of non-commute behaviors in the simulation and in part to a choice to calibrate to match observed travel times rather than speeds. If the road network is indeed less congested in these scenarios than in reality, the real feedbacks presented here would likely be even stronger, as each additional vehicle on the road network would lead to more delays as the road network becomes closer to capacity.

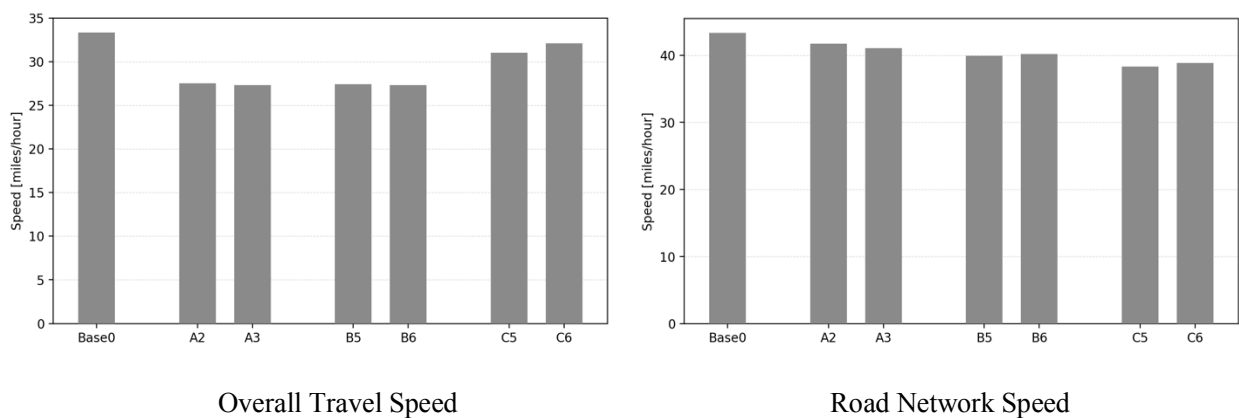


Figure 69. Left: Overall Average Travel Speed (for All Modes), Right: Average Travel Speed for Car, CAV, and Ride-hailing Trips Only.

MEP results are strongly tied to vehicle energy efficiency and roadway speeds. Vehicles in Scenarios A3, B6, and C6 are more energy efficient than the corresponding scenarios with scenarios with business-as-usual (i.e., low technology) improvements (Scenarios A2, B5, and C5, respectively), leading to higher absolute MEP scores when VTO technical research targets are met. However, the network congestion created from CAVs in Scenarios C5 and C6 (which experience the largest reduction in travel speed, coupled with increased energy consumption, with respect to Scenarios Base 5 and Base 6, respectively), results in the lowest MEP results across all scenarios (a reduction of ~3–4% from their respective baselines, i.e., Scenarios Base 5 and Base 6).

Across all of these scenarios with different land use, travel behavior, and vehicle technology assumptions, MEP provides a quantitative method for weighing different costs and benefits associated with different travel patterns. An increase in MEP over the baseline was observed for all of the workflow scenarios (Figure 70), ranging from a 35% increase for Scenario A2 to a 77% increase for Scenario B6. Increases in MEP are the most substantial in the Scenarios B6 and C6, both assuming VTO technology targets are met. Comparisons of MEP scores with respect to current day baseline (Base 0) reveal some interesting trends. First, comparing MEP scores of Scenarios A2–C6 with Base 0 (in Figure 71), it can be observed that all else remaining the same, the VTO technology scenarios have a greater MEP score than BAU scenarios (A3 > A2; B6 > B5; C6 > C5). This increase can mostly be attributed to an improvement in energy efficiency of travel in VTO scenarios. (The same trend of A3 > A2; B6 > B5; C6 > C5 can be seen in vehicle energy and energy per capita values in Table 12.) The energy efficiency improvements in these scenarios compared to Base 0 (Figure 71) counterbalance the reduction in travel speeds resulting in a net positive MEP scores.

MEP results for shared mobility scenarios (Scenarios A and B) are higher than their respective baselines, but they are lower for the privately owned automobile scenario (Scenario C), indicating shared mobility can augment vehicle technology improvements. While the magnitudes of impacts are different between workflows, the MEP scores (reflecting the comprehensive impact of travel, energy, and affordability changes across scenarios), show consistent trends. MEP scores are highest in the high sharing, high automation Scenario B (with B6 > B5), followed by the high sharing, partial automation Scenario A (with A3 ≥ A2), and finally the low sharing high automation (Scenario C) scenario (with C6 > C5). In the privately owned CAV scenario (Scenario C), networks are more congested compared to shared mobility scenarios, causing MEP scores to drop. As a result, MEP scores in Scenario C, across both workflows, perform the worst of all scenarios when compared to their respective baseline values with the same technologies.

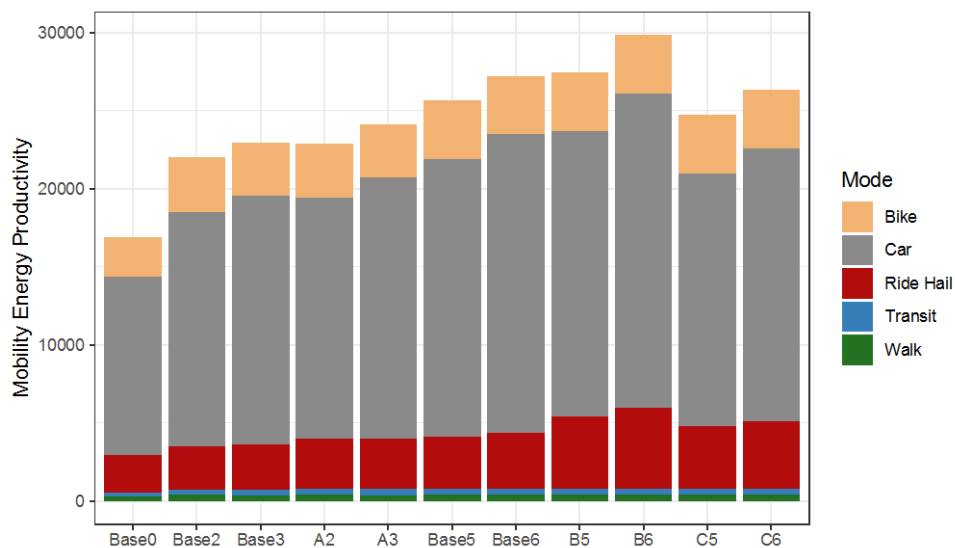


Figure 70. Aggregate BEAM MEP Values for the Workflow Scenarios

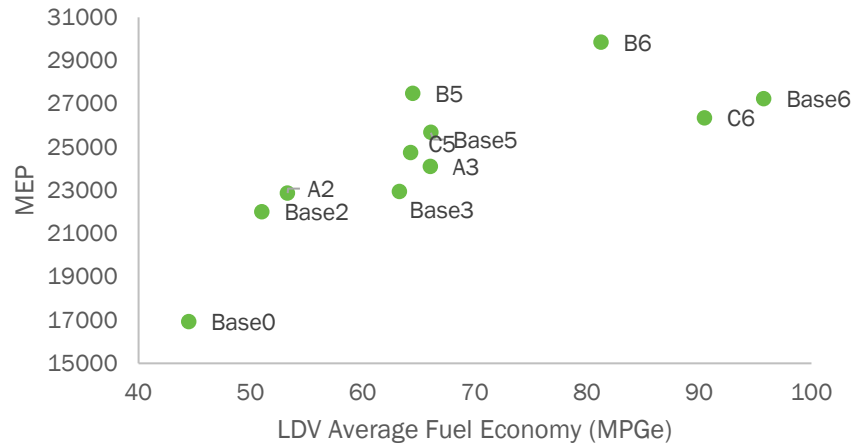


Figure 71. Relationship between MEP and Average Light-duty Vehicle Fuel Economy across Scenarios, Showing a Strong Positive Relationship.

5.1 Impact of VTO Research Targets

One of the goals of the SMART Mobility modeling workflow is to isolate the impact of VTO technology targets on transportation system energy efficiency and to explore how these impacts depend on exogenous factors such as travel behavior. Between the baselines and each future scenario, the workflow considers natural population growth, redistribution of jobs and households in response to transportation system performance and local accessibility, changes in the powertrain type and automation levels of the light-duty vehicle fleet, and different valuations of travel time.

To better distinguish the impacts of these potentially competing influences, the three main Workflow Common scenarios (Scenarios A, B, and C) are compared to their respective baselines (Bases 2, 3, 5, and 6) to distinguish changes that have to do with the vehicle fleet powertrain mix and natural population growth from changes that have to do with vehicle automation and changes in behavioral preferences. This analysis includes a set of baseline scenarios that contain the same vehicle powertrain mixes as the future scenarios but the same behavioral parameters as baseline Base 0, allowing land use and population in these scenarios evolve into the short-term future (for Base 2, Base 3, and Scenario A) and the long-term future (for Base 5, Base 6, Scenario B, and Scenario C). Thus, by comparing a workflow scenario to its equivalent with the same powertrain mix but baseline assumptions (e.g., Base 2 versus Scenario A2), it is possible to isolate the impacts of the variations in time valuation and automation on system performance. By comparing the BAU version of a workflow scenario to the VTO version, it is possible to isolate the impacts of faster advances in vehicle technology, in terms of powertrain mix and vehicle automation, from differences in behavior.

Even business-as-usual technology advancement is expected to lead to substantial decreases in per-capita light-duty vehicle energy use (up to a 32% reduction in Base 5). Advanced powertrain technologies, including electrification, remain the primary factor influencing future transportation energy consumption, having a greater impact than either vehicle sharing or automation. All of the scenarios modeled represent a substantial decrease in total energy consumption from the current baseline, despite an increase in population (Figure 72). Notably, all scenarios modeled represent an increase in the penetration of electrified vehicle powertrains into the light-duty fleet. In the short term, the lowest energy use is found in Scenario A3, representing a 35% decrease in total energy use per capita from Base 0. In the long term, the lowest energy use is found in Base 6 with baseline behavior and vehicle automation with long-term VTO powertrains, representing a 50% decrease in per-capita energy use compared to Base 0. Holding powertrain technology fixed leads to approximately a 20% variation in system-wide energy use, while varying vehicle technology (and holding behavioral parameters constant) can lead to a 30% variation in energy use. The feedbacks that limit decreases in energy

use due to sharing and increases in energy use due to VOTT reductions are explored in more detail. Dramatic improvements in the efficient operation of ride-hail fleets or automation-related increases in the frequency or distance of trips could push aggregate energy use below or above, respectively, the bounds found in these scenarios. In addition, in the Chicago results explored previously, dramatic increases in discretionary trip lengths lead to overall increases in VMT in Scenario C that are not captured by the BEAM Workflow implementation.

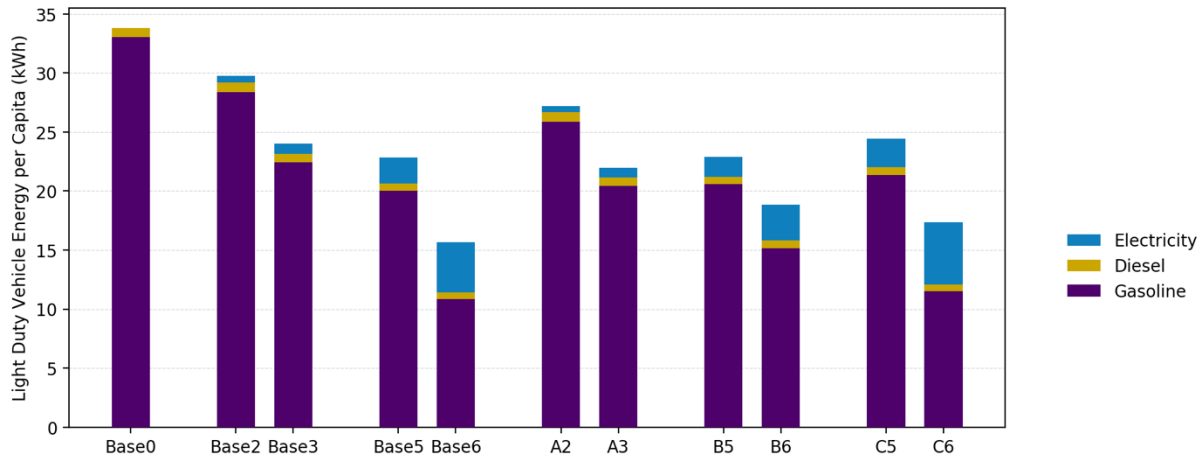


Figure 72. Total Light-duty Vehicle Energy Consumption by Fuel Type for the San Francisco Bay Area.

Meeting VTO targets, holding behavioral preferences constant, has the most substantial benefits scenarios with the most reliance on light-duty vehicles (27% decrease in per-capita energy consumption in Scenario C, versus 19% in Scenario A and 15% in Scenario B). Given conservative assumptions about the sensitivity of trip distances and frequency to perceived travel time, automation does not increase energy use more in a low-sharing versus high-sharing future. Thus, the differences in light-duty vehicle fleet powertrain makeup between scenarios have a larger impact on energy use than differences in adoption of fully automated vehicles.

The impact of VTO targets can be isolated from differing behavioral assumptions by comparing the BAU vehicle technologies and VTO target vehicle technologies alternatives of each scenario—Scenario A2 versus Scenario A3, Scenario B5 versus Scenario B6, and Scenario C5 versus Scenario C6. Doing so demonstrates that the benefits associated with meeting the VTO goals are substantial in all scenarios, but the impact on total energy use is 80% stronger in Scenario C compared to Scenario B (see Figure 73 and Table 12). There are several reasons for this, including the fact that demand for light-duty VMT is higher in Scenario C (Figure 73), so a change in the composition of the light-duty vehicle fleet will have a larger impact on overall energy use in Scenario C. In addition, the increased household vehicle retirement and resulting reliance on ride-hailing over private vehicle use from BAU vehicle technologies scenarios to VTO target vehicle technology scenarios (Scenarios B5 to B6) leads to an increase in empty VMT that proves an especially important feedback effect in Scenario B. Finally, differences in the way vehicle types are distributed and used across the personal and ride-hail fleets mean that light-duty vehicles require more energy per unit distance driven in Scenario B than in Scenario C (Table 12), reducing the impact of meeting VTO goals.

The fact that Scenario C6 has higher VMT but lower energy use than Scenario B6 is a surprising result that is explored further in Section 5.2, but in summary it shows that different behavioral assumptions can drive differences in vehicle utilization, which in turn can drive substantial differences in energy use. The way in which different vehicle powertrain types are distributed across the light-duty fleet, therefore, is an important variable to consider in understanding the energy implications of technology change. In these scenarios, the lowered light-duty vehicle energy efficiency in Scenario B is a combination of relatively higher utilization of conventional ride-hail vehicles when compared to electric ones and lower BEV energy efficiency due to traffic

conditions in Scenario B6. Notably, Scenario B5 has both lower energy use and lower VMT than Scenario C5, but Scenario B6 has higher energy use than Scenario C6 while retaining lower VMT.

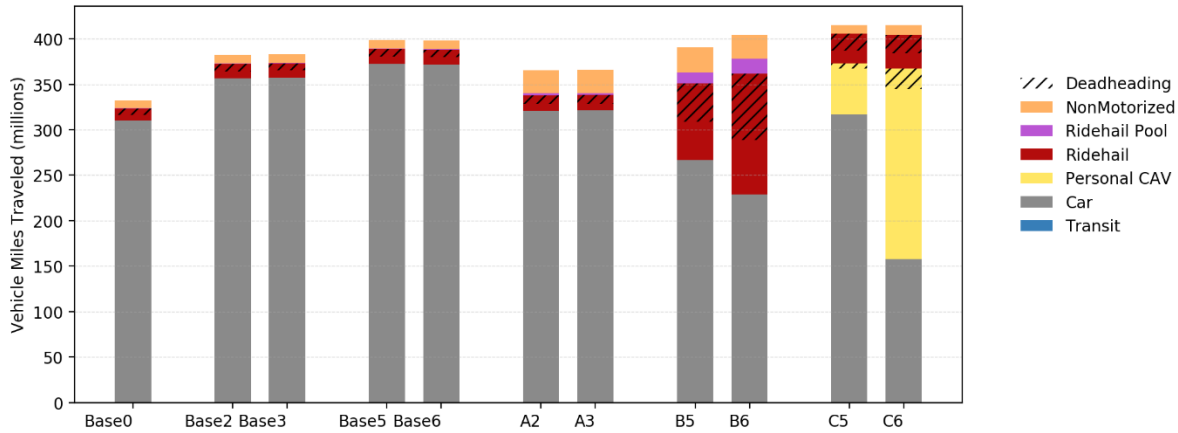


Figure 73. Total VMT for Commuting by Mode for the San Francisco Bay Area.

While pooling (increasing occupancy of light-duty vehicles) is normally expected to enable a more efficient future transportation system, scenarios focused on pooling (i.e., Scenarios B5 and B6) perform no better than those with baseline behavior and the same powertrains. This happens in part due to diseconomies of scale in the ride-hail business model. At low mode shares, ride-hail services naturally provide the trips that they can serve most efficiently. Achieving higher mode share (over a third of all trips in Scenario B6) requires serving longer trips (ride-hail trips are about 10% longer in Scenario B6 than in Base 6) that are difficult to cover with low amounts of deadheading and a high degree of pooling. This inefficiency is exacerbated in Scenario B6 where more households retire their private vehicles and the personal vehicle fleet is 22% smaller than Scenario B5 and 21% less efficient than in Scenario C6.

For the long-term scenarios, there are three scenarios each with BAU powertrains (Base 5, Scenario B5, and Scenario C5) and three with VTO research target powertrains (Base 6, Scenario B6, and Scenario C6). The impacts of automation and a preference for sharing can be isolated from differences in light-duty vehicle powertrain makeup by comparing the main workflow scenarios to a baseline scenario with the same vehicle powertrain mix—Scenarios B5 and C5 versus Base 5, and Scenarios B6 and C6 versus Base 6 (see Figure 72 and Table 12). In the both cases, the base has no automation and no preference for sharing, Scenario B has automation and a preference for sharing, and Scenario C has automation and no preference for sharing. Scenarios B6 and C6 have higher levels of automation than Scenarios B5 and C5, respectively.

Adding automation to the baseline while keeping sharing low leads to a moderate increase in energy use that is relatively similar when BAU or VTO technology assumptions are used (+7% and +10% when comparing Base 5/Scenario C5 and Base 6/Scenario C6, respectively). A similar effect is seen in the medium-term scenarios, where adding preferences for sharing and non-car modes leads to a similar reduction in energy use regardless of whether BAU or VTO technology assumptions are used (-9% when comparing Base 2/Scenario A2 and -8% when comparing Base 3/Scenario A3, respectively).

On the other hand, the behavioral assumptions in Scenario B have vastly different impacts on total energy use depending on based on whether BAU or VTO vehicle technology is assumed (0% when comparing Base 5/Scenario B5 and 20% when comparing Base 6/Scenario B6, respectively) (Figure 70). In other words, assuming moderate levels of automation and sharing has little net effect on energy use when using BAU powertrains, but assuming high levels of automation and sharing leads to a large increase in energy use when using VTO (more electrified) powertrains. This difference could be due to the differences in automation between the BAU and VTO vehicle fleets, or it could be due to the differences in electrification. The results

explored in more detail below suggest that both play a role. This difference is due in part to limitations in the ability of a shared automated ride-hailing fleet to efficiently serve large amounts of travel demand and changes in utilization to the remaining personal vehicle fleet. Scenario B6 relies heavily on automated ride-hailing vehicles to provide mobility, especially for the large number of households that give up owning a personal vehicle entirely. These AVs are online all day and therefore have more time to spend driving empty than human-driven ride-hail or personal vehicles. Due to this and other factors, explored more in Section 5.2, these ride-hail vehicles perform especially poorly in Scenario B6.

5.2 Ride-hailing

Increasing ride-hail occupancy while maintaining high enough quality service to attract travelers is a fundamentally difficult problem. Increased preference for pooled ride-hail leads to longer wait times and detours as ride-hail vehicles string together more trips, degrading customer experience and pushing riders toward solo rides. This effect limits the ability of pooled ride-hail to make up for overall fleet deadheading, even when traveler preference for pooling is very high.

Scenarios B5 and B6, with large fleets of ride-hail vehicles and widespread willingness to share rides, have the highest portion of both empty (no-passenger) VMT and the highest portion of shared miles (Figure 73). Empty miles are driven both to facilitate deadheading (moving to pick up passengers) and for repositioning or roaming while waiting for new passengers. The degree of repositioning is a calibrated parameter that was tuned to ~40% based on SMART Mobility Research in the Mobility Decision Science pillar, consistent with a recent report from the California Air Resources Board [50].

Scenario B6 has the highest portion of autonomous ride-hail vehicles, accounting for the majority of the fleet. These vehicles remain online all day and charge riders a lower price, leading to a greater ride-hail mode share but a substantial number of empty miles traveled. In calibration, researchers found that decreases to the ride-hail fleet size reduce the portion of empty miles traveled, but that they also increase wait times, which decreases the attractiveness of choosing the ride-hail mode and degrades service quality. Results suggest that ongoing developments to the algorithm that pools ride-hail riders into shared vehicles and the algorithm that moves ride-hail drivers to areas of higher demand are likely to increase the number of both shared and empty miles. However, these results also indicate that it is unlikely that fundamental constraints associated with demand patterns and the willingness of travelers to accept delays will make increasing ride-hail occupancy from less than one to a value significantly greater than one easily achievable.

Ride-hail fleets can operate most efficiently when demand is relatively dense and consistent in space and time (i.e., when a vehicle can drop off a customer and soon expect to pick up a new ride nearby). When ride-hail mode share is small, areas with a larger number of empty vehicles see shorter expected wait times and as a result appeal to more travelers, dispersing the concentration of vehicles. However, for ride-hail services to provide a large portion of typical commutes—where homes are dispersed, workplaces more concentrated, and commutes happen at the same time—they cannot rely on such natural rebalancing to match supply and demand. As an illustrative example, a ride-hail vehicle dropping off a customer in downtown San Francisco at 8:15 AM may need to drive back outside the city in order to pick up another commuter, especially if a large number of other ride-hail vehicles are dropping off riders nearby at the same time. Thus, while there are economies of scale associated with higher ride-hailing mode share (in terms of more potential customers to match with each other), there are also costs associated with meeting a large portion of typical commuting travel with ride-hailing.

While improved ride-hail matching and rebalancing algorithms could likely increase occupancy (and therefore reduce energy consumption) compared to the results presented here, these inefficiencies that emerge when ride-hail mode share is high cannot be easily overcome. Indeed, empty miles (some of which are necessary even in a perfect system) account for approximately 10% of all car (personal and ride-hail) VMT in Scenario B5 (See Figures 74 and 75). Removing these empty miles entirely, if it were possible, would decrease system energy use by at most 10%, which is still not as much as the reduction associated with meeting VTO

goals in Scenario B6. Similarly, increasing the occupancy of all non-empty ride-hail VMT to 4 would also not produce an equivalent reduction in energy use to meeting VTO technology goals.

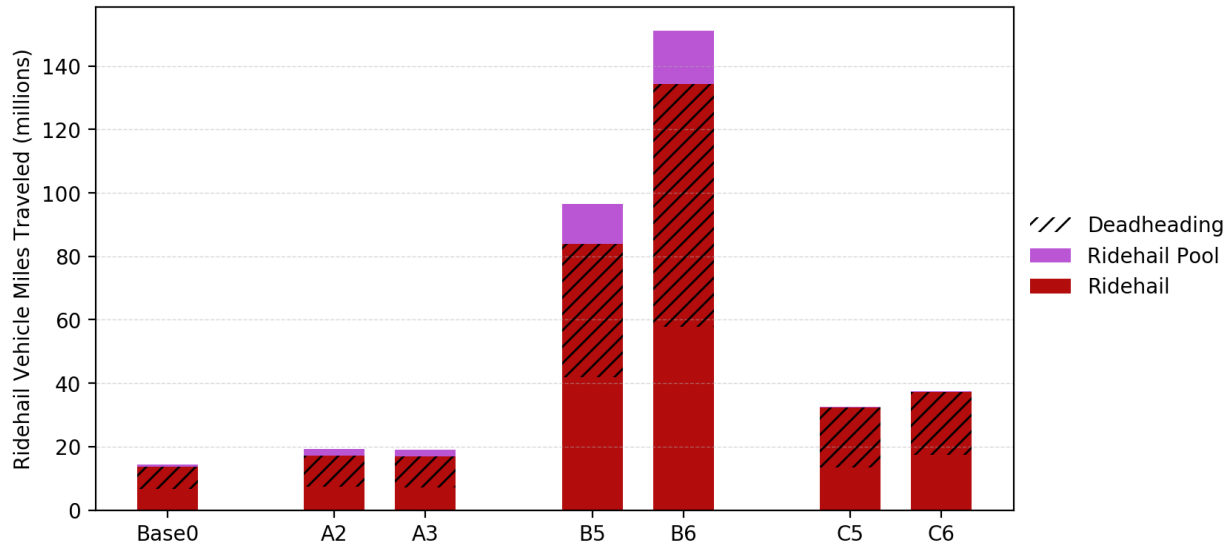


Figure 74. VMT by Ride-hails for the San Francisco Bay Area across Scenarios, Differentiating between Miles without a Passenger (Hatched) and Miles with Multiple Passengers (Purple).

Human-driven ride-hailing vehicles in a heavily utilized fleet are still empty and unmatched to passengers over 10% of the time. If ride-hailing vehicles move to increase their chances of picking up a passenger with low wait time, even if such movements happen with low probability, the result is a large number of unproductive miles traveled. Fully automated ride-hailing vehicles can operate all day, greatly increasing the supply of idle vehicles during off-peak times and potentially further increasing empty miles traveled. The total contribution of this empty driving to total VMT is sensitive to ride-hailing repositioning and matching algorithms.

One counterintuitive result is that Scenario B6, where household vehicle ownership is low and preference for sharing is high, performs worse than Scenario C6 in terms of energy use, even though the latter scenario assumes greater dependence on single-occupancy cars (Figure 68). This effect is due in large part to reduced performance of the ride-hailing fleet in Scenario B. Simulation results show that energy use is higher in Scenario B6 than both the long-term baseline (Base 6) and Scenario C6.

Despite a preference for shared rides among travelers, the matching and rebalancing algorithms simulated in BEAM are not able to substantially increase average occupancy of ride-hail vehicles from baseline levels; indeed, the average occupancy of ride-hail vehicles is less than in the baseline, due in large part to large amounts of repositioning from the ride-hail fleet (Figure 75). When local supply is higher than demand, a portion of idle ride-hail vehicles will move to locations with higher expected demand to increase their likelihood of matching a request, with this portion calibrated to match deadhead portions observed in current ride-hailing fleets [51]. Some rebalancing is necessary because ride-hailing requires low wait times in order to be competitive with other modes, and achieving low wait times requires there to be empty vehicles available for matching near potential customers. Wait times can be lowered by increasing the size of the ride-hailing fleet or by moving empty vehicles to follow demand, either decreasing the utilization of the ride-hailing fleet or decreasing its efficiency (in terms of PMT/VMT). This effect is amplified in Scenario B, where automated ride-hail vehicles operate all day and lead to an especially large oversupply of vehicles during off-peak times. When supply outstrips demand for a large portion of the day, as is the case in Scenario B, this repositioning to meet anticipated demand further inflates non-productive VMT. The inefficiency of ride-hailing would be further exacerbated if these vehicles were modeled as consuming energy and contributing to congestion or parking

constraints when they were idle, while in these simulations these idle vehicles are assumed to not consume energy but be available for matching to customers.

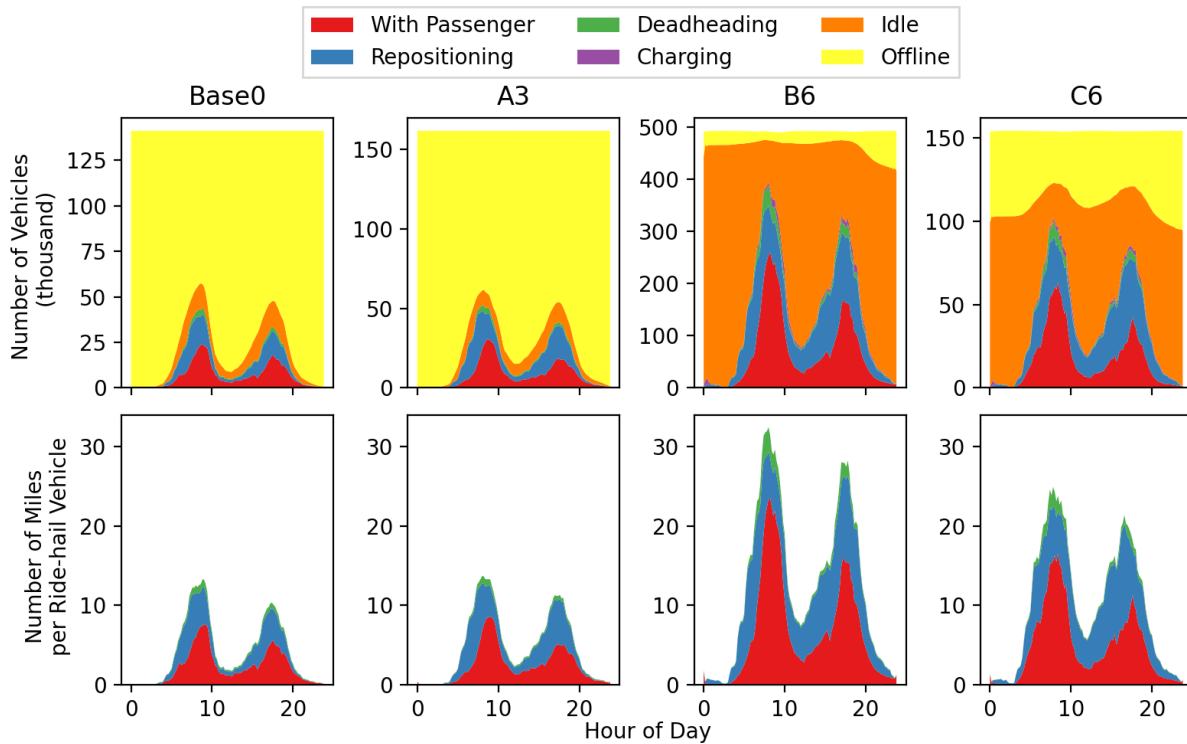


Figure 75. Utilization of Ride-hail Fleet in Base 0 and the Three VTO Scenarios. Top: Number of Ride-hail Vehicles in a State at a Given Time of Day. Bottom: Total Number of Miles Driven (Averaged per hour) by Ride-hail Fleet with Different Purposes.

Differences in the relative utilization of vehicles can lead to dramatic differences in energy use between scenarios with the same light-duty vehicle powertrain makeup, over 20% in some cases. This means that the distribution of powertrain types across different classes of use is an important driver of system-wide energy outcomes. In these high-sharing scenarios, disproportionate savings can be achieved by improving energy efficiency of the smaller (69% smaller in Scenario B6 than in Scenario C6) but heavily used (63% more VMT per vehicle) vehicles.

Average energy consumption per VMT is 5% higher in Scenario B5 than in Scenario C5, and 16% higher in Scenario B6 than in Scenario C6, canceling out or overwhelming the 5% increase in vehicle occupancy (the average number of person miles per VMT) in Scenario B compared to Scenario C. On aggregate, this means that total energy use is slightly higher in Scenario B6 than in Scenario C6, even though total light-duty VMT is lower. Even though the effective light-duty vehicle powertrain distribution is the same between those two scenarios, differences in how the vehicles are used means that overall light-duty fleet is less energy efficient (in energy per VMT) in Scenario B. Several factors combine to produce this effect. Most importantly, the powertrain composition of the personal and ride-hail fleets are different in Base 0, Scenario B, and Scenario C, even though the overall light-duty fleets are the same. For example, the scenario definitions assume that in the long-term VTO fleet, two thirds of BEVs are fully automated, despite fully automated vehicles only making up 42.5% of the total fleet. Thus, BEVs are more common in the highly automated ride-hailing fleet in Scenario B and the personal vehicle fleet in Scenario C.

Setting the ride-hail fleet size such that wait times are similar between scenarios has two important effects. On one hand, it reduces the total number of electric vehicles in Scenario B, as each automated ride-hail vehicle is

able to replace more than 10 personal vehicles. Relatedly, appropriate sizing of the ride-hail fleet means that automated ride-hail vehicles travel roughly the same distance per day in Scenarios B and C (around 300 miles on average). On the other hand, households with short commutes are modeled as more likely to retire vehicles, meaning that in Scenario B with high retirement rates, the remaining personal cars travel disproportionately far (62 miles per day on average, compared to 37 in Base 6). The result of this is that changing the behavioral and automation assumptions from Base 6 to Scenario B6 means that non-BEVs produce a larger portion of total VMT (Table 13). In addition to this effect, charging requirements of electrified ride-hail vehicles also reduce ride-hail energy efficiency in Scenario B. In Scenario B6, human-driven ride-hail PHEVs achieve 25% lower energy efficiency than personal PHEVs, and automated PHEVs get 47% lower fuel economy, as these ride-hail PHEVs rarely choose to forego fares in order to recharge their batteries and as a result primarily operate in charge-sustaining mode. These combined effects are seen in the overall fuel economy of the light-duty fleet.

Despite the same powertrain composition, when compared to Base 6 the energy consumption per unit distance driven of the light-duty vehicles is 6% higher in Scenario C6 and 23% higher in Scenario B6 relative to the baseline. In the BAU technology case, Scenarios C5 and B5 have increases in energy use per unit distance of 3% and 8%, respectively. Surprisingly, the limited range of ride-hail BEVs is not a primary driver of the lower light-duty energy efficiency in Scenario B6 than Base 6. In Scenario B, at any given time 2% of the ride-hail fleet on average will consist of plug-in vehicles that are charging, assuming ample availability of 150 kW fast chargers. The more electric vehicles are charging at once, the more likely a ride-hailing request is to be matched with one of the remaining non-plug-in vehicles, an effect that would directionally reduce fleet wide energy efficiency but is too small to lead to a significant difference in these scenarios. Occupancy (in terms of passenger miles per VMT) and utilization (VMT per unique vehicle) only differ by less than 2% between BEVs and internal combustion engine vehicles (ICEVs) in both B scenarios. In a scenario with more sparse or slower charging infrastructure, the limited range of ride-hailing BEVs might lead to further increases in energy use in Scenario B as conventional ride-hailing vehicles would need to cover more rides.

Table 13. Distribution of Light-duty Vehicle VMT across Usage (Personal vs. Ride-hail) and Powertrain Type.

		Personal Vehicle					Ride-Hail				
		Conv / HEV	Diesel	PHEV	BEV	Total	Conv / HEV	Diesel	PHEV	BEV	Total
BAU	Base5	70.8%	0.8%	7.0%	16.9%	95.5%	3.3%	0.0%	0.3%	0.8%	4.5%
	B5	64.0%	0.8%	1.2%	7.3%	73.4%	13.4%	0.1%	5.1%	8.0%	26.6%
	C5	70.3%	0.9%	5.9%	14.8%	91.9%	3.2%	0.0%	1.9%	3.0%	8.1%
VTO	Base6	47.5%	0.7%	10.7%	36.7%	95.6%	2.2%	0.0%	0.5%	1.7%	4.4%
	B6	50.6%	1.0%	1.2%	7.6%	60.4%	12.9%	0.1%	7.1%	19.5%	39.6%
	C6	42.6%	0.6%	11.1%	36.4%	90.7%	3.4%	0.0%	1.5%	4.4%	9.3%

5.3 Household CAVs

In BEAM, fully automated vehicles are treated differently than other vehicles in several respects. When CAVs are owned by a household, rather than operated by a ride-hailing fleet, household members decide how to

maximize utilization of their CAVs and then meet any remaining trips with additional vehicles and modes. When vehicles are assigned to households, CAVs are only assigned to households in roughly the top half of the overall household income distribution. These households have the highest default VOTT and hence would be least likely to take transit or non-motorized trips if faster options were available, an effect that serves to dampen increases in VMT associated with automation. In addition, partially and fully automated vehicles can participate in CACC, increasing the capacity of the road network and leading to the slight increase in road network speeds between BAU vehicle technology and VTO target vehicle technology of all workflow common scenarios with CAVs.

Vehicle automation will likely make in-car travel more comfortable and as a result has the potential to greatly increase travel distances and times. While this may be the case, this analysis uncovers several factors that will serve to limit increases to VMT in scenarios with high personal ownership of AVs, suggesting in particular that any substantial increases to travel distances are likely to come from discretionary (non-mandatory) trips.

In Scenario C, household CAVs do contribute a substantial amount to overall light-duty VMT (Figure 76), accounting for roughly half of light-duty VMT in Scenario C6 (Figure 74). Scenarios C5 and C6 both show an increase in total light-duty VMT over the other scenarios. While approximately 10% of CAV miles are driven without passengers in Scenario C, these empty miles alone do not account for the total increase in car VMT, suggesting that shifts to travel behavior and mode choice associated with convenient CAV travel and retirements of household vehicles are as important or more important of a factor than empty miles generated by CAVs.

In Scenario C6, the total number of empty CAV miles driven increases compared to Scenario C5, but the total number of light-duty VMT decreases by a greater amount. This decrease in light-duty vehicle VMT happens despite the generally greater mobility offered by CAVs compared to non-CAV light-duty vehicles. This effect is likely due to a combination of two causes: higher levels of automation, including cooperative adaptive cruise control, in the VTO scenario allow the existing road network to have a higher capacity and fewer delays, allowing vehicles to take more direct routes to their destination. In addition, Scenario C assumes that a greater reliance on CAVs and ride-hailing companies is associated with lower household vehicle ownership. This retirement of household vehicles (15% retirement in BAU, 20% in VTO) pushes some household members to rely on transit for trips that cannot be covered by a household’s vehicles. This analysis does not capture any additional trips (e.g. shopping trips and escort trips), or longer chained trips, that could be induced by CAVs. Congestion produced by these extra trips could dampen some of the accessibility benefits associated with CAV technology

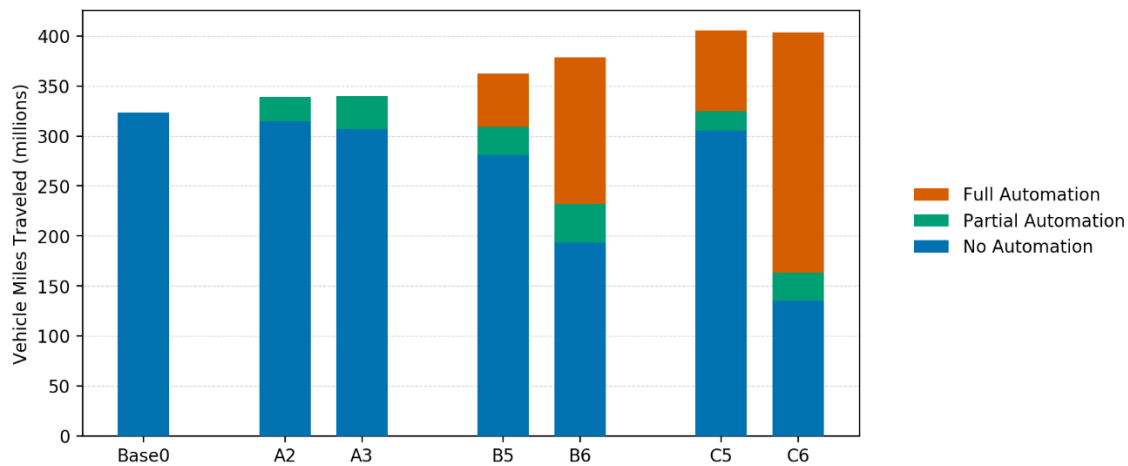


Figure 76. Light-duty VMT Disaggregated by Automation Level across Workflow Scenarios.

5.4 Land Use

Simulating multiple scenarios of vehicle automation and sharing provides insights into their implications for urban development patterns. In the workflow, a transportation demand model is linked with a land use and development model. The transportation model provides measures of accessibility that inform a simulation of the real estate market where increases in accessibility—due to either faster or less unpleasant travel options— increase the value of land and, over time, the intensity of its use. The results of this land use simulation inform models for the choice of home and work locations in ActivitySynth, where increases in the speed or favorability of travel options increases the geographical area across which agents consider home and work locations. This in turn provides the starting place for another iteration of the transportation model. The workflow is thus able to capture many of the important processes that act on different time scales that inform the evolution of urban areas, providing insight into the ways in which new technologies and changes in the perception of travel may transform cities.

Of the Workflow scenarios, Scenario B has the most reliance on expensive modes and the lowest generalized time of travel for manually operated car trips (Figure 77), which is assumed to be the primary measure of accessibility in determining what households and firms are willing to pay in rents. These differences fall in line with expectations that a reliance on modal options with higher per-use costs, such as transit and ride-hailing, lead to a downward pressure on commute times. The differences between the BAU and VTO versions of each workflow scenario tend to be muted when compared to the differences between scenarios with different behavioral assumptions.

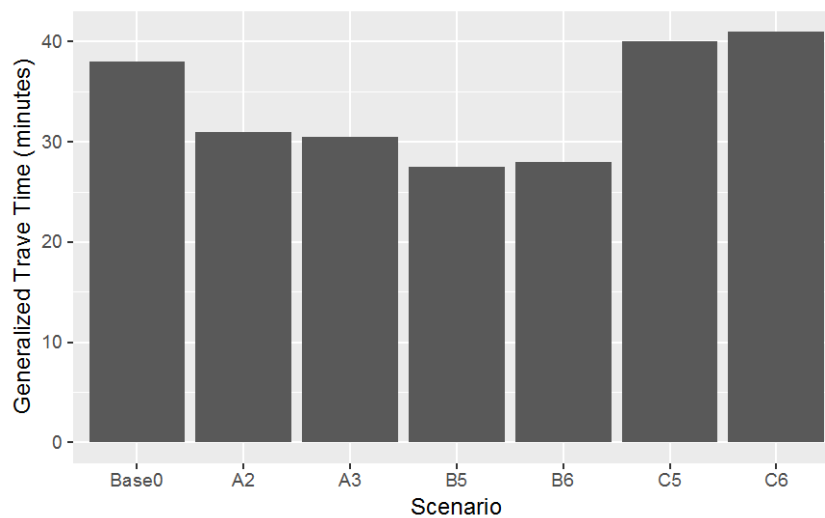


Figure 77. Average Travel Times from Home to Work for Manually Operated Car Trips, Used by Home and Workplace Location Choice Models in Urbansim.

Cities have evolved over many decades in response to changes in transportation technologies that have rapidly reduced the cost of travel (or increased speeds), resulting in a decline of the land rent gradient and density gradient of cities. To explain this phenomenon and how rent and density are related, consider that households trade off accessibility and housing prices. When transportation costs decline due to advances in transportation technology or investment in infrastructure, it increases the relative attractiveness of locations that are farther away from the urban core. Outlying places that were previously inaccessible see significant increases in their accessibility, and the demand for those locations increases. This leads to increases in land costs as competition for those locations goes up. Along the gradient from the urban core to the periphery, land costs follow a gradient of decline.

These land price patterns then translate into changes in the building stock. Those locations with low land prices tend to use more land as a factor of production, relative to capital. Those that are more expensive do the opposite: they substitute towards capital and away from land. In other words, developers build taller buildings in places that have higher land costs, and lower density in places that have lower land costs, based on production economics.

The UrbanSim models used in the BEAM workflow implementation use generalized travel time in order to account for the way people are expected to change their value of time (e.g., being transported in a partial or fully automated vehicle may be more productive to an individual than actively driving the vehicle for the same amount of time). Models including residential location choice, workplace choice and employment (firm) location choice are all sensitive to generalized travel times. As a result, the rent and density gradients change in ways that are consistent with urban economic theory. In the common SMART scenarios, it is expected that the biggest increases in costs and *perceived* travel times would lead to the most flattening of the rent gradient.

SMART workflow results from UrbanSim and BEAM demonstrate this consistency, showing that local accessibility in shared mobility scenarios is greater and more uniform, which in turn will lead to more uniform rents and less development pressure in the highest-accessibility areas. Baseline rents per square foot in residential buildings, for example, have the steepest gradient with respect to job accessibility in the C scenarios, where the network is the most congested and generalized travel times are high. On the other hand, Scenarios B5 and B6, with the shortest generalized times, show the greatest flattening of the rent gradient. In other words, in Scenario B generalized accessibility increases. As a result, there are more locations with relatively high accessibility and therefore less competition for the most favorable locations. Less competition means that the real estate market will bear less variation in rents between the central and non-central locations. These results are fully consistent with expectations.

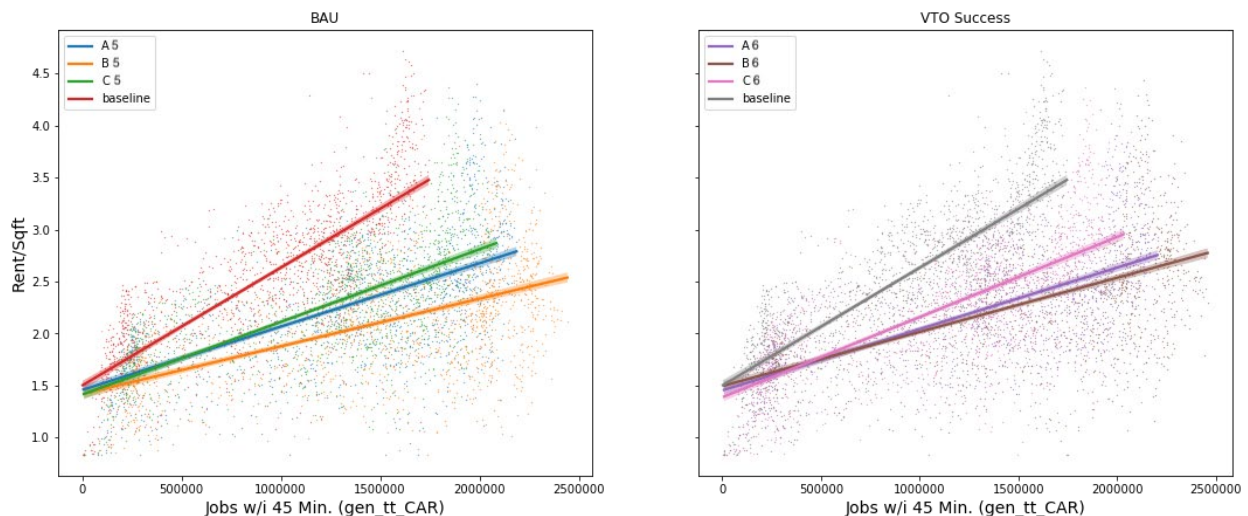


Figure 78. Relationship between Rent and Accessibility, Measured as Number of Jobs That Can Be Reached by Car within a Given Generalized Travel Time.

Examining the relationship between employment density and accessibility also shows that the steepest gradient is for the baseline scenario, while Scenarios B5 and B6 have the flattest gradient. Interestingly, even though the shared and non-motorized modes that are favored in Scenarios A and B tend to perform best in denser areas, where trips are shorter and demand more concentrated, this analysis finds that the effects of shared mobility do not in turn provide a strong market mechanism for increased density and concentration of workplaces. In the long run, the shallower rent gradient for Scenarios A and B, as shown in Figure 79, would be expected to lead to more housing and job sprawl, in turn limiting the ability to which the San Francisco Bay Area would be able to take advantage of the increased preferences for shared and non-motorized modes in

Scenarios A and B. In scenarios with more sprawl, fewer commutes will be well served by public transit, and ride-hailing services will be less able to group passengers with similar origins and destinations into pooled trips.

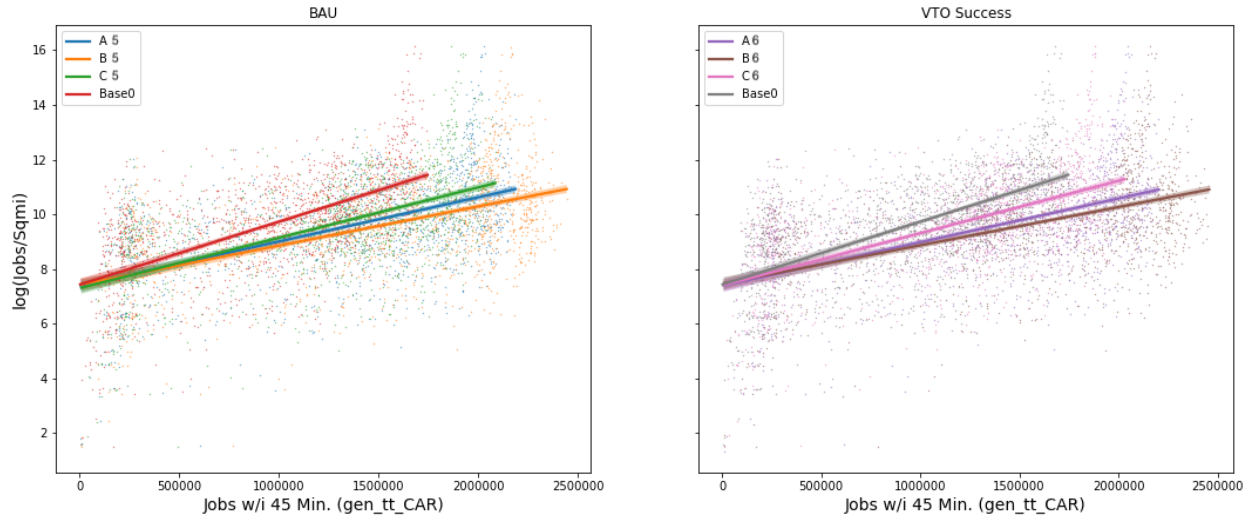


Figure 79. Relationship between Job Density and Accessibility, Measured as Number of Jobs That Can Be Reached by Car within a Given Generalized Travel Time.

5.5 Light-Duty Vehicle Charging Infrastructure

Simulation of approximately 420,000 personal and ride-hailing PEVs in San Francisco suggests that 7,770 fast-charging plugs could be necessary to meet consumer demand (a $9\times$ increase over existing infrastructure). Table 14 provides quantitative results for each workflow scenario. The PEV fleet in BEAM is comprised of two powertrain types (PHEVs and BEVs) and three use cases (personal ownership, human driven ride-hailing, and fully automated ride-hailing). In addition to previously discussed residential charging assumptions, personal and ride-hailing PEVs are assumed to have access to a network of workplace and public charging stations (PHEVs are assumed only capable of Level 2 charging). CAV ride-hailing vehicles are assumed to utilize a separate network of private fast-charging stations (as designed by FCSPlan).

Despite BEAM simulating significantly more public charging events than workplace charging events in all scenarios, the size of the workplace and public charging networks (number of stations and plugs) is similar. This demonstrates that much of the activity at public charging stations consists of fast charging (typically shorter charging times and higher vehicle throughput) and that vehicle arrival patterns at workplace stations tends to limit the ability for drivers to share charging infrastructure (i.e., drivers are assumed to plug in and begin charging immediately upon arrival at a destination). Further, despite PEV fleet sizes that can vary by up to a factor of 10 between scenarios, the relative size of the public charging network (number of plugs per electric vehicle) remains relatively constant, ranging from 27 to 31 plugs per 1,000 electric vehicles for Level 2 chargers, and 19 to 26 plugs per electric vehicle for DC fast chargers. This indicates that targets for the correct sizing of the public charging network are relatively robust to behavioral differences between scenarios. On the other hand, there is more variability in terms of the correct sizing of the Workplace Level 2 charging network, with values ranging from 34 to 57 plugs per PEV. These estimates for the required number of plugs are highest in the two C scenarios, where reliance on personal vehicles is highest. As a whole, these results suggest that there are not necessarily economies of scale to be achieved that would allow each piece of infrastructure to be utilized more heavily as the personal vehicle fleet electrifies. These results demonstrate that the design of

future charging networks can benefit from advanced simulation that quantify complex relationships between PEV fleet size, driving patterns, and infrastructure utilization.

Table 14. Summary of EVI-Pro Public Charging Networks Simulated for BEAM Workflow.

Parameter	Scenario					
	A2	A3	B5	B6	C5	C6
<i>Personal PHEVs</i>	69,860	115,270	26,250	23,950	51,660	54,440
<i>Personal BEVs</i>	93,380	162,560	150,570	159,520	280,110	357,540
<i>Human ride-hail PHEVs</i>	1,170	1,390	3,280	340	600	1,020
<i>Human ride-hail BEVs</i>	1,940	1,990	13,890	3,420	3,320	5,780
<i>Workplace charge events</i>	8,210	13,300	9,500	9,930	21,690	27,990
<i>Workplace stations</i>	880	1,190	980	1,110	1,800	2,200
<i>Public charge events</i>	36,920	63,480	39,810	37,670	70,750	79,380
<i>Public stations</i>	1,520	2,090	1,690	1,580	2,160	2,320
<i>Workplace Level 2 EVSE</i>						
<i>Plug count</i>	6,660	9,530	8,020	8,550	18,520	23,920
<i>Average events/plug</i>	1.2	1.4	1.2	1.2	1.2	1.2
<i>Average plugs/station</i>	7.6	8.0	8.2	7.7	10.3	10.9
<i>Average plugs/1,000 PEVs</i>	40	34	41	46	55	57
<i>Public Level 2 EVSE</i>						
<i>Plug count</i>	4,840	8,300	5,330	5,770	10,310	11,540
<i>Average events/plug</i>	1.5	1.5	1.3	1.2	1.3	1.4
<i>Average plugs/station</i>	3.2	4.0	3.2	3.7	4.8	5.0
<i>Average plugs/1,000 PEVs</i>	29	30	27	31	31	28
<i>Public DCFC</i>						
<i>Plug count</i>	4,110	5,860	5,080	4,380	7,620	7,770
<i>Average events/plug</i>	7.2	8.7	6.5	7.0	7.5	8.2
<i>Average plugs/station</i>	2.7	2.8	3.0	2.8	3.5	3.3
<i>Average plugs/1,000 PEVs</i>	25	21	26	23	23	19

6 Conclusions

Dedicated to furthering the understanding of the energy implications and opportunities of advanced mobility technologies and services, the DOE's SMART Mobility Consortium was formed to create tools and generated knowledge about how future mobility systems may evolve and how these evolutions will impact overall mobility, energy, and productivity.

Due to the large number of factors currently disrupting transportation, a multi-fidelity end-to-end modeling workflow is required to capture the complex interactions among mobility decision-making, technology implementation, different mobility service models and modes, land use, and EV charging infrastructure. This unique capability integrates freight and passenger movement and allows researchers to evaluate the energy, mobility, and affordability outcomes of potential future transportation scenarios. The workflow is built around two core agent-based models (ABMs) that simulate the transportation system. These two implementations of the SMART Mobility workflow were developed in parallel, and demonstrate that different tools with different levels of fidelity can be used interchangeably, employing a similar set of assumptions.

- One implementation is built around Planning and Operations Language for Agent-based Regional Integrated Simulation (POLARIS), a high-performance, open-source ABM framework developed by Argonne National Laboratory, designed for simulating large-scale transportation systems.
- Another implementation is built around the Behavior, Energy, Autonomy, and Mobility (BEAM), a modeling framework for behavior, energy, autonomy, and mobility developed by Lawrence Berkeley National Laboratory (LBNL), which extends the Multi-Agent Transportation System Framework (MATSim) to enable scalable analysis of urban transportation systems.

While both workflow implementations rely on different models to address each specific steps, they share some common elements:

- UrbanSim: a microsimulation platform for forecasting the growth and development of metropolitan regions over decade-scale time horizons, including changes to land use, demographics, and employment.
- Electric Vehicle Infrastructure Projection (EVI-Pro): a tool used to determine public charging station location and type based on plug-in vehicle (PEV) trip demand.
- Aimsun: a commercial traffic microsimulation tool used to generate traffic flow fundamental diagrams, such as the relationship between the speed, flow rate, and density of vehicles on a given transportation link, for different market penetrations of automated vehicles.
- Mobility energy productivity (MEP): a methodology that quantifies the energy, cost, and time-weighted opportunity space within a reachable area—how many goods, services, and destinations can be reached by a given mode of transport, in a specified amount of time.

Several major trends, such as vehicle connectivity, automation, sharing, and electrification are poised to have a significant impact on the transportation system. How these trends evolve (e.g., whether partial or full automation is incorporated into vehicles, what the market penetration is for new technologies or mobility services) remains uncertain. In addition, dynamic system interactions among these trends are complex, and may impact the transportation system in ways that are not fully understood. To quantify the impact of new mobility technologies independently from other parameters including land use, vehicle technology and freight, consortium members developed a series of current and future baseline scenarios that assume no/low/high vehicle technology development, but with no changes in vehicle connectivity, automation, and sharing. Three main future scenarios were created to quantify the impact of connectivity, automation, and sharing relative to the baselines:

1. **Scenario A: High Sharing, Low Automation.** This scenario represents a near-term future with a moderate increase in vehicle ride-hailing fleets along with the penetration of partially automated vehicle technologies (e.g., advanced driver assistance systems).
2. **Scenario B: High Sharing, High Automation.** This scenario represents a longer term future where fully automated driverless vehicles are owned by fleet operators and widely shared by large segments of the population. E-commerce is common among households.
3. **Scenario C: Low Sharing, High Automation.** Like Scenario B, Scenario C represents the longer term future with fully automated driverless vehicles. In Scenario C, however, those vehicles are owned by individuals and shared within the household (i.e., privately owned AVs). It is thus a low ride-hailing case alternative to Scenario B. E-commerce is common among households.

A set of high level insights were developed from the workflow, including:

- **Vehicle Repositioning to Search for Riders is a major source of Empty Miles:** In the Chicago metropolitan area, high-sharing scenarios without vehicle repositioning to search for riders (i.e., Scenarios A and B) achieve lower vehicle miles travelled (VMT) than their respective baselines due to the efficient use of ride-hailing, the small share of VMT without a passenger (below 15%), and a significant amount of ride pooling (22–27%). In the San Francisco metropolitan area, ride-hailing vehicles in a heavily utilized fleet are often empty and unmatched to passengers. If ride-hailing vehicles reposition to increase their chances of picking up a passenger – including pooled passengers – with low wait time, even if such movements happen with low probability, the increase in empty VMT from this repositioning overwhelms any VMT reductions from increased pooling, even with low prices and no consumer aversion to shared rides. These results are sensitive to ride-hailing repositioning and matching algorithms.
- **Personally Owned Driverless Vehicles Increase VMT:** The use of privately owned automated vehicles (AVs) leads to drastically increased VMT and greatly increased unloaded vehicle travel, with 1 out of 7 vehicles in the system being empty, compared to 1 out of 25 in the high-sharing, high-automation case (Scenario B6). In the Chicago metropolitan area, a 52% penetration of privately owned, fully automated vehicles (Scenario C6) leads to an increase of 25% in VMT compared to Base 6. This occurs due to two primary phenomena: the increase in VMT with no passenger due to increased vehicle repositioning in the privately owned AV case, and the increase in overall travel resulting from the assumed reduction in value of travel time (VOTT) in an AV.
- **Personally Owned Driverless Vehicles Impact Travel Behavior:** Households with AVs exhibit substantially different travel behavior compared to households without AVs. This behavior includes a propensity to travel longer during peak evening hours and to take more single-occupancy vehicle (SOV) trips. Households with AVs exhibit higher travel time compared to households without AVs; average trip travel time for AV households is approximately 7 minutes higher than for non-AV households during peak periods. In general, households with AVs tend to travel farther and for longer durations, especially for discretionary activities: for these activities, the average travel time is more than 6 minutes longer and the average travel distance is 4 miles farther than for households without AVs. The share of SOV trips for AV households is also 7% higher than that of non-AV households. These households travel farther and for longer durations by SOV, high-occupancy vehicle (HOV), and ride-hail modes compared to households without AVs. The reduced VOTT for AV travel is the major factor contributing to the differences in the travel behavior between households with and without AVs, along with unloaded vehicle repositioning as household members share the use of the AV.
- **Transit is Critical to Mobility:** Transit is vital to the overall transportation system. In a Chicago metropolitan area-based scenario with no transit, all mobility and energy metrics become substantially worse in the urban core: there is a 52% increase in VHT and a 23% decrease in travel efficiency

(passenger miles per kilowatt-hours). To analyze the effect of transit on regional mobility, an additional scenario was implemented to analyze a no-transit case. This no-transit scenario was the same as the Base 0 scenario, but with all transit links and vehicles removed in the Chicago metropolitan area. The findings indicate there would be substantial adverse effects on mobility and energy use throughout the entire region, but the negative effects are more pronounced in the urban area.

- Freight Movement Will Be Increasingly Important to Transportation Energy Use:** Medium- and heavy-duty (MD and HD) vehicles currently account for 33% of the overall transportation energy in the Chicago metropolitan area. This share is expected to grow to 50% in the future due to light-duty vehicle efficiency improvements enabled by electrification combined with increased freight demand. MD/HD truck energy represents 33% of the total energy for the Base 0 scenario and Scenario A, up to 50% for Scenario B, and up to 40% for Scenario C. The increased portion of MD/HD truck energy in future scenarios can primarily be explained by the lower level of electrification in MD/HD trucks, and the fact that their VMT is expected to increase over time. Note that in Scenario B, MD/HD trucks consume 50% of the total energy, although they are responsible for only 10% of VMT.
- An Increase in E-Commerce Lowers Overall System VMT and Energy;** E-commerce is expected to generate a large increase in last-mile delivery of goods. However, after accounting for shopping trip reductions and vehicle technology changes, simulations show that there will be an overall net reduction in VMT (34–56%) and energy use (29–54%) across the Chicago metropolitan area. The e-commerce delivery rate is assumed to increase from one delivery per household per week in the current baseline (Base 0–Base 6) to three per week in the near term (Scenarios A2, A3), and five per week in the long term (Scenarios B5, B6, C5, C6). Because the average shopping trip is 7–8 miles long and shopping trips currently constitute approximately 7% of total VMT, there is substantial potential for VMT and energy to decrease if shopping trips are replaced by deliveries. If household e-commerce deliveries triple in the short term compared to the base year (Base 0), retail-based VMT could decrease by 31%, and retail-based energy consumption could decrease by 39–49%. Over the long term, if household e-commerce deliveries were to grow to five days per week, retail-based VMT and energy consumption could decline by 36–50% and 54–72%, respectively. The VMT savings are even greater when comparing the future (Scenarios A, B, C) to their respective baselines (Base 1, Base 2, Base 3 and Base 4, Base 5, Base 6).
- MEP improvements are greater in the high sharing, high automation scenarios (B5/B6) than in the low sharing, high automation scenarios (C5/C6), demonstrating that shared mobility has additional travel cost, time, and energy benefits beyond those due to vehicle technology improvements alone.** As shown in Figure ES-10, for both workflow implementations, MEP score improvements are higher in Scenario B5/B6 than in Scenario C5/C6. This shows that reduced network congestion and increased vehicle occupancy brought out by shared mobility augment the benefits associated with vehicle technology improvements. In the privately-owned CAV scenario (Scenario C), networks are more congested compared to shared-mobility scenarios, which causes MEP scores to drop. As a result, the calculated MEP in Scenario C is lower than MEP in Scenario B with similar vehicle technology improvements.

References

1. 2018 revision of world urbanization prospects, United Nations, May 16, 2018, <https://www.un.org/development/desa/publications/2018-revision-of-world-urbanization-prospects.html>
2. McKinsey, “Urban world: The global consumers to watch,” March 2016. <https://www.mckinsey.com/featured-insights/urbanization/urban-world-the-global-consumers-to-watch>
3. Y. Hou, V. Garikapati, A. Nag, S.E. Young, and T. Grushka, 2019. “Novel and Practical Method to Quantify the Quality of Mobility: Mobility Energy Productivity Metric.” *Transportation Research Record*. <https://doi.org/10.1177/0361198119848705>
4. J. Auld, M. Hope, H. Ley, V. Sokolov, B. Xu, and K. Zhang, 2016, “POLARIS: Agent-based modeling framework development and implementation for integrated travel demand and network and operations simulations,” *Transp. Res. Part C Emerg. Technol.*
5. Argonne National Laboratory, 2020, “Autonomie,” *Autonomie*. [Online]. Available: www.autonomie.net
6. G.F. Newell, 1993, “A simplified theory of kinematic waves in highway traffic, part I: General theory,” *Transportation Research Part B: Methodological* 27(4): 281–287.
7. W. Zhang, S. Guhathakurta, and E. B. Khalil, 2018, “The impact of private autonomous vehicles on vehicle ownership and unoccupied VMT generation,” *Transp. Res. Part C Emerg. Technol.* 90: 156–165, May.
8. Y. Zhao and K.M. Kockelman, 2018, “Anticipating the Regional Impacts of Connected and Automated Vehicle Travel in Austin, Texas,” *J. Urban Plan. Dev.* 144(4): 04018032, Dec.
9. P. Bansal and K. M. Kockelman, 2017, “Forecasting Americans’ long-term adoption of connected and autonomous vehicle technologies,” *Transp. Res. Part Policy Pract.* 95: 49–63, Jan.
10. J. Auld, O. Verbas, M. Javanmardi, and A. Rousseau, 2018, “Impact of Privately-Owned Level 4 CAV Technologies on Travel Demand and Energy,” *Procedia Comput. Sci.* 130: 914–919.
11. M. Javanmardi, J. Auld, and O. Verbas, 2018, “Analyzing Intra-household Fully Autonomous Vehicle Sharing,” presented at the Transportation Research Board 97th Annual Meeting Transportation Research Board.
12. Ö. Verbas, J. Auld, H. Ley, R. Weimer, and S. Driscoll, 2018, “Time-Dependent Intermodal A* Algorithm: Methodology and Implementation on a Large-Scale Network,” *Transp. Res. Rec.* 2672(47): 219–230, Dec.
13. J. Bischoff and M. Maciejewski, 2016, “Simulation of City-wide Replacement of Private Cars with Autonomous Taxis in Berlin,” *Procedia Comput. Sci.* 83: 237–244, Jan.
14. J. Auld, O. Verbas, M. Javanmardi, and A. Rousseau, 2018, “Impact of Privately-Owned Level 4 CAV Technologies on Travel Demand and Energy,” *Procedia Comput. Sci.* 130: 914–919.
15. X.-Y. Lu, J. Lee, D. Chen, J. Bared, D. Dailey, and S.E. Shladover, 2014, “Freeway Micro-simulation Calibration: Case Study Using Aimsun and VISSIM with Detailed Field Data,” in *Proceedings of the 93rd Transportation Research Board Annual Meeting*.

16. S. Hess, A. Daly, T. Dekker, M. O. Cabral, and R. Batley, 2017, “A framework for capturing heterogeneity, heteroskedasticity, non-linearity, reference dependence and design artefacts in value of time research,” *Transp. Res. Part B Methodol.* 96: 126–149, Feb.
17. M. Harb, Y. Xiao, G. Circella, P.L. Mokhtarian, and J.L. Walker, 2018, “Projecting travelers into a world of self-driving vehicles: estimating travel behavior implications via a naturalistic experiment,” *Transportation* 45(6): 1671–1685, Nov.
18. A. Malokin, G. Circella, and P.L. Mokhtarian, 2015, “How do activities conducted while commuting influence mode choice?” *Testing public transportation advantage and autonomous vehicle scenarios*. No. 15-1179.
19. J. Gao, A. Ranjbari, and D. MacKenzie, 2019, “Would being driven by others affect the value of travel time? Ridehailing as an analogy for automated vehicles,” *Transportation*, 46: 1–14
20. E. Wood, S. Raghavan, C. Rames, J. Eichman, and M. Melaina, 2017, *Regional Charging Infrastructure for Plug-In Electric Vehicles: A Case Study of Massachusetts*, NREL/TP-5400-67436, January, <https://www.nrel.gov/docs/fy17osti/67436.pdf>
21. E. Wood, C. Rames, M. Muratori, S. Raghavan, S. Young, 2018. *Charging Electric Vehicles in Smart Cities: An EVI-Pro Analysis of Columbus, Ohio*, NREL Technical Report NREL/TP-5400-70367, <https://www.nrel.gov/docs/fy18osti/70367.pdf>
22. A. Bedir, N. Crisostomo, J. Allen, E. Wood, C. Rames, 2018. *California Plug-In Electric Vehicle Infrastructure Projections: 2017-2025*, CEC Staff Report CEC-600-2018-001, <https://www.nrel.gov/docs/fy18osti/70893.pdf>
23. M. Moniot, C. Rames, and E. Wood, 2019, *Meeting 2025 Zero Emission Vehicle Goals: An Assessment of Electric Vehicle Charging Infrastructure in Maryland*, NREL Technical Report NREL/TP-5400-71198, <https://www.nrel.gov/docs/fy19osti/71198.pdf>
24. E. Wood, C. Rames, M. Muratori, S. Raghavan, and M. Melaina, 2017, *National Plug-In Electric Vehicle Infrastructure Analysis*, DOE Office of Energy Efficiency and Renewable Energy, September, <https://www.nrel.gov/docs/fy17osti/69031.pdf>
25. G. Tal, J.H. Lee, and M.A. Nicholas, 2018, *Observed Charging Rates in California*, UCD-ITS-WP-18-02, University of California Davis, September, <https://escholarship.org/uc/item/2038613r>
26. The MATSim Book,” MATSim.org. [Online]. Available: <https://matsim.org/the-book>. [Accessed: Sept. 30, 2018]
27. R.A. Waraich, D. Charypar, M. Balmer, and K.W. Axhausen, 2015, “Performance improvements for large-scale traffic simulation in MATSim.” In *Computational Approaches for Urban Environments*, pp. 211–233. Springer, Cham
28. <https://github.com/ual/activitysynth>
29. J. Holden, et al., 2018, “Trip Energy Estimation Methodology and Model Based on Real-World Driving Data for Green-Routing Applications,” *Transportation Research Record* 2672.24: 41–48.
30. J. Alonso-Mora, S. Samaranyake, A. Wallar, E. Frazzoli, and D. Rus, 2017, “On-Demand High-Capacity Ride-Sharing via Dynamic Trip-Vehicle Assignment.” *Proceedings of the National Academy of Sciences* 114(3): 462–67. <https://doi.org/10.1073/pnas.1611675114>.

31. Krishna, K., and M. Narasimha Murty. "Genetic K-means algorithm." *IEEE Transactions on Systems, Man, and Cybernetics, Part B (Cybernetics)* 29, no. 3 (1999): 433-439
32. Liu, H., Xiao, L., Kan, X.D., Shladover, S.E., Lu, X.Y., Wang, M., Schakel, W. and van Arem, B., 2018. Using Cooperative Adaptive Cruise Control (CACC) to Form High-Performance Vehicle Streams. FINAL REPORT
33. US DOT FHWA, "Freight Analysis Framework Inter-Regional Commodity Flow Forecast Study: Final Forecast Results Report", 2012, <https://ops.fhwa.dot.gov/publications/fhwahop16043/fhwahop16043.pdf>
34. ORNL, National Household Travel survey, <https://nhts.ornl.gov/>
35. H. Park, D. Park, and I.-J. Jeong, 2016, "An effects analysis of logistics collaboration in last-mile networks for CEP delivery services," *Transport Policy* 50: p. 115–125.
36. E. Islam and all, "An Extensive Study on Sizing, Energy Consumption and Cost of Advanced Vehicle Technologies, ANL report ESD-17/17, October 2018, https://www.autonomie.net/publications/fuel_economy_report.html
37. IEA Annual Energy Outlook, www.iea.gov/aeo
38. www.eia.gov
39. N. Menon, N. Barbour, Y. Zhang, A. Rawoof Pinjari, and F. Mannering, 2019, "Shared autonomous vehicles and their potential impacts on household vehicle ownership: An exploratory empirical assessment," *International Journal of Sustainable Transportation* 13(2): 111–122.
40. R. R. Clewlow and G.S. Mishra, 2017, *Disruptive transportation: the adoption, utilization, and impacts of ride-hailing in the United States*. UCD-ITS-RR-17-07, UC Davis Institute of Transportation.
41. A. Henao and W.E. Marshall, 2018, "The impact of ride-hailing on vehicle miles traveled," *Transportation* 1: 2.
42. A. Tirachini 2019, "Ride-hailing, travel behaviour and sustainable mobility: an international review," *Transportation*, <https://doi.org/10.1007/s11116-019-10070-2>
43. J. Bischoff and M. Maciejewski, 2016, "Simulation of City-wide Replacement of Private Cars with Autonomous Taxis in Berlin," *Procedia Comput. Sci.* 83: 237–244, Jan.
44. W. Zhang, S. Guhathakurta, J. Fang, and Ge Zhang, 2015, "The performance and benefits of a shared autonomous vehicles based dynamic ridesharing system: An agent-based simulation approach." In *Transportation Research Board 94th Annual Meeting*, no. 15-2919.
45. M. Hyland and H.S. Mahmassani, 2018, "Dynamic autonomous vehicle fleet operations: Optimization-based strategies to assign AVs to immediate traveler demand requests," *Transportation Research Part C: Emerging Technologies* 92: 278–297.
46. A. Malokin, G. Circella, and P.L. Mokhtarian, 2015, "How do activities conducted while commuting influence mode choice?" *Testing public transportation advantage and autonomous vehicle scenarios* 15-1179.
47. J. Gao, A. Ranjbari, and D. MacKenzie, 2019, "Would being driven by others affect the value of travel time? Ridehailing as an analogy for automated vehicles," *Transportation* [volume 46]: 1–14.

48. M.D. Simoni, K.M. Kockelman, K.M. Gurumurthy, and J. Bischoff, 2019, "Congestion pricing in a world of self-driving vehicles: An analysis of different strategies in alternative future scenarios," *Transp. Res. Part C Emerg. Technol.* 98: 167–185, Jan.
49. C. Rodier, 2019, "Automated Vehicle Scenarios: Simulation of System-Level Travel Effects Using Agent-Based Demand and Supply Models in the San Francisco Bay Area," National Center for Sustainable Transportation.
50. California Air Resources Board, 2018 Base-year Emissions Inventory Report Technical Documentation. https://ww2.arb.ca.gov/sites/default/files/2019-12/SB%201014%20-%20Base%20year%20Emissions%20Inventory_December_2019.pdf. 2019
51. Wenzel, Tom, Clement Rames, Eleftheria Kontou, and Alejandro Henao. "Travel and energy implications of ridesourcing service in Austin, Texas." *Transportation Research Part D: Transport and Environment* 70 (2019): 18-34.

APPENDIX A – Models Validation

A.1 Autonomie (Vehicle Energy Consumption)

Argonne has been validating vehicle models for close to 20 years [1], leveraging vehicle dynamometer test data from the Advanced Mobility Technology Laboratory (AMTL). Test data were collected at Argonne from more than 60 vehicles, ranging from model year 2000 to the present. A large number of signals were collected on each vehicle for critical analysis. Signals include component efforts (torque, current, etc.) and flow (rotational speed, linear speed, etc.), as well as temperatures and direct fuel-flow measurement collected using sensors and high-speed Controller Area Network (CAN). These measurements were integrated and aligned into a single data acquisition system. Some additional parameters were estimated on the basis of measured data and other advanced-technology vehicles, (e.g., motor current as estimated from measured speed, torque and voltage). Each individual model was then independently validated. Vehicle system model validation was quantified using normalized cross correlation power (NCCP) [2] over a large number of cycles.

As a result, a large number of Autonomie vehicle models have been validated within test-to-test repeatability for a wide range of technologies and powertrain configurations. The following section illustrates some validation examples for light-duty vehicles, using AMRF data. It is worth noting that additional vehicle classes (e.g., MD and HD) and powertrain configurations including start-stop, blended plug-in hybrid electric vehicle (PHEV, e.g., Prius Prime), and battery electric vehicles (BEVs) have also been validated.

A.1.1 Conventional Powertrain

The main focus of conventional powertrain validation is on the multi-speed shifting algorithm calibration. First, the simulated vehicle speed, engine speed, and engine torque were compared with test results. For example, Figure A1.1 shows the comparison for an automatic transmission on the UDDS cycle:

- Initial calibration (simulation 1),
- Calibrated algorithm using test data (simulation 2)

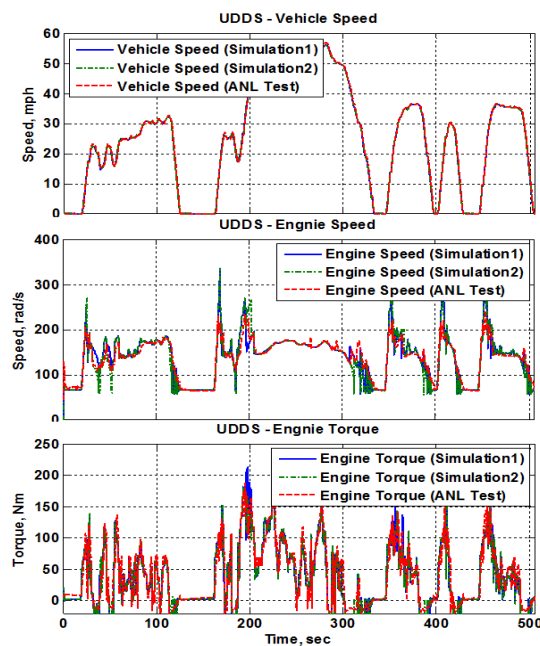


Figure A1.1. Autonomie Simulation and Testing Results on UDDS Cycle (0–505 s) for 2013 Sonata Conv. 6ATX.

In Figure A1.2, the gear numbers on the UDDS cycle are compared with the test results for both 6- and 8-speed transmissions. Both simulations are close in shifting performance to the test results. Figure A1.3 demonstrates the robust calibration of the shifting algorithm during the Normalized European Driving Cycle (NEDC).

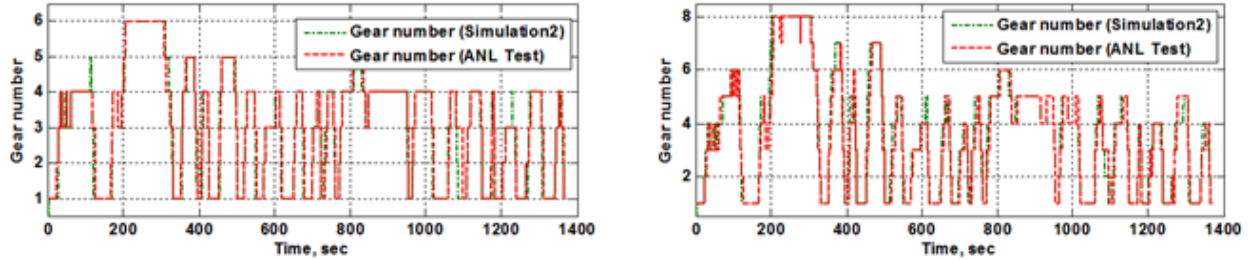


Figure A1.2. Autonomie Shifting Algorithm Validation for 2013 Sonata Conv. 6ATX (Left) and 2013 Chrysler 300 8ATX (Right) on the UDDS Cycle (0-505 s).

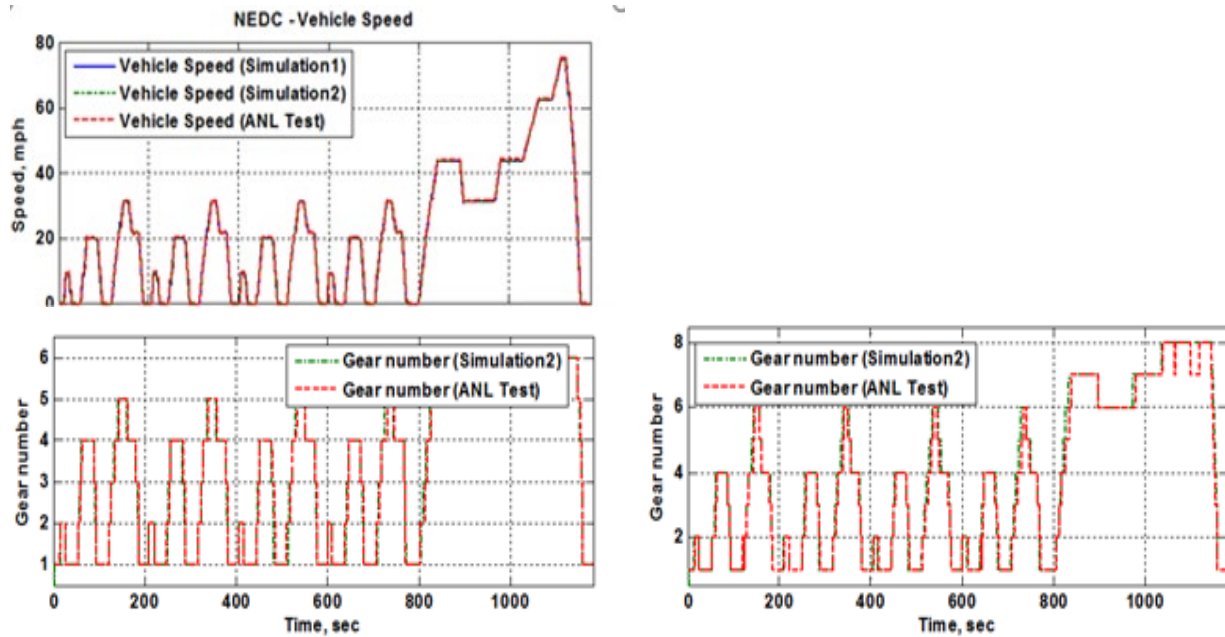


Figure A1.3. Autonomie Shifting Algorithm Validation for 2012 Fusion Conv. 6ATX (Left) and 2013 Chrysler 300 8ATX (Right) on the NEDC Cycle.

The Continuously Variable Transmission (CVT) model and shifting control strategy developed in Autonomie were also validated by comparing the simulation results with the experimental results from Argonne’s AMRF. Figure A1.4 shows the validation results for the 2012 Honda Civic HEV system on the UDDS and highway (HWFET) cycles. The simulated vehicle speed, gear ratio, engine torque and battery state of charge (SOC) behave similarly to the experimental results, demonstrating the validity of the simulation model and control strategy.

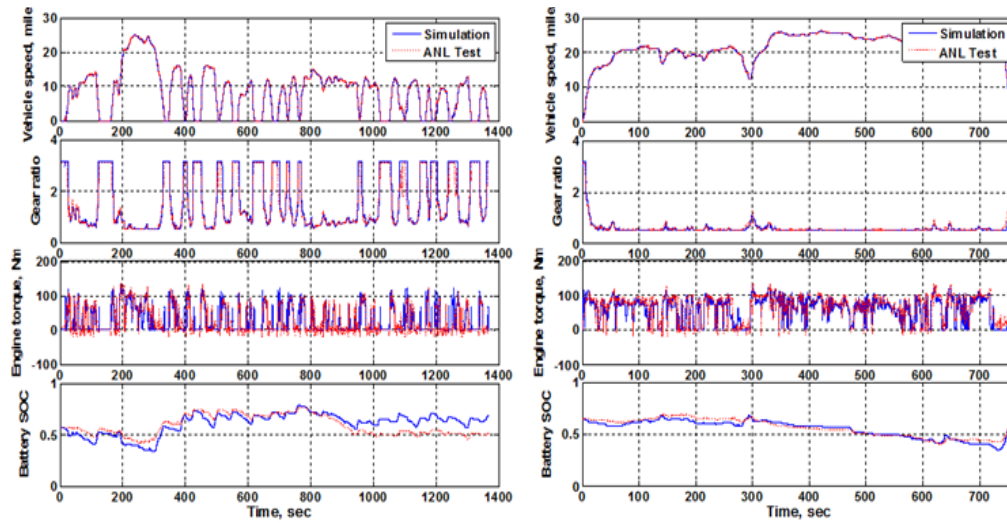


Figure A1.4. Autonomie Comparison of Simulation and Test Data for 2012 Honda Civic CVT HEV on UDDS (Left) and HWFET (Right)

A.1.2 Power-Split HEV

Multiple versions of the power-split HEV have been tested and validated since early 2000. Similarly to the other powertrains, SMART researchers focus first and foremost on validating the component operating conditions throughout the driving cycles. For example, Figure A1.5 shows consistent engine on/off, SOC control and component operating conditions (engine torque and speed) for the 2010 Toyota Prius on the UDDS cycle. The latest Toyota Prius HEV has been similarly validated.

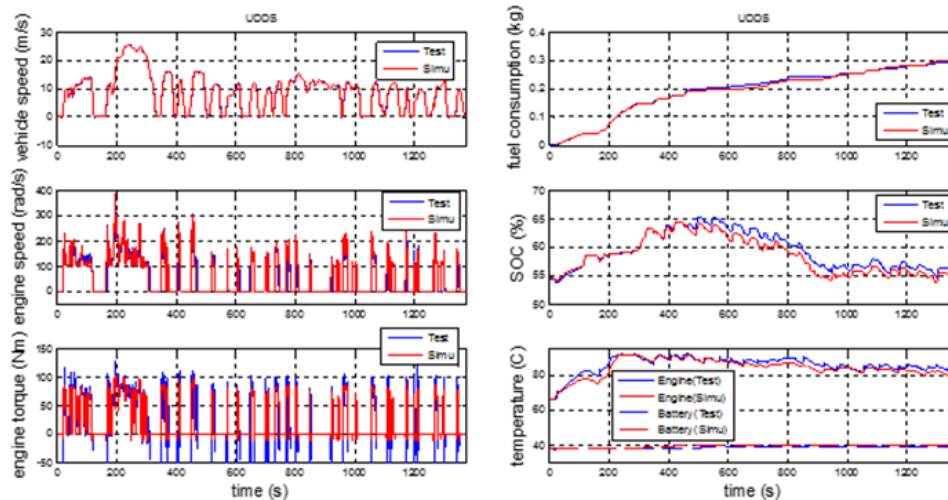


Figure A1.5. Autonomie results of simulation and testing on UDDS cycle for 2010 Toyota Prius HEV

A.1.3 Pre-transmission HEV

The pre-transmission HEV control logic was validated using Argonne AMRF test data from the 2013 Jetta DCT Hybrid. The simulation results for the vehicle speed, gear number, and battery SOC on the UDDS cycle, (see Figure A1.6) showed good correlation with the test data.

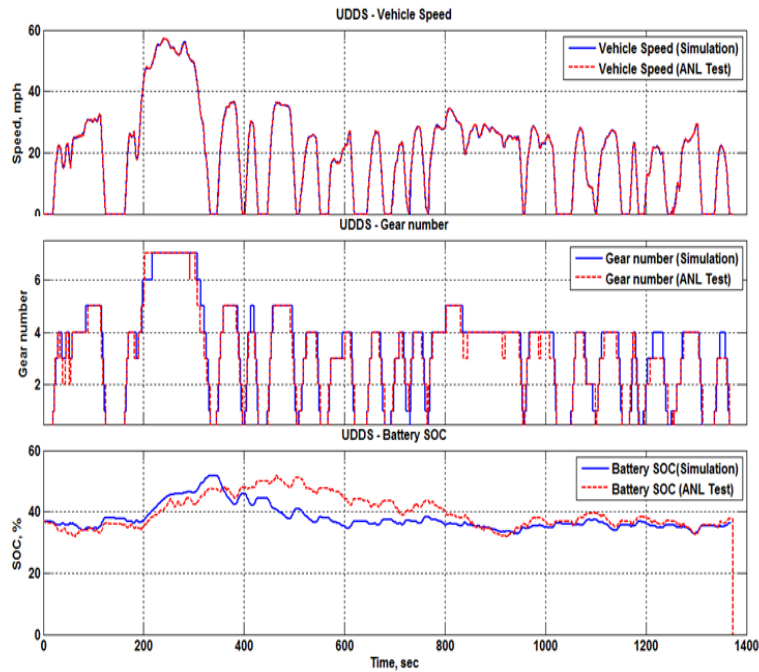


Figure A1.6. Autonomie Results of Simulation and Testing on UDDS Cycle for 2013 Jetta DCT Hybrid.

A.1.4 Range-Extender PHEV

The range-extender PHEV model was validated under different thermal conditions using AMRF test data from the second-generation GM Volt. The vehicle operating behavior, including vehicle speed, battery SOC, fuel consumption, and engine speed, torque, and temperature under ambient temperature were successfully compared with the testing results shown in Figure A1.7.

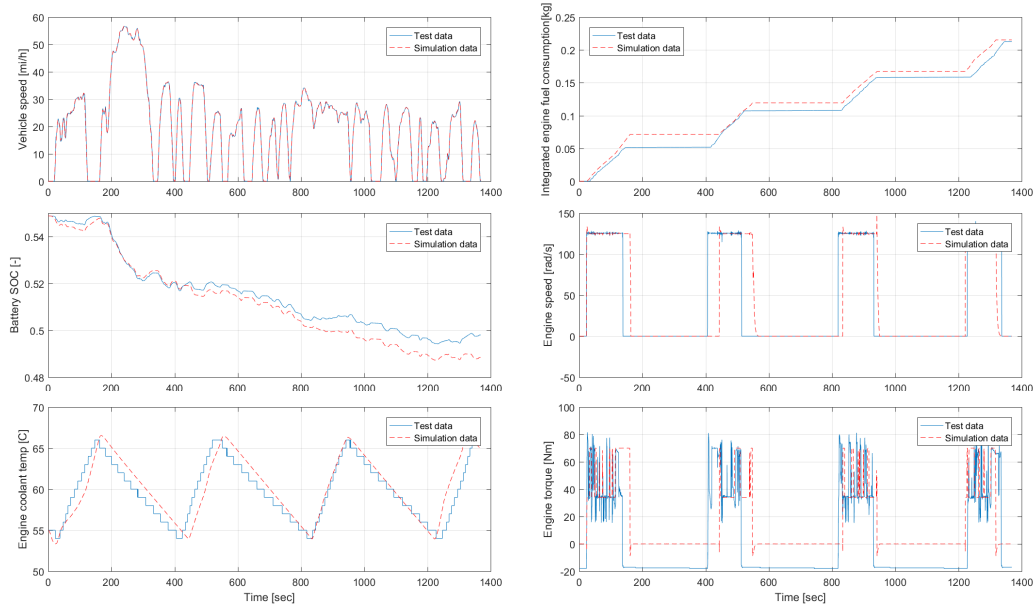


Figure A1.7. Autonomie Results of Simulation and Testing on UDDS Cycle for 2012 GM Volt PHEV.

A.2 RoadRunner (Single and Multi-Vehicle Control)

A.2.1 Truck Platooning Validation Using On-Road Data

Lawrence Berkeley Laboratory has been conducting very extensive testing of three HD tractor-trailer trucks on a closed test track. The fuel consumption for each truck in the Cooperative Adaptive Cruise Control (CACC) string was measured under several scenarios to evaluate the influence of separation distance, vehicle configuration, weight, and speed. One set of test data is then used at Argonne for validation purposes.

SMART researchers implemented in RoadRunner control algorithms inspired by the literature for the intelligent driver model (IDM), adaptive cruise control (ACC), and cooperative ACC (or CACC). These models allow simulations of close-driving platooning scenarios. In a platoon, vehicles have reduced drag coefficients as a function of both inter-vehicle spacing and the number of vehicles. The aero drag reduction coefficients are integrated into RoadRunner for short-gap driving (wind tunnel data are from Lawrence Livermore National Laboratory).

SMART researchers validated the model of a three-truck platoon in RoadRunner on the basis of test data. First, researchers validated the Autonomie models of the truck powertrain, matching signals such as gear ratio, engine torque and fuel rate for the lead vehicle in a drive cycle-following situation. The CACC controllers were then calibrated to closely match inter-vehicle gap for the following vehicles. As shown in Table A1.1, discrepancies in average inter-vehicle gap were within 5% compared to the test data, and many of the operational signals, including fuel consumption, were well matched (Figure A1.8)

Table A1.1. RoadRunner Truck Platoon Validation Summary.

Cycle (0–20,050 m)		Travel time, sec	Average gap, m	Fuel consumption, L/100 km
Veh1 (Lead)	Test	997.3	-	38.78
	Simulation	997.5	-	38.56 (-0.6%)
Veh2 (Middle)	Test	979.9	25.9	38.57
	Simulation	972.7	25.1 (-3.1%)	38.39 (-0.5%)
Veh3 (Trailing)	Test	971.0	30.3	41.05
	Simulation	969.5	29.3 (-3.3%)	39.40 (-4.0%)
CACC #1 (constant time gap)		Travel time, sec	Average gap, m	Fuel consumption, L/100 km
Veh2 (Middle)	Test	333.7	30.4	35.13
	Simulation	333.4	31.7 (4.3%)	35.31 (0.5%)
Veh3 (Trailing)	Test	350.8	31.0	36.30
	Simulation	350.0	30.4 (-1.9%)	36.19 (-0.3%)
CACC #2 (variable time gap)		Travel time, sec	Average gap, m	Fuel consumption, L/100 km
Veh2 (Middle)	Test	319.9	25.6	36.88
	Simulation	318.3	25.2 (-1.6%)	38.56 (4.6%)
Veh3 (Trailing)	Test	305.4	21.4	37.36
	Simulation	303.4	22.5 (5.1%)	40.09 (7.3%)

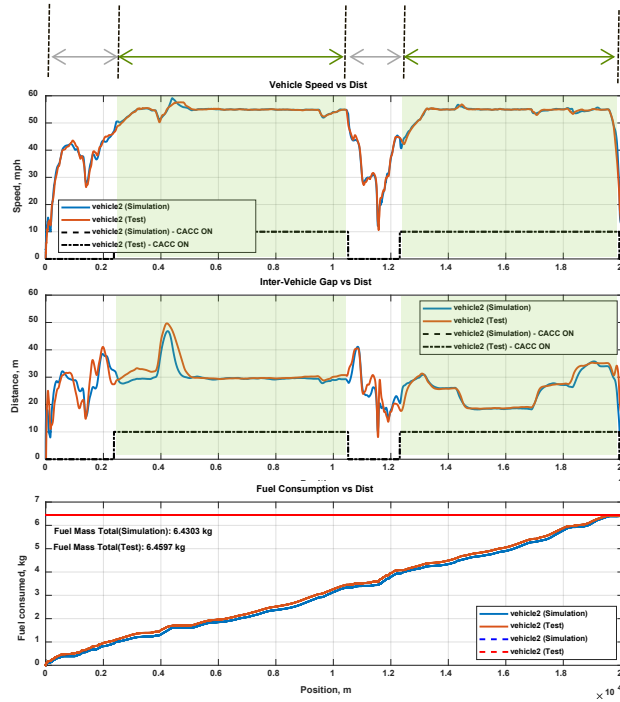


Figure A1.8. RoadRunner Simulation and Testing Results for the Middle Vehicle (Vehicle 2).

A.2.2 Toyota Prius Prime CACC Control Validation Using Vehicle Dynamometer Data

Many modern vehicles already feature partial driving automation, for example longitudinal speed control for highway driving. With ACC, the vehicle drives at a speed set by the driver if no preceding vehicle is detected (using a radar or stereoscopic cameras), and otherwise modulates its speed to maintain a safe distance with the preceding vehicles. Researchers at Argonne tested the ACC feature of the 2016 Toyota Prius, and then validated a model of the vehicle and of the ACC in RoadRunner.

The vehicle was tested on a chassis dynamometer. In order to test the ACC feature with no actual moving vehicle to detect, a method of overwriting the gap measurement from the sensor was designed and implemented. As a result it is possible to test a situation where the ACC controller commands the actual vehicle on the dynamometer to follow a virtual lead vehicle, itself following a set drive cycle. This setup allows to evaluate the automated driving controller in laboratory environment.

The data was then used to validate an ACC model in RoadRunner, and then applied to a validated Autonomic model of the Prius Prime as shown in Figure A1.9.

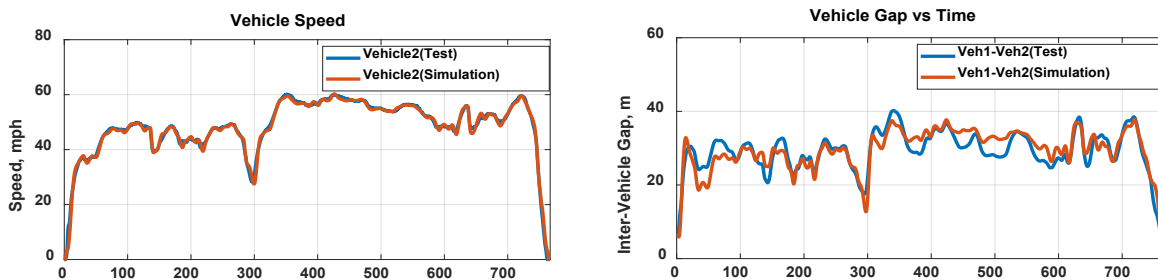


Figure A1.9. Comparison of the ACC Model in RoadRunner with Test Data.

A.2.3 Human Driver Model Development and Validation

Connected and automated vehicles (CAVs) can provide significant energy saving potential. Quantifying this potential in simulation not only depends on properly evaluating CAVs, with or without eco-driving controls, but also on a representative model of human driving. A human driver model, which serves as a baseline must capture a wide range of different driving behaviors corresponding to the surrounding environment. Researchers at Argonne have initiated the development of such model, formulating human driving as an optimal control problem with a state constraint imposed by the preceding vehicle. Deriving analytical optimal solutions by employing optimal control theory can compute human driving behaviors with low computational burden, and adding the state constraint can describe car-following features with anticipation of the preceding vehicle. On-road testing data (Figure A1.10) was collected by a highly instrumented vehicle (including dashcam video, global positioning system [GPS] coordinates, radar measurements) to validate the proposed human driver model. Results for stop scenarios at intersections demonstrates that trajectories of the proposed model are well matched with those of experimental data (Figure A1.11).

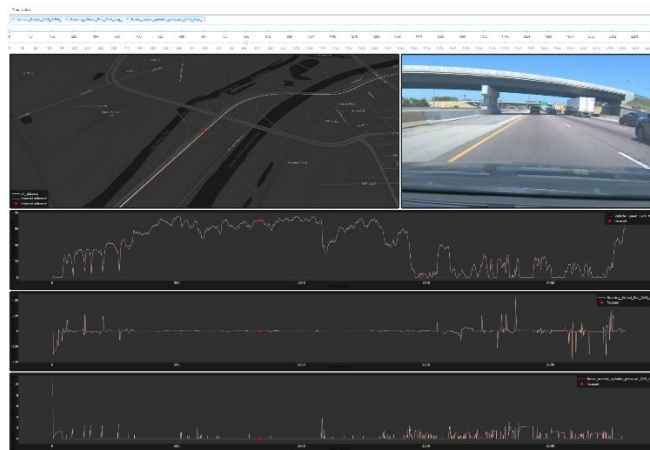


Figure A1.10. On-road Data Visualization.

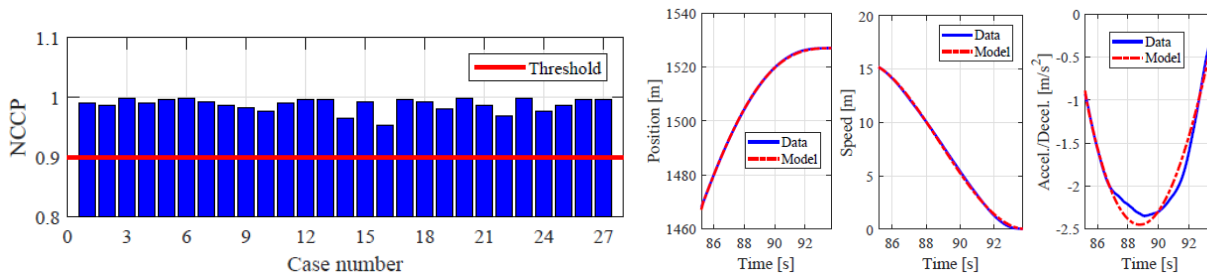


Figure A1.11. RoadRunner Human Driver Validation: Normalized Cross Correlation Power (NCCP) between experimental and Simulation Data for Several Stopping Situations (Left) and Example for One Sample (Right).

A.3 Vehicle Fleet Evolution Modeling with ADOPT and Energy Modeling with FASTSim and RouteE

The ADOPT vehicle choice model is used to estimate future vehicle powertrain adoption based on different component technology improvement scenarios (i.e., cost reductions and efficiency advancements over different timeframes for vehicle batteries, engines, electric motors). Several features of ADOPT help it to achieve strong validation performance—including its elemental representation of the vehicle fleet, its integration with the FASTSim vehicle powertrain model for evolving the fleet, and its ability to capture the impacts of policy conditions, such as Corporate Average Fuel Economy (CAFE) standards. ADOPT has been extensively validated by comparing the tool’s sales estimates to actual historic vehicle sales. Figure A1.12 shows example ADOPT validation results for nine different dimensions. The top left plot in the figure acknowledges some overestimation of national HEV sales in this example year but illustrates how ADOPT closely matches actual PHEV and BEV sales. Furthermore, the remaining plots in the figure show close alignment between ADOPT estimates and actual sales in many other dimensions, including sales by fuel economy, performance, price, size class, power, and buyer income. ADOPT’s sales estimates also match well with actual sales data for other years and for state-level and even zip-code-level sales estimates. Additional details on ADOPT can be found in the Capstone Modeling Appendix, on the website for the public-release version of the tool (www.nrel.gov/adopt) and in other published papers on ADOPT’s application [3, 4, 5]

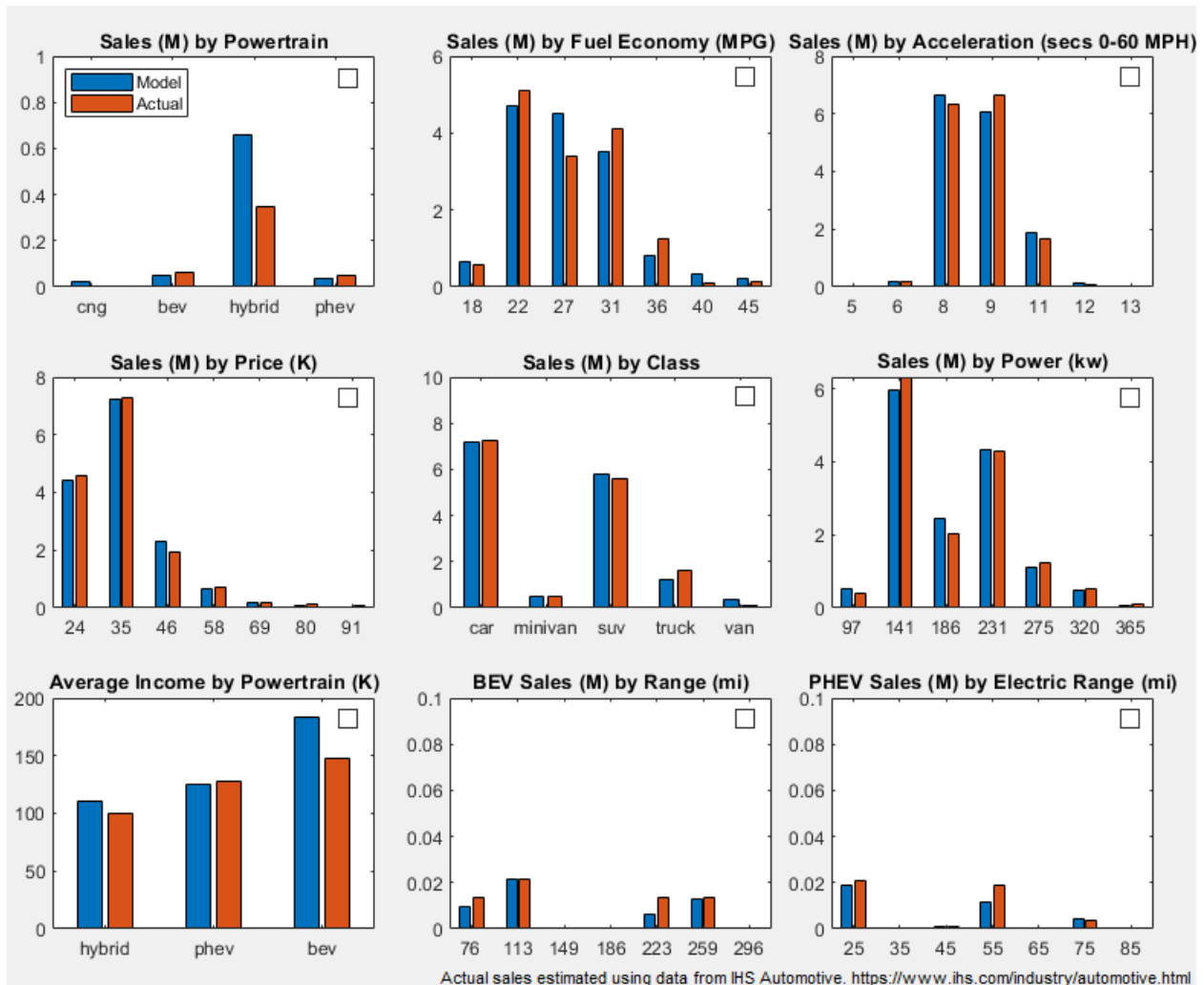


Figure A1.12. Example ADOPT Validation Comparing Model Estimates to Actual National Vehicle Sales Data in 2015.

Vehicle powertrain modeling in FASTSim focuses on the most important factors impacting vehicle efficiency, performance and cost—such as vehicle platform characteristics (mass, rolling resistance, aerodynamics, etc.) and component attributes (efficiency and power capability of the engine, motor[s], battery, etc.). FASTSim’s modeling framework is designed to balance detail, precision and speed, with the tool’s simulations performed in 1-second time steps over a specified driving profile. The driving profile may be a standardized/regulatory cycle or could represent real-world/on-road driving behavior (such as those archived in the Transportation Secure Data Center (TSDC)). FASTSim simulations can utilize base-level vehicle models comprised of representative efficiency maps for each component (which may then simply be scaled to represent hypothetical future vehicles), or highly customized models when specific vehicle component data are available, and/or when a given analysis requires additional detail, such as the influence of operating temperature on component performance. For each approach, FASTSim has been shown to accurately model vehicle efficiency as well as performance and cost (each of which are important for ADOPT vehicle choice modeling inputs), with validation activities spanning a wide range of vehicles and powertrains, including conventional, hybrid, plug-in hybrid, and battery electric. Figure A1.13 shows example fuel economy validation results for base-level FASTSim vehicle modeling. Additional details on FASTSim, its validation and example applications can be found on the website for the public-release version of the tool (www.nrel.gov/fastsim) and in published papers [6, 7, 8, 9].

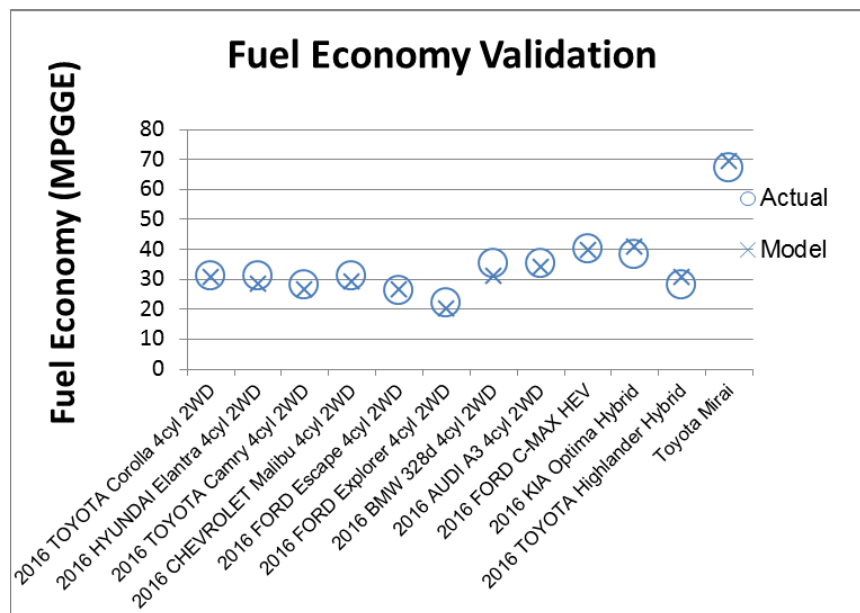


Figure A1.13. Sample Fuel Economy Validation for Base-level FASTSim Models.

As previously described, RouteE road-segment-level vehicle energy models can be trained from large-scale FASTSim simulations over TSDC-provided real-world driving data as part of the integrated ADOPT/FASTSim/RouteE tool chain. RouteE development, refinement and application activities have received support under the SMART Mobility CAVs pillar, which has included a focused validation of the tool for green routing applications (as summarized in the CAVs Capstone Report). That focused validation effort showed that RouteE reliably identified the lower fuel consuming route over each of the roughly one dozen test scenarios examined [10].

Additional validation efforts have focused on confirming that large-scale energy estimates using RouteE agree with estimates using more detailed powertrain simulation when real-world second-by-second driving data are available (such as via FASTSim simulations over TSDC driving profiles). Figure A1.14 shows that RouteE indeed achieves good agreement, and ongoing tool refinements are targeted at further reducing the areas of

greatest disagreement. Additional details on RouteE and other ways it has been applied can be found in the CAVs Capstone report, and in other published papers that have leveraged the tool [12].

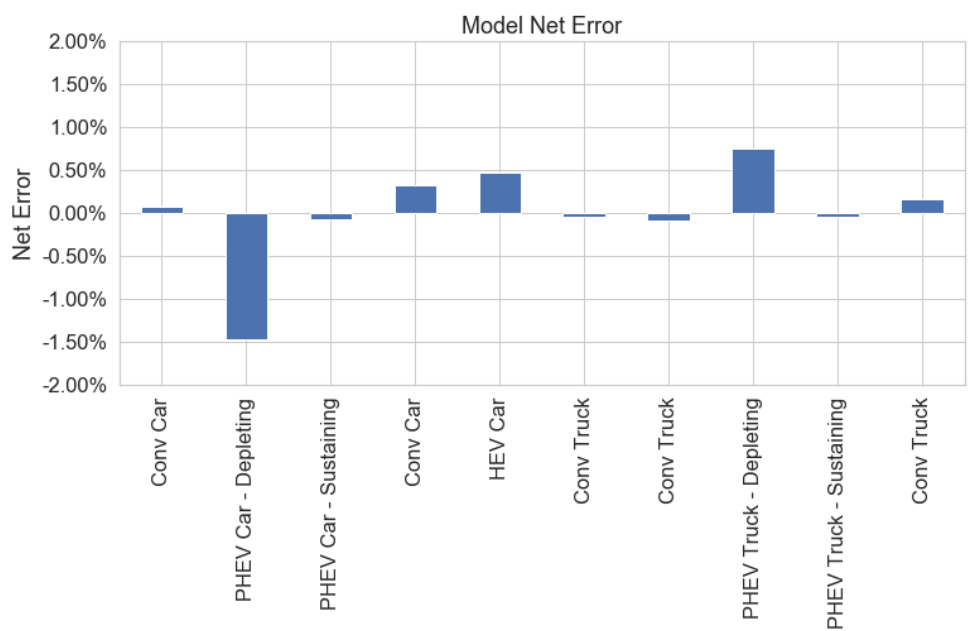


Figure A1.14. Net Error Comparison between RouteE Energy Estimates and Corresponding Energy Results from Detailed Second-by-second Simulations for a Variety of Powertrains.

A.4 Microscopic Simulation

Vehicle following and maneuvering models are essential to microscopic mixed traffic simulation. The mixed traffic means that it has both manually driven vehicles and AVs and CAVs. The critical part of the modeling is to capture the dynamic interactions between manually driven vehicles and AV/CAVs because such behaviors determine traffic-flow characteristics at local, mesoscopic, and macroscopic levels. Aimsun car following models could be calibrated for modeling traffic only with manually driven vehicles, but not with AV/CAVs. Under several U.S. Department of Transportation projects, the Berkeley team developed API (Application Program Interface) and microSDK modules for revolutionize the vehicle following behaviors in Aimsun in the following way: (a) calibrated a hybrid basic car-following model using NGSM data: the hybrid model uses Newell's rule to define the fundamental car-following pattern, and uses the Gipps model to place safety margin within the limitations of acceleration and deceleration; (b) using field collected freeway SR-99 NB corridor calibrated the freeway network model; (c) using field test data of a few CACC passenger car in public traffic modeled and ACC and CACC behavior in microscopic level. Under the DOE/VTO/EEMS program, the project team developed an HD truck ACC and CACC model based on field test data in public traffic. Those are the foundation of the microscopic traffic simulation. With the microscopic traffic simulation setup, the project team has considered the effect of managed lane and cooperative merge on mobility and energy consumption.

Currently, the default manual driving lane changing models are used in the simulation package for CAVs for several reasons at this stage:

- Although gap acceptance threshold of CAVs could be different from manually driven vehicles, CACC/ACC does not have lateral control capability yet.
- Automatic perception and lane change has not matured yet.
- There is no such calibrated maneuver model for AV or CAV in microscopic traffic simulation available yet.

- Drivers are likely to take over speed control during lane changing in mixed traffic with AVs/CAVs.
- Future human factors data collection will be necessary to model/calibrate CAV lane changing maneuvers in mixed traffic for microscopic simulation.

A.5 POLARIS

A.5.1 Polaris Physical Model Construction

The POLARIS model process starts with the construction of model representations of key transportation system infrastructure and other characteristics of the physical environment to be simulated. Examples of the POLARIS model inputs for POLARIS are shown in Figure A1.14. The physical network elements and land use environment are gathered from multiple data sources, including the local and state Departments of Transportation, the Chicago regional Metropolitan Planning Organization (CMAP) and various commercial and other partners (e.g., CoStar for land use information, parking operators for garage information, City of Chicago for parking meters, General Transit Feed Specifications (GTFS) feeds for transit, local transit agencies, etc.). These disparate data sources are combined into a single SQLITE database using various tools including QGIS and a custom-designed POLARIS network editing tool. These are used to refine the CMAP network model, correct errors in network topology or characteristics, add additional detail and refinement to areas of interest beyond what is included in the CMAP model. Going through this process has resulted in a model of the 20-county Chicago region that extends from southern Wisconsin through northwestern Indiana, and includes more than 10 million people, 32,000 road links, 290,000 parking locations (including street parking, metered areas, garages, commercial lots, etc.), 500,000 land use locations and a full representation of all transit agencies in the region.

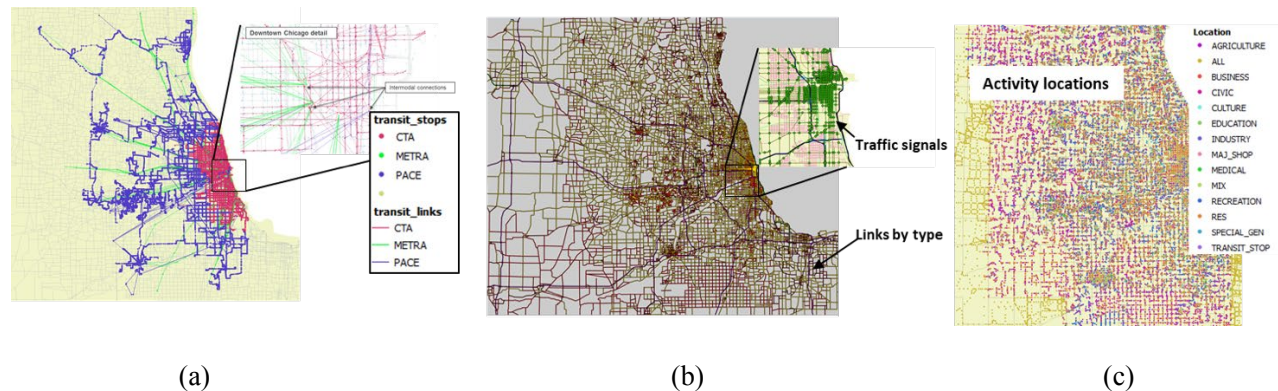


Figure A1.14. POLARIS Physical Systems Models Include (a) Transit Network, (b) Streets and Intersections, and (c) Land Use and Locations.

A.5.2 POLARIS Behavioral Model Calibration

The POLARIS behavioral models, including the activity mode choice, start time, and destination choice, have undergone extensive calibration to ensure that baseline model outputs replicate observed distributions. The observations to calibrate against are drawn from multiple data sources, including the household travel survey collected by the local metropolitan planning organization (MPO), CMAP; transit boarding and alighting counts collected by local transit agencies; road traffic counts from IDOT and Chicago DOT, and others.

For behavior model calibration, the choice constants in each model are adjusted iteratively after each calibration run, based on the difference between the observed and simulated distributions of the respective choices. If less of a given choice (e.g., transit mode) is obtained from simulation than in the observed distribution, the alternative constant for that choice is increased in the next run. Because many models are combined in the POLARIS simulator, all of the choice constants for each model are adjusted simultaneously, as increasing a mode choice constant can effect a destination choice constant and vice versa. After iteratively

adjusting population constants, the observed baseline distributions can be replicated in POLARIS, as shown in Figure A1.15, for the mode choice and start time choice.

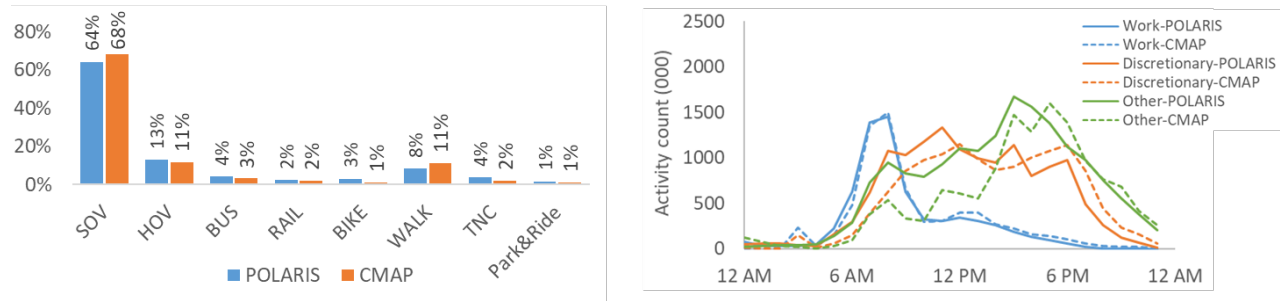


Figure A1.15. POLARIS Behavioral Model Calibration.

A.5.3 POLARIS Network Validation

Because POLARIS is an integrated activity-based model and network simulator, it is important to ensure that both the activity model and network results are converged before running scenarios. To test the function of the traffic flow model, two sources of data are compared: vehicle in-network curves and link-based traffic counts. The in-network curve for a POLARIS run shows the instantaneous number of vehicles in the network throughout the simulation, and is a key indicator of model performance because it is very sensitive to misspecifications or errors in activity generation, trip distribution, mode choice, activity timing, routing and traffic flow. Differences in any of these models can drastically change the shape of the in-network curve (destination choice that under-weights travel times will greatly increase vehicles in network; poor timing choice models shift location of the AM/PM traffic peaks, etc.). Although the in-network curve comparison is highly underdetermined (i.e., many different model specifications can lead to the same observation), similarity in these curves is indicative of good model performance.

Figure A1.16 compares the baseline POLARIS in-network curve for autos to an in-network curve derived from the CMAP household travel survey self-reported travel times. Note that this comparison removes freight vehicles, ride-hailing vehicles, and other non-privately owned automobile travel because these would not be reported in the household travel survey, but the background effects of these vehicles on travel are still captured. The simulated and observed in-network curves match very closely, with some underestimation of vehicles in network during a short time in the PM peak period, but this is potentially due to a survey artifact with travel survey respondents rounding actual arrival times. The pre-peak AM congestion growth, AM-peak, mid-day travel, and post-PM-peak congestion release all match almost exactly.

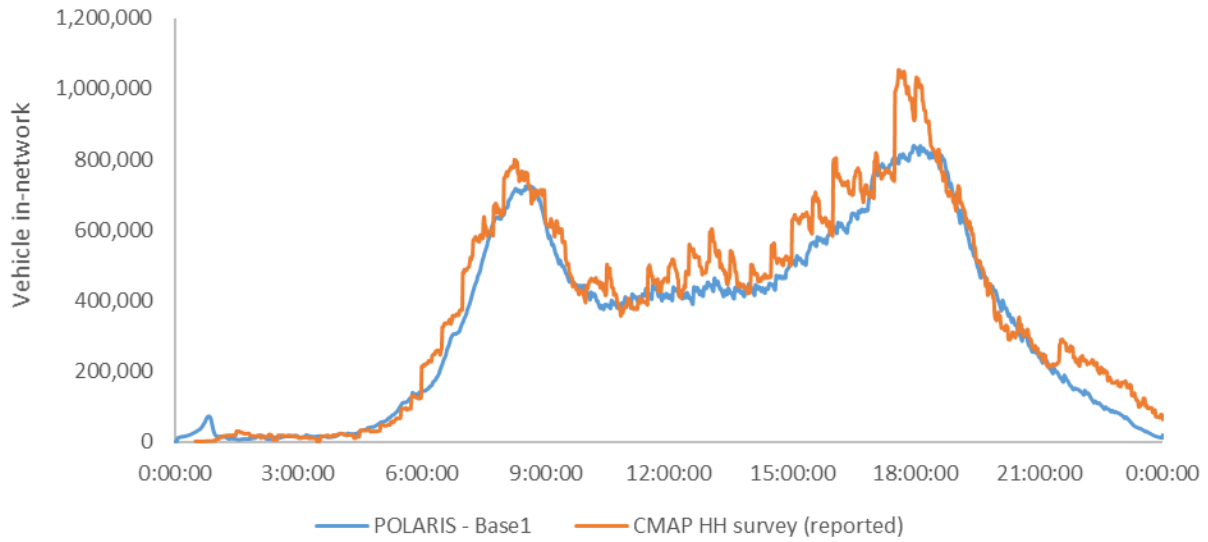


Figure A1.16. In-network Vehicles Curve for POLARIS Baseline Compared to CMAP Survey Observation.

The simulated traffic counts by link from POLARIS can also be compared against observations to validate network performance. Figure A1.17 is a map of daily traffic counts by link from the POLARIS baseline model compared against traffic counts reported in the IDOT highway performance monitoring system. This comparison is good for providing a general sense of network function, although IDOT HPMS data is updated infrequently and there are many missing observations, even for some freeways and expressways in the area. Overall, similar traffic patterns can be seen in the POLARIS results and observed data, although POLARIS generally demonstrates higher traffic counts on arterial streets, likely due to infrequent updates and approximate count measures on such roads in the HPMS.

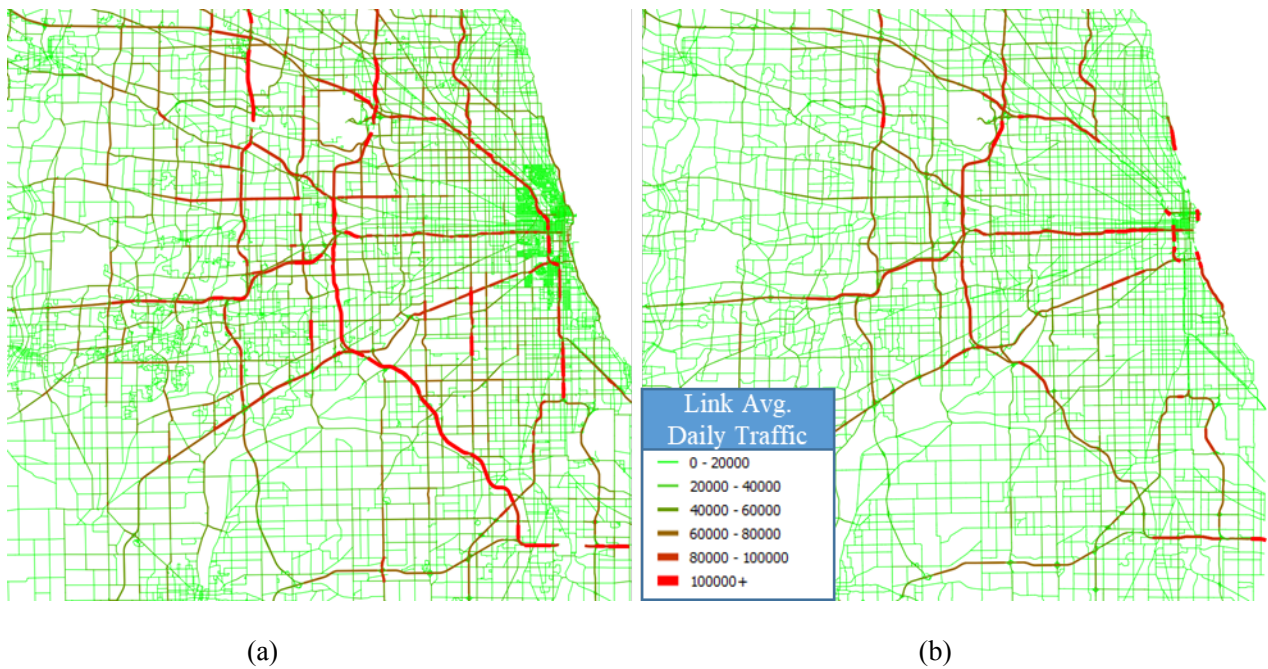


Figure A1.17. Daily Traffic Counts from (a) POLARIS and (B) IDOT Traffic Counters.

A.6 BEAM

SMART researchers apply the BEAM model to the San Francisco Bay Area. The calibration process involves coupling the BEAM simulation model to a cloud-based Bayesian Optimization service called SigOpt. For this study, the SigOpt API was used to calibrate behavioral parameters for mode choice. Potential future work includes calibration across traffic counts, transit ridership, and ride-hail use.

A.6.1 Mode Choice Parameters

SMART researchers calibrated the mode choice model in BEAM for the San Francisco Bay Area model based on estimates of modal split from the Metropolitan Transportation Commission (MTC). The following objective function is used for the mode calibration runs:

$$\begin{aligned}
 f_{obj_{mode}} = & \sum_{mode=i}^n |obs_i - sim_i| + \sum_{mode=i}^n 0.1 [sim_i > 0] \\
 & + sim_{car} \cdot 0.1 [sim_{car} - obs_{car} \cdot 0.8 > 0] \\
 & + sim_{drive_transit} \cdot 0.1 [sim_{drive_transit} - obs_{drive_transit} \cdot 0.3 > 0] \\
 & + sim_{ride_hail} \cdot 0.1 [sim_{ride_hail} - obs_{ride_hail} \cdot 0.3 > 0] \\
 & + sim_{ridehail_transit} \cdot 0.1 [sim_{ridehail_transit} - obs_{ridehail_transit} \cdot 0.3 > 0] \\
 & + sim_{walk} \cdot 0.1 [sim_{walk} - obs_{walk} \cdot 0.3 > 0] \\
 & + sim_{walk_transit} \cdot 0.1 [sim_{walk_transit} - obs_{walk_transit} \cdot 0.3 > 0]
 \end{aligned}$$

where obs_i and sim_i are observed versus simulated mode shares. It was found that while a root mean square percentage error objective function could be used, it places too much weight on modes with small shares. SMART researchers therefore used an objective function with an absolute error component (first sum term), followed by a component focusing on mode diversity (second sum term) and further ensuring a minimal representation of all modes (last six sum terms). These mode calibrations are typically done with one to two BEAM iterations and typically involve 50–150 calibration runs.

A.6.2 Network Flow Parameters

Ideally, mode and network flow parameter calibration would be conducted jointly; however, this is not possible for practical reasons. For example, network flow calibration runs typically take 20–30 iterations to reach equilibrium, which would lead to prohibitive calibration costs in terms of time and computation. Therefore, calibration is performed by iterating between doing calibrations of mode, then network, then mode, etc. Furthermore, up-to-date network travel times are fed from the network flow parameter calibration into the mode calibration run, requiring fewer iterations to reach equilibrium. Outliers remain which are largely due to mis-specified network data. For example, if a road has the wrong capacity or speed setting, certain trips can take substantially longer than observed. Work continues to improve our network data to minimize such outliers in travel times.

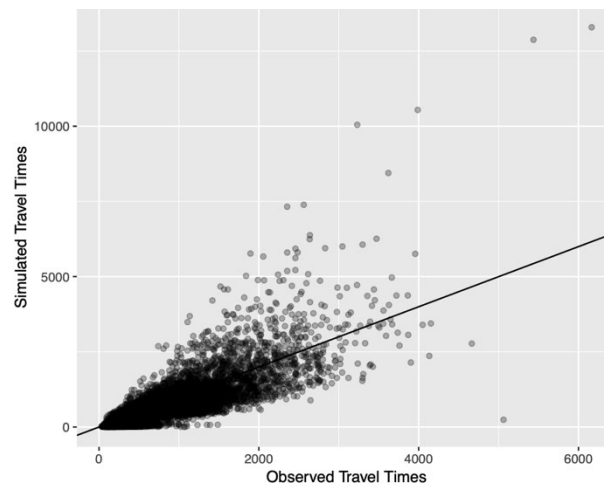


Figure A1.17. Simulated travel times (in seconds) from calibrated BEAM baseline run versus observed travel times from Uber Movement.

A.6.3 Transit Ridership

Next, the daily profile of BEAM-simulated transit ridership is compared to observed ridership data from the Clipper RFID payment system used by the four major transit agencies in the Bay Area (Figure A1.18). Because Clipper is only a subset of riders and there are no reliable data sources to allow us to correct for the under-sample, only hourly distribution of ridership can be compared, not the absolute magnitude. In addition, there is likely bias in ridership data from Clipper. For example, there could be underrepresentation of low-income riders due to a lack of credit cards or insufficient funds to prepay.

That said, there is a high degree of alignment between the daily ridership patterns between the base BEAM simulation and the Clipper data. The AC Transit comparison shows the most agreement. The other transit agencies show a less pronounced evening peak in the BEAM output. In addition, the midday ridership estimates from BEAM are higher than the observed midday lows for BART. In further analysis these discrepancies will be explored in further detail.

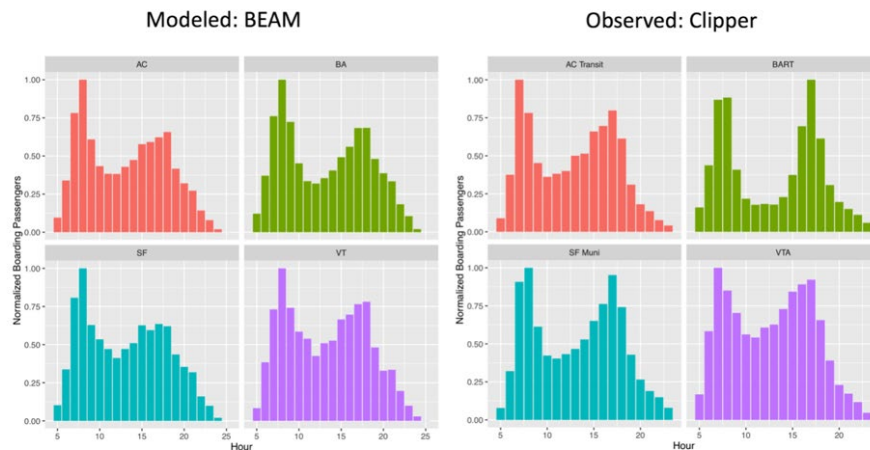


Figure A1.18. Modeled versus Observed Transit Ridership Hourly Distributions.

A.6.4 Ride-Hail Trip Distributions

Finally, the San Francisco County Transportation Authority (SFCTA) conducted a study called “TNC Today” of ride-hail usage in the City of San Francisco in 2017. Data were collected through API scraping, allowing them to observe the approximate pickup and drop-off locations of all trips in the city over ~5 weeks. They shared the origin-destination data with our team to allow comparison of the spatial distribution of ride-hail trip starting and ending locations to BEAM model predictions. In Figure A1.19, the spatial distributions from ride-hailing are plotted next to the BEAM output. There is a high degree of agreement between the observed and simulated trip pickup densities.

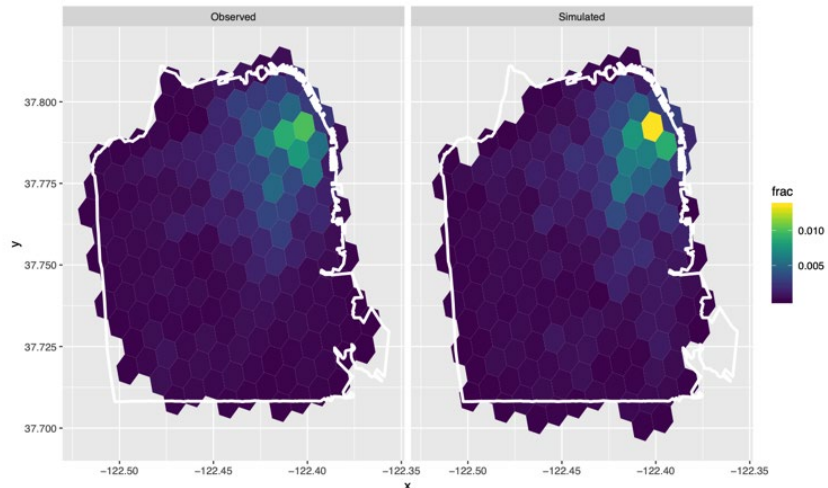


Figure A1.19. Trip starting Location Density for a Typical Weekday in the Ridehail Today Database and from the BEAM Simulation.

A.7 References

1. https://www.autonomie.net/publications/papers_validation.html
2. SAE 2011-01-0881, “Test Correlation Framework for HEV System Model,” Ford Motor Company
3. A. Brooker, J. Gonder, S. Lopp, and J. Ward, 2015, “ADOPT: A Historically Validated Light Duty Vehicle Consumer Choice Model,” 2015-01-0974, SAE Technical Paper www.nrel.gov/docs/fy15osti/63608.pdf
4. C. Johnson, E. Newes, A. Brooker, R. McCormick, S. Peterson, P. Leioby, R. Uria Martinez, G. Oladosu, and M. Brown, 2015, *High-Octane Mid-Level Ethanol Blend Market Assessment*, NREL/TP-5400-63698, National Renewable Energy Laboratory.
5. E. Hale, H. Horsey, B. Johnson, M. Muratori, E. Wilson, et al., 2018, *The Demand-side Grid (dsgrid) Model Documentation*. NREL/TP-6A20-71492. Golden, CO: National Renewable Energy Laboratory. www.nrel.gov/docs/fy18osti/71492.pdf.
6. A. Brooker, J. Gonder, L. Wang, E. Wood, et al., 2015, “FASTSim: A Model to Estimate Vehicle Efficiency, Cost and Performance,” 2015-01-0973, SAE Technical Paper, doi:10.4271/2015-01-0973.
7. J. Gonder, A. Brooker, E. Wood, and M. Moniot, 2018, *Future Automotive Systems Technology Simulator (FASTSim) Validation Report*. NREL TP-5400-71168.
8. E. Wood, J. Gonder, and F. Jehlik, 2017, “On-Road Validation of a Simplified Model for Estimating Real-World Fuel Economy,” *SAE Int. J. Fuels Lubr.* 10(2):2017, doi:10.4271/2017-01-0892.
9. J. Gonder, T. Markel, M. Thornton, and A. Simpson, 2007, “Using Global Positioning System Travel Data to Assess Real-World Energy Use of Plug-In Hybrid Electric Vehicles.” *Journal of the Transportation Research Board (TRB)*, p. 26.
10. J. Holden, et al., 2018, “Trip Energy Estimation Methodology and Model Based on Real-World Driving Data for Green-Routing Applications,” *Transportation Research Record* 2672(24): 41–48.

11. L. Zhu, J. Holden, E. Wood, and J. Gonder, 2017, “Green Routing Fuel Saving Opportunity Assessment: A Case Study Using Large-Scale Real-World Travel Data,” Proceedings of the 2017 IEEE Intelligent Vehicles Symposium (IV’17), June, Redondo Beach, CA. Pre-print: <https://www.nrel.gov/docs/fy17osti/68194.pdf>.
12. L. Zhu, H. Holden, and J. Gonder, 2018, “Navigation API Route Fuel Saving Opportunity Assessment on Large-Scale Real-World Travel Data for Conventional Vehicles and Hybrid Electric Vehicles.” *Transportation Research Record: Journal of the Transportation Research Board*. October. doi.org/10.1177/0361198118797805.

APPENDIX B – POLARIS Household E-Commerce Demand Model

Variables	Estimates	t-stat
Binary probit model: HH's decision to participate in e-commerce		
Constant	-0.007	-0.07
Number of adults in the household	-0.047	-1.17
Household income <\$20K	-0.456	-2.33
Household income \$25K-\$50K	-0.533	-3.33
Household income \$50K-\$100K	-0.151	-1.4
Household Income >\$200K	0.398	3.74
Walking distance to nearest transit stop	0.076	1.16
Ordered probit model: Delivery to retail shop ratio		
Constant	2.703	11.41
Number of adults in the household	-0.184	-3.12
Household Income >\$200K	0.389	3.48
Household walk accessibility	-0.047	-2.45
Number of vehicles in the household	-0.145	-2.27
Threshold 1	0	Fixed
Threshold 2	1.52	12.76
Threshold 3	2.095	16.86
Threshold 4	2.639	20.32
Threshold 5	3.377	23.28

APPENDIX C – Main Vehicle Technologies Assumptions

B.1 Light-Duty Vehicle Main Assumptions

B.1.1 Engine

Scenarios	Base0/1/4	Base2, A2	Base3, A3	Base5, B5, C5	Base6, B6, C6
Naturally Aspirated GASOLINE for Conventional					
IC Engine eff	36	40	43	44	47
Engine eff at 2bar at 2000rpm	24	26			
Engine eff at 20% at 2000rpm	24	26	30	31	35
Engine eff at 3bar at 1300rpm		31	35	36	39
DIESEL					
IC Engine eff	42	44	50	48	52
Engine eff at 2bar at 2000rpm	26	29			
Engine eff at 20% at 2000rpm	30	37	42	41	46
Engine eff at 3bar at 1300rpm	32	35	39	39	43
Downsized, Boosted, Gasoline Engine Pathway (Turbo)					
IC Engine eff	35.9	39	43	42	46
Engine eff at 2bar at 2000rpm	24.0	25			
Engine eff at 20% at 2000rpm	29.1	32	36	36	41
Engine eff at 3bar at 1300rpm	27.0	29	38	34	40
GASOLINE for HEVs based on Atkinson Cycle					
IC Engine eff	39	41	46	45	50
Engine eff at 2bar at 2000rpm	25.1				
Engine eff at 20% at 2000rpm	23.7	26	30	31	35
Engine eff at 3bar at 1300rpm		31	35	36	39

B.1.2 Electric Machine

	Scenarios	Base0/1/4	Base2, A2	Base3, A3	Base5, B5, C5	Base6, B6, C6
Parameter	Tech Progress	Low	Low	High	Low	High
Boost Converter Cost [PC2]	\$/kW	8	4.8	2.7	4.5	2
High Voltage System Cost (without boost*)	\$/kW	17	10	6	6.3	4
DC/DC Buck Converter Cost [PC]	\$/kW	65	50	30	29	18
On-board Charger cost	\$	125	65	35	33	18

B.1.3 Energy Storage

	Scenarios	Base0/1/4	Base2, A2	Base3, A3	Base5, B5, C5	Base6, B6, C6
Parameter	Tech Progress	Low	Low	High	Low	High
High Power APPLICATIONS						
Specific Power @ 70% SOC	W/kg	2750	4000	5000	5000	6000
Power Term	\$/W	20	19	15	17	13
High Energy APPLICATIONS (PHEV)						
Energy Density (Wh/kg) - Blended PHEV	Wh/kg	60	105	125	115	170
Energy Density (Wh/kg) - EREV PHEV	Wh/kg	70	105	125	115	170
Energy Term - based on USABLE Energy - Blended PHEV	\$/kWh	530	210	160	160	120
Energy Term - based on USABLE Energy - EREV PHEV	\$/kWh	500	210	160	160	120
BEV						
Energy Density (Wh/kg)	Wh/kg	170	230	310	280	320
Energy Term - based on USABLE Energy - AEV	\$/kWh	220	144	125	120	80

B.1.4 Light Weighting

	Scenario	Base2, A2	Base3, A3	Base5, B5, C5	Base6, B6, C6
Cost of Lightweighting	\$/ kg-saved	\$17.00	\$11.00	\$15.00	\$9.00
Compact Car					
Vehicle Mass Reference	kg	1320			
Glider Cost Reference (Lab Year 2015)	\$	7949			
Glider mass reduction (Lab Year 2015)	%	5%	18%	5%	19%
Total Glider Cost	\$	\$ 8,847	\$ 9,837	\$ 8,741	\$ 9,612
Midsize Car					
Vehicle Mass Reference	kg	1595			
Glider Cost Reference (Lab Year 2015)	\$	10671			
Glider mass reduction (Lab Year 2015)	%	10%	25%	10%	32%
Total Glider Cost	\$	\$ 12,701	\$ 13,955	\$ 12,462	\$ 14,110
Small SUV					
Vehicle Mass Reference	kg	1636			
Glider Cost Reference (Lab Year 2015)	\$	12617			
Glider mass reduction (Lab Year 2015)	%	10%	18%	18%	28%
Total Glider Cost	\$	\$ 14,564	\$ 14,963	\$ 15,807	\$ 15,675
Midsize SUV					
Vehicle Mass Reference	kg	1737			
Glider Cost Reference (Lab Year 2015)	\$	13773			
Glider mass reduction (Lab Year 2015)	%	13%	20%	21%	30%
Total Glider Cost	\$	\$ 16,431	\$ 16,514	\$ 17,681	\$ 17,148
Pick-Up					
Vehicle Mass Reference	kg	2006			
Glider Cost Reference (Lab Year 2015)	\$	14710			
Glider mass reduction (Lab Year 2015)	%	14%	21%	22%	28%
Total Glider Cost	\$	\$ 18,120	\$ 17,901	\$ 19,224	\$ 18,245

B.2 Medium-Duty (MD) and Heavy-Duty (HD) Vehicle Main Assumptions

B.2.1 Engine

Peak Efficiency (%)	Base0/1/4	Base2, A2	Base3, A3	Base5, B5, C5	Base6, B6, C6
Class 3	40%	43%	50%	46%	51%
Class 4	40%	43%	50%	46%	51%
Class 5 & 6	43%	47%	53%	50%	55%
Transit Bus	47%	50%	55%	53%	59%
Class 7 & 8	47%	53%	55%	55%	59%

B.2.2 Electric Machine

	Base0/1/4	Base2, A2	Base3, A3	Base5, B5, C5	Base6, B6, C6
Boost Converter Specific Power slope (W/kg)	11000	11110	11782	11333	12019
High Voltage System Specific Power slope (without boost* W/kg)	10000	10000	10000	10000	10000
High Voltage System Peak Efficiency (w/o boost)(%)	91%	94%	94%	96%	96%
High Voltage System Cost (without boost*) (\$/kw)	22	10	6	6.3	4
DC/DC Buck Converter Cost (\$/kw)	95	50	30	29	18

B.2.3 Energy Storage

	Base0/1/4	Base2, A2	Base3, A3	Base5, B5, C5	Base6, B6, C6
High Power					
Specific Power @ 70% SOC (W/kg)	375	1000	1500	1000	1500
Usable Pack Energy Density (Wh/kg)	50	105	120	115	120
Cost of Power (\$/kW)	20	19	15	17	13
High Energy (PHEVs)					
Specific Power @ 70% SOC (W/kg)	375	1000	1500	1000	1500
Usable Pack Energy Density (Wh/kg)	160	220	310	280	320
Usable Energy Cost (\$/kWh)	3	225	110	166	80
BEVs					
Specific Power @ 70% SOC (W/kg)	375	1000	1500	1000	1500
Usable Pack Energy Density (Wh/kg)	160	220	310	280	320
Usable Energy Cost (\$/kWh)	3	225	110	166	80

B.2.4 Light Weighting

Glider Weight Reduction (%)	Base0/1/4	Base2, A2	Base3, A3	Base5, B5, C5	Base6, B6, C6
Class 3	0%	8%	12%	15%	20%
Class 4	0%	8%	12%	15%	20%
Class 5 & 6	0%	6%	12%	12%	20%
Transit Bus	0%	5%	8%	9%	15%
Class 7 & 8	0%	6%	8%	9%	15%

APPENDIX D – VOTT Changes Under Different Uncertainties

VOTT Factor High Impact				VOTT Factor Low Impact			
Congestion	Time Sensitivity	AV-level	Multiplier Highway/Arterial	Congestion	Time Sensitivity	AV-level	Multiplier Highway/Arterial
Low	Low	Partial	0.7/1.0	Low	Low	Partial	0.9/1.0
Low	Low	Full	0.5/0.5	Low	Low	Full	0.7/0.7
Low	High	Partial	0.9/1.0	Low	High	Partial	1.0/1.0
Low	High	Full	0.7/0.7	Low	High	Full	0.9/0.9
High	Low	Partial	0.5/1.0	High	Low	Partial	0.7/1.0
High	Low	Full	0.35/0.35	High	Low	Full	0.5/0.5
High	High	Partial	0.7/1.0	High	High	Partial	0.7/1.0
High	High	Full	0.5/0.5	High	High	Full	0.7/0.7

APPENDIX E – Main Vehicle Fleet Assumptions

C.1 Evolution of Light-Duty Vehicle Classes

Evolution of Light Duty Vehicle Classes

	Base0/1/4	Base2/A2	Base3/A3	Base5/B5/C5	Base6/B6/C6
Compact Car	21.6%	18.5%	18.5%	13.0%	13.0%
Midsize Car	20.5%	21.0%	21.5%	22.0%	23.0%
Large Car	7.1%	7.0%	7.0%	6.0%	6.0%
Compact SUV	15.0%	17.5%	18.0%	27.5%	26.5%
Midsize SUV	20.0%	20.0%	20.0%	18.0%	18.0%
Full Size SUV	4.0%	4.0%	4.0%	3.0%	3.0%
Pickup	11.8%	12.0%	11.0%	10.5%	10.5%

C.2 Evolution of Light-Duty Vehicle Powertrains

Evolution of Light Duty Vehicle Powertrains

	Base0/1/4	Base2/A2	Base3/A3	Base5/B5/C5	Base6/B6/C6
Conv Gas	95.8%	67.0%	59.0%	11.0%	16.0%
Conv Gas 48V	0.0%	16.0%	21.0%	35.0%	21.0%
Conv Diesel	2.0%	1.0%	1.0%	0.5%	0.5%
HEV	2.0%	9.0%	7.0%	28.0%	12.0%
PHEV	0.1%	3.0%	5.0%	7.5%	11.5%
BEV	0.1%	4.0%	7.0%	18.0%	39.0%

C.3 Evolution of Light-Duty Vehicle Automation

Evolution of Light Duty Vehicle Automation

	Base0/1/4	Base2/A2	Base3/A3	Base5/B5/C5	Base6/B6/C6
No Automation	100.0%	90.0%	89.0%	77.5%	40.5%
Partial Automation	0.0%	10.0%	11.0%	5.0%	8.0%
Full Automation	0.0%	0.0%	0.0%	17.5%	51.5%

C.4 HEV Powertrain Distribution per Class (Light-Duty Vehicle)

HEV Powertrain Distribution per Class (LDV)

	Base0/1/4	Base2/A2	Base3/A3	Base5/B5/C5	Base6/B6/C6
Compact Car	1.5%	2.0%	1.0%	5.0%	4.0%
Midsize Car	0.5%	2.0%	2.0%	8.0%	4.0%
Large Car	0.0%	2.0%	0.0%	3.0%	0.0%
Compact SUV	0.0%	1.0%	2.0%	8.0%	3.0%
Midsize SUV	0.0%	2.0%	2.0%	4.0%	1.0%
Full Size SUV	0.0%	0.0%	0.0%	0.0%	0.0%
Pickup	0.0%	0.0%	0.0%	0.0%	0.0%

C.5 PHEV Powertrain Distribution per Class (Light-Duty Vehicle)

PHEV Powertrain Distribution per Class (LDV)

	Base0/1/4	Base2/A2	Base3/A3	Base5/B5/C5	Base6/B6/C6
Compact Car	0.0%	0.0%	0.0%	0.0%	0.0%
Midsize Car	0.0%	2.0%	3.0%	4.0%	5.0%
Large Car	0.1%	1.0%	2.0%	0.0%	0.0%
Compact SUV	0.0%	0.0%	0.0%	3.5%	4.5%
Midsize SUV	0.0%	0.0%	0.0%	0.0%	2.0%
Full Size SUV	0.0%	0.0%	0.0%	0.0%	0.0%
Pickup	0.0%	0.0%	0.0%	0.0%	0.0%

C.6 BEV Powertrain Distribution per Class (Light-Duty Vehicle)

BEV Powertrain Distribution per Class (LDV)

	Base0/1/4	Base2/A2	Base3/A3	Base5/B5/C5	Base6/B6/C6
Compact Car	0.1%	2.0%	4.0%	5.0%	9.0%
Midsize Car	0.0%	2.0%	3.0%	4.0%	10.0%
Large Car	0.0%	0.0%	0.0%	1.0%	4.0%
Compact SUV	0.0%	0.0%	0.0%	7.0%	11.0%
Midsize SUV	0.0%	0.0%	0.0%	1.0%	5.0%
Full Size SUV	0.0%	0.0%	0.0%	0.0%	0.0%
Pickup	0.0%	0.0%	0.0%	0.0%	0.0%

C.7 Evolution of MD/HD Truck Classes

Evolution of MDT/HDT Classes

	Base0/1/4	Base2/A2	Base3/A3	Base5/B5/C5	Base6/B6/C6
Class 3 Box	13.0%	13.0%	13.0%	13.0%	13.0%
Class 3 Shuttle	2.0%	2.0%	2.0%	2.0%	2.0%
Class 4 Delivery	20.0%	20.0%	20.0%	20.0%	20.0%
Class 6 P&D	20.0%	20.0%	20.0%	20.0%	20.0%
Transit Bus	5.0%	5.0%	5.0%	5.0%	5.0%
Line Haul	40.0%	40.0%	40.0%	40.0%	40.0%

C.8 Evolution of MD and HD Vehicle Powertrains

Evolution of Medium & Heavy Duty Vehicle Powertrains

	Base0/1/4	Base2/A2	Base3/A3	Base5/B5/C5	Base6/B6/C6
Conv Gas	15.0%	12.0%	7.0%	0.0%	0.0%
Conv Gasoline 48V	0.0%	3.0%	6.0%	5.0%	5.0%
Conv Diesel	82.5%	60.0%	56.0%	52.0%	44.0%
Conv Diesel 48V	0.0%	20.0%	16.0%	12.0%	10.0%
HEV	2.5%	5.0%	13.0%	20.0%	22.0%
PHEV	0.0%	0.0%	0.0%	0.0%	4.0%
BEV	0.0%	0.0%	2.0%	11.0%	15.0%

C.9 Evolution of MD and HD Vehicle Automation

Evolution of Medium & Heavy Duty Vehicle Automation

	Base0/1/4	Base2/A2	Base3/A3	Base5/B5/C5	Base6/B6/C6
No Automation	100%	95%	90%	78%	45%
Partial Automation	0%	5%	10%	20%	40%
Full Automation	0%	0%	0%	2%	15%

C.10 HEV Powertrain Distribution per Class (MD/HD Trucks)

HEV Powertrain Distribution per Class MDT/HDT)

	Base0/1/4	Base2/A2	Base3/A3	Base5/B5/C5	Base6/B6/C6
Class 3 Box	0.0%	0.0%	2.0%	8.0%	8.0%
Class 3 Shuttle	0.0%	0.0%	0.0%	0.0%	0.0%
Class 4 Delivery	0.0%	0.0%	4.0%	4.0%	8.0%
Class 6 P&D	0.0%	0.0%	4.0%	6.0%	6.0%
Transit Bus	0.0%	0.0%	0.0%	0.0%	0.0%
Line Haul	0.0%	0.0%	0.0%	0.0%	0.0%

C.11 PHEV Powertrain Distribution per Class (MD/HD Trucks)

PHEV Powertrain Distribution per Class MDT/HDT)

	Base0/1/4	Base2/A2	Base3/A3	Base5/B5/C5	Base6/B6/C6
Class 3 Box	0.0%	0.0%	0.0%	0.0%	0.0%
Class 3 Shuttle	0.0%	0.0%	0.0%	0.0%	0.0%
Class 4 Delivery	0.0%	0.0%	0.0%	0.0%	4.0%
Class 6 P&D	0.0%	0.0%	0.0%	0.0%	0.0%
Transit Bus	2.5%	5.0%	3.0%	2.0%	0.0%
Line Haul	0.0%	0.0%	0.0%	0.0%	0.0%

C.12 BEV Powertrain Distribution per Class (MD/HD Trucks)

BEV Powertrain Distribution per Class MDT/HDT)

	Base0/1/4	Base2/A2	Base3/A3	Base5/B5/C5	Base6/B6/C6
Class 3 Box	0.0%	0.0%	0.0%	0.0%	0.0%
Class 3 Shuttle	0.0%	0.0%	0.0%	2.0%	2.0%
Class 4 Delivery	0.0%	0.0%	0.0%	4.0%	4.0%
Class 6 P&D	0.0%	0.0%	0.0%	2.0%	4.0%
Transit Bus	0.0%	0.0%	2.0%	3.0%	5.0%

APPENDIX F – GREET Greenhouse Gas Emission Factors

Fuel	GHG	Base 0	Base 2, Base 3, A2, A3	Base 5, Base 6, B5, B6, C5, C6
		WTW g/MJ		
Gasoline	CO ₂ (w/C in VOC and CO)	87	86	86
	CH ₄	0.113	0.113	0.113
	N ₂ O	0.004	0.004	0.004
	GHGs	91.11	90.74	90.70
North American Natural Gas	CO ₂ (w/C in VOC and CO)	65	65	65
	CH ₄	0.269	0.265	0.267
	N ₂ O	0.003	0.003	0.003
	GHGs	74.06	73.53	73.44
Low Sulfur Diesel	CO ₂ (w/C in VOC and CO)	88	88	88
	CH ₄	0.135	0.133	0.137
	N ₂ O	0.000	0.000	0.000
	GHGs	92.52	92.37	92.41
Electricity U.S. Mix	CO ₂ (w/C in VOC and CO)	132	115	107
	CH ₄	0.252	0.227	0.219
	N ₂ O	0.002	0.002	0.002
	GHGs	140.28	122.13	114.35

(This Page Intentionally Left Blank)

U.S. DEPARTMENT OF
ENERGY

Office of
**ENERGY EFFICIENCY &
RENEWABLE ENERGY**

For more information, visit:
energy.gov/eere/vehicles

DOE/EE-2066 • July 2020